ORNL/Sub-7434/1
80-EES-12-02

THE DESIGN AND DEVELOPMENT OF A SPLIT EVAPORATOR HEAT PUMP SYSTEM

M. H. Somerville
S. G. Penoncello

Date Published: December 1981

Report Prepared by
Engineering Experiment Station
University of North Dakota
Grand Forks, North Dakota 58202
under
Subcontract Number 7434
for
OAK RIDGE NATIONAL LABORATORY
Oak Ridge, Tennessee 37830
operated by
UNION CARBIDE CORPORATION
for the
U.S. Department of Energy
Contract No. W-7405-eng-26

TABLE OF CONTENTS

PAGE

LIST OF TABLES vi

LIST OF FIGURES ix

ABSTRACT 1

ACKNOWLEDGMENTS 3

1.0 INTRODUCTION 7

1.1 Background to the Project 7
1.2 Project Objectives Under Subcontract 7434 16
1.3 Overview of the Project Results 18
1.4 Report Objectives 19

2.0 DEVELOPMENT OF A PARALLEL EVAPORATOR - MULTIPLE SOURCE HEAT PUMP 23

2.1 Introduction 23
2.2 Objective 24
2.3 Experimental Equipment 24
2.4 Test Procedure 30
2.4.1 Detailed Procedure 32
2.5 Analysis of Results 33
2.5.1 Air Side Tests 33
2.5.2 Ice Side Tests 41
2.6 Conclusions 43

3.0 THE DUAL SERIES EVAPORATOR DESIGN AND DEVELOPMENT 44

3.1 Introduction 44
3.2 The Dual Series Evaporator Configuration 44
3.3 Dual Series Evaporator Configuration 47
3.3.1 Thermal Electric Expansion Valve 47
3.3.2 Accumulator 48
3.3.3 Four-Way Reversing Valve 48
3.3.4 Restrictor 50
3.4 Laboratory Test Facility 50
3.5 Results and Analysis of the Dual Series Evaporator Tests . 52
3.5.1 Test One - Four-Ton Modified Tetco Unit 52
3.5.2 Test Two - 2½ Ton Janitrol Unit 55
3.6 Conclusions and Recommendations 62

4.0 DEVELOPMENT OF A MULTI-SOURCE HEAT PUMP WITH PARALLEL EVAPORATORS WITH ACTIVE SUBCOOLING 64

4.1 Introduction 64
4.2 The Parallel Multiple Source Heat Pump with Active Subcooling 64

TABLE OF CONTENTS (Continued)

PAGE

4.3 System Description 67
4.4 Test Procedure 72
4.5 Experimental Results 75
4.5.1 Results of Test 1 75
4.5.2 Results of Test 2 80
4.5.3 Results of Test 3 83
4.6 Conclusions and Recommendations 89

5.0 DESIGN PROCEDURE FOR MULTIPLE SOURCE HEAT PUMPS 90

5.1 Introduction 90
5.2 Development of the Desktop Design Procedure for Dual Series Heat Pump Systems 91
5.2.1 Compressor Model 91
5.2.2 Condenser Model 92
5.2.3 Active Evaporator Model 97
5.2.4 Restrictor Model 101
5.2.5 Expansion Device Model 107
5.2.6 Inactive Evaporator Model 111
5.2.7 Graphical Solution Procedure 111
5.3 Development of the Analytical Model 118
5.3.1 Design Philosophy 118
5.3.2 Dual Series Model 123
5.3.3 Modification of the Dual Series Model to a General Multiple Source Heat Pump Model 126

APPENDIX 5.A - COMPUTER PROGRAM LISTING . . microfiche, inside back cover

6.0 WEATHER DATA ANALYSIS 132

6.1 Background 132
6.1.1 Historical 132
6.1.2 New Thermal Design Constraints 133
6.1.3 Existing Weather Data 135
6.1.4 Load Calculations 136
6.2 Presentation of Weather Data 138
6.2.1 Heating Season 138
6.2.2 Cooling Season 147
6.3 Weather Data Analysis 149
6.4 Design Use of the Weather Data 158
6.5 Conclusions and Recommendations 158

7.0 HEAT TRANSFER CHARACTERISTICS OF A FLAT PLATE ICE-MAKER 162

7.1 Introduction and Summary of the Work 162
7.1.1 Summary of Work 162
7.1.2 Typical Application 163
7.2 Intent of the Summary 168

TABLE OF CONTENTS (Continued)

PAGE

7.3 Analytical Model 168
7.3.1 Analytical Model Development and Solution Procedure 168
7.3.2 The Governing Differential Equations. 169
7.3.3 Calculation of the Film Coefficient 171
7.3.4 Calculation of the Ice Formation Rate 172
7.4 Experimental Equipment 174
7.5 Experimental Procedure 175
7.6 Analytical and Experimental Results. 178
7.6.1 Analytical Results. 178
7.6.2 Experimental Results. 187
7.7 Conclusions and Recommendations. 187

APPENDIX 7.A - NOMENCLATURE. 194

8.0 THE ICE/EARTH SOURCE EVAPORATOR 199

8.1 System Description 200
8.2 Analytical and Experimental Efforts with the ETS Facility. 204
8.3 Recommendations. 207

9.0 RELATIVE ECONOMICS OF THE MULTIPLE SOURCE HEAT PUMP SYSTEM. . . . 208

9.1 Introduction 208
9.2 Analysis Assumptions 208
9.3 Analysis Procedure 211
9.3.1 Determination of the Procurred Energy During the Heating Season. 211
9.3.2 Determination of the Procurred Energy During the Cooling Season. 214
9.3.3 Determination of the Total Procurred Energy and Annual COP for the Heating/Cooling Systems. . 216
9.3.4 The Influence of an Off-Peak to Demand Cost Ratio in the Electrical Rate Structure. 216
9.4 Results of Analysis. 218
9.4.1 Thermal Performance 218
9.4.2 Economic Performance. 218
9.5 Recommendations. 224

10.0 CONCLUSIONS AND RECOMMENDATIONS. 225

10.1 Conclusions. 225
10.2 Recommendations. 226

REFERENCES 227

LIST OF TABLES

TABLE NO.		PAGE
1.1	ORIGINAL PROJECT SPONSORS	8
1.2	COMPARISON OF COMMONLY USED WEATHER DATA PARAMETERS WITH SOME STATISTICAL PARAMETERS	15
1.3	LIST OF REPORTS RELATED TO ORNL SUBCONTRACT 7434	20
2.1	MANUFACTURER'S AIR TO AIR PERFORMANCE DATA OF JANITROL 38 HEATING ONLY HEAT PUMP AT 1200 CFM	28
2.2	RAW DATA FOR THE DUAL, PARALLEL ALTERNATING, EVAPORATOR HEAT PUMP IN THE ICE MODE	34
3.1	HEAT PUMP PERFORMANCE	54
4.1	DATA REQUIRED TO ANALYZE THE THERMAL PERFORMANCE OF A MSHP SYSTEM	74
4.2	HEATING CAPACITY, WORK INPUT AND HEATING COEFFICIENT OF PERFORMANCE FOR TEST II OF THE AIR/ICE MSHP	82
4.3	TEST III, MSHP - STATE POINT PRESSURES AND TEMPERATURE DURING ACTIVE AIR EVAPORATOR TEST	86
4.4	CALCULATED EVAPORATOR EXIT TEMPERATURE	87
4.5	HEATING CAPACITY, WORK INPUT AND HEATING COEFFICIENT OF PERFORMANCE FOR TEST III OF THE AIR/ICE MSHP	88
5.1	ENTHALPY CHANGE ACROSS THE CONDENSER ASSUMING SATURATED VAPOR INTO THE COMPRESSOR, 50 PERCENT ISENTROPIC COMPRESSION EFFICIENCY, AND 10°F SUBCOOLING AT THE EXIT FROM THE CONDENSER	96
5.2	HEATING CAPACITY OF THE CONDENSER AS A FUNCTION OF THE CONDENSING TEMPERATURE	98
5.3	ENTHALPY CHANGE ACROSS THE ACTIVE EVAPORATOR	100
5.4	ACTIVE EVAPORATOR HEAT TRANSFER RATES	102
5.5	CRITICAL PRESSURES AND MASS FLOW RATES AFTER TUBE DIMENSION CORRECTION	106
5.6	CRITICAL PRESSURE CORRECTION FACTORS (ϕ_2)	109
5.7	REFRIGERANT 22 - TONS OF REFRIGERATION	119

LIST OF TABLES (Continued)

TABLE NO.		PAGE
5.8	INPUT PARAMETERS FOR SYSTEM SIMULATION PROGRAM	128
5.9	EXAMPLE OF COMPUTER MODEL OUTPUT	130
6.1	EXAMPLE OF DOD BIN WEATHER DATA - BOSTON, MASSACHUSETTS - SEPTEMBER	140
6.2	CALCULATION OF THE CUMULATIVE °F-HRS FOR BOSTON, MASSACHUSETTS - SEPTEMBER	141
6.3	SEASON 1 CUMMULATIVE FRACTION HEATING LOADS FOR BOSTON, MASSACHUSETTS - OCTOBER 1 TO MAY 31	142
6.4	ESTAR AND VSTAR VALUES FOR BOSTON, MASSACHUSETTS, OCTOBER 1 TO MAY 31	144
6.5	SEASON 2 CONDUCTION CUMMULATIVE FRACTION COOLING LOADS FOR BOSTON, MASSACHUSETTS, JULY 1 TO AUGUST 31	148
6.6	LATENT COOLING LOAD DUE TO AN AIR CHANGE FOR BOSTON, MASSACHUSETTS, JULY 1 TO AUGUST 31	150
6.7	TOTAL (LATENT PLUS SENSIBLE) COOLING LOAD DUE TO AN AIR CHANGE FOR BOSTON, MASSACHUSETTS, JULY 1 TO AUGUST 31	151
6.8	COOLING LOAD DUE TO CONDUCTION IN DEGREE HOURS, BOSTON, MASSACHUSETTS	152
6.9	COOLING LOAD DUE TO AIR CHANGE IN B.T.U. HOURS PER LB. DRY AIR FOR BOSTON, MASSACHUSETTS	153
6.10	HEATING LOAD DUE TO CONDUCTION IN DEGREE HOURS FOR BOSTON, MASSACHUSETTS	154
6.11	LISTING OF CITIES WEATHER DATA STUDIED BY A.S.H.R.A.E. DEGREE DAYS	156
6.12	LIST OF OUTPUT TABLES BY OWDA	159
7.1	RESULTS OF FILM COEFFICIENT LABORATORY TESTS WATER FLOW RATE = 99.5 LBS/MIN	188
7.2	RESULTS OF FILM COEFFICIENT LABORATORY TESTS WATER FLOW RATE = 65.5 LBS/MIN	189
7.3	COMPARISON OF ANALYTICAL AND EXPERIMENTAL FILM CO-EFFICIENTS WATER FLOW RATE = 99.5 LBS/MIN (45.1 KG/MIN)	191
9.1	THE FIVE MAJOR CITIES CHOSEN FOR THE THERMAL AND ECONOMIC STUDY	209

LIST OF TABLES (Continued)

TABLE NO.		PAGE
9.2	CALCULATION OF HEATING SEASON COP FOR THE FOUR SYSTEMS ANALYZED FOR BOSTON, MASSACHUSETTS	212
9.3	DETERMINATION OF THE PROCURRED ENERGY DURING THE COOLING SEASON FOR BOSTON, MASSACHUSETTS	215
9.4	DETERMINATION OF THE TOTAL PROCURRED ENERGY AND ANNUAL COP OF THE FOUR HEATING SYSTEMS FOR BOSTON, MASSACHUSETTS	217
9.5	THE INFLUENCE OF AN OFF-PEAK INCENTIVE ON THE PERCENT SAVINGS IN PROCURRED ENERGY FOR BOSTON, MASSACHUSETTS	219
9.6	THERMAL ANALYSIS OF THE FOUR CASE SYSTEMS	220
9.7	FRACTION OF ACES STORAGE VOLUME REQUIRED FOR A MSHP SYSTEM (ACES = 1.00)	222
9.8	SUMMARY OF PERCENT OPERATING COST SAVINGS FOR VARIOUS O/D RATIOS AND RELATIVE CAPITAL COST OF THE SYSTEM FOR THE FIVE CITIES CONSIDERED	223

LIST OF FIGURES

FIGURE NO.		PAGE
1.1	MEAN CUMULATIVE TEMPORAL FREQUENCY OF OCCURENCE OF TEMPERATURES AND HEAT LOAD FRACTION AT OR ABOVE A GIVEN TEMPERATURE, CASE 2 - MID-POINT OF EACH TEMPERATURE RANGE, NOME, ALASKA 64 30'N, 166 02'W . . .	11
1.2	MEAN CUMULATIVE TEMPORAL FREQUENCY OF OCCURENCE OF TEMPERATURES AND HEAT LOAD FRACTION AT OR ABOVE A GIVEN TEMPERATURE, CASE 2 - MID-POINT OF EACH TEMPERATURE RANGE, GRAND FORKS, NORTH DAKOTA, 47 40'N, 97 03'W	12
1.3	MEAN CUMULATIVE TEMPORAL FREQUENCY OF OCCURENCE OF TEMPERATURES AND HEAT LOAD FRACTION AT OR ABOVE A GIVEN TEMPERATURE, CASE 2 - MID-POINT OF EACH TEMPERATURE RANGE, MINNEAPOLIS, MINNESOTA 44 53'N, 93 16'W .	13
1.4	THEORETICAL PERFORMANCE OF A MULTIPLE SOURCE HEAT PUMP .	17
2.1	MULTIPLE SOURCE CHARACTERISTIC AND INDIVIDUAL HEAT PUMP CHARACTERISTICS	25
2.2	SCHEMATIC OF A MULTIPLE SOURCE HEAT PUMP WITH A PARALLEL ALTERNATING EVAPORATOR ARRANGEMENT	26
2.3	THE EXPERIMENTAL MULTI-SOURCE HEAT PUMP WITH A PARALLEL EVAPORATOR ARRANGEMENT	27
2.4	MAKE-UP OF WATER DISTRIBUTION SYSTEM USED IN LABORATORY TESTS	31
2.5	PARALLEL DUAL EVAPORATOR HEAT PUMP TEMPORAL PERFORMANCE, OPERATING ON THE AIR SIDE EVAPORATOR	40
2.6	PARALLEL DUAL EVAPORATOR HEAT PUMP TEMPORAL PERFORMANCE, OPERATING ON TWO ICE MAKER EVAPORATORS	42
3.1	SCHEMATIC OF SERIES AIR AND ICE-MAKER EVAPORATOR HEAT PUMP SYSTEM	45
3.2	DUAL SERIES EVAPORATOR HEAT PUMP CYCLE	46
3.3	COMPARISON OF BIDIRECTIONAL THERMAL ELECTRIC EXPANSION VALVE TO A THERMOSTATIC EXPANSION VALVE SET-UP	49
3.4	TEST CONFIGURATION OF MAJOR LABORATORY EQUIPMENT	51

LIST OF FIGURES (Continued)

FIGURE NO.		PAGE
3.5	OUTPUT OF DUAL-SERIES EVAPORATOR HEAT PUMP AT VARIOUS SUBCOOLING AIR TEMPERATURES. ACTIVE ICE-MAKER	56
3.6	OUTPUT OF DUAL-SERIES EVAPORATOR HEAT PUMP AT VARIOUS SUBCOOLING AIR TEMPERATURES. ACTIVE ICE-MAKER	57
3.7	OUTPUT OF DUAL-SERIES EVAPORATOR HEAT PUMP AT VARIOUS SUBCOOLING AIR TEMPERATURES. ACTIVE ICE-MAKER	58
3.8	EFFECT OF INCREASED RESTRICTION BETWEEN CONDENSER AND SUBCOOLER ON OUTPUT. ACTIVE ICE-MAKER	59
3.9	DEFROST PERFORMANCE OF A DUAL-SERIES EVAPORATOR HEAT PUMP AT VARIOUS RESTRICTOR SETTINGS	60
4.1	MULTIPLE SOURCE HEAT PUMP SYSTEM	65
4.2	IDEAL AND ACTUAL P-h DIAGRAMS OF AN MSHP SYSTEM	66
4.3	SCHEMATIC DIAGRAM OF TESTED MSHP SYSTEM	68
4.4	MODIFIED TUBE-IN-TUBE AIR EVAPORATOR DESIGN	71
4.5	THE PRESSURE ENTHALPY DIAGRAM FOR THE ACTIVE AIR EVAPORATOR TEST (ICE MAKERS INACTIVE)	76
4.6	THE PRESSURE ENTHALPY DIAGRAM FOR THE ACTIVE ICE EVAPORATOR TEST (INACTIVE AIR EVAPORATORS)	77
4.7	TEMPERATURE VS. TIME PLOT FOR AIR/ICE MSHP TEST DURING ICE-MAKING, TEST I	78
4.8	MSHP TEST I, EXPERIMENTAL DATA, AIR EVAPORATOR ACTIVE	79
4.9	PLOT OF TEMPERATURE VS. TIME FOR TEST II OF MSHP SYSTEM	81
4.10	EXPERIMENTAL RESULTS FOR TEST III OF THE AIR/ICE MSHP SYSTEM - AIR EVAPORATOR ACTIVE	84
4.11	PROPOSED DESIGN FOR A CO-AXIAL COPPER TUBE FOR USE IN A MSHP FINNED TUBE AIR COIL	85
5.1	REFRIGERATION EFFECT IN THE EVAPORATOR	93
5.2	COMPRESSOR CHARACTERISTICS	94
5.3	CONDENSOR CHARACTERISTICS	99
5.4	ACTIVE EVAPORATOR CHARACTERISTICS	103

LIST OF FIGURES (Continued)

FIGURE NO.		PAGE
5.5	CAPILLARY FLOW FACTORS (REFRIGERANTS 12 AND 22)	104
5.6	BASIC RATING CURVES FOR .064 IN. I.C., 80 IN. LONG CAPILLARY	105
5.7	CRITICAL CORRECTION FACTOR (REFRIGERANTS 12 AND 22)	108
5.8	RESTRICTOR CHARACTERISTICS	110
5.9	EXPANSION VALVE CHARACTERISTICS	112
5.10	COMPRESSOR - CONDENSER OVERLAY OF FIGURES 5.2 and 5.3	113
5.11	CONDENSING UNIT CHARACTERISTICS	114
5.12	EVAPORATOR - CONDENSING UNIT OVERLAY	115
5.13	SYSTEM CHARACTERISTICS (FIRST TRIAL)	117
5.14	SYSTEM CHARACTERISTICS (FINAL RESULT)	122
5.15	EFFECTS OF PRESSURE DROPS DUE TO FLUID FRICTION	124
5.16	PARALLEL PIPE FLOW SYSTEM	127
7.1	FLAT PLATE ICE-MAKER EVAPORATOR CONFIGURATION	165
7.2	ICE-MAKER PLATE HEAT TRANSFER SITUATION	167
7.3	COORDINATES FOR THE VELOCITY AND THERMAL BOUNDARY LAYERS FOR FORCED LAMINAR FLOW ALONG A FLAT PLATE	170
7.4	NOMENCLATURE FOR THE OVERALL HEAT TRANSFER ANALYSIS	173
7.5	ANALYTICAL CALCULATIONS OF MEAN NUSSELT NUMBER	179
7.6	ANALYTICAL CALCULATIONS OF MEAN NUSSELT NUMBER	180
7.7	ANALYTICAL CALCULATIONS OF MEAN NUSSELT NUMBER	181
7.8	ANALYTICAL CALCULATIONS OF MEAN NUSSELT NUMBER	182
7.9	ANALYTICAL CALCULATIONS OF LOCAL NUSSELT NUMBER	183
7.10	VARIATION IN MEAN NUSSELT NUMBER WITH RESPECT TO THE RELATIVE AIR TEMPERATURE, Θ	184
7.11	ANALYTICAL DETERMINATION OF ICE FORMATION FOR AVERAGE CONDUCTION EVAPORATORS	185

LIST OF FIGURES (Continued)

FIGURE NO.		PAGE
7.12	EFFECT OF AIR ENVIRONMENT ON ICE FORMATION RATE AT A WATER FLOW RATE OF 65.5 LBS/MIN (29.7 KG/MIN)	190
8.1	CROSS-SECTION OF TEST FACILITY	201
8.2	TYPICAL E.T.S. UNIT	202
8.3	REVERSE-RETURN HYDRAULIC SYSTEM	203
8.4	DETAIL OF SUBCOOLING TUBE ENTRY, EARTH EVAPORATOR	205
8.5	ICE MELT OFF VERSUS TIME	206

ABSTRACT

The work presented is a summary of a five year effort to design, build, laboratory test and field test experimental multiple source heat pumps. The results presented are a summary of detailed technical reports, which have been issued throughout the project.

The designs and experimental results of three types of multiple source heat pumps are presented. The three designs are the parallel evaporator, the series evaporator, and the parallel evaporator with active subcooling. Of the three, the parallel evaporator with the active subcooling shows, by far, the most promise and offers a potential solution to the problem of defrosting of air evaporators.

Three design procedures for multiple source heat pumps were developed. One of these is a hand calculational procedure, the others are computer based. All three predict the performance characteristics of the multiple source heat pump reasonably well (within ten percent). The models are based upon the refrigerant flow rate, rather than the refrigeration effect of the evaporator.

The technical results of a detailed analytical and experimental model of the heat transfer rates on a flat plate ice maker are presented. It is shown, both analytically and experimentally, that the temperature of the air surrounding the flat plate ice maker can play a dominant role in the rate of ice formation.

A detailed weather analysis for forty cities located throughout the nation was completed. These data were processed to allow easy computation

of thermal storage requirements for full, partial, or minimum ACES systems, or upon other design requirements, such as off-peak air conditioning.

The results of an innovative ice storage system that is thermally coupled to the earth are described. This system has the potential for meeting both the off-peak air conditioning needs and the thermal storage requirements for the heating cycle.

Finally, an economic and energy comparison of multiple source heat pumps with ACES, and air-to-air heat pump systems is presented. The comparison shows that air-to-air systems and multiple source heat pump systems will probably be developed before ACES systems are, even though ACES systems are generally more energy efficient.

The major conclusions of this work are:

* It is possible to build a multiple source heat pump;
* The potential for building an air-to-air multiple source heat pump that would solve the defrost cycle problem, while improving the steady-state COP, is high;
* Insufficient weather data exists to properly design short to intermediate term (weekly or more) thermal storage systems;
* The environmental air temperature surrounding a flat plate ice-maker can have a pronounced impact (doubling) upon the ice formation rate, at air temperatures greater than 32°F (0°C); and
* It is likely that the air-to-air and multiple source heat pumps will be developed prior to ACES system.

ACKNOWLEDGMENTS

This report summarizes almost five years of work, three of which were sponsored by the Department of Energy, Division of Conservation and Solar Applications, through the Oak Ridge National Laboratory, under Subcontract Number 7434. Although some of the people who have made this work possible can be recognized, it is not possible to recognize all of them because they number in the hundreds. The people cited below have made major contributions to this work.

Mr. Harry C. Fischer deserves special recognition for his role as the designer and advocate of the Annual Cycle Energy System (ACES); the early support that the project received from Harry is much appreciated and recognized. Dr. Robert Minturn, the program manager, provided invaluable advice, appropriate prodding, and support throughout the project. Program management of a task the size and complexity of this one is difficult; Dr. Minturn did an outstanding job. Dr. Len Abbatiello provided technical advice and critiques of our work on a regular basis; we found this to be valuable, and appreciated his assistance. The assistance of Mr. Mel Koons, the contract monitor, is also recognized.

In addition to the support received under Subcontract #7434, several other sponsors offered major financial support. These include the Northern States Power Company, Ottertail Power Cooperative, Minnkota Power Cooperative, and the Westinghouse Electric Corporation. Mr. Lee Tuskey and Mr. Conrad Aas, both of N.S.P., contributed not only financial support, but also provided information concerning the needs and future requirements of the utility industry. These data were crucial in the development of the

multi-source heat pump concept. Mr. Lou Hine, of Westinghouse, provided much insight into the market requirements of air-to-air heat pumps and residential HVAC equipment.

Special recognition should go to Mr. James Stover, his wife Sherry, and Mr. Richard Widseth for their part in a very ambitious undertaking; they agreed to have their homes act as a field laboratory for our experimental heating systems. Their cooperation and assistance is greatly appreciated. Mr. David Hart, of TETCO, provided not only financial support, but also invaluable design information and assistance. His encouragement and continuing support are most appreciated.

A project of the magnitude of this one, carried out in a university climate, involves the assistance of students. During the last five years, over fifty students have actively participated in this project. For many, it was their first exposure in the practice of engineering; the project, in term, benefited from their creativity and willingness to work hard for little renumeration. The students cited below all made significant contributions to this project, without them and their peers, little would have been accomplished.

Greg Loken, Carl Svard and Larry Albrecht, the initial students involved in the project, made outstanding contributions in the technical and economic modeling effort, the initial design; and the construction of multiple source heat pumps. Major contributions to the monitoring effort were made by Tony Pascuzzi, Jon Olson, and Dean Anderson. The work of Larry Albrecht in the multiple source heat pump area was continued and expanded by Joe Wood and Steve Penoncello. Both Steve and Joe made significant contributions in the design of the series and parallel with active subcooling multiple source heat pumps. Jim Wendschlag's contribution to the project

was the completion of an outstanding modeling and experimental effort in measuring the heat transfer coefficient of the water film on the ice maker plates. His work documented for the firt time the impact of air temperature on ice formation rates. A.C. Lindem, Jon Olson, and Janet Viestenz all made contributions to both the monitoring effort and analysis of the weather data. Norm Cox and Jim Fristad carried out much of the detailed design work and were responsible for the construction of the earth-ice thermal storage system.

Special recognition should go to Lloyd Nordling, the School's Research Machinist, for his continued support and advice throughout the project and for his outstanding technician and machinist skills. David Schmit, the project's technician, was responsible for construction of the multiple source heat pump system's located at Crookston and much of the system located at Larimore. Mr. Donald E. Nelle redesigned the system in Larimore, and was responsible for the detailed design of much of Crookston's system.

This project has resulted in some thirty-one (31) major reports, totaling over three thousand pages. The clerical effort required to produce these reports and conduct the project has been enormous. The staff of the Engineering Experiment Station should be recognized for their part in this project and their outstanding support; were it not for them, the results of the work would not have been published. In particular, the efforts of Ms. Debbie Haley, Ms. Alice Corrigan, Ms. Beverly Biberdorf, Ms. Anne Ecklund, Ms. Cheryl Thompson, Ms. Rox Hochstetler, Mr. John Betcher, Ms. Linda Coye, Ms. Jackie Daugherty, Mr. Ron Enabnit, Ms. Annette Hanson, Ms. Nancy Heidlebaugh, Mr. Steve Larson, Ms. Laju Nankani, Ms. Carol Preston, and Ms. Rita Wolbeck are both recognized and deeply appreciated.

The project would not have been successful were it not for the efforts of both Professors William G. Barney and Don V. Mathsen. Professsor Barney was responsible for the supervision, procurement, and installation of the monitoring equipment. Professor Mathsen served as Co-principal Investigator throughout the project, was responsible for the design of the solar collectors in Larimore, and all of the field operations. Don's support and contributions to the project were truly outstanding; as is his design creativity.

This report, which is a summary of the entire project, was written by Mr. Steve Penoncello and Mr. Norm Cox, in concert with the Principal Investigator. Steve authored Chapters three and five, and co-authored Chapter nine; Norm authored Chapter eight.

Finally, Mr. John Hutchinson of Westinghouse, Dean Alan G. Fletcher, and the University of North Dakota should be recognized for their support of the project and the Principal Investigator. Dean Fletcher's willingness to provide the Principal Investigator, the faculty, staff, and students the flexibility and freedom required to conduct a project of this magnitude is most deeply appreciated. It is very likely that this project would not have been carried out at all, were it not for his foresight and creative vision.

1.0 INTRODUCTION

1.1 Background to the Project

In January 1976, the University of North Dakota, Engineering Experiment Station, was approached by Mr. James Stover of Larimore, North Dakota, to design and construct a "solar" heating system. Almost simultaneously, the Station was approached by the Andro Corporation to test a new uni-directional heat pump which had been designed specifically for northern climates. The two requests were analyzed, and accepted under the following conditions:

1. Andro would donate nine heat pumps, only one of which was to be field tested in a typical situation.

2. Eight of the heat pumps were to be used in the development of an experimental "solar" heating system.

3. The "solar" system that was to be installed in Stover's house was to be experimental as opposed to prototypical.

4. The Station was to solicit the support of commercial firms and industry in building the experimental system.

5. The Station was to have access to the experimental solar system for the purposes of monitoring and modification.

Dr. Mason H. Somerville and Mr. Don V. Mathsen were the two initial co-principal investigators on the Stover project. In an attempt to protect Mr. Stover from the extremely high cost of developing an experimental solar heating system, the Station actively pursued the financial aid of industry. Subsequently, several companies joined the project with donations of time, money, and/or equipment. The original sponsors and participants in the project are listed in Table 1.1.

Several of the sponsors had vested interests in the project. The home-owners (Stover, later joined by a second experimental system owner, Widseth)

TABLE 1.1

ORIGINAL PROJECT SPONSORS

U.N.D. Engineering Experiment Station, Grand Forks, ND
Mr. Jim Stover, Larimore, ND
Engineering Associates, Grand Forks, ND
Marvin Windows, Warroad, MN
Northern States Power, Grand Forks, ND
Minnkota Power, Grand Forks, ND
Otter Tail Power, Fergus Falls, MN
Nodak Power Cooperative, Grand Forks, ND
Trane Company, LaCrosse, WI
Johnson Controls, Fargo, ND
Andro Corporation, Columbus, OH
Tappan, Elyria, OH
Techo, Inc., Columbus, OH
B.F. Goodrich General Products Company, Akron, OH
Burke Rubber Company, San Jose, CA
Canton Redwood Yard, Inc., Minneapolis, MN
Foam Form, Inc., Scarborough, Ontario
McIntyre Plumbing, Heating & Air-Conditioning Inc., Grand Forks, ND
Owens-Corning Insulation, Granville, OH
Meland Lumber Company, Larimore, ND
Wholseale Building Supply, Inc., East Grand Forks, MN
Mr. Gary Johnson, Grand Forks, ND
Mr. Arnold Hanson, Devils Lake, ND
Mr. Dick Widseth, Crookston, MN
Mr. Lloyd Nordling, Alvarado, MN

wanted to have warm houses at low operating and capital costs, the contractors wanted experience at building a solar system, the utilities wanted a system that would not be a "peaking only" system, and the manufacturers wanted a place to try out their products. In short, the constraints that were placed upon the development of the experimental system were representative of what a manufacturer of heat and air conditioning equipment would face in the open marketplace. These constraints, in particular the first three, played a dominant role in guiding the development of the overall project, including the work produced under Subcontract 7434 with Oak Ridge National Laboratory.

The initial design objective for the Larimore (Stover) project was to build a series, or parallel, solar assisted heat pump system. This design was to allow testing of the theory comparing the two basic design philosophies. An analytical model was designed and programmed which described the performance of the system in several operating modes (Loken, 1977). The results of this work indicated that the maximum yearly COP resulted from a hybrid type system which utilized a variable source and an isothermal source. The utility company's constraint that the system not be a peaking one was judged to be fundamentally sound. Thus, the initial design tried to accomplish two major goals:

* maximization of years coefficient of performance (COP), and
* minimization of the use of peak electrical power.

The resulting experimental system was quite complex but did provide some very valuable design information. The experience of constructing the Larimore experimental system (Somerville et al., 1977; Svard et al., 1977; Mathsen et al., 1977; and Somerville and Wendschlag 1977) indicated that the following general conclusions were probably valid, at least for a climate with a high heating load:

1. A simple one or two mode system was highly desirable;

2. The use of a constant temperature source, such as found in the ice making technology associated with the Annual Cycle Energy System (ACES), (Fisher, 1976 A and B) was highly desirable;

3. The use of direct gain solar thermal collectors in a thermal climate similar to North Dakota's would be unlikely to compete with an isothermal source heat pump; and

4. That future research efforts in the program should be directed toward reduction of the capital investment of the ACES system, while maintaining or improving the seasonal and instantaneous coefficient of performance.

As part of the introductory work, an analysis of available weather data had been completed. Sources of data which were analyzed included:

* local climatalogical data;

* the American Society of Heating, Air Conditioning, and Refrigeration Engineers;

* the National Climatic Center weather tapes;

* the U.S. Department of Defense bin weather data.

Originally, the weather data were only used to support the modeling effort and grew into supporting the total heating system design effort. Two conclusions became apparent as a result of this work. The first was that the existing weather data base was not in a format that allowed one to design an ACES easily. The second was that the heating load characteristics of a given region offered a unique opportunity to build a machine whose behavior would approach that of an annual cycle energy system (e.g., an isothermal heat pump) without the immense storage required by ACES.

The bin weather data were analyzed and the cumulative heat load fraction and the temporal frequency of occurrence of the temperature were both determined. Results of this type of analysis yield an "S" shaped cumulative frequency curve. Examples for these type of data are given in Figures 1.1, 1.2, and 1.3 for Nome, AK, Grand Forks, ND, and Minneapolis, MN.

ORNL-DWG 81-17884

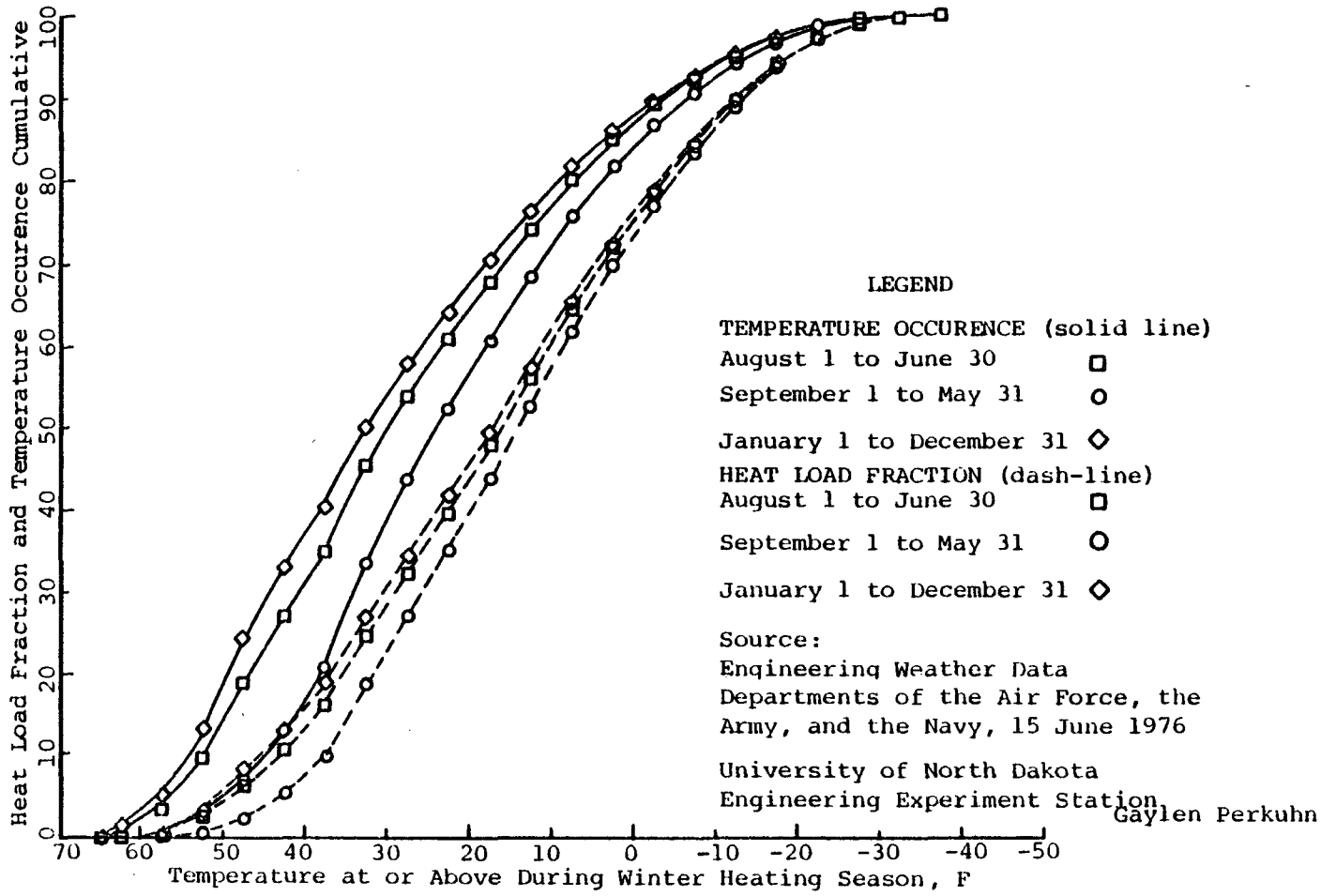

FIGURE 1.1 - MEAN CUMULATIVE TEMPORAL FREQUENCY OF OCCURENCE OF TEMPERATURES AND HEAT LOAD FRACTION AT OR ABOVE A GIVEN TEMPERATURE
CASE 2 - MID-POINT OF EACH TEMPERATURE RANGE
NOME, ALASKA 64 30'N, 166 02'W

ORNL-DWG 81-17885

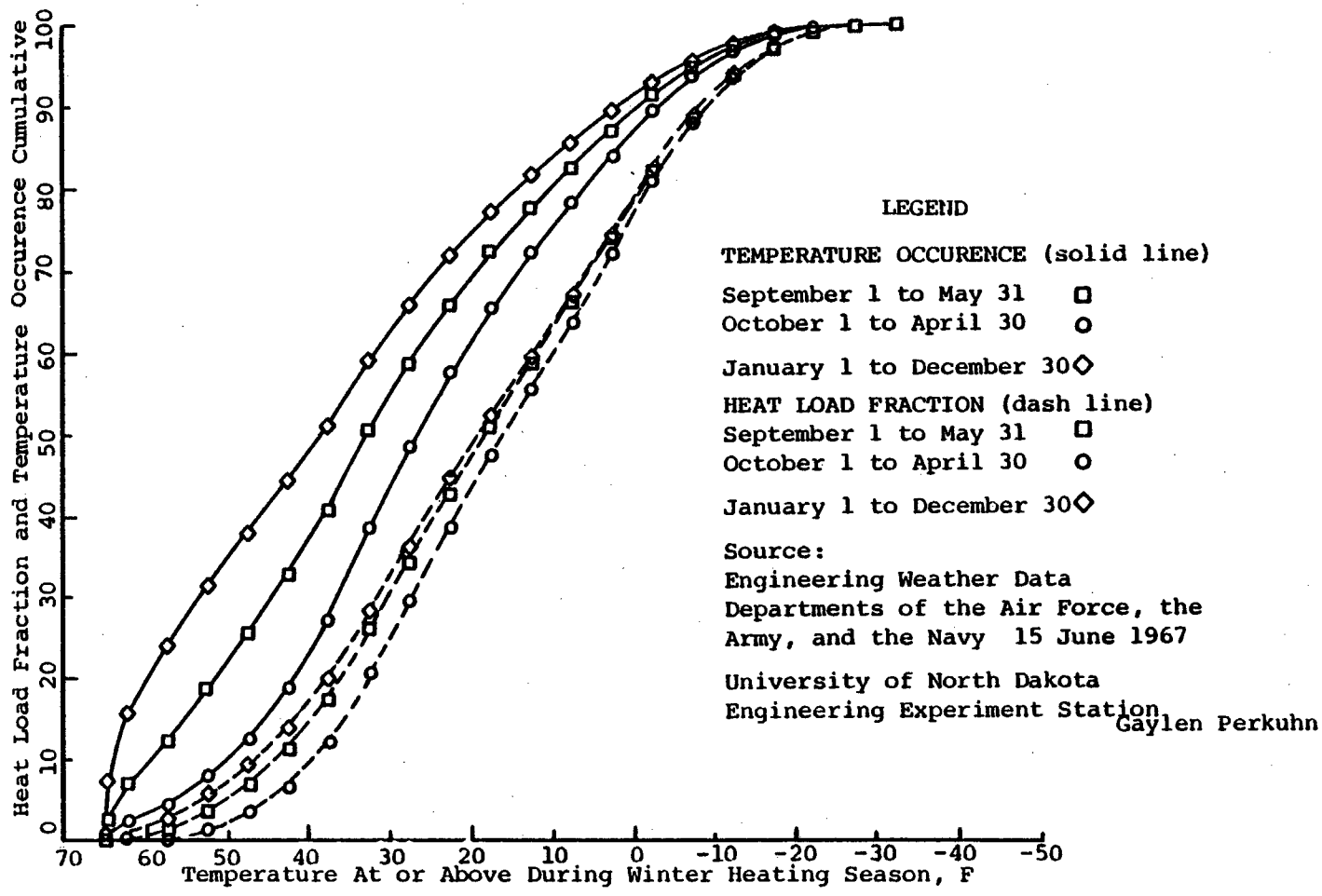

FIGURE 1.2 - MEAN CUMULATIVE TEMPORAL FREQUENCY OF OCCURENCE OF TEMPERATURES AND HEAT LOAD FRACTION AT OR ABOVE A GIVEN TEMPERATURE
CASE 2 - MID-POINT OF EACH TEMPERATURE RANGE
GRAND FORKS, NORTH DAKOTA 47 40'N, 97 03'W

ORNL-DWG 81-17886

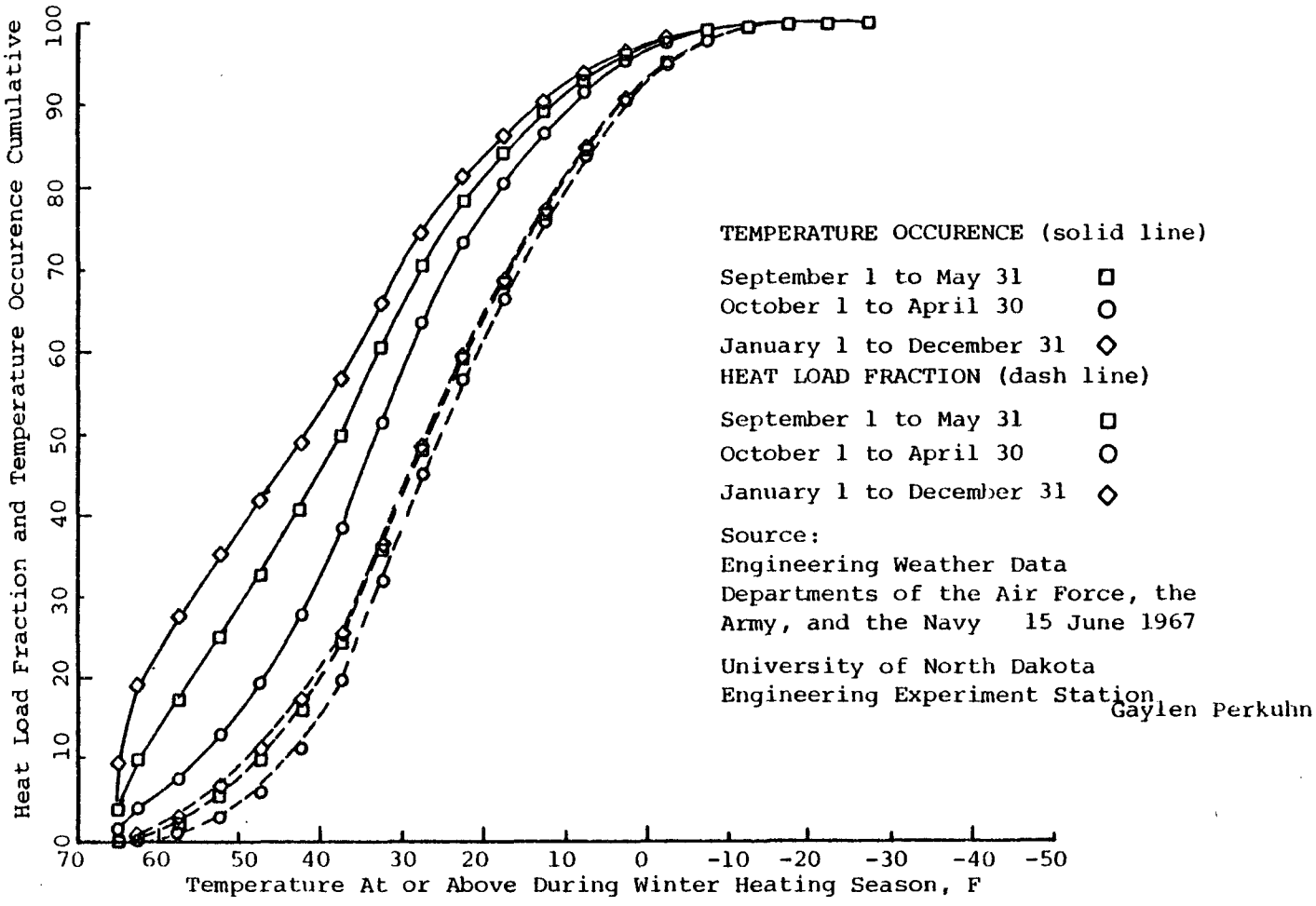

FIGURE 1.3 - MEAN CUMULATIVE TEMPORAL FREQUENCY OF OCCURENCE OF TEMPERATURES AND HEAT LOAD FRACTION AT OR ABOVE A GIVEN TEMPERATURE
CASE 2 - MID-POINT OF EACH TEMPERATURE RANGE
MINNEAPOLIS, MINNESOTA 44 53'N, 93 16'W

Comparison of the ASHRAE degree-day data with data from these Figures provides some insights that reveal an opportunity for the designer of vapor compression machines (heat pumps).

Such a comparison is done in Table 1.2. The total energy requirements for heating vary from 2061 to 14,171 Degree-Days (^{o}F - days). These data are, of course, well known; however, the other data are not. Namely, the temperature at or above which half the heat load occurs for most of the nation is at or above 27°F (-2°C). The fraction of the heat load that occurs at or above 32°F (0°C) is large (> 40 percent) for most of the nation; and the fraction of the heat load occurring above 10°F (-12°C) is in excess of 80 percent for most of the nation.

The data of Table 1.2 are encouraging because most of the nation's population reside at or below 44°N latitude. Consequently, the task of the thermal designer is to design a machine that provides the energy transfer required, but that avoids utilizing ambient air as a source at low temperatures, due to the basic thermodynamics involved. The annual cycle energy system (ACES), of course, avoids utilizing air as an energy source, altogether. Unfortunately, the economics of thermal storage are such that the ACES system is not competitive in the present U.S. market, even though its life cycle costs are. The goal of the designer is, of course, to save energy <u>and</u> money with a design that will compete in the market in the near term (5 to 10 years). Consequently, we sought a solution to this problem by minimizing capital cost, by reducing the size of the thermal storage unit required by ACES. We recognized that this could be done because of the data in Table 1.2. That is, we thought it was possible to design and build a vapor compression machine that would use two (or more) energy sources for the purpose of heating (and air conditioning). One of these

TABLE 1.2

COMPARISON OF COMMONLY USED WEATHER DATA PARAMETERS WITH SOME STATISTICAL PARAMETERS

Location	ASHRAE Degree-Days °F - Days	Air Temperature at or above Which Half (50%) of the Cumulative Heat Load Occurs, °F (°C)	Fractional Heat Load that Occurs at or above an Air Temperature of 10°F and 32°F
Nome, AK	14171	16, (-9)	60, 24
Grand Forks, ND	9901	18, (-8)	63, 30
Minneapolis, MN	8382	27, (-3)	80, 40
Other data not included in Figures 1.1, 1.2, 1.3			
Boston, MA	5634	34, (1)	93, 57
Memphis, TN	3232	41, (5)	99, 81
Los Angeles, CA	2061	57, (14)	100, 100

sources was to be ambient air, the second an isothermal source similar to that used in ACES technology (Ice-maker). We also recognized that such a multiple source heat pump could:

* provide a seasonal COP equivalent to ACES due to the high average temperature at which it could operate;

* provide off-peak air conditioning;

* provide a known thermal output, independent of ambient air temperatures, particularly at low ambient temperatures (See Figure 1.4);

* minimize the use of thermal storage, thereby, minimizing capital cost;

* utilize much of the existing heat pump technology;

* represent a path which would allow a continual transition from existing technology to an energy conserving technology, as well as, an air conditioning load management technology; and

* be easily built with four variable switch-over temperatures (see Figure 1.4). This would allow a manufacturer to build a given size machine with variable thermal storage size that would meet a large fraction of this U.S. heating and air conditioning market simply by changing the set point on the switch over temperature.

1.2 Project Objectives Under Subcontract 7434

The principal goal was to develop a split (multiple-source) ice-maker/air heat pump. Secondary objectives were: to complete monitoring of the experimental system in Larimore, and the experimental system in Crookston (a multiple source (air/ice) heat pump); develop a design procedure for designing a multiple source heat pump, and to analyze the impact upon a utilities load duration curves of wide spread usage of ACES systems.

As the project grew and matured and the effort to develop a design procedure continued, it became very clear that a detailed analysis of the weather data for the U.S. was required. This was particularly true in the determination of the air conditioning load. In both an off peak air conditioning system and a thermal storage system for heating, the size of the

ORNL-DWG 81-17887

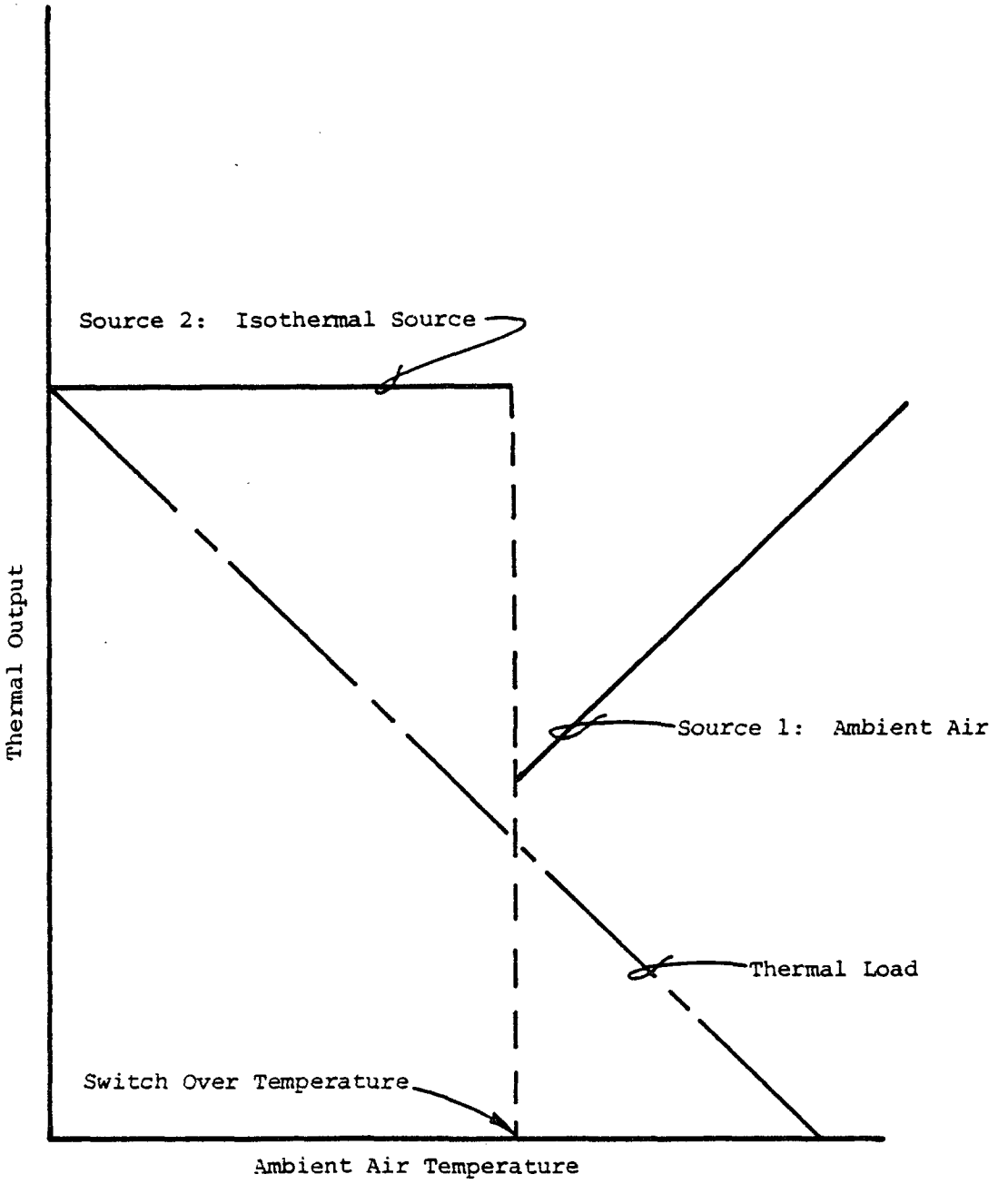

FIGURE 1.4 - THEORETICAL PERFORMANCE OF A MULTPLE SOURCE HEAT PUMP

storage unit must be determined. For systems that are designed to provide only diurnal energy requirements, this task becomes easy because a "worse case" approach can be used. This approach, however, cannot be used for intermediate periods, such as a week to a month, because the economics depend heavily upon the size of the thermal storage unit. Consequently, a detailed analysis of the bin weather data was undertaken to determine what the thermal load characteristics would be and consequently, the size of the thermal storage that would be required. This objective was added to the project because it is fundamental to the entire project including ACES design. Without these data, it is impossible to design either an off-peak air conditioning system or a thermal storage multiple source heat pump heating system. Thus, an objective of performing the required analysis of weather data was added and completed during the project, which was not included in the original project.

1.3 Overview of the Project Results

The majority of the objectives of the project were accomplished. The only major objective not accomplished was the monitoring of the experimental systems due to the continual failure of the monitoring equipment. This failure is documented in a separate report.

Several multiple source heat pumps were developed; they include a parallel evaporator, a series evaporator, and a parallel evaporator with active subcooling design. Part of the required utility study was completed and the results published (Kipp, 1978). The utility study demonstrated that the penetration of ACES into a utilities load, displacing an electrical heating load, could both reduce the peak load and flatten the load duration curve. An extensive effort was completed in the analysis of the bin weather data for forty major U.S. cities. The heat transfer characteristics of

a flat plate ice maker were determined, and an innovative ice-earth source evaporator was designed and built. A total of thirty-one (31) technical reports were written and published, and are listed in Table 1.3.

1.4 Report Objectives

This report summarizes the results of the project in all of the above areas except for the monitoring effort and the utility study. Chapters 2 3, and 4 describe the chronological development of the multiple source heat pumps. They are presented in chronological order because the lessons learned in each development support the subsequent development effort. In all cases, the designs utilized only commercially available equipment. In several cases this constraint caused the equipment to operate improperly because it was not designed to operate under the conditions imposed upon it by the system the equipment was installed in. Much of this equipment was pedestrian, e.g., solenoid valves and expansion valves.

Chapter 5 presents a summary of the work that was done in developing a design procedure for designing a multiple source heat pump. The procedures developed include both computer based procedures and a hand calculational procedure. Chapter 6 describes the work in analyzing the weather data and its design use; Chapter 7 presents the results of the work to determine the heat transfer characteristics of flat plate ice maker. Chapters 8 and 9 describe the ice-earth source evaporator and the relative economics of the multiple source system. The conclusions and recommendations are given in Chapter 10.

TABLE 1.3

LIST OF REPORTS RELATED TO ORNL SUBCONTRACT 7434

Report No.	Title
Pre Contract Reports	
1.	"The Design and Analysis of a North Dakota Annual Cycle Residential Solar Heating System," by M.H. Somerville, D.V. Mathsen, G.R. Loken, C.D. Svard, and J.C. Wendschlag, April 1977, Bulletin No. 77-04-EES-01.
2.	"A Flat-Plate Solar Collector Using Non-Black Absorber Elements," by D.V. Mathsen, M.H. Somerville, and G.R. Loken, April 1977, Bulletin No. 77-04-EES-02.
3.	"The Heating Only Heat Pump, An Application in the Annual Cycle System," by M.H. Somerville, and J.C. Wendschlag, April 1977, Bulletin No. 77-04-EES-03.
4.	"The Economics of Solar Space Heating and Cooling," by C.D. Svard, M.H. Somerville, and D.V. Mathsen, April 1977, Bulletin No. 77-04-EES-04.
5.	"A Computer Model for Performance Analysis of a Solar Heated Residential Home in North Dakota," by G.R. Loken, M.H. Somerville, and D.V. Mathsen, April 1977, Bulletin No. 77-04-EES-05.
6.	"A Mathematical Model of Residential Heating and Cooling Annual Cycle Solar Energy System" by G.R. Loken, July 1977-March 1978, Bulletin No. 77-07-EES-01.
Post Contract Award Publications	
7.	"The Development of a Hybrid Annual Cycle Energy System Heat Pump and Related Solar System" by M.H. Somerville, April 1977-March 1978, Bulletin No. 78-04-EES-01.
8.	"The Dual Evaporator Heat Pump with the Parallel Alternating Arrangement," by L.S. Albrecht, M.H. Somerville, April 1978, Bulletin No. 78-04-EES-02.
9.	"The Development of a Hybrid Annual Cycle Energy System Heat Pump and Related Solar Systems," by M.H. Somerville, W.G. Barney, J.A. Wood, and J.C. Wendschlag, April 1978-June 1978, Bulletin No. 78-07-EES-02.

TABLE 1.3 (continued)

LIST OF REPORTS RELATED TO ORNL SUBCONTRACT 7434

Report No.	Title
10.	"Data Acquisition Requirements for Monitoring Experimental Solar Energy Houses," by A. Pascuzzi, August 1978, Bulletin No. 78-08-EES-01.
11.	"Annual Cycle Energy System (ACES) Impact Upon a Utilities Load Duration Curve," by C.P. Kipp, September 1978, Bulletin No. 78-10-EES-01.
12.	"The Development of a Hybrid Annual Cycle Energy System Heat Pump," by M.H. Somerville, W.G. Barney, J.A. Wood, and J.C. Wendschlag, July 1978-September 1978, Bulletin No. 78-10-EES-01.
13.	"Progress Report: Fluke Data Acquisition System Computer Programs," J. Viestenz, and M.H. Somerville, May 1979, Bulletin No. 79-05-EES-01.
14.	"Development of an Ice/Ice Evaporator Heat Pump System," by M.H. Somerville, and S.G. Penoncello, May 1979, Bulletin No. 79-05-EES-02.
15.	"ACES Programmer's Users Guide for Computer-Based Statistical Analysis of Department of Defense Weather Data for Use in the Design of Solar and Hybrid Energy System," by A.C. Lindem III, June 1979, Bulletin No. 79-06-EES-01.
16.	"Isothermal Heat Transfer Through a Thin Fluid Film Undergoing a Phase Change with a Secondary Heat Transfer from a Warm Environment," by J.C. Wendschlag, June 1979, Bulletin No. 79-06-EES-02.
17.	"A Practical Design Procedure for Dual Evaporator Heat Pumps," by J.A. Wood, June 1979, Bulletin No. 79-06-EES-03.
18.	"The Effect of Subcooling on the Performance on a Dual-Series Evaporator Heat Pump," by G. Mondry, June 1979, Bulletin No. 79-06-EES-04.
19.	"Processed Bin Weather Data for Use in the Design of Renewable Energy Based Heating and Air Conditioning for Forty Cities, by M.H. Somerville, W.G. Barney, and A.C. Lindem III, July 1979, Bulletin No. 79-07-EES-01, Volumes A, B, C, and D.
20.	"Statistical Analysis of United States Weather Data for Use in the Design of Solar and Hybrid Heating Systems," by G. Perkuhn, and M.H. Somerville, May 1979, Bulletin No. 79-06-EES-02.

TABLE 1.3 (continued)

LIST OF REPORTS RELATED TO ORNL SUBCONTRACT 7434

Report No.	Title
21.	"The Development of a Monitoring System for a Solar-Assisted Heating System," by J.R. Olson, December 1979, Bulletin No. 79-12-EES-02.
22.	"Energy Flow Through an Annual Cycle Energy System," by P. Wacker, December 1979, Bulletin No. 79-12-EES-03.
23.	"Development of a Thermal Storage System Coupled to the Earth Utilizing Phase Change Materials," by J. Fristad, April 1980, Bulletin No. 80-04-EES-01.
24.	"The Design and Development of Multi-Source Heat Pump Using an Air-Ice Evaporator or an Air-Earth Evaporator," by M.H. Somerville, April 1980, Bulletin No. 80-04-EES-02.
25.	"Analytical Solution for the Determination of the Instantaneous Thermal Storage of an Earth Thermal Storage Facility" by N.R. Cox, April 1980, Bulletin No. 80-04-EES-03.
26.	"The Development of an Air-Icemaker Multiple Source Heat Pump System," by M.H. Somerville, S.G. Penoncello, June 1980, Bulletin No. 80-05-EES-01.
27.	"A Summary of the 1979-80 Monitoring Effort on the Jim Stover Residence," by D. Anderson and M.H. Somerville, May 1980, Bulletin No. 80-05-EES-05.
28.	"Operation of and Technical Description of a Dual Evaporator Heat Pump Control System," by D.E. Nelle, and M.H. Somerville, June 1980, Bulletin No. 80-07-EES-02.
29.	"Technical Description of the Computer Programs to Process the Fluke/Kennedy Data Tapes," by J. Viestenz, and M.H. Somerville, June 1980, Bulletin No. 80-07-EES-03.
30.	"A Technical Description of the In-Bin ACES Heat Exchanger and Associated Solar Equipment Located in Larimore, North Dakota," by M.H. Somerville, N. Cox, and J. Fristad, June 1980, Bulletin No. 80-07-EES-04.
31.	"Technical Operation and Control of an Experimental ACES/SOLAR Heating System Located in Larimore, North Dakota," by M.H. Somerville, D.E. Nelle, July 1980, Bulletin No. 80-07-EES-06.
32.	"The Analytical Prediction and Experimental Verification of the Thermal Performance of a Multiple Source Heat Pump System," by S.G. Penoncello, and M.H. Somerville, August 1980, Bulletin No. 80-07-EES-05.

2.0 DEVELOPMENT OF A PARALLEL EVAPORATOR - MULTIPLE SOURCE HEAT PUMP

2.1 Introduction

A heat pump is a refrigeration machine which transfers heat from a low temperature source to a high temperature sink by absorbing work. The concept of the heat pump has been known for seventy years (Trellis, 1978); the implementation of it began in the 1930's. In the 1950's the promotion and sales of heat pumps increased dramatically, but their service records and performance data were poor because many of the units were underdesigned due to excessive price competition. Common problems were compressor failure and control malfunction, especially in northern climates where the heat pumps were used mainly for heating, and cold frost was a major problem. By 1960 these problems and others were partially corrected by heat pump manufacturers.

The fixes that were employed, were, for the most part, ones that addressed only a particular problem. Many of the fixes utilized the use of electrical energy to solve the problem. Examples of this can be found in the hot-gas by-pass defrost, crank case heaters, accumulator design and four-way valve designs. Although most of the available heat pump systems operate satisfactorily, many of them have become unduly complex due to the number and variability of the fixes employed. What is needed is a fresh approach to the design of heat pumps that stresses simplicity, reliability, and energy efficiency at reasonable (not necessarily the lowest) cost.

The concept of a multiple source heat pump utilizing low temperature thermal storage has the potential to solve many of the "old maid" problems, including evaporator frost accumulation, charge migration, and inefficient

operation in the heating mode due to air-conditioning design constraints. The initial attempt to "design" and build a multiple source heat pump was based around a parallel evaporator design, and is described below. This design was chosen because we had experience in design and construction of heat pumps with both types of proposed evaporators, the air and the flat-plate ice-maker.

The characteristics of the heat pumps (air and the ice-maker) that we had built are shown in Figure 2.1. The design problem was to couple the two evaporators to one compressor and condenser, thereby minimizing the cost of the multiple source unit. The addition of the flat-plate evaporator to the unit can be accomplished for $50 to $100, and is strongly dependent upon the type of flat-plate evaporator used. A schematic of the system as built is shown in Figure 2.2. In this system one of the evaporators is selected by a controller to be the active evaporator; the other remains inactive. This controller can be as simple as an environmental thermostat or as complex as a small computer that has been programmed to provide maximum annual COP, based upon local weather conditions. The selection is accomplished by opening valves V1 and V3 to make the air side active, or V2 and V4 to make the ice side active.

2.2 Objective

It was the objective of this portion of the research to design, build, and test a multi-source heat pump with parallel evaporators.

2.3 Experimental Equipment

A graphical display of the components used is shown in Figure 2.3. A donated 2½ ton (condenser load) commerical heat pump was modified to a multi-source heat pump. Table 2.1 presents a summary of its performance. The modified heat pump was a Janitrol 38 heating only heat pump. The

ORNL-DWG 81-17888

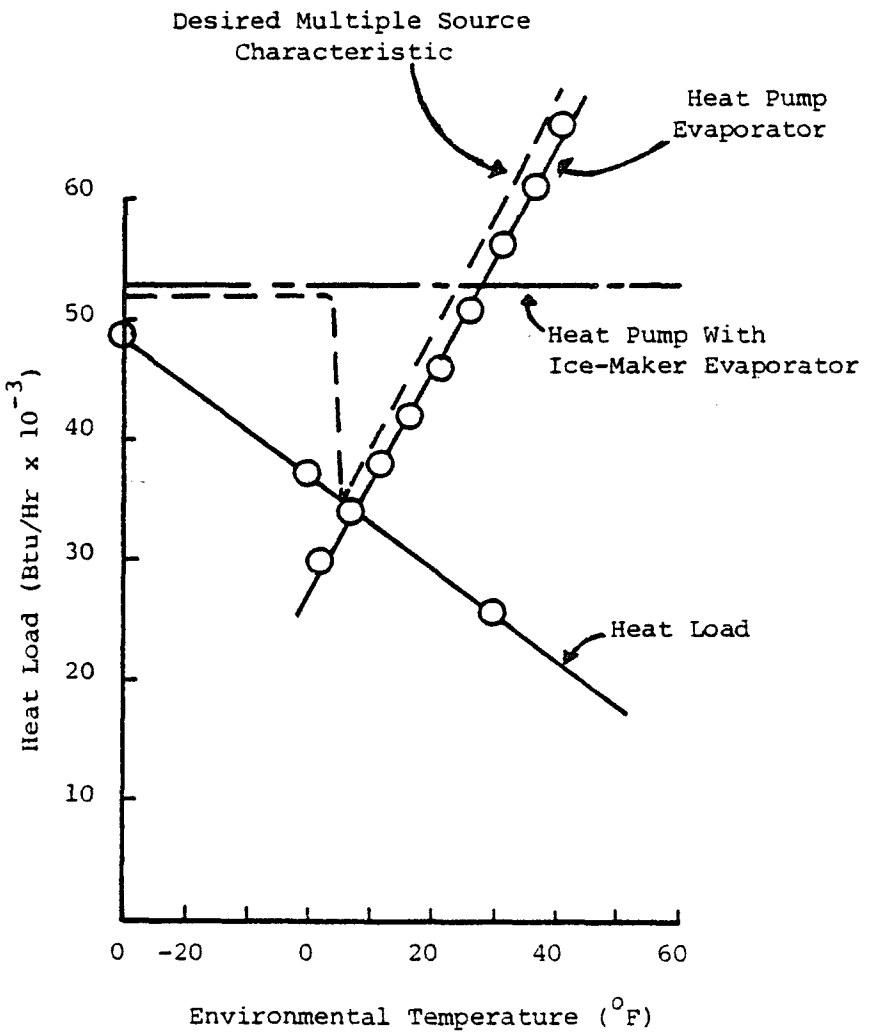

FIGURE 2.1 - MULTIPLE SOURCE CHARACTERISTIC AND INDIVIDUAL HEAT PUMP CHARACTERISTICS

ORNL-DWG 81-17889

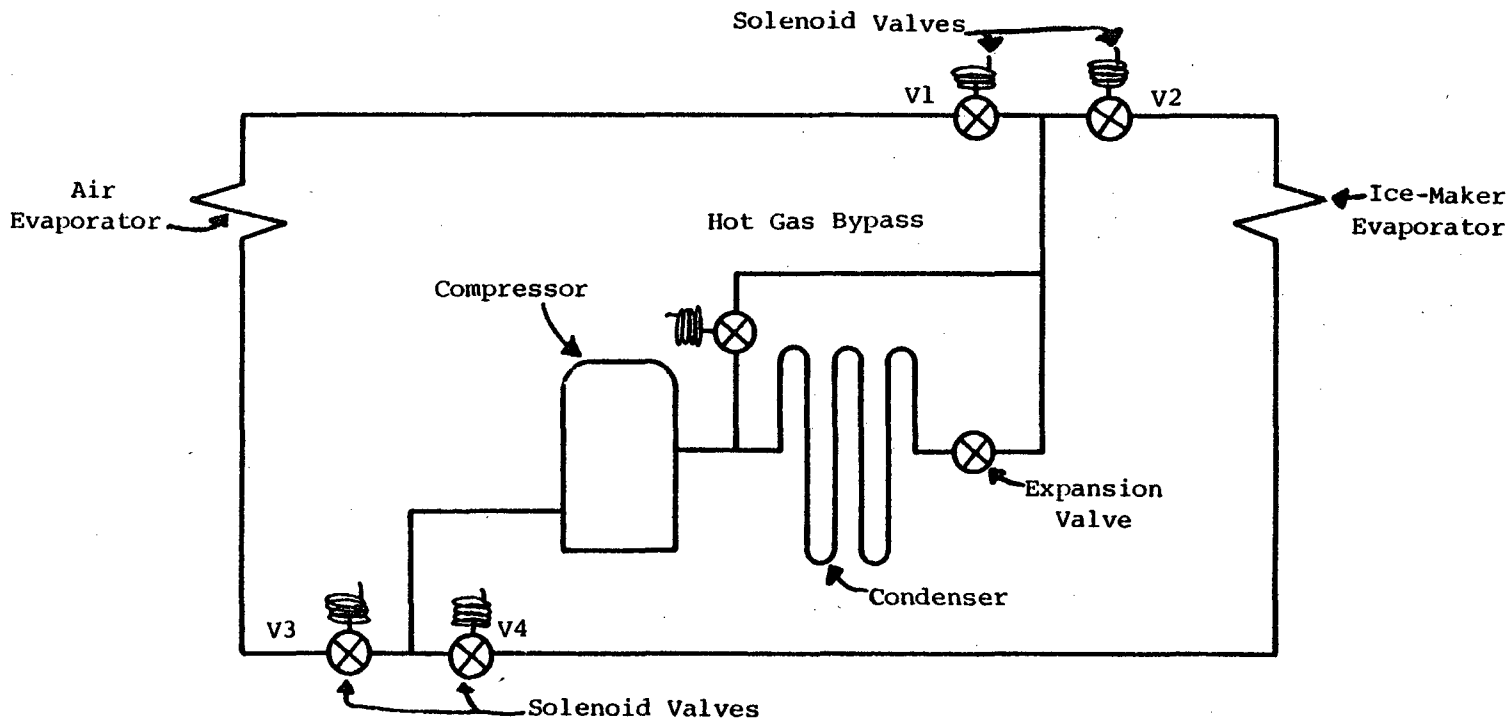

FIGURE 2.2 - SCHEMATIC OF A MULTIPLE SOURCE HEAT PUMP WITH A PARALLEL ALTERNATING EVAPORATOR ARRANGEMENT

ORNL-DWG 81-17890

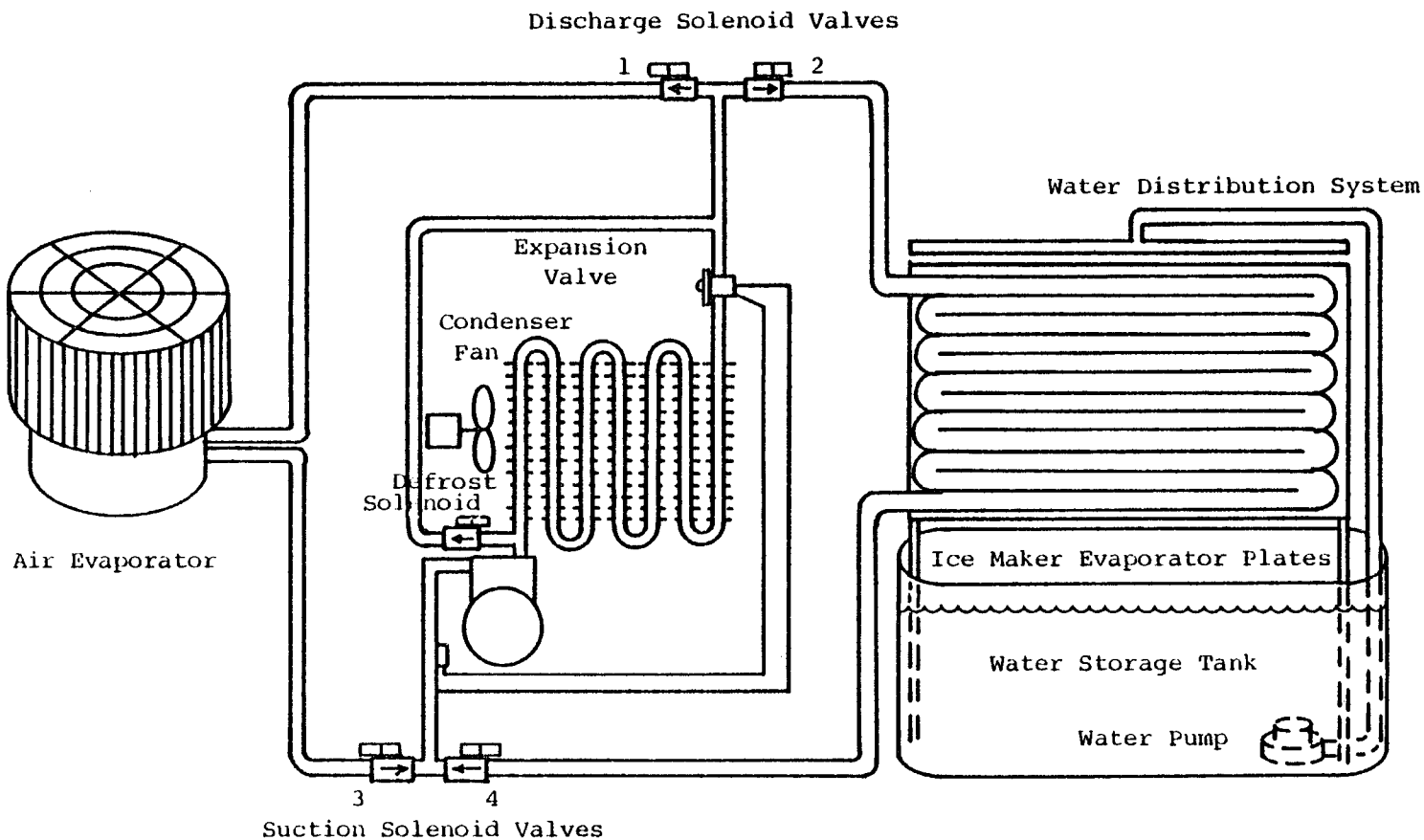

FIGURE 2.3 - THE EXPERIMENTAL MULTI-SOURCE HEAT PUMP WITH A PARALLEL EVAPORATOR ARRANGEMENT

TABLE 2.1

MANUFACTURER'S AIR TO AIR PERFORMANCE DATA OF JANITROL 38
HEATING ONLY HEAT PUMP AT 1200 CFM

Evaporator Temperature (°F, °C)	C.O.P.	Indoor Temperature Rise - °F	Operating Pressures			Discharge Gas Temperature °F
			Suction PSIG	Discharge (Head) PSIG	Compression Ratio	
62 (16.7)	3.4	34.0	71	226	2.81	194
57 (13.9)	3.3	32.4	65	219	2.93	191
52 (11.1)	3.2	30.1	59	212	3.08	188
47 (8.3)	3.2	28.2	53	205	3.25	186
42 (5.5)	3.1	26.2	49.0	198	3.34	182
37 (2.8)	2.9	24.3	45.0	192	3.46	178
32 (0)	2.8	22.4	41.0	185	3.59	174
27 (-2.8)	2.6	20.4	37.0	179	3.75	179

TABLE 2.1 (Continued)

MANUFACTURER'S AIR TO AIR PERFORMANCE DATA OF JANITROL 38
HEATING ONLY HEAT PUMP AT 1200 CFM

Evaporator Temperature (°F, °C)	C.O.P.	Indoor Temperature Rise - °F	Operating Pressures			Discharge Gas Temperature °F
			Suction PSIG	Discharge (Head) PSIG	Compression Ratio	
22 (- 5.5)	2.5	18.5	33.0	172	3.91	166
17 (- 8.3)	2.3	16.6	29.0	166	4.14	162
12 (-11.1)	2.1	15.0	26.0	161	4.32	158
7 (-13.9)	1.9	13.5	23.5	157	4.49	155
2 (-16.7)	1.7	12.0	21.0	153	4.70	152
-3 (-19.4)	1.6	10.8	18.5	149.0	4.93	150
-8 (-22.2)	1.5	9.6	15.5	146	5.32	147
-12 (-24.4)	1.4	8.9	13.0	144	5.73	143

operating characteristics of this pump are also given in Table 2.1. The pump was modified by the addition of four, two ton, solenoid valves (1 through 4 in Figure 2.3) and two flat-plate ice-makers. The stainless steel flat-plate ice-makers used for this project were manufactureed by Turbo Refrigeration, in Denton, Texas. The total wetted surface area of the two plates was 32 Ft^2 (2.97 m^2). Both sides of both plates were used to manufacture ice. Water was distributed along the top of each plate by a ½ in. (1.3 cm) copper tube with 0.14 in. (0.36 cm) holes drilled along the axis at 0.50 in. (1.3 cm) intervals. The larger holes are located at the center of the distribution manifold, where the supply of water is fed (See Figure 2.4). An inexpensive (and inefficient) ½ horsepower sump pump was used to provide water to the plates. The pump was capable of providing 25 GPM (95 lpm) at 20 ft (6.1 m). A flow of 2.0 $\frac{GPM}{ft}$ (24.8 $\frac{Liters}{Min\text{-}m}$) was used for the tests. Although not quantified at the time of this work, we had observed that the rate of ice formation was relatively insensitive to the water flow rate at values above this number, but that it was also strongly dependent upon the air temperature surrounding the plates. Consequently, the entire ice making system was placed in an insulated enclosure and the water storage tank was insulated. All tests were performed at an ice-maker chamber air temperature of 43°F (6°C).

2.4 Test Procedure

The following test procedure was developed to provide proof of principle test data. It was not intended to provide conclusive operational test data because this was the first multi-source heat pump, within our knowledge, that had been built. Further, the testing facilities that were available to us were marginal at best. This forced us to design a test procedure that would maximize the effectiveness of the support facilities,

ORNL-DWG 81-17891

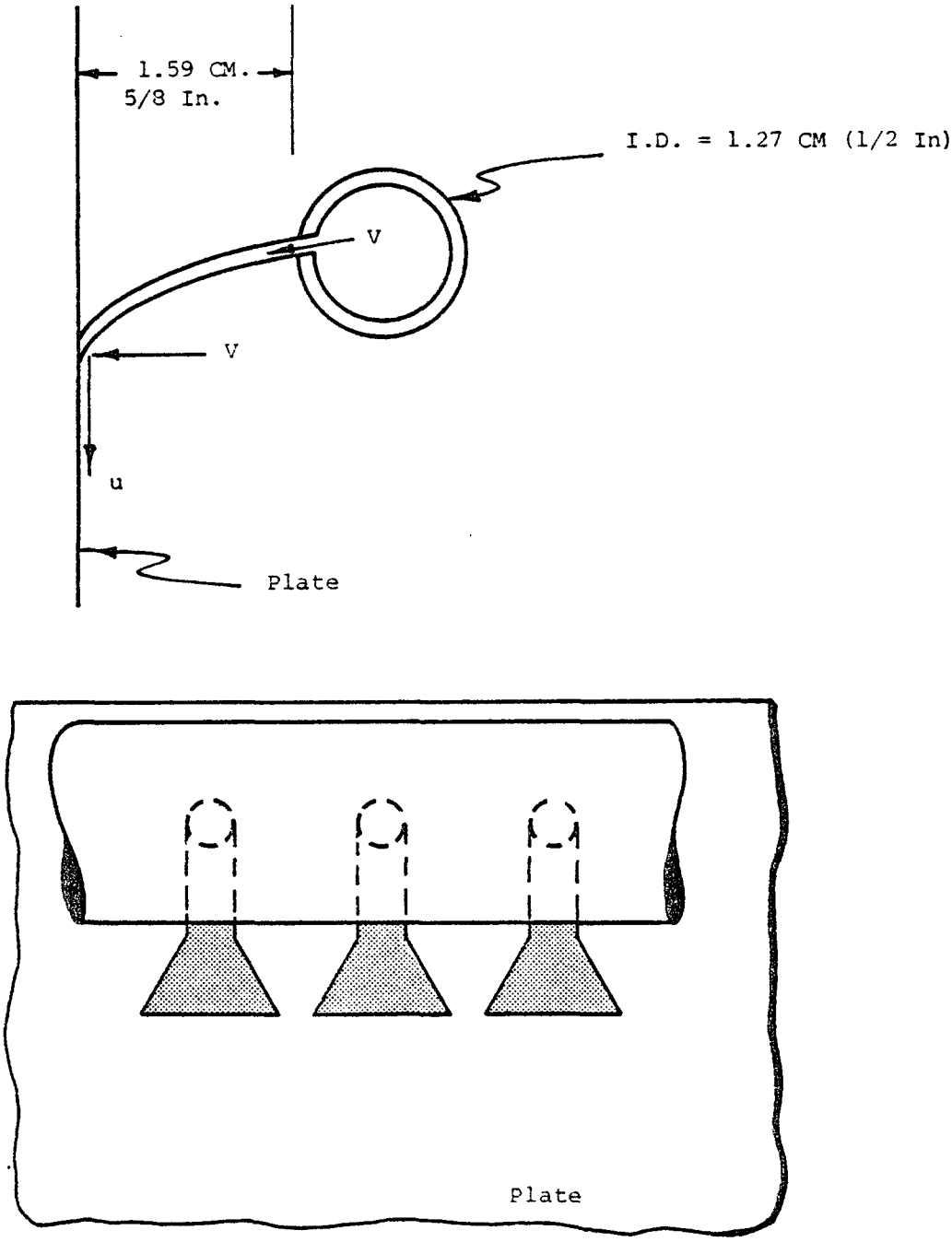

FIGURE 2.4 - MAKE-UP OF WATER DISTRIBUTION SYSTEM USED IN LABORATORY TESTS

as well as test the design. In this case, the unit being tested had to act as the environmental control unit, as well as the unit being tested. The detailed procedure outlined below was utilized in its entirety three times to provide the data that are presented below.

2.4.1 Detailed Procedure

Valve Status[1] 1	2	3	4		
c	c	c	c	1.	The entire system is allowed to reach room temperature, including both the ice and air side environmental chambers.
c	o	o	c	2.	The compressor is started. Valves 2 and 3 are opened until the suction pressure starts to drop rapidly in the air evaporator. This pumps down the air evaporator and ensures that the charge is on the ice side. This requires approximately 30 seconds. Following this, Valve 3 is closed and Valve 4 is opened.
c	o	c	o		
				3.	The unit is run continuously, decreasing the water temperature from room temperature to 32 to 33°F (0 to 1°C). This typically requires three to four hours. The unit is then run through four cycles of ice manufacture for another two hours. This process lowers the air temperature in the ice chamber to 43°F (6°C) which remains relatively constant due to its large thermal inertia.
o	c	c	o	4.	Valve 2 is closed and Valve 1 opened. This pumps down the ice side evaporator and requires approximately 30 seconds to complete. Pump down is continued until the suction pressure starts to drop rapidly.
o	c	o	c	5.	Valve 4 is closed and Valve 3 is opened. This allows the air evaporator to become active and starts to cool off the sealed air evaporator environmental chamber. Temperature equilibrium is reached in approximately two hours at 28°F.
				6.	The air side test is initiated at 28°F and runs for approximately forty minutes.
c	o	o	c	7.	Following completion of the air test, Valve 1 is closed and Valve 2 is opened, this pumps down the

1. Refer to Figure 2.3, c = closed, o = open

c o c o		air evaporator. Following pump down (~ 30 seconds), Valve 3 is closed and Valve 4 opened.
	8.	The ice-maker performance is measured for 30 minutes (approximately ½" (1.25 cm) of ice) while the raw data are collected (See Table 2.2)
defrost solenoid opened	9.	The defrost solenoid is opened for three minutes and accomplishes defrost of the plates.
defrost solenoid closed	10.	The defrost solenoid is closed and the second cycle of ice-making in initiated. Steps 9 and 10 are repeated as often as desired.
c c c c	11.	The equipment is shut down.

2.5 Analysis of Results

2.5.1 Air Side Tests

This test operated in a mode where the active evaporator was at a lower temperature than the inactive evaporator. The results of the test are shown in Figure 2.5 and show that the output of the unit continually decreased. This phenomena was repeated in three separate tests which were run on three different days. Since the system was allowed to regain equilbrium with the environment (nominally room temperature), in between each of the three tests, one reaches the conclusions that the results are being controlled by a physical phenomena as opposed to a test error. In all three tests, an accumulation of frost on the air side evaporator was observed. Thus, the performance of the parallel system is identical to that of a conventional system with a frosted coil. Unfortunately, a hot gas defrost was not performed. If it had been, it is very likely that significantly reduced performance would have been observed following the defrost. The reasons for this are below in more detail.

TABLE 2.2

RAW DATA FOR THE DUAL, PARALLEL ALTERNATING, EVAPORATOR HEAT PUMP IN THE ICE MODE[1]

Time Min.	Evap.	T_0 °F	T_1 °F	T_2 °F	T_3 °F	T_4 °F	T_5 °F	T_6 °F	T_7 °F	T_8 °F	T_9 °F	T_{10} °F	P_S psig	P_D psig	Power Heat/Water Pump Watts	Current H.P. Amps	Solenoids Open
0	air	--	--	26	141	137	169	71	90	32	42	28	39.5	183	2820/ ---	15.85	1,3
5	ice	26	24	35	138	135	162	70	95	32	42	28	43.0	186	2900/ 326	15.95	2,4
15	ice	24	23	33	139	137	160	70	95	32	42	28	42.0	184	2910/ 326	16.00	2,4
25	ice	25	22	35	138	136	161	71	94	32	42	28	40.0	180	2860/ 329	15.90	2,4
30		Ice Harvest															
35	ice	28	25	40	141	139	168	70	85	32	42	28	41.5	177	2920/ 328	16.00	2,4
45	ice	29	25	39	145	141	171	71	87	32	42	28	45.0	173	2880/ 328	15.90	2,4
55	ice	28	23	41	144	142	173	71	85	32	42	28	44.0	170	2820/ 230	15.85	2,4
65	ice	28	24	37	142	140	172	71	85	32	42	28	46.0	168	2800/ 229	15.80	2,4
End Trial 1 - Start Trial 2																	
0	air	--	--	25	143	138	170	70	89	32	42	28	38.5	185	2900/ ---	15.95	1,3
5	ice	29	25	38	142	139	169	71	97	32	42	28	44.5	192	2940/ 228	16.10	2,4
15	ice	28	26	38	143	140	170	70	96	32	42	28	43.0	190	2880/ 228	15.90	2,4

1. List of symbols are at the end of the table.

TABLE 2.2 (Continued)

RAW DATA FOR THE DUAL, PARALLEL ALTERNATING, EVAPORATOR HEAT PUMP IN THE ICE MODE

Time Min.	Evap.	T_0 °F	T_1 °F	T_2 °F	T_3 °F	T_4 °F	T_5 °F	T_6 °F	T_7 °F	T_8 °F	T_9 °F	T_{10} °F	P_S psig	P_D psig	Power Heat/Water Pump Watts	Current H.P. Amps	Solenoids Open
25	ice	27	25	37	140	138	168	70	95	32	42	28	40.5	185	2820/ 227	15.85	2,4
30		Ice Harvest															
35	ice	28	26	40	142	139	174	70	82	32	42	28	41.5	173	2840/ 228	15.90	2,4
45	ice	29	24	37	142	136	172	71	85	32	42	28	40.0	170	2840/ 229	15.90	2,4
55	ice	29	26	39	141	138	172	70	82	32	42	28	41.0	169	2820/ 230	15.85	2,4
65	ice	29	25	37	140	135	170	70	81	32	42	28	39.5	168	2800/ 230	15.80	2,4
- End Trial 2 - Start Trial 3 -																	
0	air	--	--	25	139	137	163	70	91	32	42	28	40.5	181	2920/ ---	16.00	3,1
5	ice	25	22	39	142	138	163	70	96	32	42	28	43.5	190	2880/ 300	15.95	2,4
15	ice	24	23	39	141	139	165	70	94	32	42	28	44.0	186	2860/ 300	15.95	2,4
25	ice	25	23	38	143	140	166	71	94	32	42	28	42.0	185	2820/ 228	15.90	2,4
30		Ice Harvest															
35	ice	27	25	39	144	142	170	70	84	32	42	28	40.5	179	2820/ 228	15.90	2,4
45	ice	28	26	40	144	144	173	70	85	32	42	28	41.0	175	2820/ 229	15.90	2,4

TABLE 2.2 (Continued)

RAW DATA FOR THE DUAL, PARALLEL ALTERNATING, EVAPORATOR HEAT PUMP IN THE ICE MODE

Time Min.	Evap.	T_0 °F	T_1 °F	T_2 °F	T_3 °F	T_4 °F	T_5 °F	T_6 °F	T_7 °F	T_8 °F	T_9 °F	T_{10} °F	P_S psig	P_D psig	Power Heat/Water Pump/Watts	Current H.P. Amps	Solenoids Open
55	ice	28	25	38	145	143	171	70	83	32	42	28	44.0	173	2800/ 300	15.85	2,4
65	ice	27	25	37	145	143	171	70	83	32	42	28	43.0	170	2780/ 300	15.85	2,4

- End Trial 3 -

Evaporator	Evap. Temp.	T_6 °F	T_7 °F	ΔT	Q	Power in Watts / Btu/hr	C.O.P.	Comp. Ratio
air	28	71	90	19	5220/17800	2820 / 9600	1.85	3.67
ice	32	70	95	25	5800/23400	3220 / 11000	2.13	3.50
ice	32	70	95	25	5800/23400	3240 / 11000	2.12	3.53
ice	32	71	94	23	5300/21500	3190 / 10900	1.974	3.58
	Ice Harvest							
ice	32	70	85	15	4100/14000	3250 / 11100	1.26	3.43
ice	32	71	87	16	4400/15000	3210 / 11000	1.37	3.16
ice	32	71	85	14	3800/13100	3150 / 10800	1.22	3.16

TABLE 2.2 (Continued)

RAW DATA FOR THE DUAL, PARALLEL ALTERNATING, EVAPORATOR HEAT PUMP IN THE ICE MODE

Evaporator	Evap. Temp.	T_6 °F	T_7 °F	ΔT	Q	Power in Watts / Btu/hr	C.O.P.	Comp. Ratio
ice	32	71	85	14	3800 / 13100	3050 / 10300	1.26	3.02
- - - - - - - - - - - - - - - - - - End Trial 1 - Start Trial 2 - - - - - - - - - - - - - - - - - -								
air	28	70	89	19	5210	2900	1.79	3.75
ice	32	71	97	26	7130	3240	2.20	3.49
ice	32	70	96	26	7130	3180	2.24	3.54
ice	32	70	95	25	6860	3120	2.19	3.62
	Ice Harvest							
ice	32	70	82	12	3290	3140	1.04	3.34
ice	32	71	85	14	3740	3140	1.22	3.37
ice	32	70	82	12	3290	3120	1.05	3.29
ice	32	70	81	11	3020	3100	.97	3.37
- - - - - - - - - - - - - - - - - - End Trial 2 - Start Trial 3 - - - - - - - - - - - - - - - - - -								
air	28	70	91	21	5760	2920	1.97	3.54
ice	32	70	96	25	6860	3180	2.16	3.52

TABLE 2.2 (Continued)

RAW DATA FOR THE DUAL, PARALLEL ALTERNATING, EVAPORATOR HEAT PUMP IN THE ICE MODE

Evaporator	Evap. Temp.	T_6 °F	T_7 °F	ΔT	Q	Power in Watts / Btu/hr	C.O.P.	Comp. Ratio
ice	32	70	94	24	6580	3160	2.08	3.42
ice	32	71	94	23	6310	3120	2.02	3.52
	Ice Harvest							
ice	32	70	84	14	3840	3120	1.23	3.51
ice	32	70	85	15	4110	3120	1.32	3.41
ice	32	70	83	13	3560	3100	1.15	3.14
ice	32	70	83	13	3560	3080	1.16	3.20
- End Trial 3 -								

Name of Tester: Larry Albrecht
Date: February 17, 1980

Barometric Pressure: 38.97

Notes: Charge increased to 50 lbs.

TABLE 2.2 (Continued)

DEFINITION OF SYMBOLS USED ON LABORATORY DATA SHEETS

T_0	Temperature of freon leaving ice-maker evaporator
T_1	Temperature of freon entering ice-maker evaporator
T_2	Suction temperature of freon entering heat pump
T_3	Temperature of freon entering condenser coil
T_4	Temperature of freon leaving oil separator
T_5	Discharge temperature of freon leaving compressor
T_6	Temperature of air entering heat pump
T_7	Temperature of air leaving heat pump
T_8	Water temperature in storage tank
T_9	Air temperature in water storage tank
T_{10}	Ambient air temperature
P_S	Heat pump suction pressure
P_D	Heat pump discharge pressure

Solenoid numbers correspond to Figure 7 of Senior Honors Thesis.

ORNL-DWG 81-17892

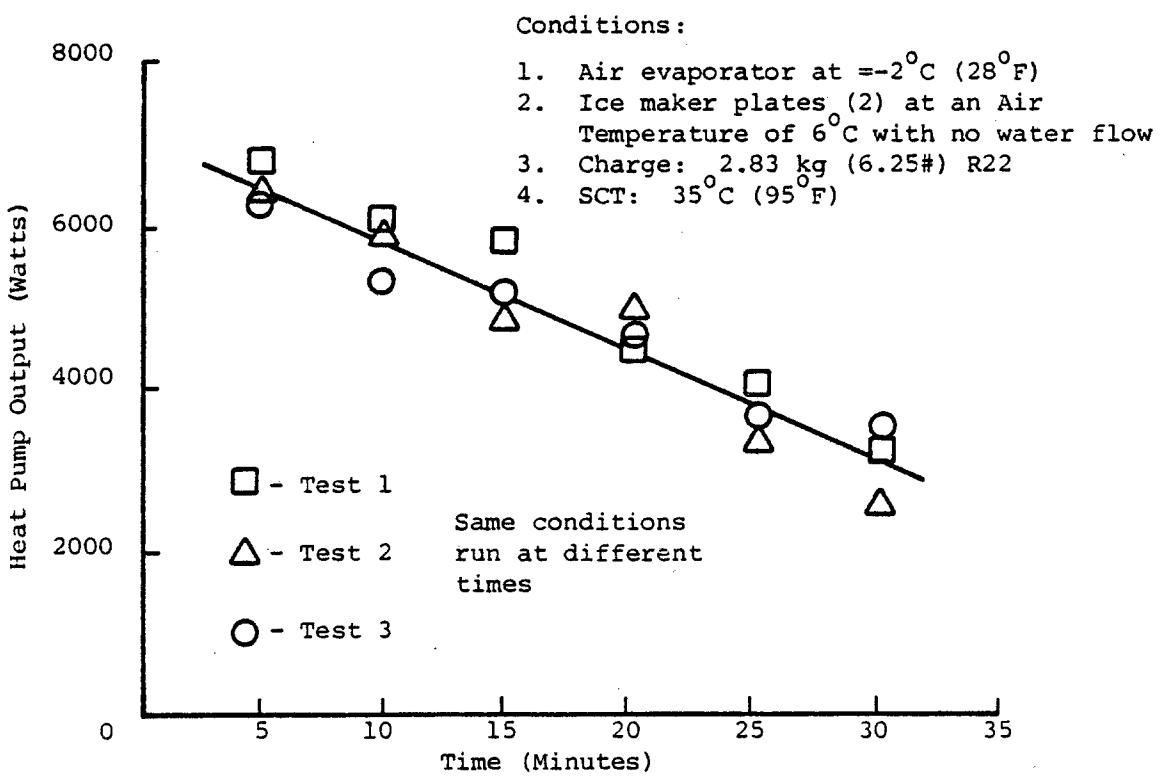

FIGURE 2.5 - PARALLEL DUAL EVAPORATOR HEAT PUMP TEMPORAL PERFORMANCE, OPERATING ON THE AIR SIDE EVAPORATOR

2.5.2 Ice Side Tests

The results of the ice side test are shown in Figure 2.6. During this test the air evaporator was at a temperature of 28°F (-2°C), while the saturated evaporating temperature was 23 to 24°F (-5°C). Some superheating of the freon takes place between the exit of the evaporator and the suction of the compressor (typically 5 to 10 F° (2 to 5 C°)). However, the ice-maker pressure is less than the pressure in the inactive air evaporator because the air evaporator environment temperature (28°F, -2°C) is greater than the saturated evaporating temperature on the ice-maker side (23 to 24°F). Consequently, the refrigerant does not leak past Valve 3 (Figure 2.3) into the air evaporator and the ice-maker performs reasonably well (See Figure 2.6) during the first thirty minutes of operation. However, at the end of the first thirty minutes, the defrost solenoid is opened and the ice-makers are defrosted. This operation forces high pressure (~ 100 psig), warm (50 to 70°F (10 to 21°C)) vapor/liquid mixture past the Valve 4 on the way to the compressor. Unfortunately, solenoid Valve 3 (which theoretically is closed) is forced open by this action, and a portion of the refrigerant charge is forced into the cold air evaporator where it immediately condenses. Following completion of the defrost, the defrost solenoid valve is closed, and the unit starts to make ice. However, we now observe a drastically reduced output due to the fact that the unit is undercharged. This can be seen in Figure 2.6 by comparing the pre and post defrost heat pump output values (6800 vs 4000 watts). The same performance would undoubtedly have been observed had the frosted air side coil been defrosted.

ORNL-DWG 81-17893

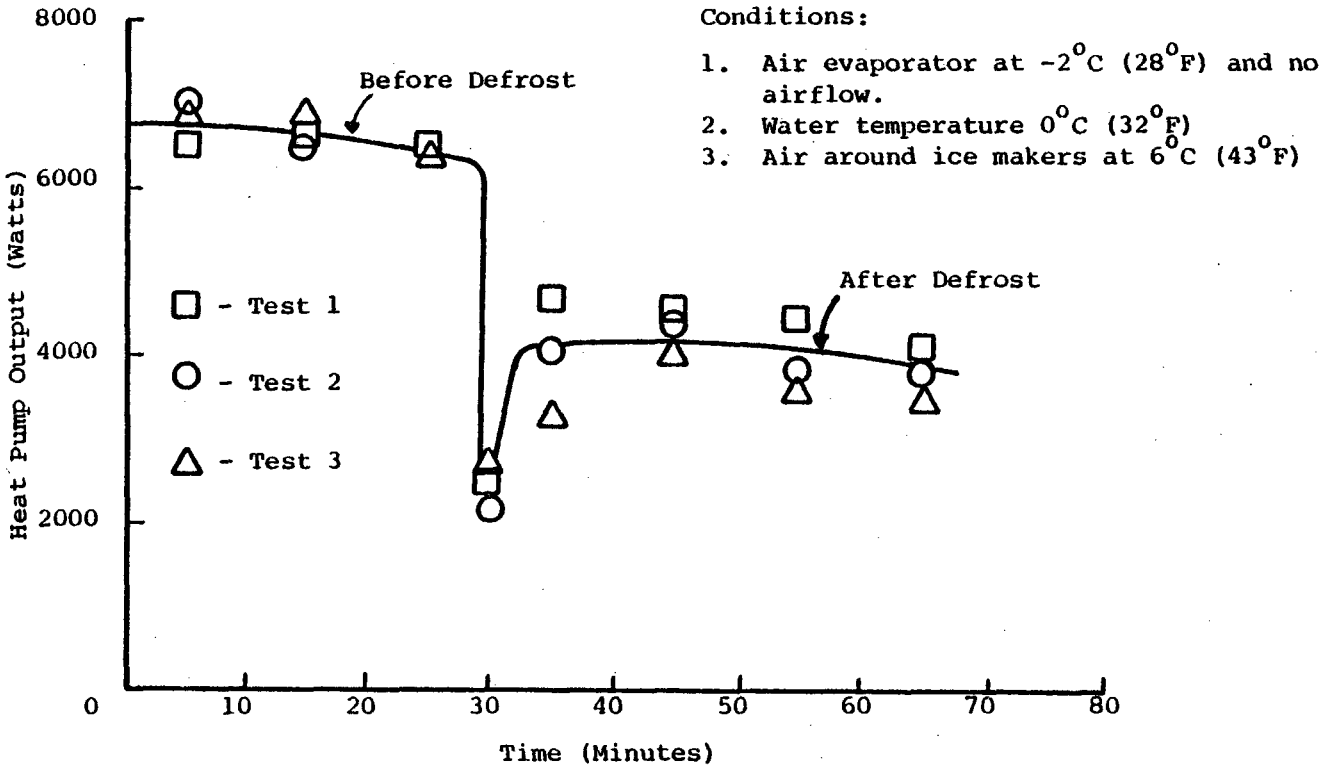

FIGURE 2.6 - PARALLEL DUAL EVAPORATOR HEAT PUMP TEMPORAL PERFORMANCE, OPERATING ON TWO ICE MAKER EVAPORATORS.

2.6 Conclusions

The objective of a multi-source heat pump is to take advantage of the highest temperature energy source available. This infers that the inactive evaporator(s) environment will be the colder one. Consequently, there will usually be a pressure difference across the suction side inactive solenoid valve that will tend to force the low pressure freon into the inactive evaporator. The greater the temperature difference between the evaporators, the greater the pressure difference and flow rate of freon to the inactive evaporator will be.

This is a serious problem because it attacks the basic philosophy of a multiple source heat pump. The solenoid valves that are available are all unidirectional, and many are pilot operated, thus, the simple solution of using better or different valves does not exist.

The major problems that this work revealed were:

* freon migration to the inactive evaporator had to be controlled;
* a parallel system with solenoid valves alone required a complex operating strategy (pump down before switch over);
* the defrost problem still existed and the traditional method had not been displaced;
* commercially available inexpensive solenoid valves cannot be relied upon to prevent freon migration, especially under negative pressure gradients with long or short term exposure.

These problems, together with the background provided by our sponsors, lead us to the design, building and testing of a multi-source heat pump with a series evaporator arrangement. This heat pump is described in the following chapter.

3.0 THE DUAL SERIES EVAPORATOR DESIGN AND DEVELOPMENT

3.1 Introduction

The refrigerant charge migration problem experienced with the dual parallel evaporator arrangement was the main reason for abandoning further development of a parallel evaporator configuration. If a configuration could be developed that provided no possible means for refrigerant "back-flow", the migration problem can be eliminated. By arranging the evaporators in a series configuration, only one flow path is provided for the refrigerant, and thus, the problem of migration is eliminated. This is the premise used in the design of the dual series evaporator configuration.

Subsequent sections will discuss in detail:

1. The series evaporator configuration;
2. The series evaporator heat pump system description;
3. The laboratory test facility;
4. Results and analyses of the dual series evaporator tests; and
5. Conclusions and recommendations concerning the dual series evaporator configuration.

3.2 The Dual Series Evaporator Configuration

Figure 3.1 shows a schematic of the dual series evaporator configuration. The dashed arrows in the figure show the path of the refrigerant during ice-making. In this case the air evaporator is used as a subcooler (i.e., an "extended" condenser) for the refrigerant. The solid arrows show the path of the refrigerant during air evaporating. In this case, the ice-makers serve as the subcooler. A pressure-enthalpy diagram of the dual series evaporator heat pump system is shown in Figure 3.2.

ORNL-DWG 81-17894

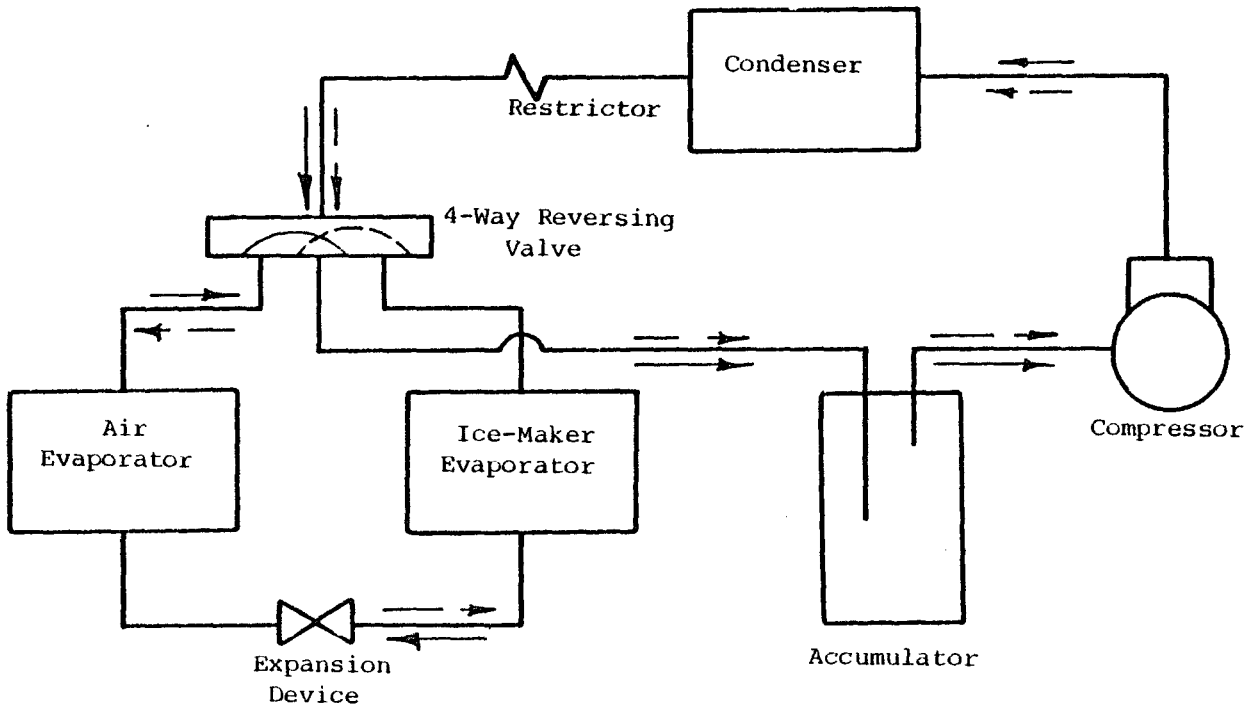

FIGURE 3.1 - SCHEMATIC OF SERIES AIR AND ICE-MAKER EVAPORATOR HEAT PUMP SYSTEM

ORNL–DWG 81–17895

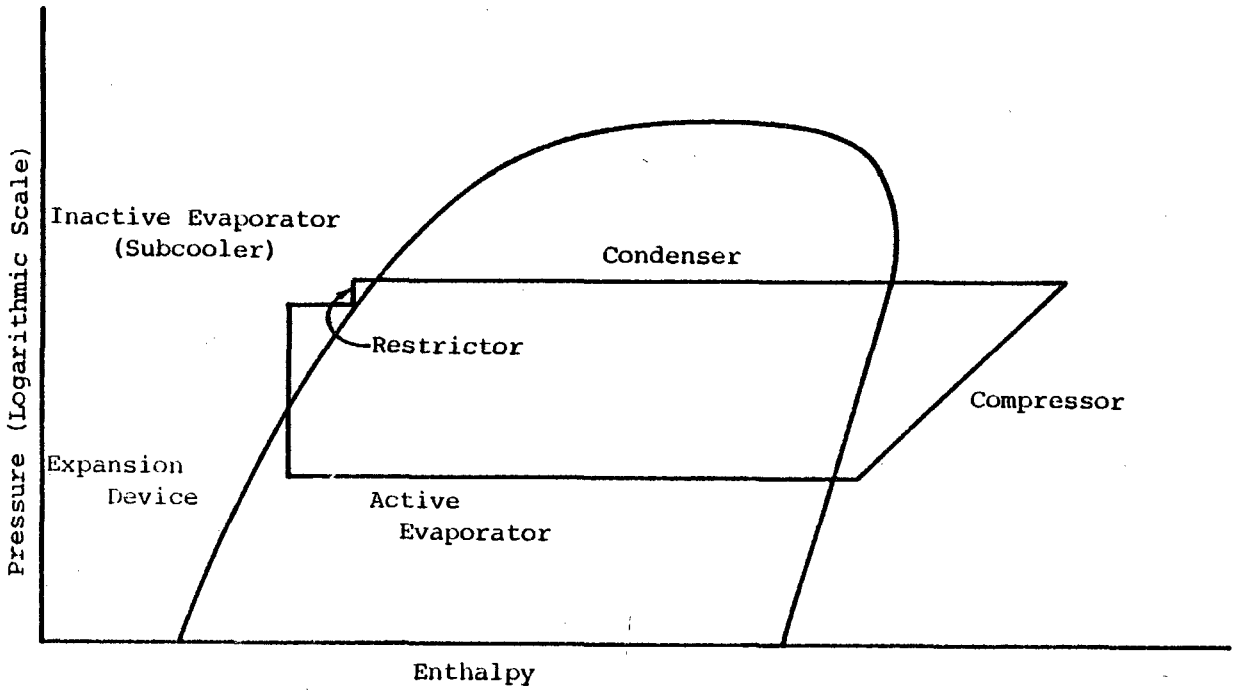

FIGURE 3.2 - DUAL SERIES EVAPORATOR HEAT PUMP CYCLE

The series evaporator configuration has the advantage that it can defrost the inactive evaporator (subcooler) by utilizing the energy rejected during the subcooling process for the defrost. This defrost scheme has the potential to raise the system heating coefficient of performance (COP_h). The reason for the higher COP_h is because the energy utilized for the hot gas bypass defrost (supplied by the compressor) is no longer needed in the series subcooling defrost.

Another advantage of the series configuration is that during the defrost cycle, the thermal load of the residence can be supplied (either partially or totally, depending on the source) by the evaporator which served as the system subcooler previous to the initiation of defrost.

This section has provided a general overview of the dual series evaporator configuration. The following section will discuss the actual dual series evaporator heat pump system tested in the laboratory.

3.3 Dual Series Evaporator Heat Pump System Description

In order to convert a unitary air-to-air heat pump to a dual series heat pump, several system modification were made. The air evaporator, condenser, compressor, and most of the electrical control wiring are suitable in their unitary configuration. The equipment added to the system will be discussed below (reference to Figure 3.1 would be helpful).

3.3.1 Thermal Electric Expansion Valve

The thermal electric expansion valve was installed primarily because of its bidirectional flow capability and its proven performance in previous laboratory tests. The bidirectional flow capability of this valve results in considerable simplification of the system design. The more common thermostatic expansion valves allow flow control in only one direction. Thus, each evaporator would need a separate expansion

valve. Check valves would need to be installed to assure the proper expansion valve is used with the active evaporator. Figure 3.3 compares the two expansion valve arrangements. A capillary tube could also have been used, but it was rejected because of the wide temperature range over which the air evaporator would be operating. The capillary tube would be properly sized over only a limited portion of this range.

3.3.2 Accumulator

The accumulator was installed to protect the compressor from filling with liquid freon during the evaporator switchover process. The line from the condenser to the subcooling evaporator, the subcooling evaporator itself, and the line from the subcooling evaporator to the expansion device are all filled primarily with liquid freon. In the case of subcooling in the air evaporator, the total volume can hold more than 20 pounds of liquid freon in a given system. During switchover, this charge flows from the high pressure subcooling evaporator to the low pressure suction of the compressor. The accumulator must be sized to prevent this liquid from entering the compressor.

3.3.3 Four-way Reversing Valve

The four-way reversing valve was installed immediately after the condenser discharge. This valve provides the selection of which evaporator will act as the subcooler. To initiate a defrost, the four-way valve is simply switched, thus, making the previously active evaporator (the one requiring defrost) the new subcooler. The subcooling energy is then rejected to the media of the subcooler, thus, causing a defrost.

ORNL-DWG 81-17896

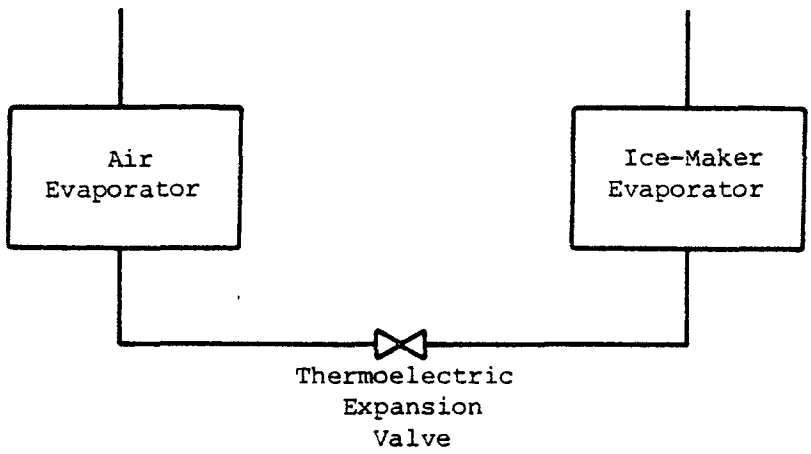

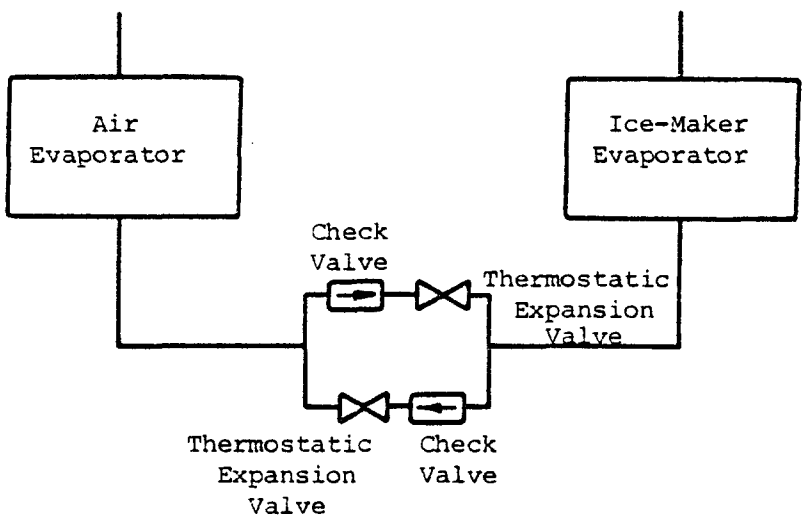

FIGURE 3.3 - COMPARISON OF BIDIRECTIONAL THERMAL ELECTRIC EXPANSION VALVE TO A THERMOSTATIC EXPANSION VALVE SET-UP

3.3.4 Restrictor

Previous laboratory tests indicate the need for the restrictor between the condenser and the four-way valve. Without the restrictor, the condenser performance is adversely affected, as condensation of the gaseous freon takes place in the inactive (subcooling) evaporator. The restrictor assures that only liquid freon exits from the condenser, thus, maintaining its performance. The restrictor size is affected by the rate of subcooling in the inactive evaporator. The effect of the restriction size on the subcooling rate has been determined by Mondry (1979) and will be presented in the results portion of this chapter.

3.4 Laboratory Test Facility

A drawing of the laboratory test facility is shown in Figure 3.4. Heat output data for the heat pump was obtained primarily on the basis of thermocouple temperatures. An Omega digital thermometer gave a direct temperature readout of these thermocouples. The temperature rise across the condenser, together with the condenser air flow rate was used to determine the heat output. The air flow rate was measured with a vane anemometer.

The (voltage)(current) product for the compressor established the electrical power input to the compressor. The electrical current to the compressor was monitored by an ammeter. The voltage across the compressor was measured before each test. The power requirements of the water pump, air evaporator fan, and condenser fan were measured prior to testing and assumed to be constant.

Control of the equipment used and the evaporator switching were facilitated by a single control panel. This allowed individual on-off control of the heat pump, the water pump, and the air evaporator fan. The

ORNL-DWG 81-17897

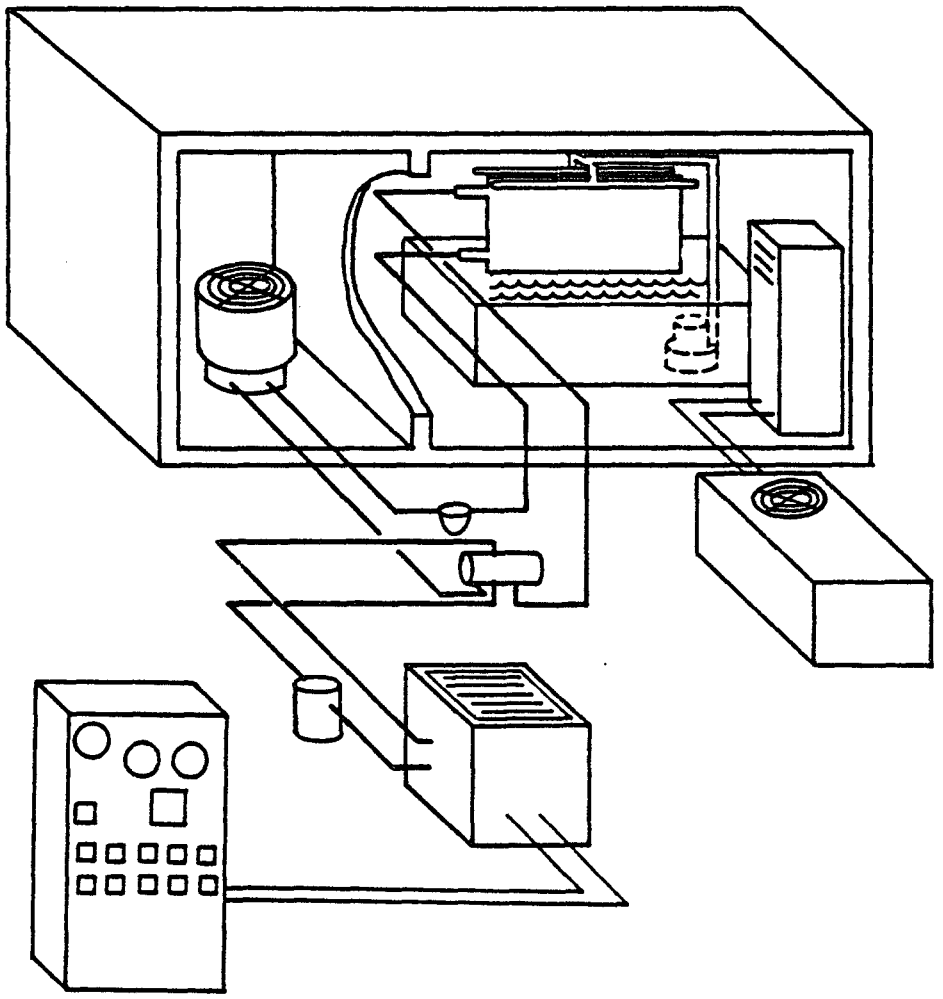

FIGURE 3.4 - TEST CONFIGURATION OF MAJOR LABORATORY EQUIPMENT

selection of which evaporator was being used was also controlled by a switch for the four-way valve, located on the control panel.

The enclosures surrounding the two evaporators were to control the environments under which they were operating. In order to properly evaluate the performance of the ice-maker evaporators it is necessary to operate them with a surrounding air temperature similar to what it would be over an actual water storage tank. This temperature may be as low as 32°F (0°C). Operating with surrounding air temperatures significantly above this may have significant effects on both the ice formation rate and the ice harvesting characteristics. The magnitude of these effects has been determined by Wendschlag (1979) (See Chapter 7.0).

The enclosure surrounding the air evaporator enables its performance to be evaluated over a wide range of temperatures. In an actual application, the heat pump may be required to operate at temperatures as low as -30°F (-34.4°C) when harvesting of the ice-maker evaporator is required. Therefore, the laboratory tests must be able to allow evaluation of the air evaporator performance at temperatures below 0°F (-17.8°C), and as close to -30°F (-34.4°C) as can be achieved.

3.5 Results and Analysis of the Dual Series Evaporator Tests

Two tests were conducted of the dual series evaporator heat pump system. The first test was conducted on a four-ton modified Tetco heat pump. This pump was to be installed in the Widseth home. The second test was conducted on a laboratory test pump. The test pump was a Janitral 2½ ton heat pump, modified to the series configuration.

3.5.1 Test One - Four-ton Modified Tetco Unit

The first thing determined during the laboratory tests was the amount of freon charge required. The Tetco heat pump, when used in a

conventional manner with the air evaporator, operates with about four pounds (1.816 kg) of freon. However, by adding the second evaporator (the ice-maker evaporator) and subcooling in one of the evaporators, the charge required for efficient operation increases significantly. This is due to the volumes of the subcooled evaporator and extra line required, both of which are nearly filled with liquid freon. The determination of correct charge was made by adding freon to the heat pump until the suction and discharge pressures achieved corresponded to those encountered when the heat pump is operated in the conventional manner. The system in the laboratory required 28 pounds (12.712 kg) of freon.

Once the correct amount of freon charge was determined, data was taken to evaluate the performance of the heat pump. Table 3.1 presents the test results for both evaporators in the active mode.

Besides heat pump output and efficiency, the major objective of the preliminary tests was to determine the time required to harvest the ice-maker evaporator, while operating on the air evaporator. Ice harvesting was performed both with the water running over the plates and without this water flow. The time to completely harvest the plates with the water running was consistently around 15 minutes. Without the water flow, harvesting was achieved in about 10 minutes. Thus, the best harvesting scheme also eliminates the need for running the water pump during the harvest.

The time difference between the two ice harvesting schemes can be attributed to the loss of subcooling energy to the flowing water, when the water pump is left on. Since the hot liquid freon from the condenser enters the defrosting ice-maker plates at the top of the

TABLE 3.1

HEAT PUMP PERFORMANCE

Mode Description	Condenser Air Flow (lbm/hr) (kg/hr)	Compressor Power Current (amps)	Voltage (volts)	Power (watts)	Condenser Output (Btu/hr) (watts)	Compressor only COP	System* COP
Evaporating in ice-maker evaporator, Subcooling in air evaporator	4830 (2193)	16.7	195	3260	37,100 (10,870)	3.3	2.4
Harvesting ice-maker plates, evaporating in air evaporator with average air temperature of 50°F	4830 (2193)	14.5	195	2930	29,000 (8,497)	3.0	2.3
Subcooling in ice-maker evaporator with no ice on plates, evaporating in air evaporator with air temperature of -1°F	4830 (2193)	11.5	195	2240	16,300 (4,776)	2.1	1.6

*Water Pump Power = 900 Watts, Air Evaporator Fan Power = 300 Watts, Condenser Fan Power = 450 Watts

plates, the ice melts free from the plates from the top down. When the water is running over the plates as the ice is being melted, it can get between the ice and the plate. The water, thus, cools the liquid freon from the top of the plate down to the point that the ice has not yet melted free. This leaves less energy in the freon to melt the remaining ice from the plate; and a longer harvesting time is required.

As shown in Table 3.1, the system COP while operating with the ice-maker evaporator is 2.3. When harvesting the ice-maker evaporators, the COP of the system will be a function of the ambient air conditions of the air evaporator. With the average temperature of the air evaporator enclosure at $50^{\circ}F$ ($10^{\circ}C$), the system COP was 2.3 when harvesting the plates. As the ambient conditions become more severe, it can be expected the COP will approach one at temperatures well below $0^{\circ}F$ ($-17.8^{\circ}C$). This is still significantly better than a harvest scheme, such as the hot gas bypass, for which no energy is rejected at the condenser (COP = 0) during ice harvesting.

3.5.2 Test Two - 2½ Ton Janitral Unit

The second set of tests was performed on the Janitral 2½ ton modified heat pump system. These tests were primarily concerned with the performance of the dual series configuration as a function of the restrictor size and subcooling environment temperatures. The results of these tests are shown in Figures 3.5 through 3.9. Tabulated data can be seen in the text of Mondry's report (Mondry, 1979).

Figure 3.5 is a plot of output vs. time, with no restriction between the condenser and subcooler. The output is high at high subcooling temperatures because the refrigerant is close to the subcooling

ORNL-DWG 81-17898

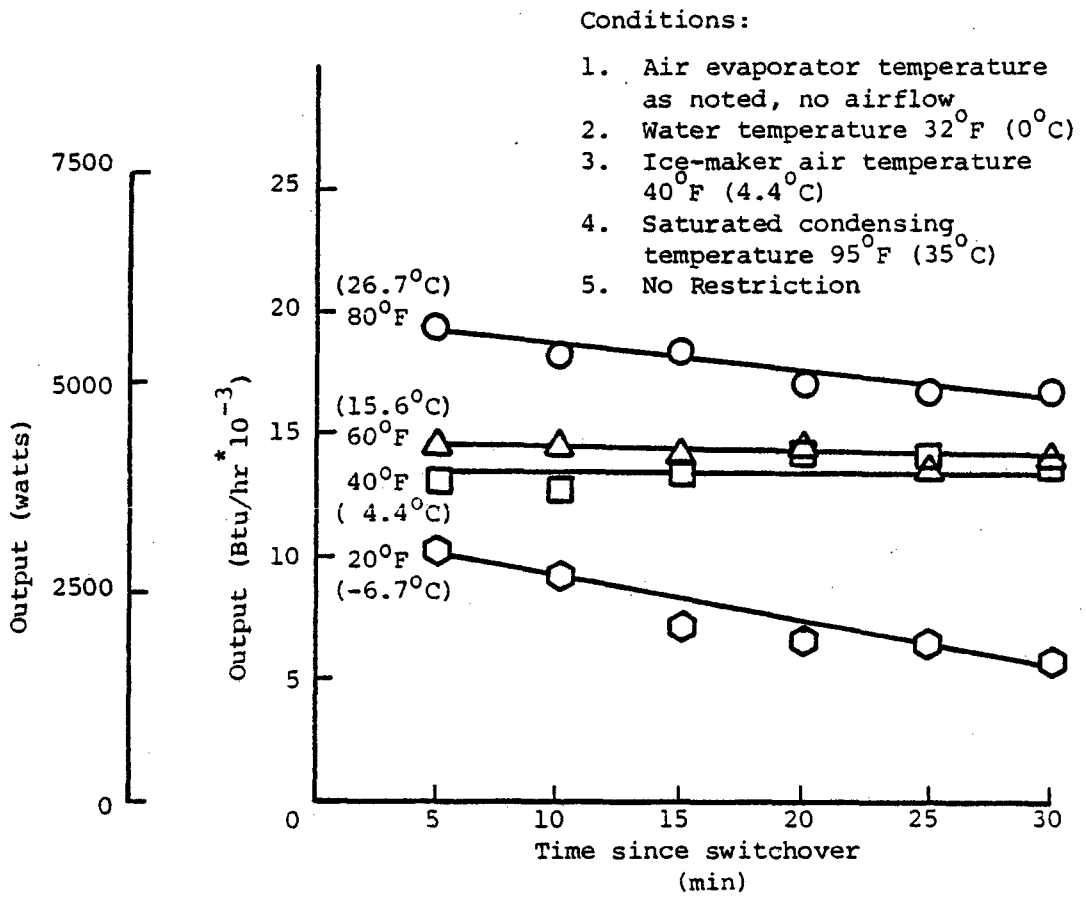

FIGURE 3.5 - OUTPUT OF DUAL-SERIES EVAPORATOR HEAT PUMP AT VARIOUS SUBCOOLING AIR TEMPERATURES. ACTIVE ICE-MAKER

ORNL-DWG 81-17899

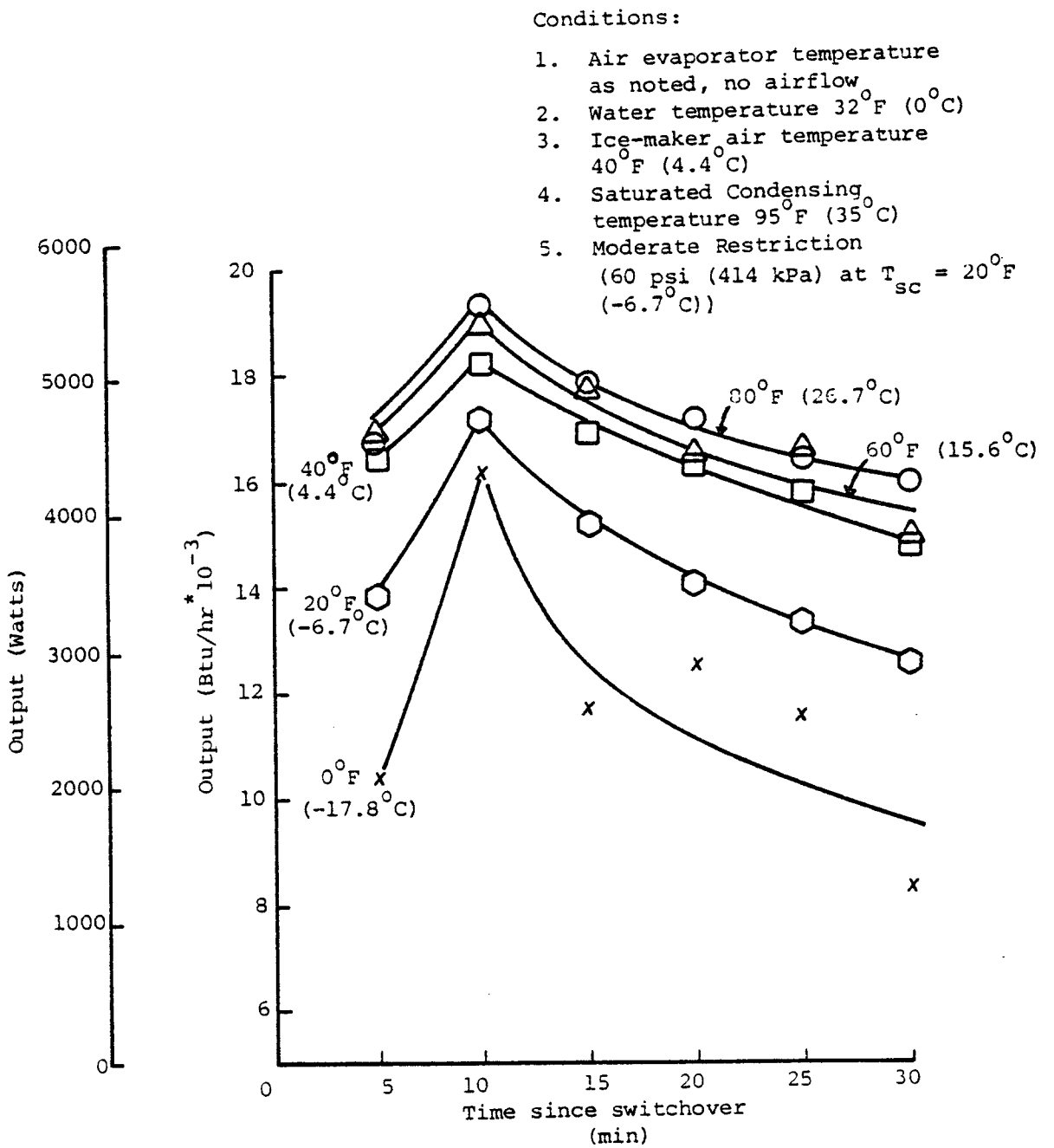

FIGURE 3.6 - OUTPUT OF DUAL-SERIES EVAPORATOR HEAT PUMP AT VARIOUS SUBCOOLING AIR TEMPERATURES. ACTIVE ICE-MAKER

ORNL-DWG 81-17900

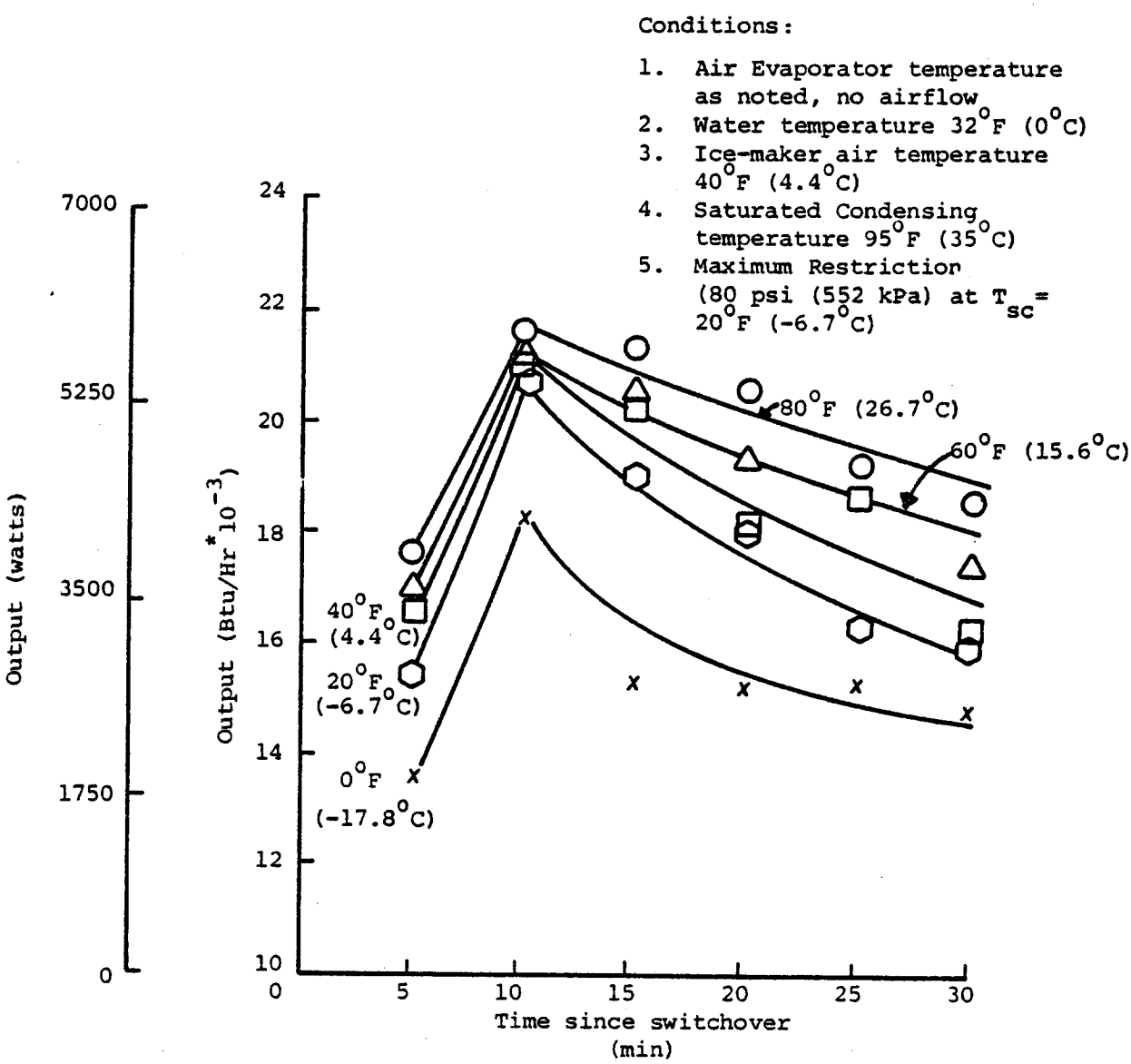

FIGURE 3.7 - OUTPUT OF DUAL-SERIES EVAPORATOR HEAT PUMP AT VARIOUS SUBCOOLING AIR TEMPERATURES. ACTIVE ICE-MAKER

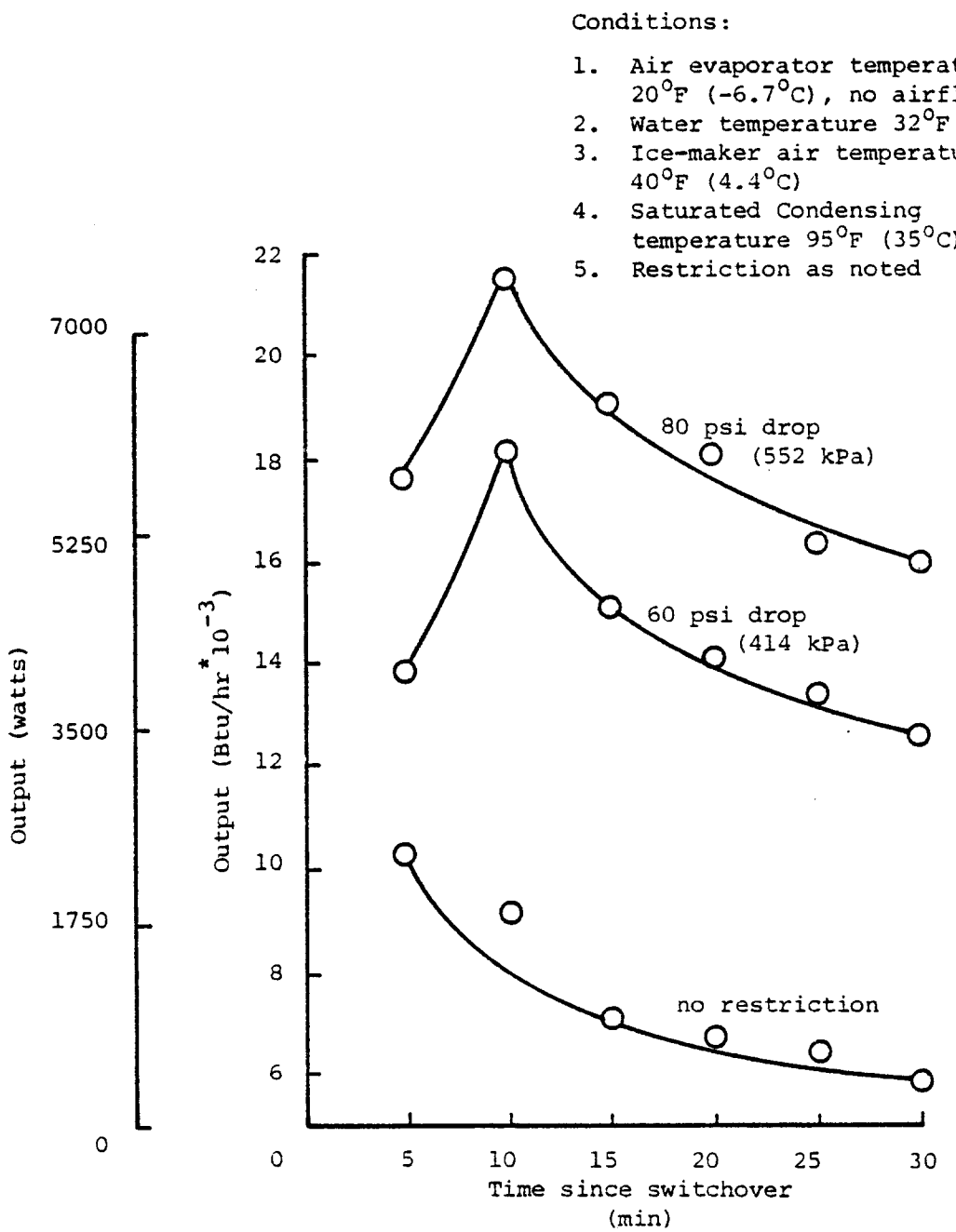

FIGURE 3.8 - EFFECT OF INCREASED RESTRICTION BETWEEN CONDENSER AND SUBCOOLER ON OUTPUT. ACTIVE ICE-MAKER

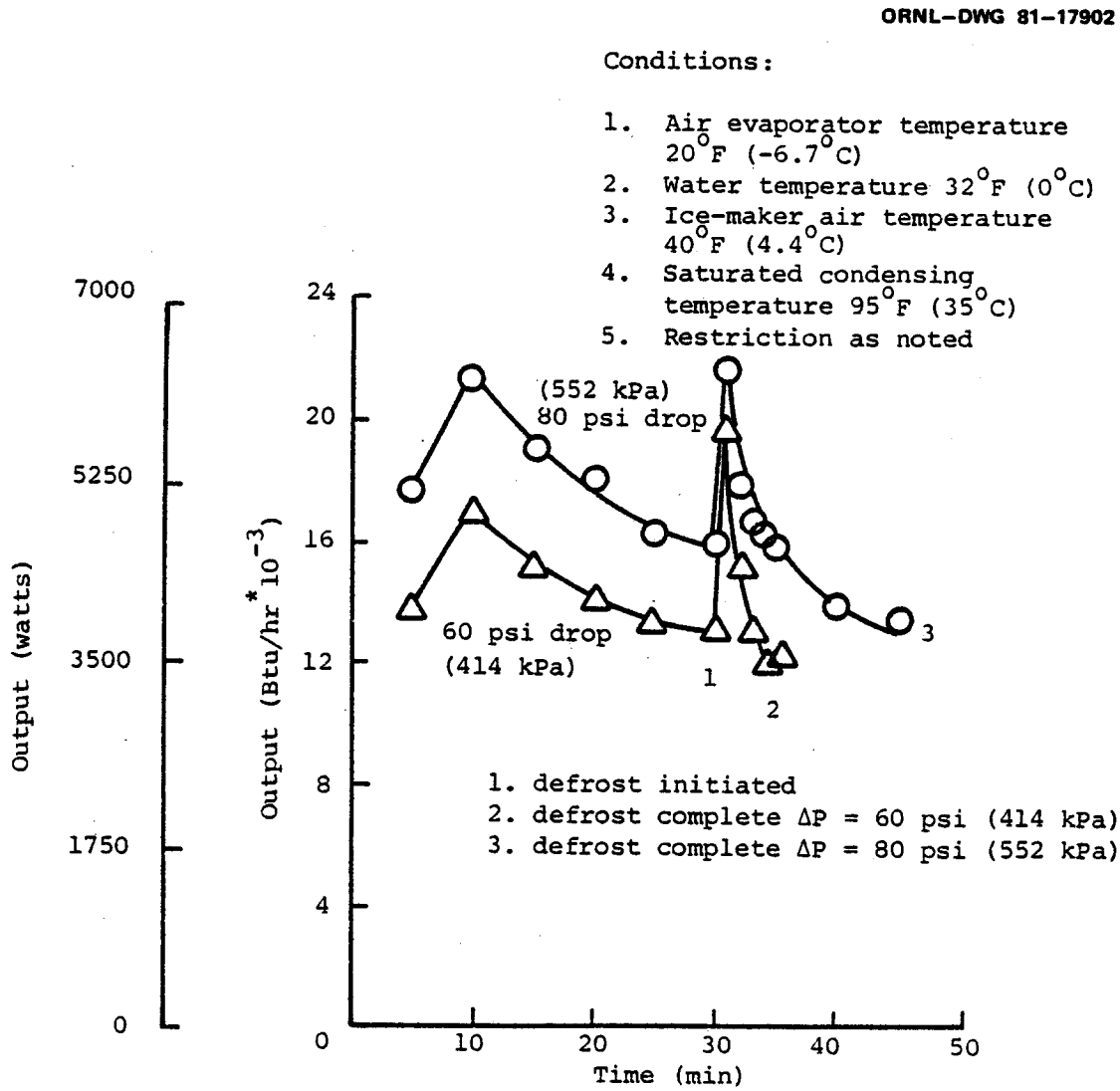

FIGURE 3.9 - DEFROST PERFORMANCE OF A DUAL-SERIES EVAPORATOR HEAT PUMP AT VARIOUS RESTRICTOR SETTINGS

air temperatures and very little subcooling occurs. However, as the subcooling temperature decreases, the output falls off drastically. It drops by 9000 Btu/hr (4392 W-^{o}C) with a decrease in subcooling temperature from 80°F (26.7^{o}C) to 20°F (-6.7^{o}C). At 20°F (-6.7^{o}C), after running on the ice-maker evaporator for 15 minutes, the system COP fell below one. At this point it became apparent that the refrigerant was not completely condensing in the condenser coil, but, rather, was moving to the cold subcooling coil and condensing, thereby, losing heat to the subcooling air. The tests with no restriction served to verify this characteristic, which had been anticipated at the outset of testing.

To alleviate this problem, a restriction was introducted between the condenser and the subcooler. This had the effect of restricting the flow of refrigerant out of the condenser until it was fully condensed. It also forced the condensing pressure up, with a corresponding increase in the saturated condensing temperature and heat output.

This increased restriction had a detrimental effect on defrost, however. As the pressure drop across the restrictor increased, so did defrost time. This happened because as the pressure drop increased, the refrigerant pressure in the subcooler dropped, with a corresponding drop in temperature. The subcooling effect was, thus, reduced, but it is precisely this subcooling that is relied on for the defrost of the evaporator plates.

The recovery time after defrost remained relatively constant at approximately 10 minutes. This loss in performance was due to the dumping of all the liquid refrigerant from the ice-maker plate into the accumulator, when switched back to active ice-maker from the active air mode. The system then had to boil off all of the liquid before

the output peaked. The subsequent gradual drop in performance was due to reduced heat transfer as ice was built up on the ice-maker plate.

Although the defrost time increased with the pressure drop across the restrictor, the system output was higher during defrost, also (Figure 3.9). The system COP during defrost, however, was typically only 1.2 as compared to about 2.0 during ice-making.

3.6 Conclusions and Recommendations

Both of the dual series heat pump systems tested exhibit identical characteristics. There are two main disadvantages seen in this series configuration: the large freon charge requirement, and the lengthy recovery period after system switchover.

Both of these disadvantages are caused due to the inherently large size of the subcooler. The subcooler (when used as the active evaporator) must be sized to accomodate the heat load of the house. This requirement places a minimum size on the volume of the evaporator, and hence the subcooler. Since this minimum size is rather large (to provide a COP_h in excess of 1.0), there is a large volume associated with the evaporator. Therefore, since the subcooler is flooded with liquid, a rather large freon charge must be incorporated into the system.

When the system experiences a switchover, the large freon charge in the subcooler is dumped into the accumulator. In order for the system to reestablish equilibrium (and thus maximize the COP), the liquid in the accumulator must be completely boiled off, soley by the suction pressure at the compressor inlet. This process takes a rather long period of time to complete and thus, the recovery time for the system is long.

Because of these disadvantages, further development of the dual series configuration was abandoned. It was decided to revert back to the parallel

design configuration. The problem of the freon migration was controlled thermally. The lessons learned from both parallel and series configuration lead to the design of the parallel evaporator multiple source heat pump system, with active subcooling. This is the topic of the next chapter.

4.0 DEVELOPMENT OF A MULTI-SOURCE HEAT PUMP WITH PARALLEL EVAPORATORS WITH ACTIVE SUBCOOLING

4.1 Introduction

The failures of both the original parallel alternating design and the series evaporator design provided important data that led to the third and most successful design. Some of the lessons learned included:

* It was obvious that freon migration problems would be difficult or perhaps impossible to control mechanically through the use of solenoid valves. This left only one alternative, the migration had to be controlled thermally.

* The use of subcooling energy for defrosting both the air and ice evaporators was an attractive alternative; it increased the system average COP markedly by eliminating the hot gas defrost.

* The series concept of using all of the evaporators (either as subcoolers or evaporators) all of the time seemed valid in spite of the problems encountered.

* The use of a large charge was to be avoided, if at all possible.

* The charging of an experimental heat pump system is, at best, an art. Theoretical calculation of displacement, with quality assumptions, gave some direction but were often in error by 50 percent or more.

* Restrictor size was crucial to the successful operation of a heat pump utilizing active subcooling. Little or no analytical information existed that could be used to size the restrictor; its size had to be determined experimentally.

It was on the basis of the above and other information that we designed the third prototype of a multi-source heat pump.

4.2 The Parallel Multiple Source Heat Pump with Active Subcooling

The multiple source heat pump (MSHP) system described here incorporates the concept of subcooling in all evaporators simultaneously. Figure 4.1 shows a schematic of a MSHP. The ideal and actual pressure-enthalpy (P-h) diagrams for this cycle are shown in Figure 4.2. The deviations from the

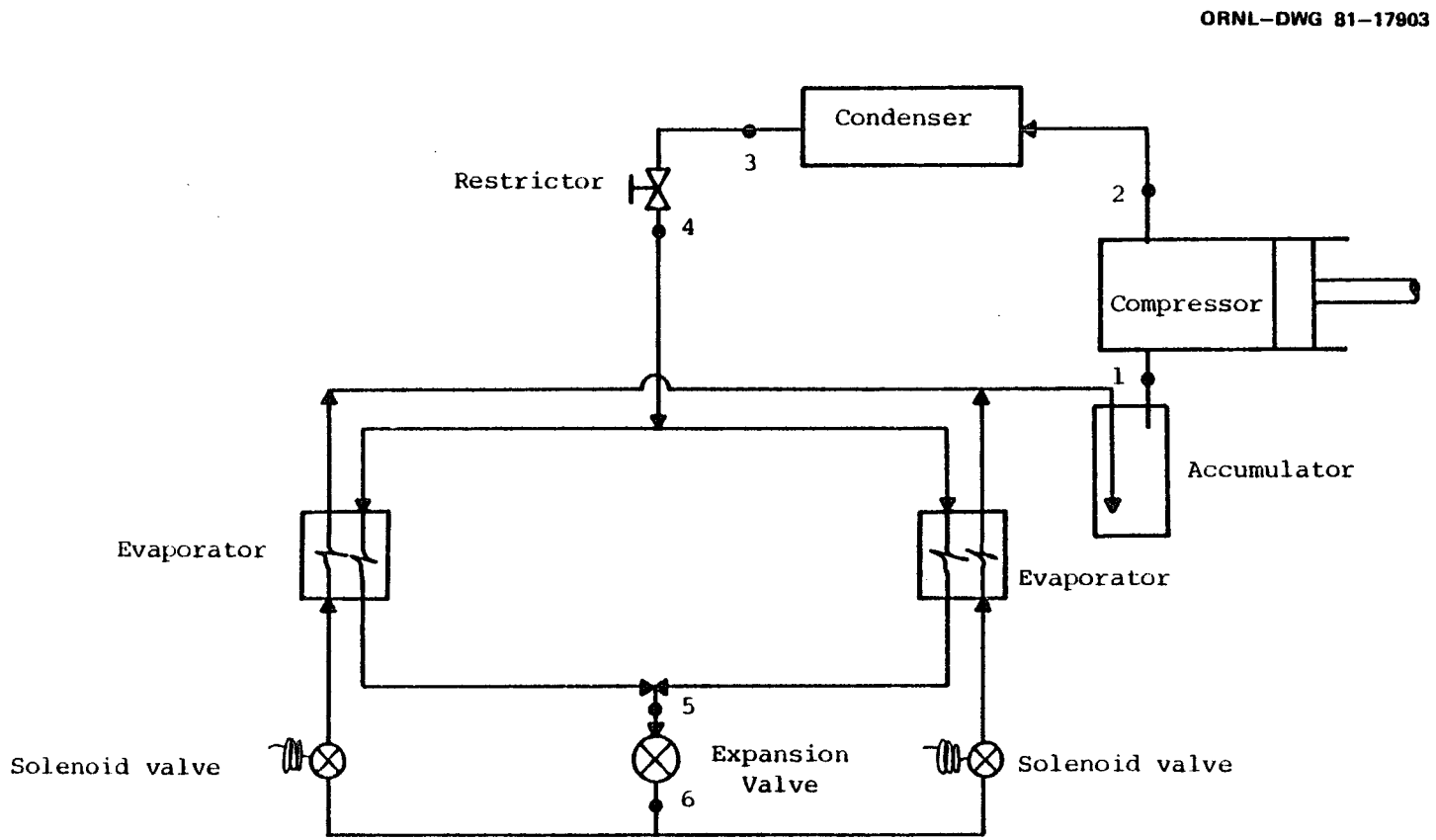

FIGURE 4.1 - MULTIPLE SOURCE HEAT PUMP SYSTEM

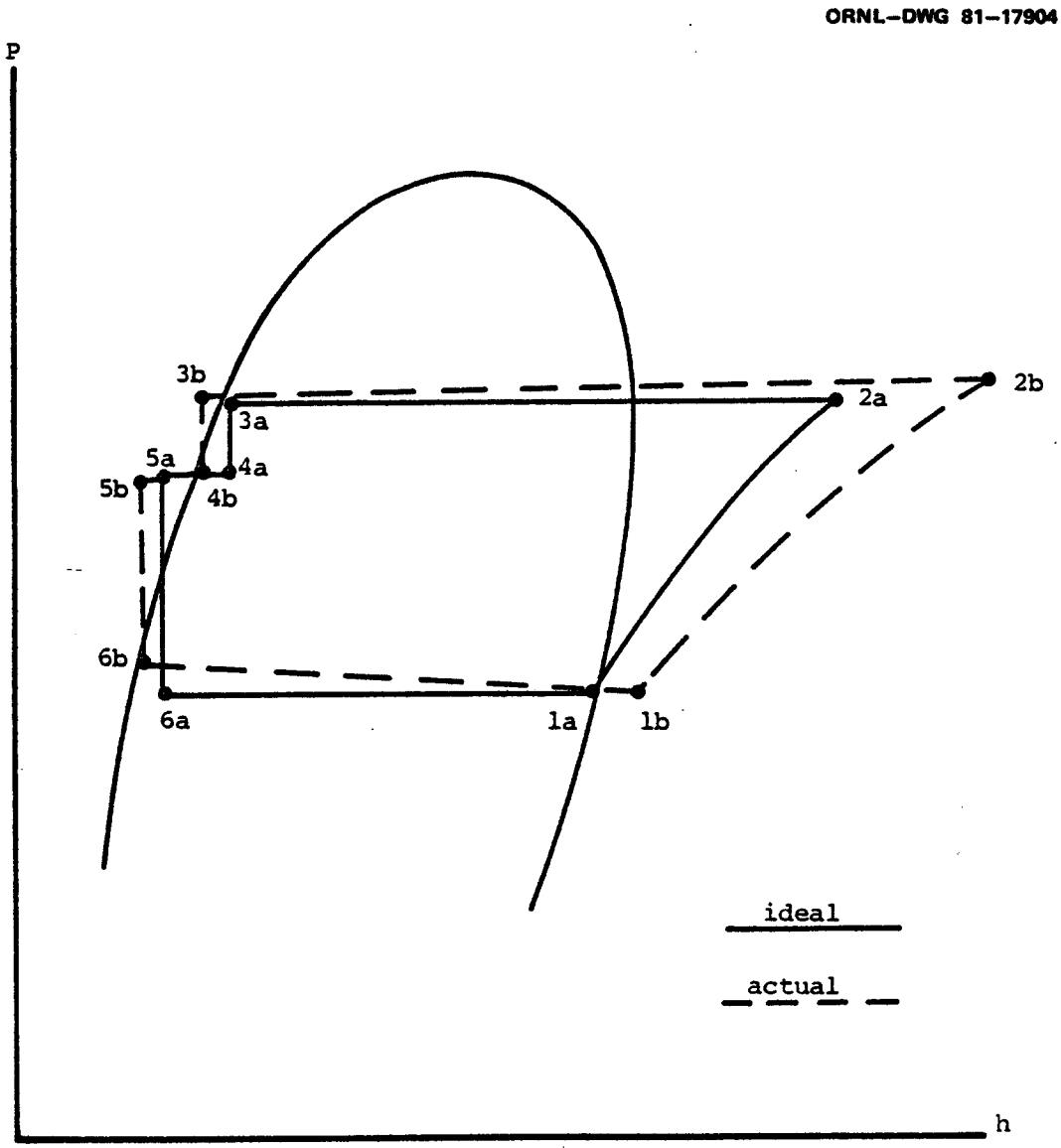

FIGURE 4.2 - IDEAL AND ACTUAL P-h DIAGRAMS OF AN MSHP SYSTEM

ideal cycle are due to pressure drops through system components and the non-isentropic compression process.

In the case of ice-maker evaporators, the multiple source configuration provides a unique method for defrost of any of the evaporators. Closing the solenoid valve upstream of the evaporator requiring defrost (see Figure 4.1) allows only subcooling refrigerant to pass through the evaporator. Since the evaporation section of the evaporator is inactive, the warm subcooling refrigerant releases its energy to the ice surrounding the plate, thus causing a defrost to occur. The advantage of this defrost scheme is that the flow of liquid from the condenser is never interrupted or diverted by mechanical means, such as with a four-way reversing valve. This means that there is very little chance of filling the accumulator with liquid refrigerant, thereby, eliminating the lengthy recovery period seen in the series described above.

Two MSHP systems were designed and tested for the purpose of residential application (in Crookston, Minnesota, at the home of Widseth). The first a five-ton MSHP using four ice-maker evaporators, the second a four-ton unit utilizing four ice-maker evaporators and an air source evaporator. Only the air/ice unit is described here, as the other, although the same design, incorporates only one source.

4.3 System Description

A schematic of the air/ice MSHP system is shown in Figure 4.3. The heat pump consists of a four-ton Westinghouse compressor, a finned-tube, four-ton condenser, a three-ton thermostatic expansion valve, a five-ton finned tube air evaporator and four Olin roll bonded ice-maker plate evaporators. The four-ton Westinghouse compressor was installed when the original Tecumseh compressor failed due to oil return problems during a

ORNL-DWG 81-17905

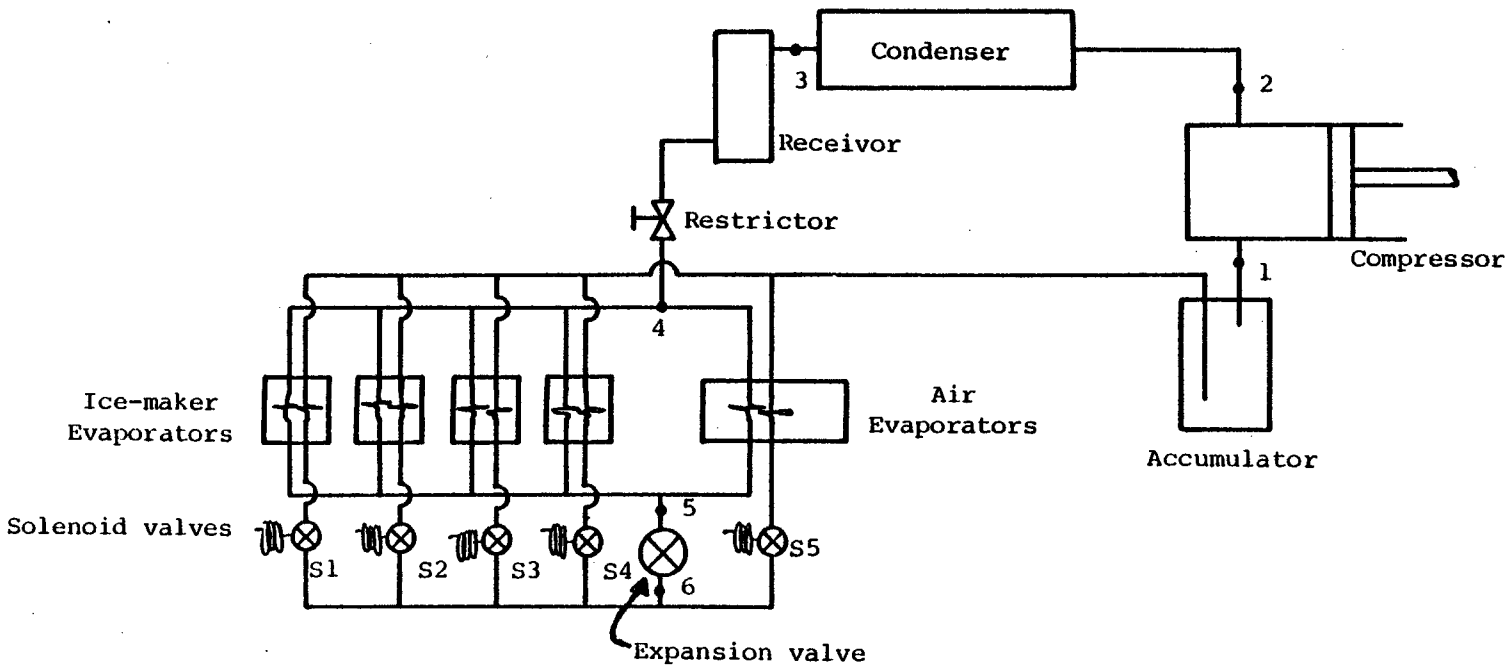

FIGURE 4.3 - SCHEMATIC DIAGRAM OF TESTED MSHP SYSTEM

series MSHP air/ice-maker test. A new condenser was needed to accomodate the higher mass flow rate produced by the larger Westinghouse compressor. The new condenser was obtained from the Greer and Snow Company. An accumulator was installed to protect the new compressors.

A receiver-restrictor assembly was built and installed on the condenser exit to serve as both the pressure drop component to provide a place for liquid refrigerant to collect under varying charge situations (i.e., varying evaporator conditions and configurations). The receiver is a section of three-inch copper tube capped at both ends. Sight glasses were installed at various heights on the receiver to detect the liquid level. An adjustable micrometer needle valve was used as a restrictor.

The original design called for a three-ton thermostatic expansion valve manufactured by the Sporlan Company. During a test of the air evaporator, the expansion valve was suspected of being undersized. This was detected by an excessive pressure drop (in excess of 120 psi) across the air evaporator. This was verified by removing the feeler bulb from the suction line and exposing it to the ambient air. Under this condition, the expansion valve should detect excessive superheat and attempt to counteract this condition by opening the valve orifice, thereby, allowing more liquid to pass and flood the evaporator, thus, decreasing the pressure drop across the evaporator. However, this change did not impact either system performance or the pressure drop across the evaporator. This inferred that the valve was fully opened and consequently undersized. By replacing the three-ton valve with a four-ton valve, this problem was remedied.

Type A3, normally closed Sporlan Solenoid valves were used in the system. The size of the solenoid valve can be critical. A larger solenoid

valve will have the tendency to leak refrigerant, thus allowing some evaporation to occur, which can have a detrimental effect on the defrost time. An undersized valve introduces a pressure drop that lowers the COP.

The ice-maker evaporators used were manufactured by Olin, through Energy Management Engineering Incorporated. These plates have seven independent flow paths. Four of these are used for the evaporator, while the other three are used as subcoolers.

The air evaporator used was a modified five-ton Janitrol finned tube coil. A subcooling run consisting of a 5/16 inch (0.8 cm) refrigeration tube was installed coaxially through the evaporation tubes in the coil in Figure 4.4. Since the flow rate (and thus the velocity) of the refrigerant is proportional to the cross sectional area of the tube, and the pressure drop is nominally proportional to the square of the fluid velocity, a change in tube area can have a significant impact on the evaporator pressure drop. The ratio of the pressure drops in the modified unit (subscript "m") to the original unit (subscript "o") can be shown in the following fashion:

$$\frac{\Delta P_m}{\Delta P_o} = \left(\frac{V_m}{V_o}\right)^2$$

$$\frac{\Delta P_m}{\Delta P_o} = \left(\frac{(\dot{m}/\rho A)_m}{(\dot{m}/\rho A)_o}\right)^2$$

or

$$\frac{\Delta P_m}{\Delta P_o} = \left(\frac{A_o}{A_m}\right)^2 \left(\frac{\rho_o}{\rho_m}\right)^2 \left(\frac{\dot{m}_m}{\dot{m}_o}\right)^2$$

Since the mass flow rate is proportional to the density, the above equation becomes:

ORNL-DWG 81-17906

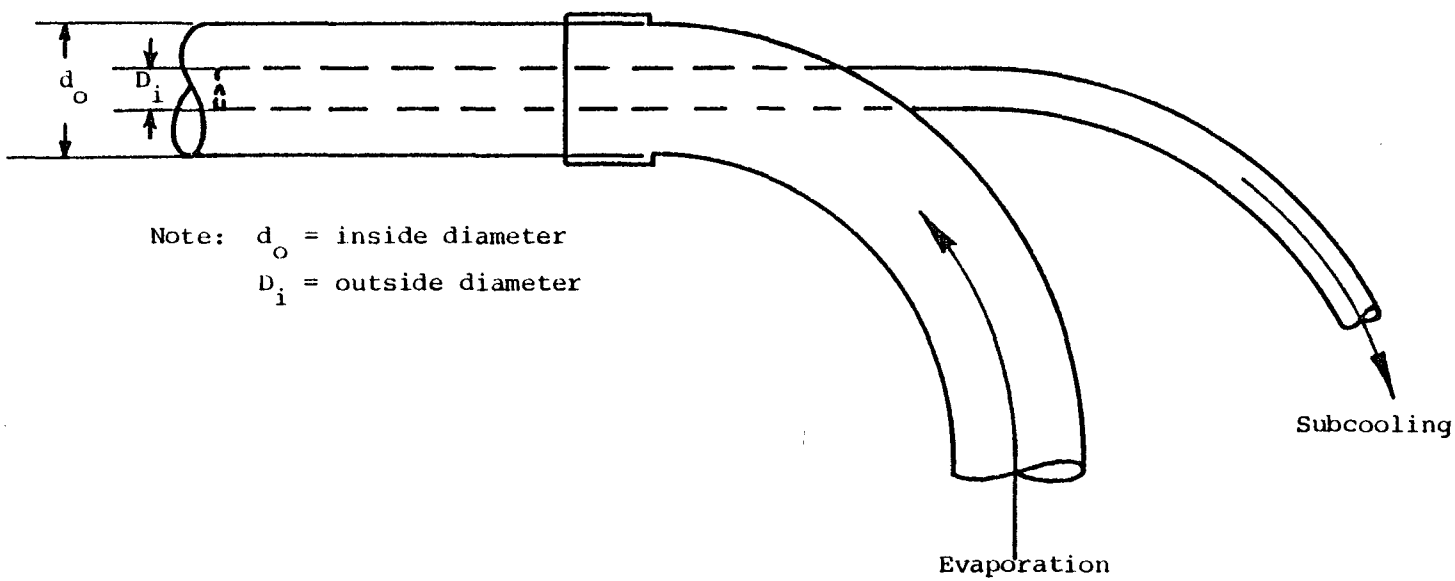

FIGURE 4.4 - MODIFIED TUBE-IN-TUBE AIR EVAPORATOR DESIGN

$$\frac{\Delta P_m}{\Delta P_o} = \frac{1}{\left[1 - \left(\frac{D_i}{d_o}\right)^2\right]^2}$$

where:

d_o = inside diameter of the outer pipe (Figure 4).

D_i = outside diameter of the inner pipe (Figure 4).

For the system tested, d_o is 0.50 inches (1.25 cm) and D_i is 0.31 inches (0.79 cm). Thus the ratio $\Delta P_m/\Delta P_o$ is approximately 2.7. This means the pressure drop in the modified unit can be expected to be 2.7 times greater than in the original unit. This is the reason that the experimental pressure drop reported below is so large. The modified unit was used in spite of this because the time and funds required to modify the design were not available. Consequently, the results presented below cannot be expected to represent an optimum design.

4.4 Test Procedure

The objective of the test program was to evaluate the thermal performance of the MSHP system by at least two independent methods. One of the principal parameters used in evaluating the thermal performance of a heat pump is the heating coefficient of performance (COP_h). This parameter can be experimentally determined by two methods. The first method is to perform an energy balance on the condenser air and to measure compressor work, this yields:

$$COP_h = \frac{\dot{Q}_R}{\dot{W}_c} = \frac{\dot{m}_a \, c_p \, (\Delta T)_{air}}{\dot{W}_c} \qquad 4.1$$

where:

$\dot{Q}_R = \dot{m}_a \, c_p \, (\Delta T)_{air}$

$\dot{W}_c$ = power input into the compressor (BTU/hr).

The second method is to perform an energy balance on the freon. This method yields:

$$COP_h = \frac{h_2 - h_3}{h_2 - h_1} \qquad 4.2$$

where:

h_1 = enthalpy at the compressor suction inlet

h_2 = enthalpy at the compressor discharge port

h_3 = enthalpy at the condenser exit

The enthalpy values at points 1, 2, and 3 (see Figure 4.3) can be determined from pressure and temperature measurements at these points, since the freon is generally not in a saturated state at these points.

Table 4.1 summarizes the data that needs to be collected to determine the COP_h, as described in Equations 4.1 and 4.2.

All tests were conducted during steady state operation of the system. Each evaporator was tested individually, since that is how the system will operate in the field. The tests were run under the following conditions:

A. Ice-Maker Tests. The ice-makers were tested starting with a water source temperature of approximately 50°F. Energy was drawn from the tank until ice formation. At this point the four ice-makers were put into a cyclic defrost mode, until all plates were defrosted at least once. During this test the air evaporator was inactive and the air subcooling environmental temperature was sustained at 55°F by a separate environmental control unit.

B. Air-evaporator tests. The air evaporator was tested while attempting to keep the control chamber at a constant temperature. During the first test the control chamber was maintained at 45°F. However, due to a large temperature fluctuation (±10 F°) the average air temperature was 54.9°F. The temperature fluctuation in the source air could also be detected on the suction pressure gauge. In an attempt to keep a constant source temperature, the second set of tests run used room air (72°F) as the source.

Data was taken at five-minute intervals. A Fluke 2240B data acquisition system was used to record system temperatures and compressor power. Pressures were read manually on standard U.S. Test Gauges which had been calibrated. A real time computer program was used to analyze the data.

TABLE 4.1

DATA REQUIRED TO ANALYZE THE THERMAL PERFORMANCE OF A MSHP SYSTEM

	Data	Yields
A.	ρ_a - density of air through the condenser A - area of the condenser exit duct $\overline{V}$ - average velocity of the air through the condenser	$\dot{m}_a$ - mass flow rate of the air through the condenser
B.	T_{in} - temperature of the inlet air to the condenser T_{out} - temperature of the exit air from the	ΔT_{air} - temperature difference of the air across the condenser c_p - constant pressure specific heat of the air at the condenser exit temperature $^*c_p$ - $6.667\ (10^{-6})\ T_{out} + 0.2398$
C.	R_v - watt-transducer reading in volts (compressor)	$\dot{W}_c$ - compressor power requirement
D.	P_1 - pressure at the compressor suction T_1 - temperature at the compressor suction	h_1 - enthalpy at the compressor suction
E.	P_2 - pressure at the compressor discharge T_2 - temperature at the compressor discharge	h_2 - enthalpy at the compressor discharge
F.	P_3 - pressure at the condenser exit T_3 - temperature at the condenser exit	h_3 - enthalpy at the condenser exit

* See Somerville, M.H. and Penoncello, S.G., 1980, Appendix E for the derivation of this expression

4.5 Experimental Results

A series of three tests were run on the system. The initial test was run using the original system components with the undersized expansion valve. Both air evaporator and ice-maker data were collected. A second test was run on the air evaporator to determine the operation of the thermostatic expansion valve. When the valve proved to be undersized, a third test was run on both the air evaporator and the ice-makers using a larger expanion valve. The complete tests results are reported by Somerville and Penoncello (1980). A summary of the test results is presented below. These data are intended to portray only the results of the tests; they do not represent a complete data set.

4.5.1 Results of Test 1

Figure 4.5 through 4.8 present the results of Test 1 The following important facts can be noted by examining Figures 4.5 and 4.6. The pressure drop in the modified air evaporator is enormous (80 psid), the pressure drop in the ice maker is large (22 psid), the saturated condensing temperature is very low (150°F at discharge), and the entropy decreases across the compressor. Figure 4.7 shows that the MSHP behaves normal while operating on the ice-maker evaporators except for the low discharge temperature. Ice making was initiated at approximately 1200 (two hours into the test), the first defrost was initiated at 12:45. Performance is observed to be constant, due to the ice formation. It should also be noted that the defrost operation does not impact heat pump performance. Interpretation of Figure 4.8 shows that the subcooling effect gradually warms the cold ice-makers (the existing freon temperature warms from 30°F (3°C) to 82°F (28°C) in approximately one hour. The data also shows that the

ORNL-DWG 81-17907

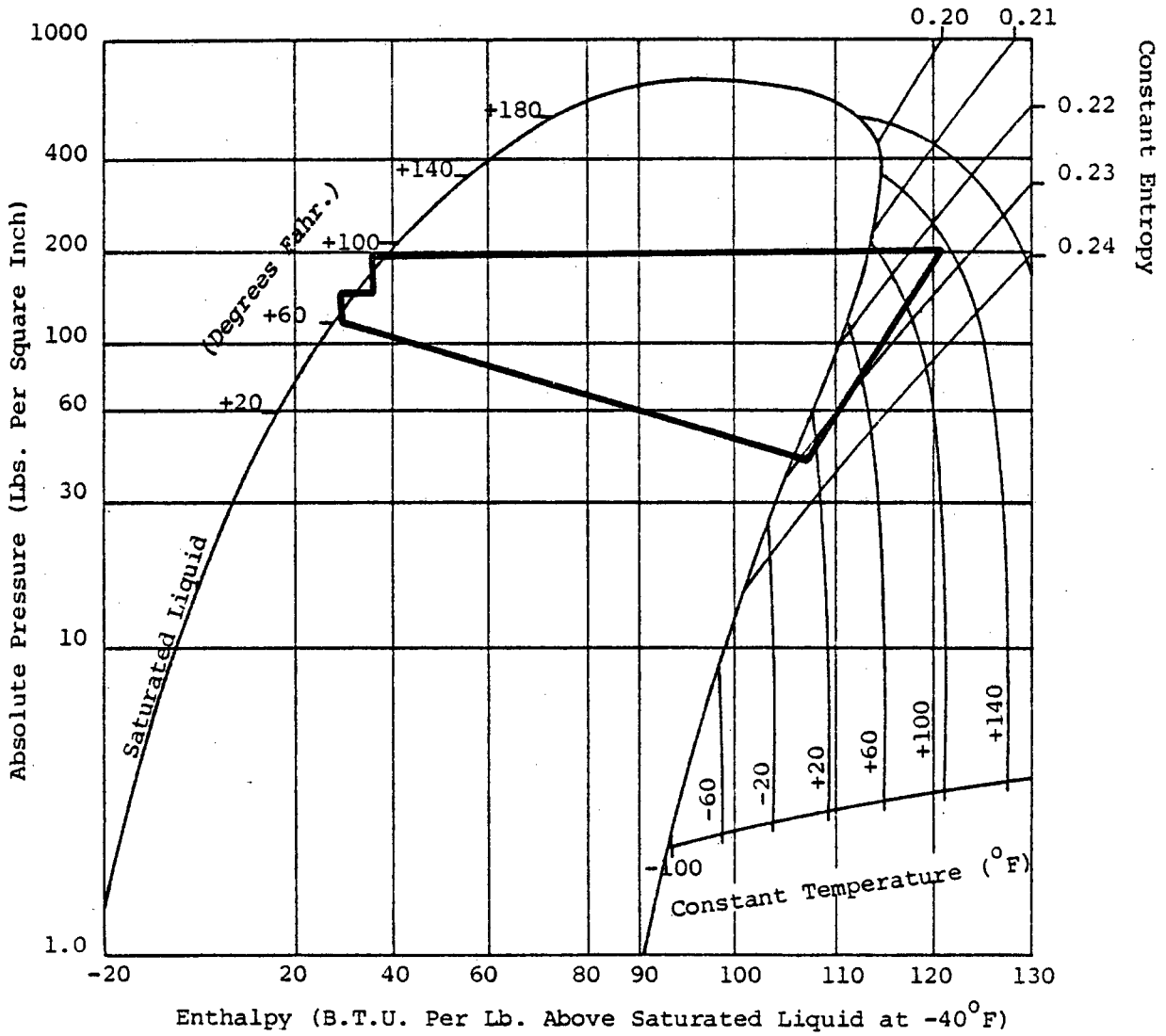

FIGURE 4.5 - THE PRESSURE ENTHALPY DIAGRAM FOR THE ACTIVE AIR EVAPORATOR TEST (ICE MAKERS INACTIVE)

ORNL-DWG 81-17908

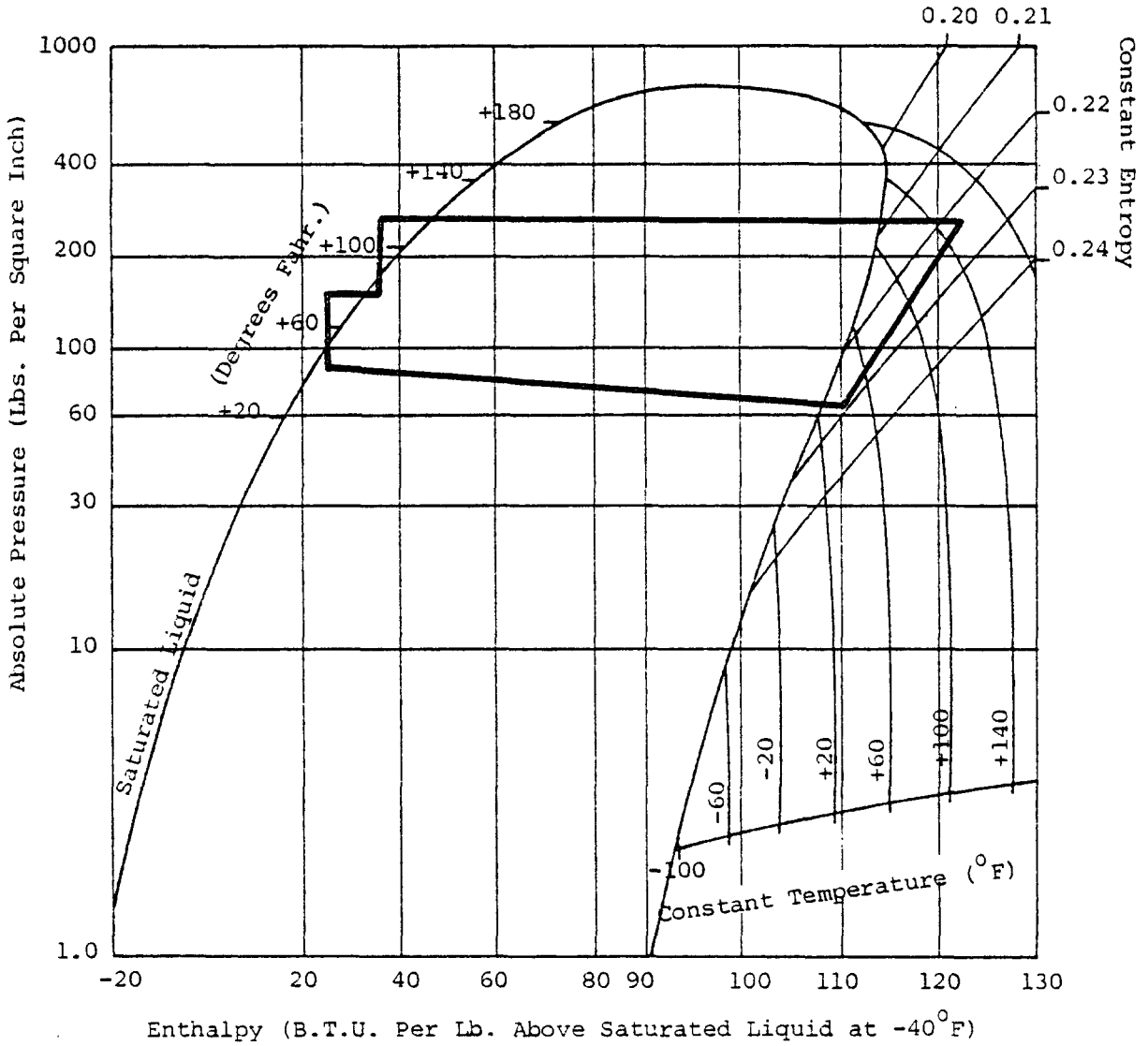

FIGURE 4.6 - THE PRESSURE ENTHALPY DIAGRAM FOR THE ACTIVE ICE EVAPORATOR TEST (INACTIVE AIR EVAPORATORS)

ORNL-DWG 81-17909

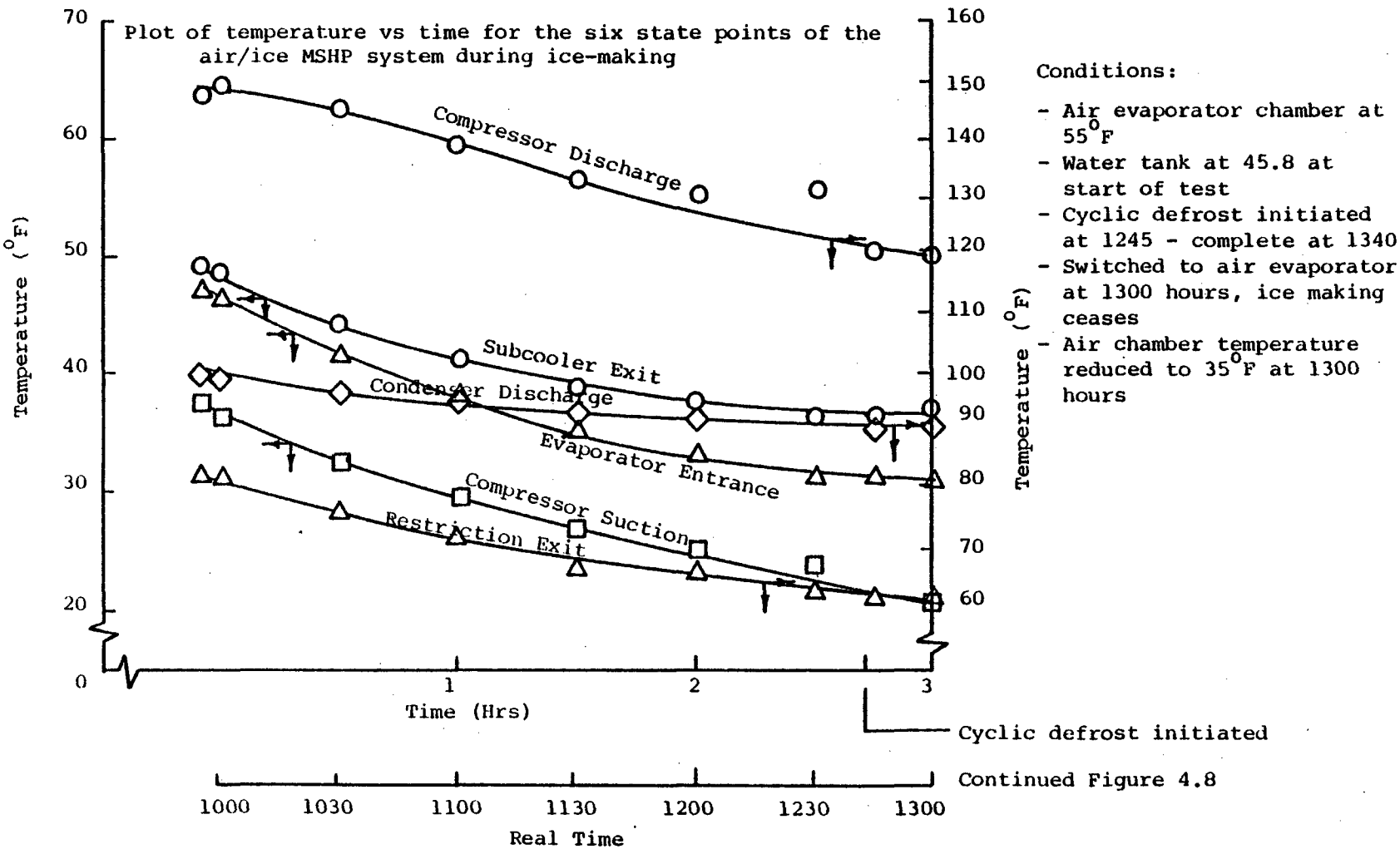

Continued Figure 4.8

FIGURE 4.7 - TEMPERATURE VS. TIME PLOT FOR AIR/ICE MSHP TEST DURING ICE-MAKING, TEST I

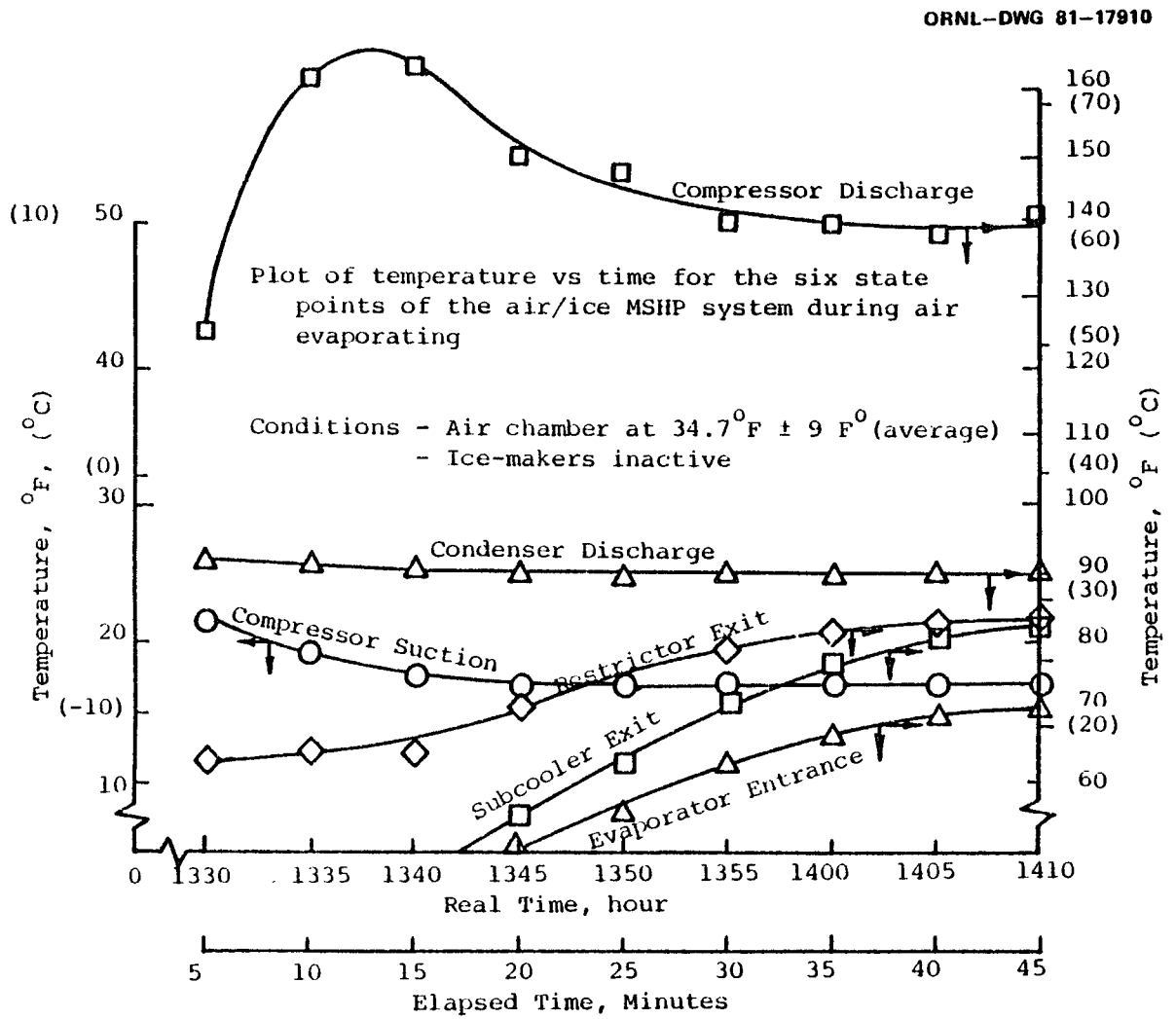

Note: air temperature changed to 35°F at 1300. Thirty minutes allowed for chamber equalization

FIGURE 4.8 - MSHP TEST I, EXPERIMENTAL DATA, AIR EVAPORATOR ACTIVE

heat transfer rate on the air side subcooler is minimal, as there is virtually no temperature drop between the restrictor exit and subcooler exit. We are unable to explain the increase in the compressor discharge from 1330 through 1340.

The conclusions that we reached from this test were:

* The thermocouple on the compressor discharge was erroneous;
* The modified air evaporator pressure drop is unacceptably high to the change in cross sectional area;
* The expansion valve is undersized (virtually no throttling takes place across the valve, indicating it was completely opened).

4.5.2 Results of Test 2

The purpose of this short test was to determine whether or not the expansion valve was sized properly. This was done by allowing the system to run normally, then removing the feeler bulb of the valve assembly and noting the system performance. The experimental data are shown in Figure 4.9. Table 4.2 shows the results of the performance calculations. Considering the source temperature of 71.1^{o}F, the COP_h seems to be slightly low. This can be expected because of the excessive air evaporator pressure drop. (Resources were not available to build a second evaporator.)

The feeler bulb of the expansion valve was removed midway through the test. Again referring to Table 4.2, it can be seen that the COP_h and heating capacity remain unchanged during system operation. Since the performance was virtually unchanged by removing the feeler bulb, the conclusion drawn was that the expansion valve was undersized.

The original three-ton expansion valve was replaced with a four-ton expansion valve and the final test was performed on the air evaporator.

ORNL-DWG 81-17911

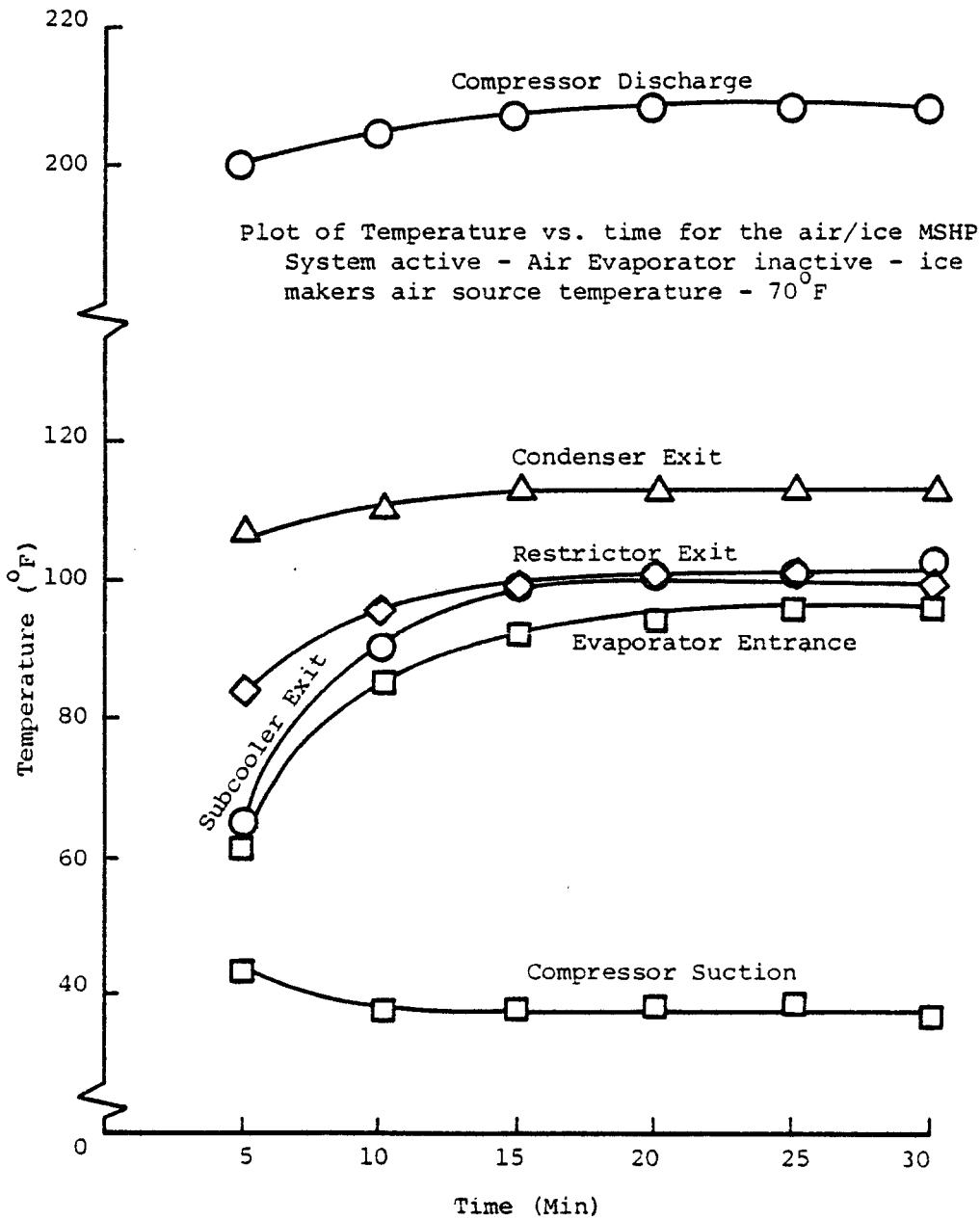

FIGURE 4.9 - PLOT OF TEMPERATURE VS. TIME FOR TEST II OF MSHP SYSTEM

TABLE 4.2

HEATING CAPACITY, WORK INPUT AND HEATING COEFFICIENT OF PERFORMANCE FOR TEST II OF THE AIR/ICE MSHP

Time	$\dot{Q}_R$ (Btuh)	$\dot{W}_c$ (Btuh)	Δh_{1-2}	Δh_{2-3}	$COP_h = \frac{\dot{Q}_R}{W_c}$	$COP_h = \frac{\Delta h_{2-3}}{\Delta h_{1-2}}$
1545	40548	14284	23.32	89.70	2.84	3.84
1550	45268	14280	22.70	88.61	3.17	3.90
1555	46877	14298	22.85	88.22	3.28	3.86
1600	47414	14283	23.00	88.12	3.32	3.83
1605	47413	14287	22.99	88.60	3.32	3.85
1610	47199	14285	23.04	88.16	3.30	3.83

Conditions - $\dot{m}\, c_{p\ air}$ = 1072.71 Btu/hr - F

- Air evaporator source temperature at 71.1 F (average) ± 1.2 F
- Feeler bulb removed at 1600

4.5.3 Results of Test 3

The results of the third test are shown in Figure 4.10 and Tables 4.3 through 4.5. The experimental data are graphically presented in Figure 4.10 and tabulated in Table 4.3. A comparison of the evaporator's entrance temperature with its exit temperature (the saturation temperature at the suction pressure) reveals that frost should have formed on the coil, as it did. The impact of the new expansion valve which is flooding the evaporator can also be seen; the pressure drop across the evaporator has been reduced to 35 to 40 psid from its earlier 80 psid. This is due to the entrance of warm liquid into the evaporator. The evaporation of the entering freon is retarded by the close approach (15 F^o, 8 C^o) to the room temperature. Thus, less vapor forms near the entrance to the evaporator and more forms near the end. This effectively reduces the fluid velocity in the tubes and consequently reduces the pressure drop. This, however, is only a temporary fix to the real problem, which is the greatly reduced flow area in the air evaporator, which is caused by the co-axial subcooling tube. This problem can only be cured by a complete re-design and construction of an air evaporator whose tubes have adequate cross sectional flow area, as well as a subcooling flow. A proposed design for such a tube is shown in Figure 4.11. The cross sectional area of the tube, A_E, is designed to handle the two phase evaporating flow, while the subcooling flow, which is entirely liquid, can be handled by the smaller tube. The smaller inner tube must have a good thermal contact with the outer tube to effectively accomplish defrost. It is important that the smaller tube be located at the bottom of the larger one so that condensing freon will be boiled off during the period of time (cold weather) that the air coil is inactive.

ORNL-DWG 81-17912

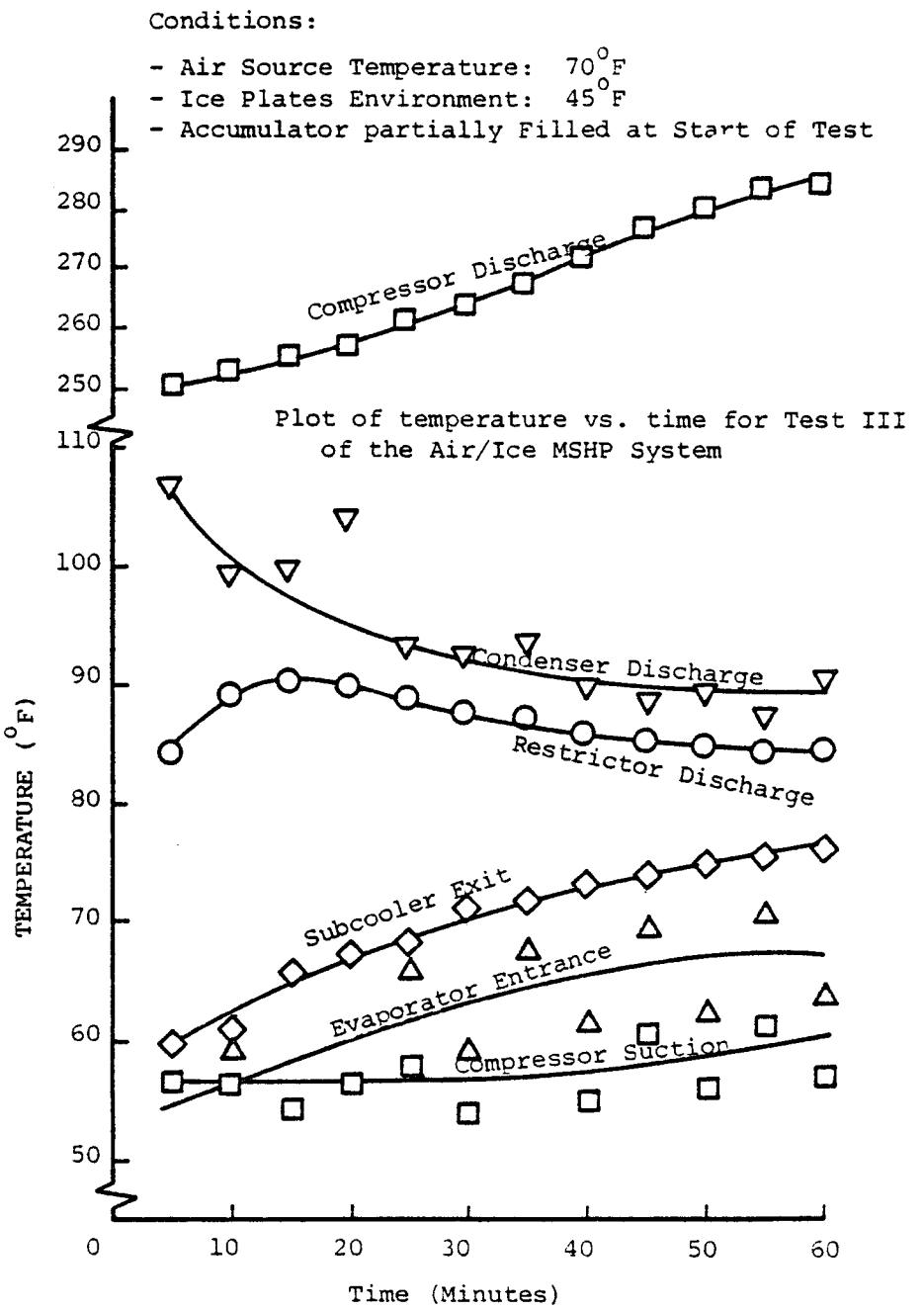

FIGURE 4.10 - EXPERIMENTAL RESULTS FOR TEST III OF THE AIR/ICE MSHP SYSTEM-AIR EVAPORATOR ACTIVE

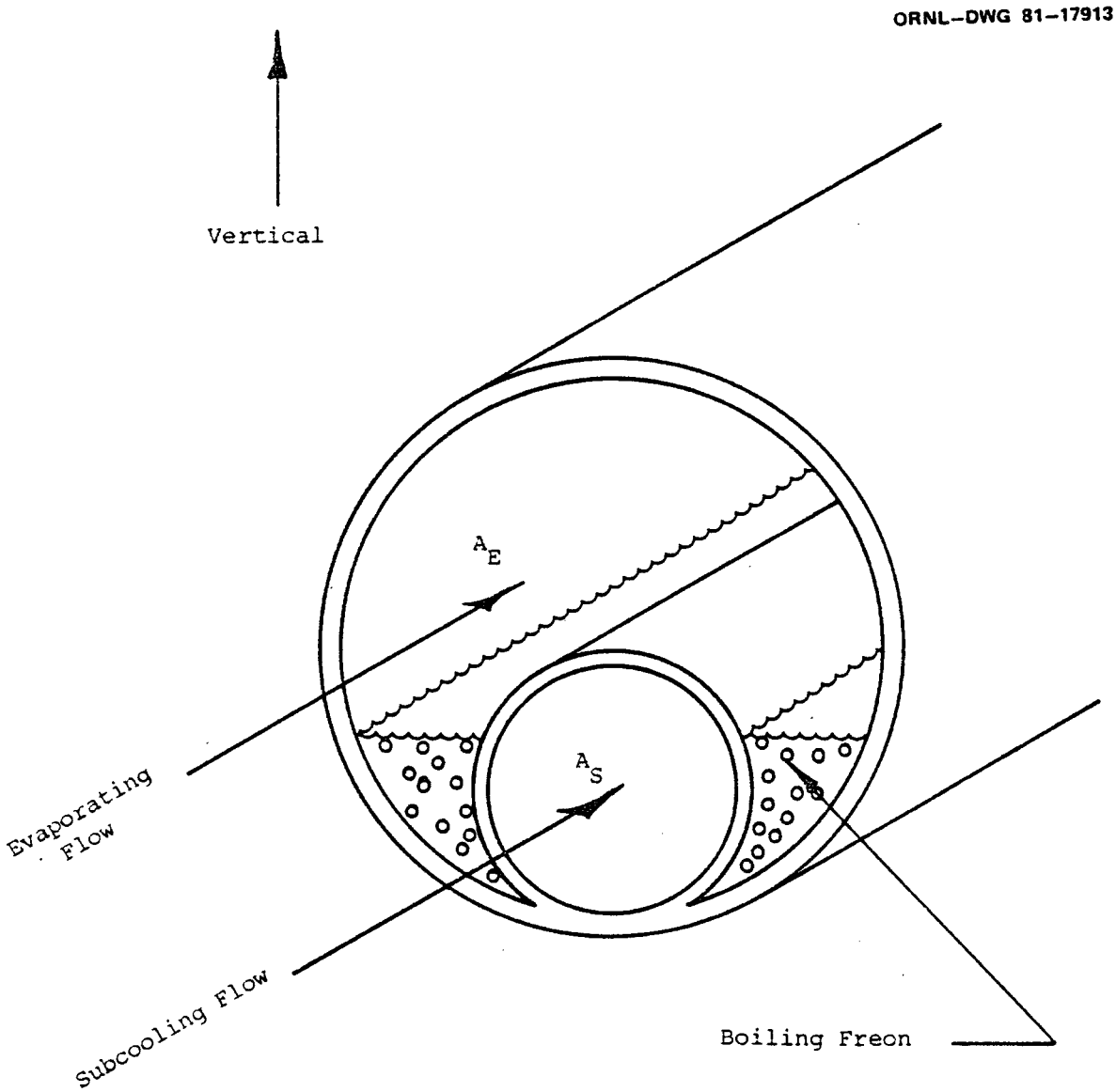

FIGURE 4.11 - PROPOSED DESIGN FOR A CO-AXIAL COPPER TUBE FOR USE IN A MSHP FINNED TUBE AIR COIL

TABLE 4.3

TEST III, MSHP
STATE POINT PRESSURES AND TEMPERATURES DURING
ACTIVE AIR EVAPORATOR TEST

	Compressor Suction		Compressor Discharge		Condenser Discharge	
Time	T (^{o}F)	P (psig)	T (^{o}F)	P (psig)	T (^{o}F)	P (psig)
1530	56.5	61.0	250.3	248.0	106.6	246.0
1535	56.3	58.0	253.3	245.0	99.3	243.0
1540	54.2	56.0	255.3	249.0	99.5	248.0
1545	56.4	42.0	257.0	249.0	103.9	254.0
1550	57.8	60.0	261.2	254.0	92.8	254.0
1555	53.7	61.0	263.9	270.9	92.2	271.0
1600	60.0	65.0	267.5	262.0	93.2	262.0
1605	54.9	63.0	271.3	286.0	89.6	286.0
1610	60.5	65.0	276.2	273.0	88.4	272.0
1615	55.7	64.0	279.4	294.0	88.8	295.0
1620	61.0	65.0	282.6	279.0	87.0	277.0
1625	56.8	66.0	283.4	300.0	90.3	300.0

	Restrictor Exit		Subcooler Exit		Evaporator Entrance	
Time	T (^{o}F)	P (psig)	T (^{o}F)	P (psig)	T (^{o}F)	P (psig)
1530	84.2	195.0	59.7	200.0	52.6	86.0
1535	89.1	166.0	61.0	163.0	59.1	100.0
1540	90.2	205.0	65.8	202.0	54.9	106.0
1545	89.9	221.0	67.2	221.0	56.6	94.0
1550	88.8	186.0	68.2	185.0	65.8	111.0
1555	87.7	239.0	71.2	238.0	59.0	99.0
1600	87.3	240.0	71.6	240.0	67.6	101.0
1605	85.7	253.0	73.2	253.0	61.2	102.0
1610	85.0	240.0	73.9	242.0	69.1	115.0
1615	84.6	259.0	74.8	260.0	62.4	115.0
1620	84.2	203.0	75.2	202.0	70.4	125.0
1625	84.5	264.0	76.0	264.0	63.5	108.0

TABLE 4.4

CALCULATED EVAPORATOR EXIT TEMPERATURE

	Compressor Suction			Evaporator Entrance	
	Measured		Evaporator Exit Calculated	Measured	
Time	Pressure (psig)	Temperature (°F)	Sat. Temp.* (°F)	Pressure (psig)	Temperature (°F)
1530	61	56.5	34.6	86	52.6
1535	58	56.3	32.4	100	59.1
1540	56	54.2	30.9	106	54.9
1545	52	56.4	27.7	94	56.6
1550	60	57.8	33.9	111	65.8
1555	61	53.7	34.0	99	59.0
1600	65	60.0	38.5	101	67.6
1605	63	54.9	36.1	102	61.2
1610	65	60.5	37.5	115	69.1
1615	64	55.7	36.8	115	62.4
1620	65	61.0	37.5	125	70.4
1625	66	56.8	37.6	108	63.5

* Calculated by linear interpolation from R-22 saturation data

TABLE 4.5

HEATING CAPACITY, WORK INPUT AND HEATING COEFFICIENT OF PERFORMANCE FOR TEST III OF THE AIR/ICE MSHP

Time	$\dot{Q}_R$ (Btuh)	$\dot{W}_c$ (Btuh)	Δh_{1-2}	Δh_{2-3}	$COP_h = \frac{\dot{Q}_R}{W_c}$	$COP_h = \frac{\Delta h_{2-3}}{\Delta h_{1-2}}$
1530	35164	14254	29.833	99.984	2.47	3.34
1535	33531	14261	30.392	102.866	2.35	3.38
1540	34299	14259	30.946	103.092	2.41	3.33
1545	36317	14259	31.151	101.984	2.55	3.27
1550	36221	14254	31.626	106.117	2.54	3.36
1555	38911	14258	32.552	106.342	2.73	3.27
1600	38623	14244	32.612	107.041	2.71	3.28
1605	40832	14243	33.594	108.104	2.87	3.22
1610	40352	14238	34.045	109.871	2.83	3.23
1615	41793	14254	34.999	109.739	2.93	3.14
1620	41123	14251	35.134	111.404	3.89	3.17
1625	41601	14259	35.612	109.963	2.92	3.09

Conditions - Air evaporator environment temperature = 69.9°F

- Ice-makers inactive

4.6 Conclusions and Recommendations

The purpose of these tests was to perform a proof of principle test for the multi-source heat pump concept, with parallel evaporators with active subcooling. The following major conclusions can be drawn from the work:

1. The concept of a multi-source heat pump can be successfuly carried out with a parallel evaporator arrangement, with active subcooling in each evaporator.

2. The concept of utilizing the subcooling energy to control freon migration appears to be sound, but will require that a new tube be designed with new fittings for finned tube coils.

3. Defrosting of both the ice-maker and the air coil can be successfully accomplished without loss of performance or degradation of the units COP.

4. Additional design and development work is required, but it appears that with properly sized evaporators and condenser, both the accumulator and receiver could be eliminated.

5. Since we have also built an ice/ice multi-source heat pump using this concept, there is no reason visible to us that would prevent us from building an air/air unit that would eliminate the need for a hot gas defrost cycle.

It is recommended that a split finned tube coil be designed, built, and tested to determine if the concept of active subcooling can be used to solve defrost problems.

5.0 DESIGN PROCEDURE FOR MULTIPLE SOURCE HEAT PUMPS

5.1 Introduction

With the advent of dual evaporator technology, it became apparent that a design procedure for heat pumps with the dual evaporator configurations needed to be developed. This task was initiated during the design and development of the dual series evaporator system (Wood, 1979), and progressed through the parallel evaporator with active subcooling system (Penoncello, 1980).

There were two methods of solution sought after in this design procedure. The first solution method was analytical. A computer model was written that simulates the operation and performance of a dual series heat pump system. By variation of various input parameters, a dual series heat pump system could be sized, based on the system performance determined analytically. After the dual series system was abandoned and the development of the parallel configuration with active subcooling was well under way, the analytical model was then revised so that the active subcooling configuration was included in the simulation algorithm.

The second solution method was to be an easy-to-use, "desktop" method that did not require the use of a computer. This method was developed for the dual series configuration.

Subsequent sections will discuss in detail:

1. The development of the desktop design procedure, and
2. The development of the analytical model for both the dual series system and the parallel system with active subcooling.

5.2 Development of the Desktop Design Procedure for Dual Series Heat Pump Systems

In this section, a procedure is presented by which a graphical model of a dual series evaporator heat pump, during steady state operation, can be constructed. This model allows the user to predict the system operating characteristics in a simple manner, without requiring the use of a computer.

Several assumptions are made during model construction, as discussed in later sections, to simplify the procedure. As a result, the graphical model will not represent the actual system as accurately as the analytical model would. However, because of its simplicty, the graphical model should be used prior to the analytical model to avoid possible wasted effort because of component missizing. Component missizing is readily visible with the graphical method.

The procedure for developing each of the graphical component models is discussed in a separate section below, along with any simplifying assumptions which were made. Then, after each of the components models has been developed, the procedure for combining these models to form the system model is outlined.

5.2.1 Compressor Model

Compressor performance curves which are published by manufacturers usually present the refrigeration capacity as the dependent variable as a function of the saturated evaporating and condensing temperatures (TEVAP and TCOND). However, in this procedure, the refrigerant mass flow rate is used as the dependent variable instead of the refrigeration capacity, because it is then a simple matter to use the continuity equation to predict component interactions. Therefore, compressor curves which are based on the refrigeration capacity must be converted to a mass flow rate basis.

The first step in converting to a mass flow basis is to calculate the refrigeration effect across the evaporator, with the conditions stated on the compressor capacity curves. For the model presented here, a Sundstrand 2.5 ton compressor, model H20A323AB, was used as the basis. The specified test conditions for this model were: $95^{o}F$ ($35^{o}C$) vapor at the entrance to the compressor and 15 F^{o} (9 C^{o}) of subcooling at the exit from the condenser, with refrigerant 22. Therefore, the enthalpy at the entrance to the evaporator is the enthalpy which corresponds to 15 F^{o} (9 C^{o}) of subcooling at the saturated condensing pressure and the enthalpy at the exit from the evaporator is the enthalpy of $95^{o}F$ ($35^{o}C$) superheated vapor at the saturated evaporating pressure. By using either a pressure-enthalpy diagram or refrigerant tables, the change in enthalpy of the refrigerant in the evaporator (refrigeration effect) can be calculated for several values of the saturated evaporating and condensing temperatures. This has been done for the above compressor test conditions and is shown graphically in Figure 5.1.

Then, dividing the refrigeration capacity given by the manufacturers' curves by the corresponding refrigeration effect from Figure 5.1, at various values of evaporating and condensing temperatures, a series of curves which represent the compressor characteristics on a mass flow rate basis can be developed. The curve for this example is shown in Figure 5.2.

5.2.2 Condenser Model

As with the compressor model, the condenser model is constructed with the refrigerant mass flow rate as the dependent variable. If condenser capacity curves are available, they must again be converted to a mass flow rate basis.

ORNL-DWG 81-17914

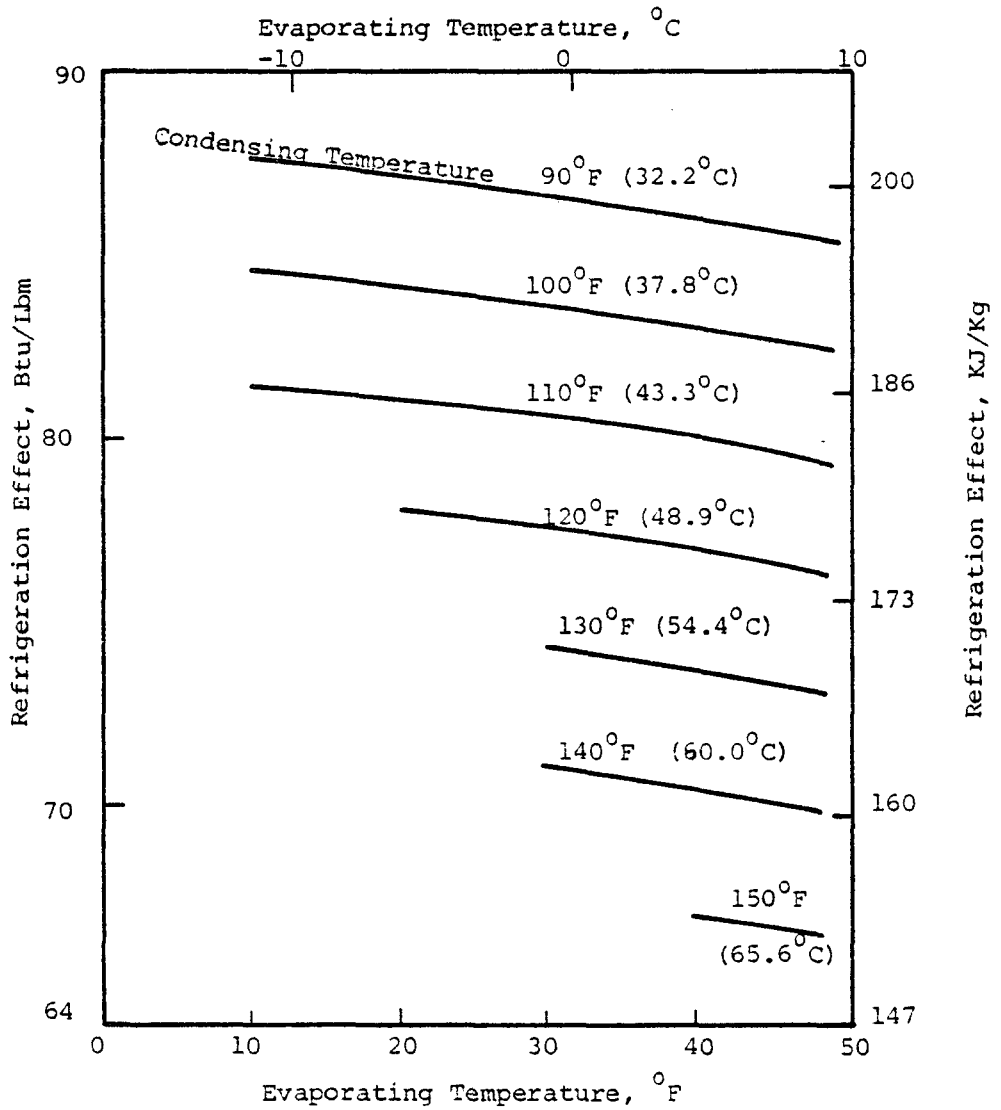

FIGURE 5.1 - REFRIGERATION EFFECT IN THE EVAPORATOR

ORNL-DWG 81-17915

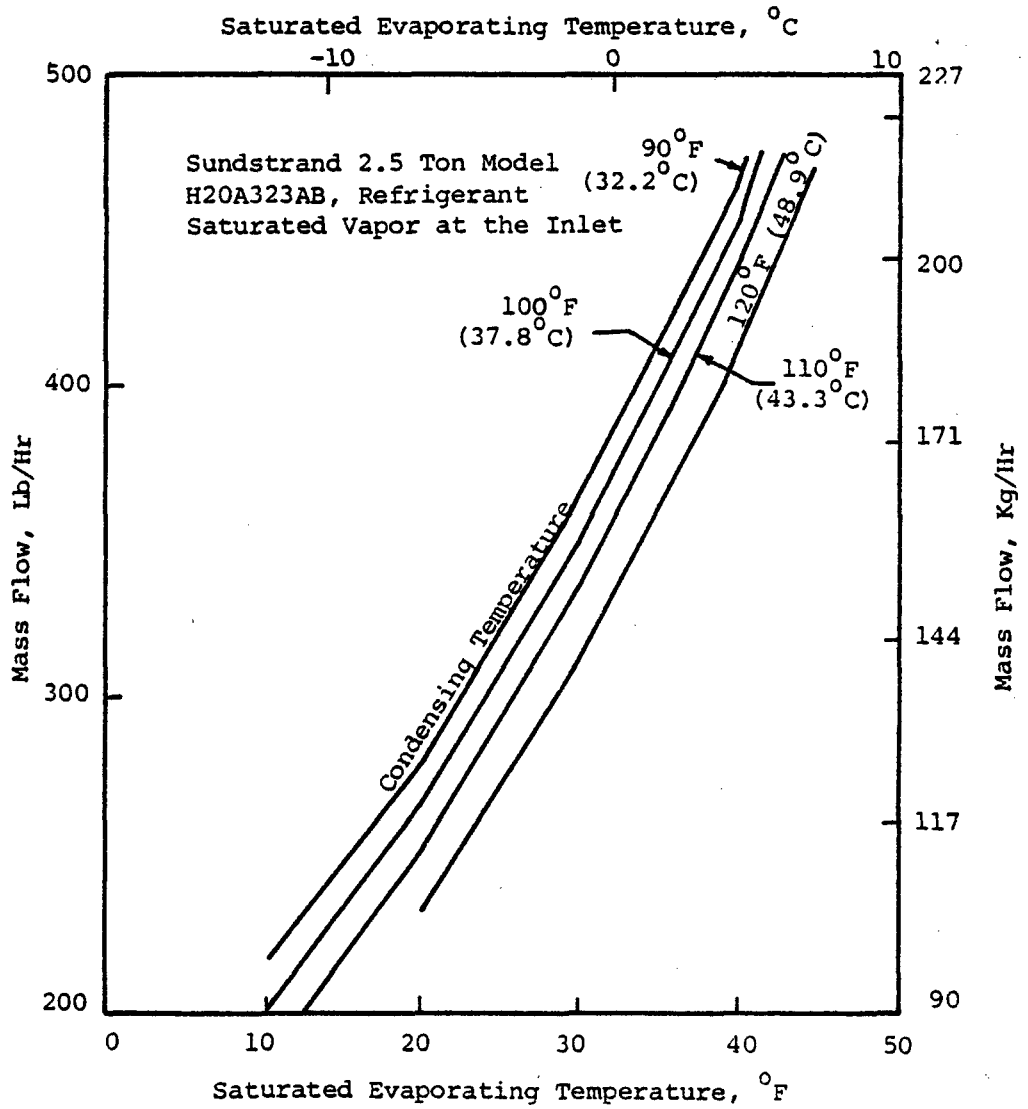

FIGURE 5.2 - COMPRESSOR CHARACTERISTICS

The condenser used in this model is based on a UA product of 800 Btu/hr-^{o}F (391 W-^{o}C). In addition, the following assumptions were made concerning the condenser:

1. There is 10 F^{o} (6 C^{o}) of subcooling at the exit from the condenser.

2. The compressor has an isentropic efficiency of 50 percent.

3. The house air temperature is constant over the entire face of the condenser and equal to 70°F (21°C).

4. The saturation zone overall heat transfer coefficient and temperature difference can be used for the entire condenser area.

5. The refrigerant enters the compressor as a saturated vapor (a thermal-electric expansion valve is used).

By using refrigerant tables or diagrams, the refrigerant enthalpy at the exit from the compressor, assuming isentropic compression, can be calculated for several values of evaporating and condensing temperatures. Then, the difference between this isentropic enthalpy at the exit from the compressor and the enthalpy at the entrance to the compressor (H1) is multiplied by 2 (50 percent isentropic compressor efficiency), and added to H1 to give the actual enthalpy at the exit from the compressor (H2). Finally, the change in enthalpy of the refrigerant as it flows through the condenser can be calculated by subtracting the enthalpy which corresponds to 10 F^{o} (6 C^{o}) of subcooling at the condenser exit from H2 as calculated above. This has been done for several values of evaporating and condensing temperatures, and this enthalpy change is listed in Table 5.1.

Next, the heat transfer characteristics of the condenser must be calculated with Newton's law of cooling which states:

$$CAPH = UA(TCOND - TSINK) \qquad 5.1$$

TABLE 5.1

ENTHALPY CHANGE ACROSS THE CONDENSER ASSUMING SATURATED VAPOR INTO THE COMPRESSOR, 50 PERCENT ISENTROPIC COMPRESSION EFFICIENCY, AND 10°F SUBCOOLING AT THE EXIT FROM THE CONDENSER

	TEVAP, °F*					
TCOND, °F*	0	10	20	30	40	50
90	122.00	115.60	110.70	105.80	99.50	94.90
100	123.04	117.94	111.44	106.54	101.74	96.94
110	125.40	118.80	113.70	108.70	102.20	97.30
120	127.90	121.20	114.40	109.30	104.30	99.30
130	128.60	121.70	116.50	111.30	106.10	101.10
140	129.10	123.70	115.70	111.40	106.20	101.00
150	131.20	124.10	118.60	111.50	106.10	100.80

* $^{o}C = \frac{5}{9}\,(^{o}F - 32)$

where CAPH is the rate of heat transfer from the refrigerant to the house air, TCOND is the condensing temperature, and TSINK is the temperature of the sink ($70^{o}F$ or $21.1^{o}C$).

The energy equation can be used to balance the energy change of the refrigerant as it passes through the condenser, with the rate of heat transfer from the refrigerant to the house air.

Therefore, dividing the heating capacity from Table 5.2 by the change in enthalpy across the condenser from Table 5.1, the mass flow rate of refrigerant through the condenser can be calculated. This has been done for several values of evaporating and condensing temperatures, and is shown in Figure 5.3.

5.2.3 Active Evaporator Model

The model presented here is based on a UA of 1800 Btu/hr-^{o}F (878 W-^{o}C) and a source temperature of $32^{o}F$ ($0^{o}C$). In addition, the following assumptions were made concerning the active evaporator:

1. The enthalpy at the entrance was assumed to be the enthalpy corresponding to 10 F^{o} (6 C^{o}) of subcooling at the saturated condensing pressure. This assumption will be corrected later, after the effects of subcooling have been determined.

2. The values of the overall heat transfer coefficient and temperature difference can be approximated by the values in the saturation region throughout the evaporator.

3. The refrigerant exits from the evaporator as a saturated vapor (a thermal-electric expansion valve is used).

The first step in development of the model is to calculate the change in enthalpy of the refrigerant across the active evaporator. With the conditions assumed above, refrigerant tables can be used to determine this enthalpy change for various values of condensing and evaporating temperatures. The enthalpy changes for this model are shown in Table 5.3.

TABLE 5.2

HEATING CAPACITY OF THE CONDENSER AS A FUNCTION OF THE CONDENSING TEMPERATURE

TCOND, ^{o}F*	CAPH, Btu/hr**
90	16,000
100	24,000
110	32,000
120	40,000

* $^{o}C = \frac{5}{9}(^{o}F - 32)$

** kW = 3.413 Btu/hr

ORNL-DWG 81-17916

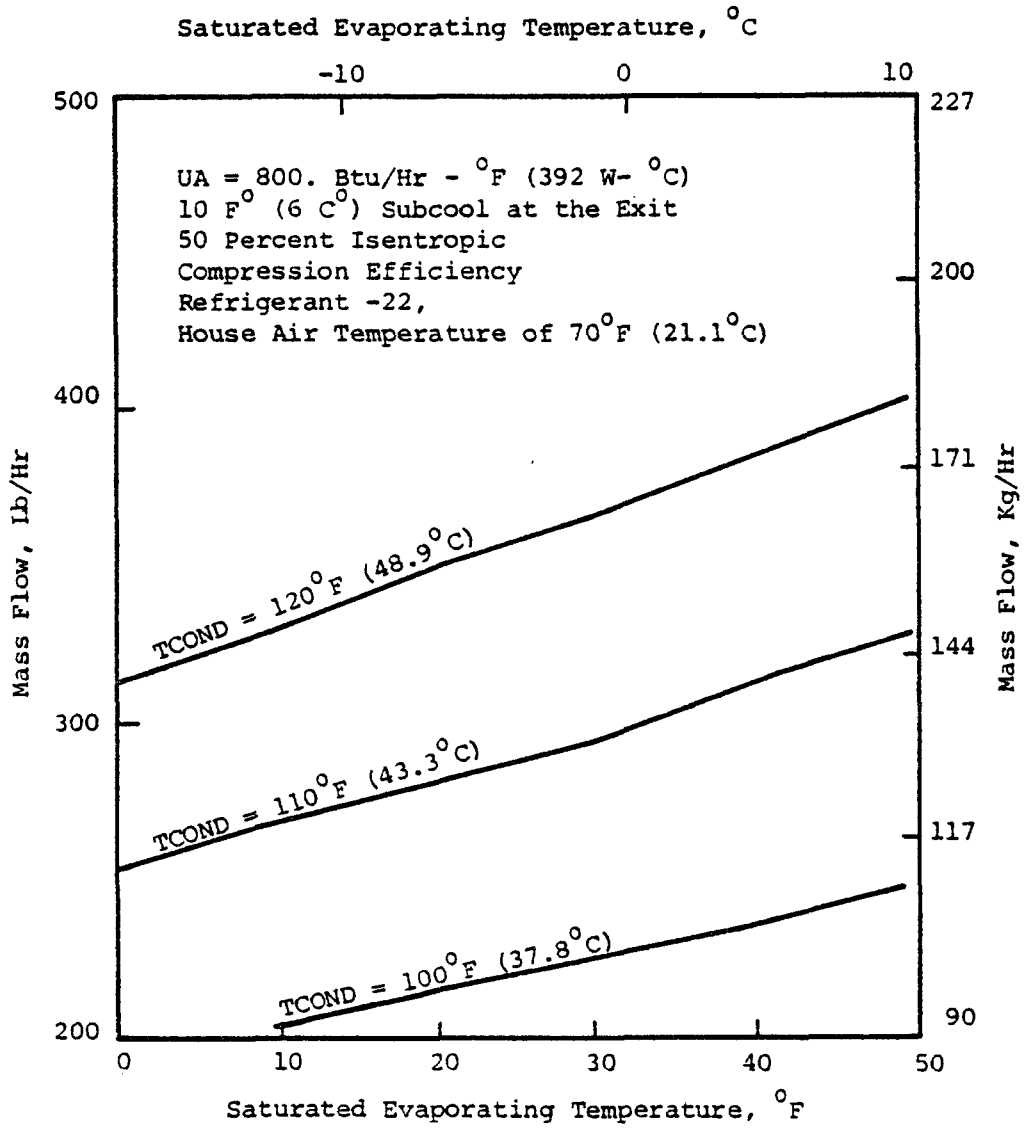

FIGURE 5.3 - CONDENSER CHARACTERISTICS

TABLE 5.3

ENTHALPY CHANGE ACROSS THE ACTIVE EVAPORATOR

TCOND, ^{o}F*	TEVAP, ^{o}F*				
	10	15	20	25	30
90	72.3	72.8	73.3	73.7	74.2
100	69.3	69.8	70.3	70.7	71.2
110	66.1	66.6	67.1	67.5	68.0
120	63.	63.5	64.	64.4	64.9

* $^{o}C = \frac{5}{9}\,(^{o}F - 32)$

Next, the heat transfer characteristics of the active evaporator must be determined by using Newton's law of cooling which states:

$$QEVAP = UA\ (TSOURCE - TEVAP) \qquad 5.2$$

Where QEVAP is the active evaporator heat transfer rate, TEVAP is the evaporating temperatuer, and TSOURCE is the source temperature ($32^{o}F$ or $0^{o}C$). The rates of heat transfer for several values of TEVAP were calculated and are listed in Table 5.4.

Finally, dividing the heat transfer rates of Table 5.4 by the corresponding changes in enthalpy across the evaporator from Table 5.3, the refrigerant mass flow rate is calculated. This mass flow rate then represents an energy balance between the energy change of the refrigerant and the heat transfer rate of the evaporator. Figure 5.4 represents the resulting evaporator characteristics.

5.2.4 Restrictor Model

The restrictor used in this model is composed of three parallel capillary tubes, each with an L/1250•D ratio of .2 and a flow factor (ϕ_1) from Figure 5.5 of 1.85.

In the construction of this model, it is assumed that the entering refrigerant is subcooled 10 F^{o} (6 C^{o}) which agrees with the condenser model.

The first step in modeling the restrictor is to use Figure 5.6 to determine the mass flow rates through a standard size capillary tube with inlet pressure corresponding to various values of the condensing temperature of 10 F^{o} (6 C^{o}) of subcooling. The mass flow rates from Figure 5.6 are then multipled by the dimensional correction factor (ϕ_1). The resulting mass flow rates (MR1) are listed in Table 5.5.

TABLE 5.4

ACTIVE EVAPORATOR HEAT TRANSFER RATES

TEVAP, ^{o}F*	QEVAP, Btu/hr**
10	39,600
15	30,600
20	21,600
25	12,600
30	3,600

* $^{o}C = \frac{5}{9}(^{o}F - 32)$

** kW = 3.413 Btu/hr

ORNL-DWG 81-17917

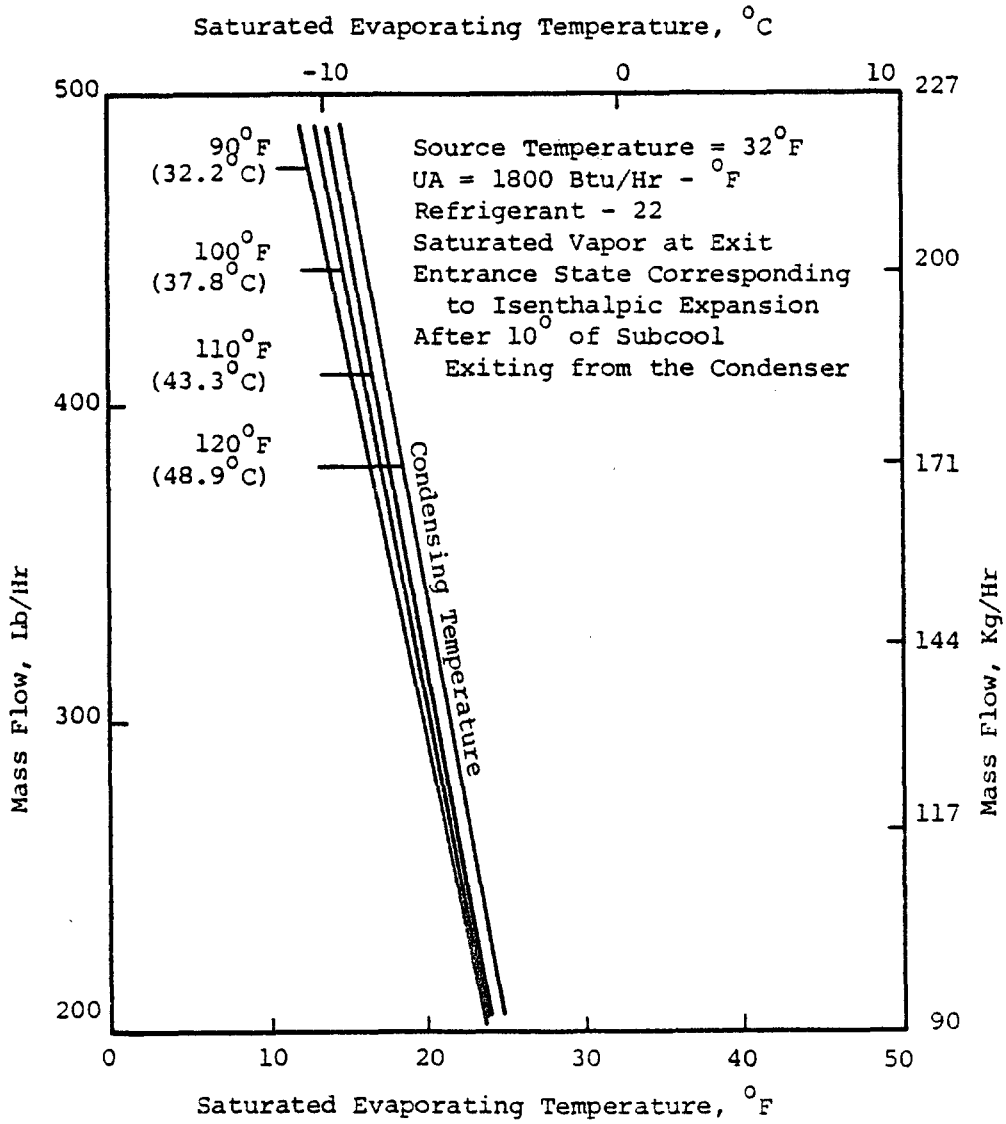

FIGURE 5.4 - ACTIVE EVAPORATOR CHARACTERISTICS

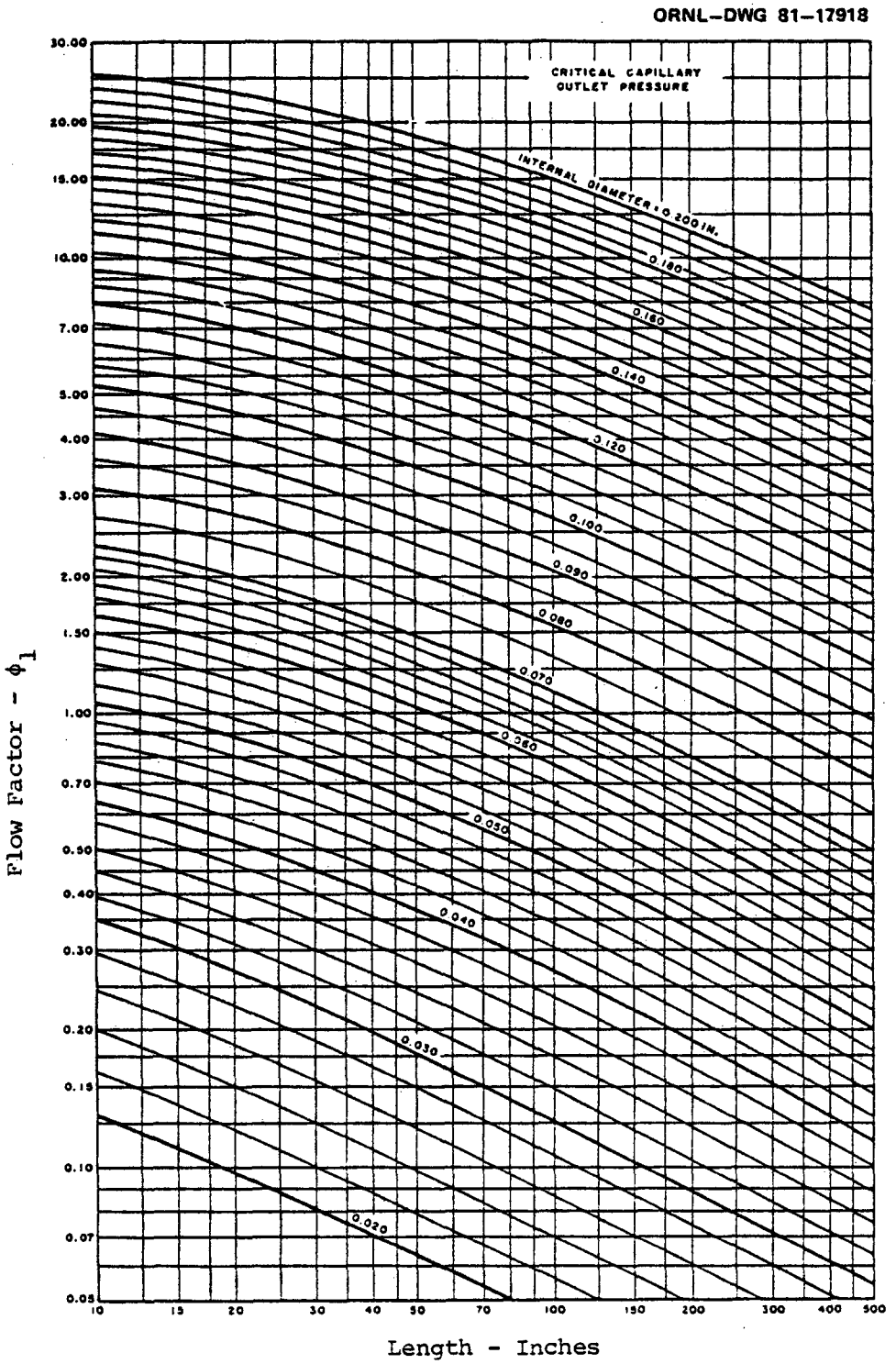

FIGURE 5.5 - CAPILLARY FLOW FACTORS (REFRIGERANTS 12 AND 22)

ORNL-DWG 81-17919

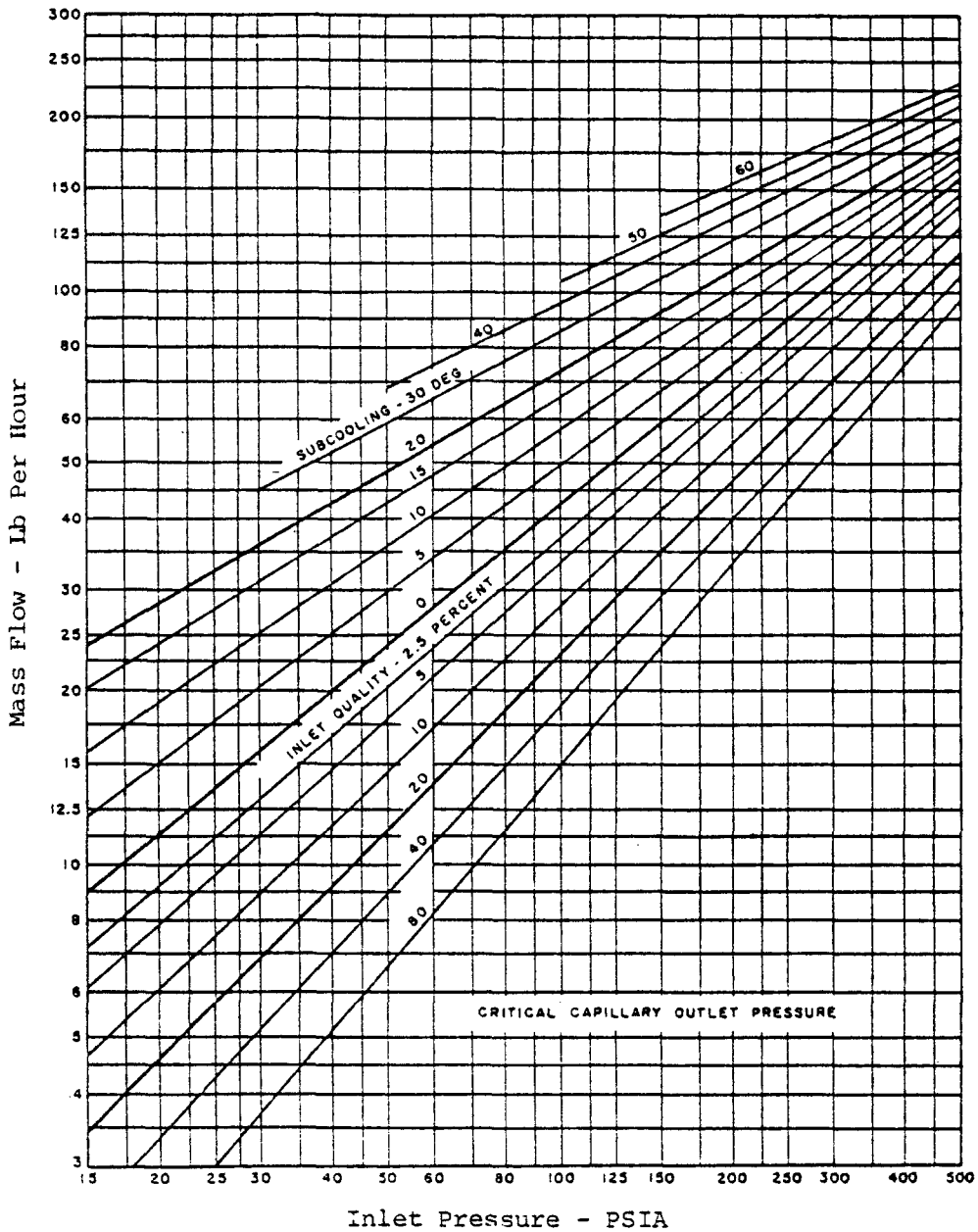

FIGURE 5.6 - BASIC RATING CURVES FOR .064 IN. I.C., 80 IN. LONG CAPILLARY

TABLE 5.5

CRITICAL PRESSURES AND MASS FLOW RATES
AFTER TUBE DIMENSION CORRECTION

TCOND, ^{o}F*	MR1, lb/hr**	PC, psia***
90	92.5	110
100	109	126
110	122	143
120	139	160

* $^{o}C = \frac{5}{9}(^{o}F - 32)$

** 1 Kg/hr = 2.2 lb/hr

*** 1 kPa = 6.895 psi

Once the critical pressures have been determined, Figure 5.7 is used to calculate the critical pressure correction factor (ϕ_2) for various values of the inactive evaporator pressure (see Table 5.6).

Finally, the mass flow rates through each tube with various values of the condensing temperatures and the inactive evaporator pressure are calculated by multiplying the mass flow rates of Table 5.5 by the correction factors of Table 5.6. The total restrictor mass flow rate is then obtained by multiplying the above mass flow rate by three (three parallel tubes). The resultant model is shown in Figure 5.8.

5.2.5 Expansion Device Model

The expansion device used in this model is a Singer Controls thermal-electric expansion valve with an orifice size of .062 inches (.158 cm). The manufacturer's capacity charts were used to determine the mass flow rate through the valve.

As with the compressor curves, most manufacturers present the valve characteristics in terms of refrigeration capacity, and it is necessary to convert to a mass flow rate basis.

For this model, the enthalpy at the entrance to the evaporator is assumed to be the enthalpy corresponding to 100°F (37.8°C) saturated liquid and the enthalpy at the exit from the evaporator is that of saturated vapor at the saturated evaporating temperature (TEVA). With these assumptions, it is possible to determine the refrigeration effect in the evaporator for various values of TEVAP.

Dividing the refrigerating capacity of the valve from the manufacturer's chart by the corresponding refrigerating effect, the mass flow rate through the valve is determined for various values of evaporating temperature and pressure drops across the valve.

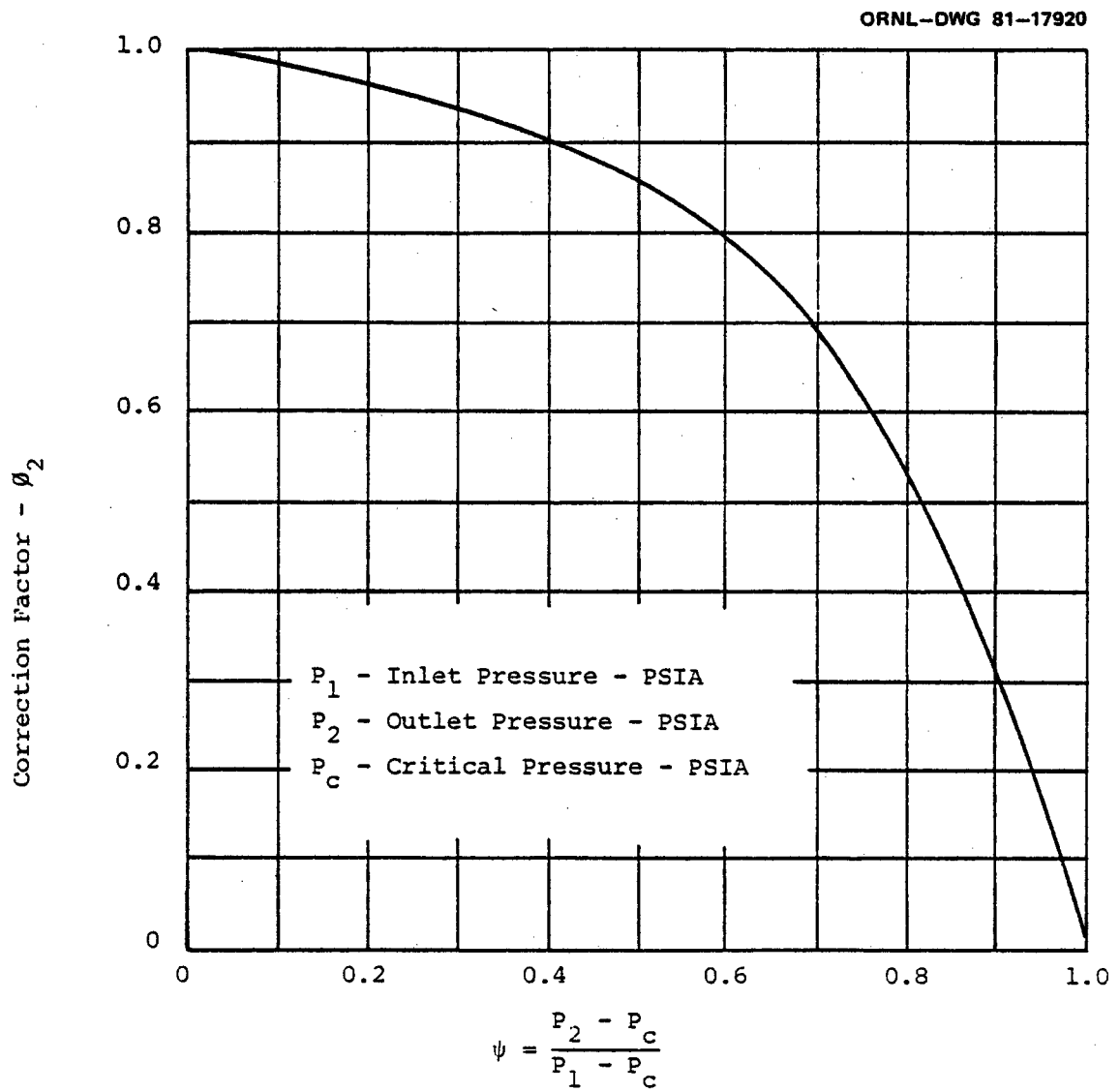

FIGURE 5.7 - CRITICAL CORRECTION FACTOR (REFRIGERANTS 12 AND 22)

TABLE 5.6

CRITICAL PRESSURE CORRECTION FACTORS (ϕ_2)

	Inactive Evaporator Pressure, psia**				
TCOND, °F	160	180	200	220	240
90	.72	.15	0	0	0
100	.90	.77	.42	0	0
110	.97	.92	.81	.57	.69
120	1.00	.97	.93	.85	.69

* $^{o}C = \frac{5}{9}\,(^{o}F - 32)$

** 1kPa = 6.895 psi

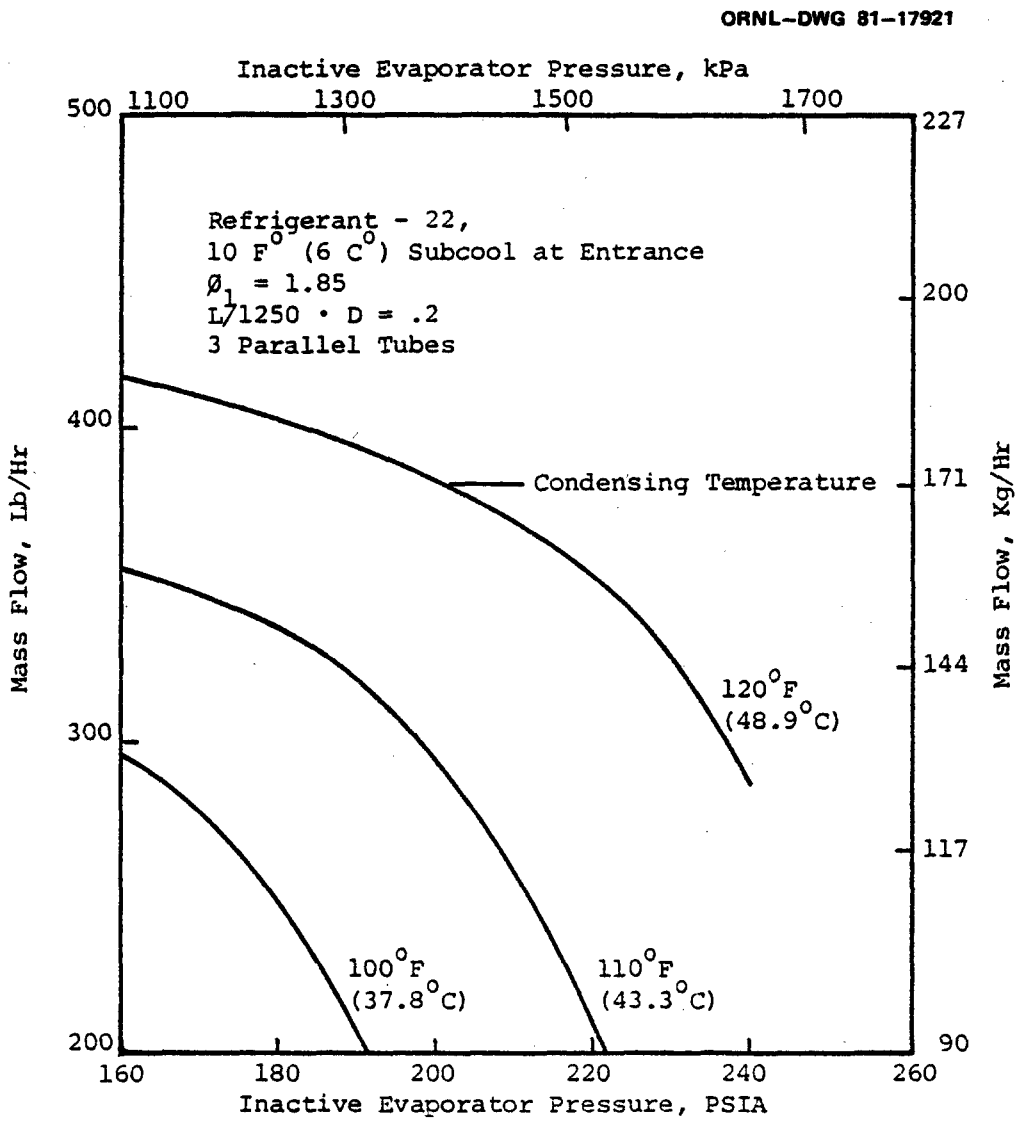

FIGURE 5.8 - RESTRICTOR CHARACTERISTICS

The mass flow rates obtained above can then be plotted, versus the inactive evaporator pressure (P4). This pressure is obtained by adding the pressure drop across the valve to the saturated evaporating pressure. This was done in Figure 5.9.

Corrections for entering temperatures other than 100°F (37.8°C) are discussed in a later section.

5.2.6 Inactive Evaporator Model

The inactive evaporator model which is used in this example is based upon a UA of 180 Btu/hr-°F (87.8 W-°C), which would be reasonable for a conventional air evaporator with free convection. The environmental temperature is assumed to be 0°F (-17.8°C).

5.2.7 Graphical Solution Procedure

Since the energy equation was used to construct the graphical models of each of the components, the continuity equation is used to combine the component models to form the system model. Simply stated, the graphical procedure determines the operating point which produces equal mass flow rates in all components. For clarity, this procedure is presented in English units.

The stepwise procedure is as follows:

1. The performance characteristics of the compressor can be superimposed on the characteristics of the condenser as shown in Figure 5.10. The intersections of equal condensing temperatures represent possible solutions to the governing equations of the two components as a unit (condensing unit). Therefore, a curve can be constructed through these intersections which represents the operating characteristics of the condensing unit (see Figure 5.11).

2. In a similar manner, the active evaporator characteristics can be superimposed over the condensing unit characteristics, as shown in Figure 5.12. As the figure demonstrates, there will be a coincident point where the mass flow through the condensing unit and active evaporator balance. This coincident point represents a possible steady state solution for

ORNL-DWG 81-17922

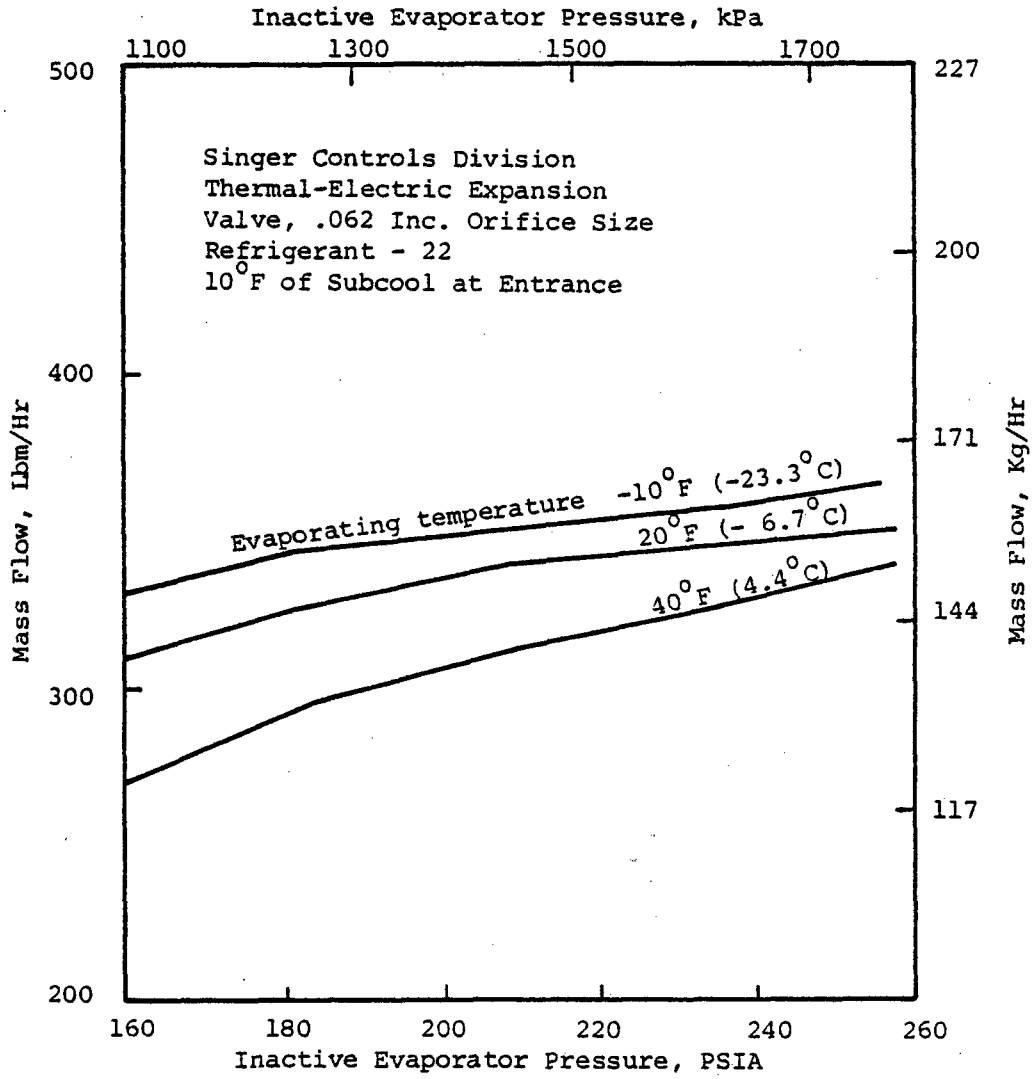

FIGURE 5.9 - EXPANSION VALVE CHARACTERISTICS

ORNL-DWG 81-17923

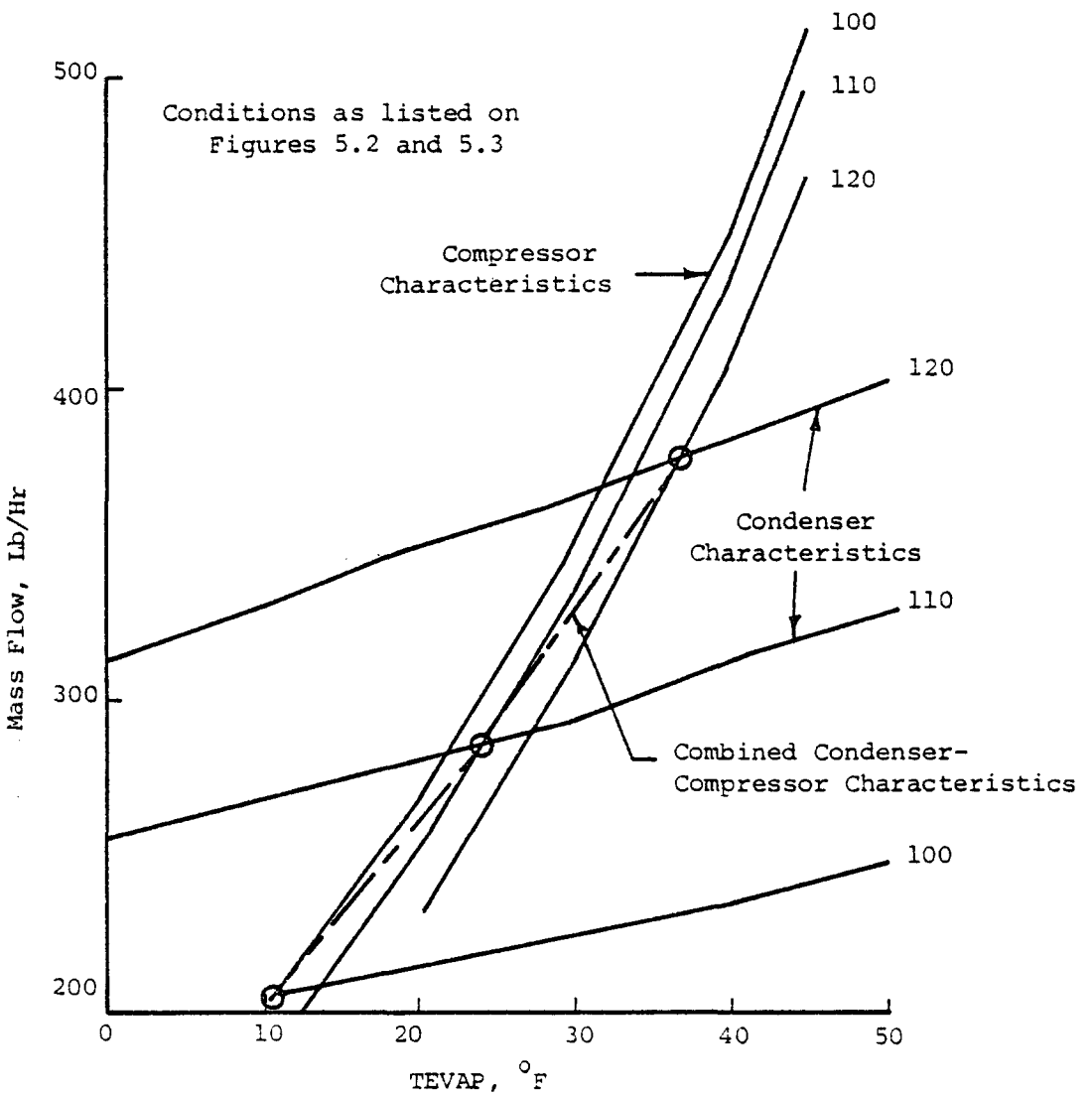

FIGURE 5.10 - COMPRESSOR - CONDENSER OVERLAY OF FIGURES 5.2 AND 5.3

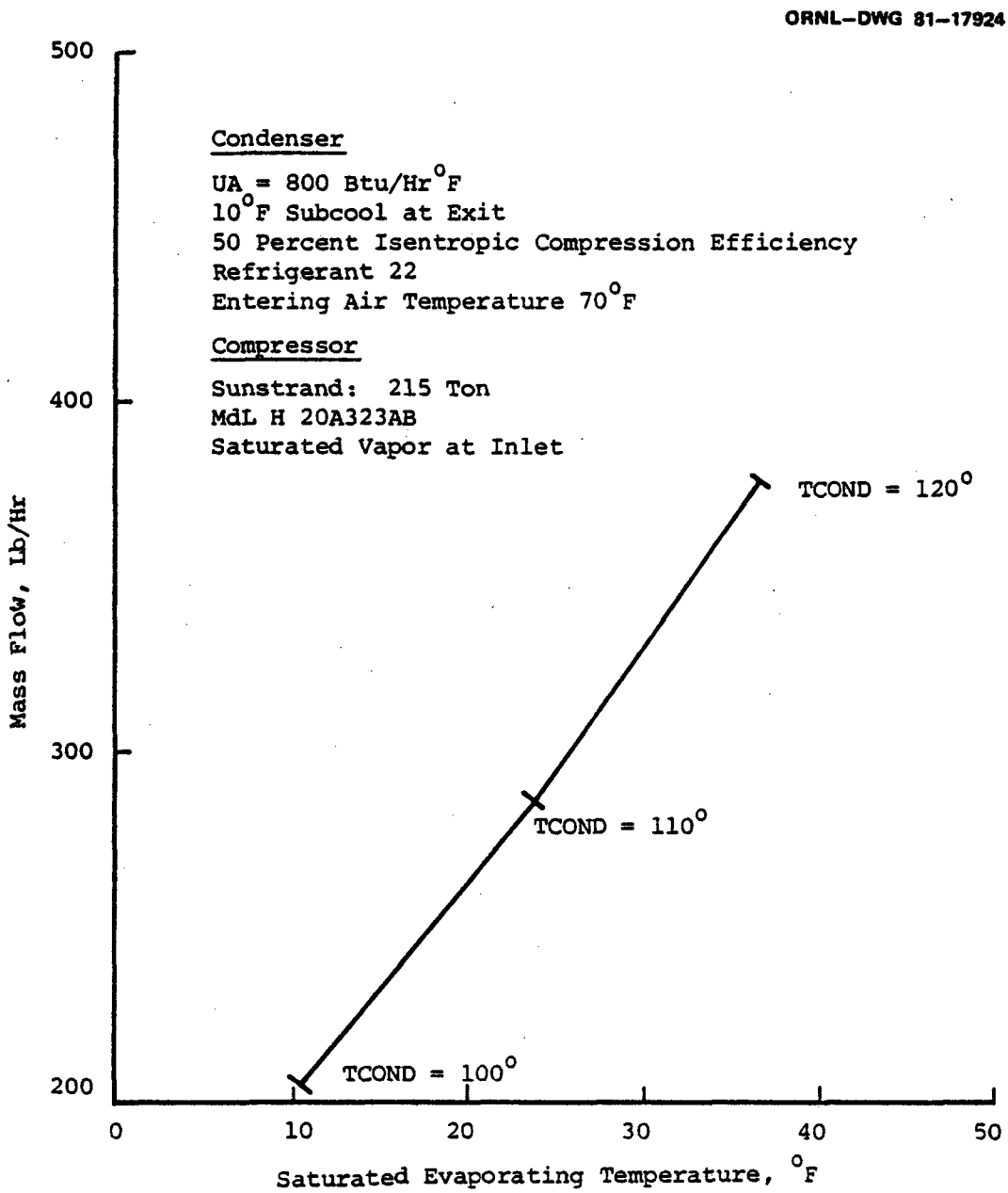

FIGURE 5.11 - CONDENSING UNIT CHARACTERISTICS

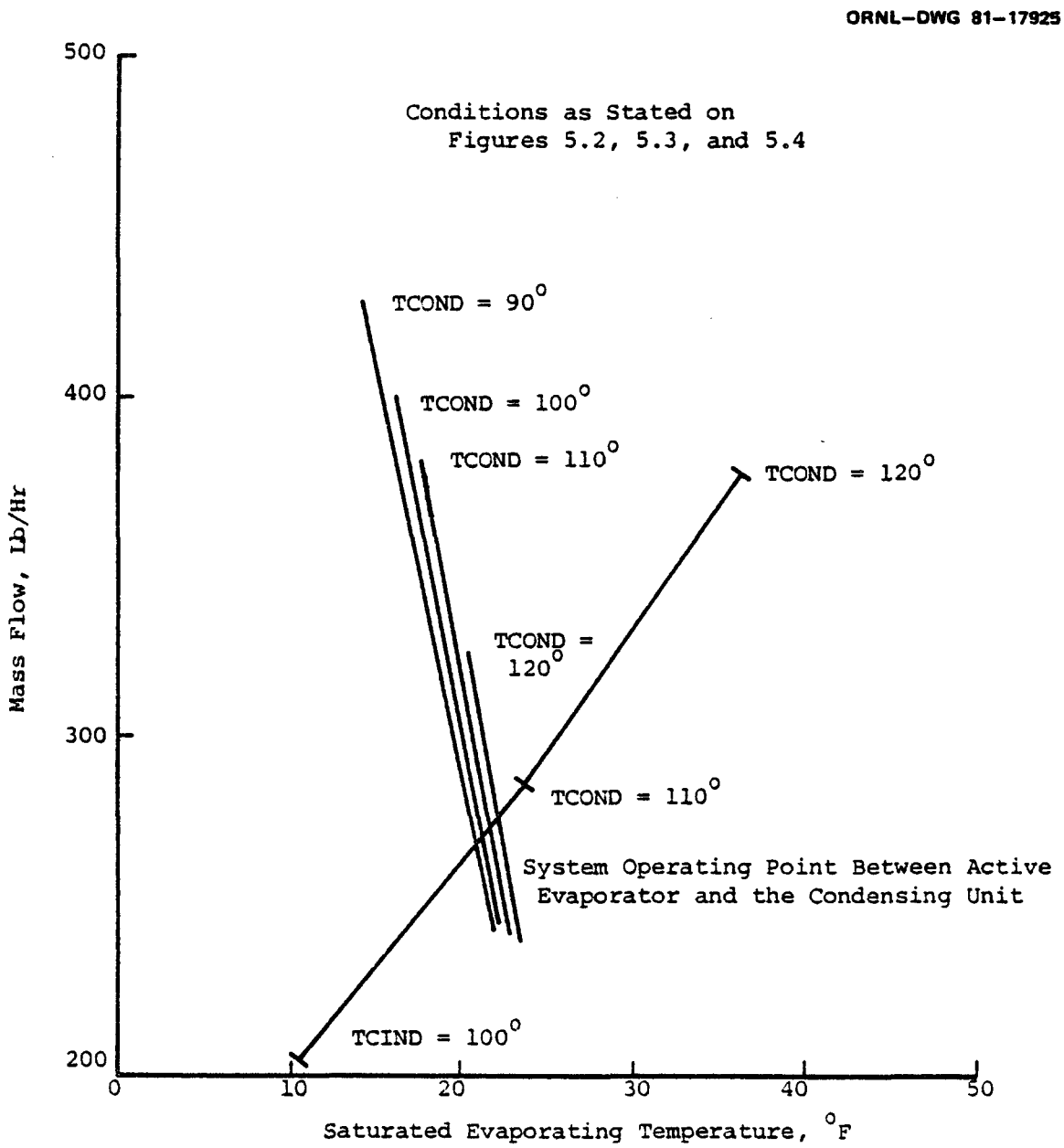

FIGURE 5.12 - EVAPORATOR - CONDENSING UNIT OVERLAY

the system, assuming no subcooling takes place in the inactive evaporator. The effects of subcooling must be analyzed next.

3. In order to analyze the amount of subcooling which takes place in the inactive evaporator, P4 must first be determined. The restrictor and expansion device characteristics must be examined to determine P4. Therefore, the characteristics of the expansion device are first superimposed over the restrictor characteristics. Next, the coincident point from Figure 5.12, which represents the operating characteristic of the evaporator, condenser and compressor, is also superimposed on the restrictor curve by matching the mass flow rate and saturated condensing temperature with equal values (See Figure 5.13). The location of this point will determine P4. Since the expansion valve is able to vary the mass flow rate it passes by monitoring the refrigerant state at the exit from the active evaporator, its performance characteristics vary with time (hunting). Therefore, as long as the valve is not undersized, it will adjust to pass the flow rate which allows the other components to balance.

4. The operating characteristics of the system will be affected by subcooling, since the enthalpy at the entrance to the evaporator will change, as the amount of subcooling is changed. As a result, the rate at which the active evaporator is able to boil the refrigerant will decrease, since it will require additional energy. Also, if the temperature at the entrance to the expansion valve is different from 100°F, the expansion valve characteristics will change. P4, as determined by the first trial (Figure 5.13), was found to be approximately 200 psia, and the condensing temperature was found to be approximately 108°F. Using either a pressure-enthalpy diagram or refrigerant tables, it can be seen that the refrigerant will enter the inactive condenser at 98°F and as a low quality liquid. The inactive evaporator characteristics are then used to determine the change in enthalpy of the refrigerant prior to entering the expansion device. The temperature at the exit from the inactive evaporator is calculated by:

$$T_s - T_c \; (T_{in} - T_c) \exp - (UA/\dot{m}c_p)$$

where: T_c = subcooler environment temperature
T_{in} = refrigerant temperature at the entrance to the subcooler
UA = subcooler UA product

The mass flow rate which is used for this calculation is the mass flow rate predicted by the coincident point of Figure 5.13 (270 lb/hr), and the specific heat will be approximately 0.3 Btu/lbm-°F. Solving this equation yields an exciting temperature of 11°F, with a corresponding enthalpy of 13.4 Btu/lbm.

5. The enthalpy at the exit from the inactive evaporator, which was calculated in step 4, can now be used to correct the

ORNL-DWG 81-17926

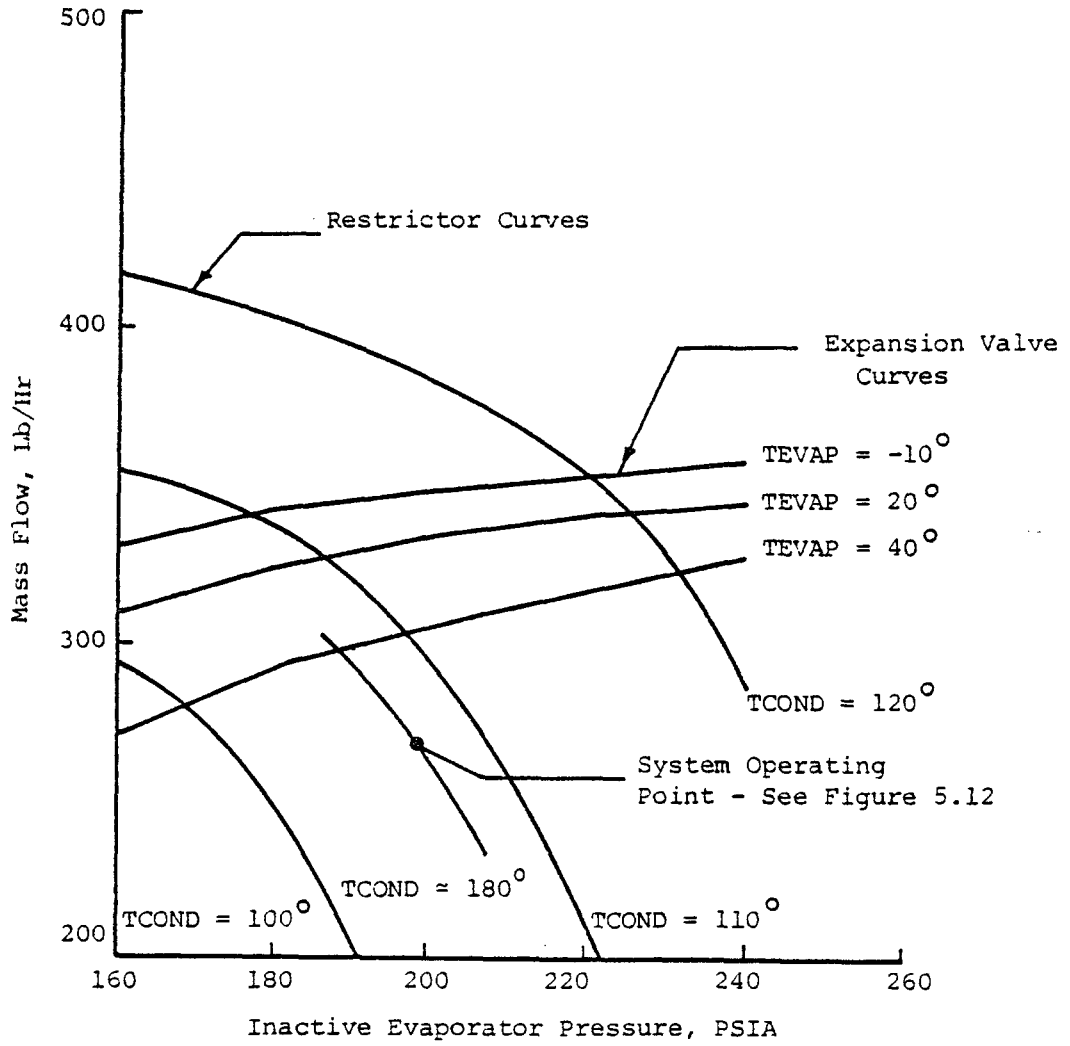

FIGURE 5.13 - SYSTEM CHARACTERISTICS (FIRST TRIAL)

evaporator curves and redo steps 2 through 4. In addition, the expansion valve characteristics must be corrected to reflect an entering liquid temperature other than 100°F. However, since the actual entering temperature is lower than 100°F, the expansion valve will be able to pass a greater mass flow rate and will not limit system operation (see correction factors from Table 5.7). This iterative process (steps 2 4) should be repeated until the predicted enthalpy at the exit from the inactive evaporator is in reasonable agreement with the value which was used for the active evaporator model. This interative process was followed, and the results are shown on Figure 5.14. The results predict that the system will operate with a TCOND of 106°F and a TEVAP of 18.5°F, at a mass flow rate of 255 lb/hr.

6. The heating capacity (CAPH) and heating coefficient of performance can be calculated next. Using Equation 5.1, and the predicted saturated condensing temperature from step 5, the heating capacity for this example was found to be 28,000 Btu/hr.

7. The power draw of the compressor must be calculated, prior to calculating the heating coefficient of performance (COPH). One way in which this can be done is to use refrigeration tables to determine the enthalpy at the entrance to the compressor and the enthalpy at the exit from the condenser. Once these have been determined, the change in enthalpy across the condenser (ΔH) can be calculated by dividing CAPH by the mass flow rate. Then, the work of compression (W) is calculated as follows:

$$W = (\Delta H + H3) - H1$$

The power of compression is then the product of the work of compression and the mass flow rate. For this example, the power of compression is calculated to be 11,409 Btu/hr. COPH can then be calculated by dividing CAPH by the power of compression. The COPH for this example is calculated to be 2.52.

5.3 Development of the Analytical Model

5.3.1 Design Philosophy

The purpose of the mathematical model is to provide a sizing tool which can be used in the design of dual evaporator heat pumps. It is intended that the model will provide a reasonably accurate (±10 percent) prediction of a heat pump's performance, given the basic operating characteristics of the individual components.

TABLE 5.7

REFRIGERANT 22 - TONS OF REFRIGERATION

	Evaporator Temperatures (^{o}F)									
	+40°					+20°				
	Pressure Drop Across Valve (PSIG.)									
Orifice Size	75	100	125	150	175	100	125	150	175	200
.031	.486	.560	.626	.689	.740	.540	.604	.662	.715	.765
.047	.938	1.08	1.21	1.33	1.43	1.04	1.17	1.28	1.38	1.48
.062	1.31	1.51	1.69	1.86	2.00	1.46	1.63	1.79	1.93	2.07
.070	1.56	1.79	2.01	2.21	2.37	1.69	1.88	2.07	2.23	2.38
.078	2.39	2.75	3.08	3.39	3.63	2.66	2.97	3.26	3.52	3.76
.093	3.29	3.80	4.25	4.67	5.02	3.63	4.06	4.45	4.81	5.14
.109	4.05	4.67	5.23	5.76	6.17	4.47	5.00	5.48	5.93	6.34
.125	4.70	5.42	6.06	6.66	7.15	5.16	5.77	6.33	6.83	7.32
.140	5.43	6.16	6.89	7.58	8.12	5.82	6.51	7.14	7.71	8.25
.187	7.84	9.04	10.1	11.1	11.9	8.50	9.49	10.4	11.2	12.0

TABLE 5.7 (continued)

REFRIGERANT 22 - TONS OF REFRIGERATION

	Evaporator Temperatures (°F)									
	-10°					-40°				
	Pressure Drop Across Valve (PSIG.)									
Orifice Size	125	150	175	200	225	150	175	200	225	250
.031	.556	.610	.659	.704	.746	.554	.598	.640	.678	.715
.047	1.08	1.18	1.28	1.36	1.45	1.07	1.16	1.24	1.31	1.38
.062	1.50	1.65	1.78	1.91	2.02	1.50	1.62	1.73	1.84	1.94
.070	1.68	1.84	1.99	2.12	2.24	1.60	1.73	1.84	1.95	2.06
.078	2.73	3.00	3.24	3.46	3.67	2.72	2.94	3.14	3.33	3.51
.093	3.73	4.09	4.42	4.72	5.01	3.66	3.95	4.23	4.48	4.73
.109	4.55	5.00	5.40	5.77	6.12	4.42	4.77	5.11	5.41	5.71
.125	5.22	5.72	6.18	6.61	7.00	5.06	5.46	5.84	6.19	6.53
.140	5.87	6.44	6.95	7.44	7.88	5.69	6.15	6.57	6.97	7.34
.187	8.62	9.43	10.2	10.9	11.5	8.34	9.00	9.63	10.2	10.7

TABLE 5.7 (continued)

The ratings on the previous pages are based on 100°F vapor-free liquid refrigerant entering the valve. To determine valve ratings for other liquid refrigerant temperatures entering the valve, multiply the capacities on the previous pages by the proper multiplier factor listed below.

Liquid Refrigerant Temp. (°F) Entering Valve	Multiplier Factor
80°	1.12
90°	1.06
100°	1.00
110°	.940
120°	.880
130°	.815
140°	.751

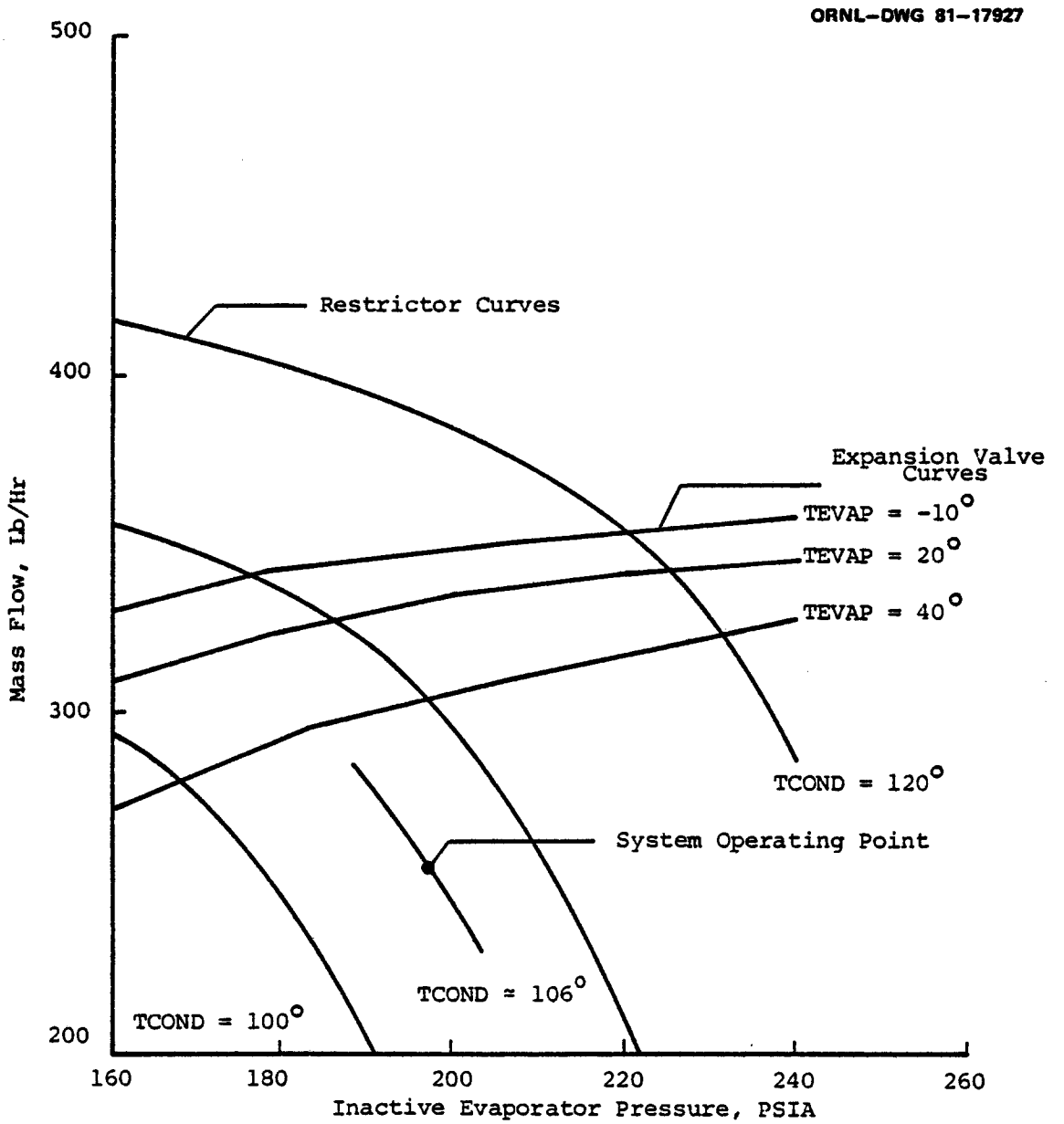

FIGURE 5.14 - SYSTEM CHARACTERISTICS
(FINAL RESULT)

A simplified cycle which neglects pressure drops due to fluid friction is used as the basis of the heat pump model. A comparison of the simplified cycle with an actual cycle is shown in Figure 5.15. The deviation from the actual cycle is exaggerated for emphasis. In order to model the actual cycle, it would be necessary to include specific tube diameters and lengths throughout the heat pump. Not only does this type of model increase the complexity of the computer program considerably, it also increases the amount of input data which is required. Programs of this type can be very cumbersome to use in an approximate sizing operation, where tube dimensions are often unknown. Therefore, in keeping with the purpose of the model, a simplified cycle was used.

However, it is extremely important that the pressure drops are not neglected in the finalized design, since large pressure drops can drastically reduce the performance of a heat pump. As shown in Figure 5.15, refrigerant in the vapor state is especially sensitive to pressure drop, due to fluid friction. This is because the density of the refrigerant vapor decreases rapidly as the pressure decreases, with a resulting rapid increase in the vapor's velocity. Therefore, special care should be taken to design the evaporator-to-compressor and compressor-to-condenser plumbing to minimize these pressure drops.

5.3.2 Dual Series Model

The analytical model determines the overall performance by modeling each individual component in the system. The overall system model is based on three basic principles: the energy equation (first law of thermodynamics), the continuity equation (mass flow balance), and the momentum equation (pressure balance). Therefore, the model for each

ORNL-DWG 81-17928

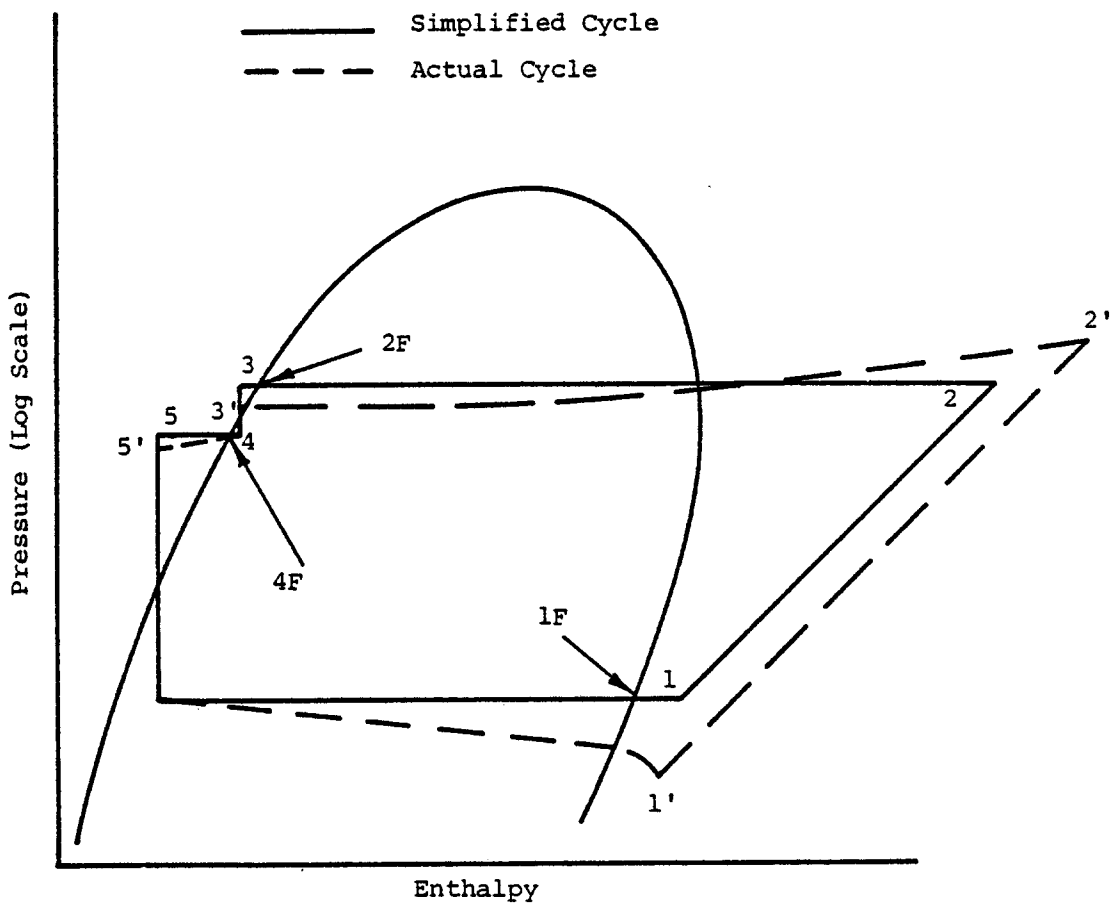

FIGURE 5.15 - EFFECTS OF PRESSURE DROPS DUE TO FLUID FRICTION

individual component must supply the following information to the overall system model: energy loss or gain in the component, mass flow through the component, and pressure increase or drop through the component.

Each component model is contained in a separate subroutine and is called by the overall system model. Therefore, any of the subroutines can be tailored to model an actual component, without affecting the other component models. For the dual series model, there are nine such subroutines.

Once the component processes have been defined, the three fundamental principles (i.e., the energy equation, the continuity equation and the momentum equation) are used to determine the component interactions. Stated simply, the governing equations require an overall energy balance for the cycle, a mass flow balance between all the components and an overall pressure balance for the cycle.

The solution to the governing equations is obtained in the system model by varying three parameters--the saturated evaporating temperature (TEVAP), the saturated condensing temperature (TCOND), and the inactive evaporator pressure (P4)--units all governing equations are satisfied within reasonable accuracy. In the process, the system calls upon individual component models to determine either state points on the cycle or predicted mass flow rates. The component models have been written such that the governing equations for each component are automatically satisfied.

For a more detailed description of the dual series model, the reader should consult (Wood, 1979).

5.3.3 Modification of the Dual Series Model to a General Multiple Source Heat Pump Model

In the multiple source configuration, the total mass flow splits at the restrictor exit and fractional flow is present in each of the subcoolers. This is the main problem in revision of the dual series analytical model. To determine the mass flow rate of refrigerant in each subcooler, it was recognized that the flow system represented the parallel pipe flow problem from fluid mechanics (see Figure 5.16). The known parameters are: the pressure at the inlet, the total mass flow at the inlet and the exit, the length to diameter ratio of each pipe, and the roughness of each pipe. The solution of this type of problem involves the iterative use of the Moody friction factor ob tained from the Moody Chart. Hiller and Glicksman, of the Massachusetts Institute of Technology, have developed a computer subroutine (FRICT) that determines the general Moody friction factor for single phase flow in tubes. The input parameters to this subroutine are: the Reynolds number of the flow, the surface roughness of the passage, and the equivalent diameter of the flow passage (Ellison, 1978). This subroutine is used in the computer program that determines the subcooling mass flow rates.

Once the mass flow rate through each subcooler is calculated, the state variables at the subcooler exits can be determined.

For a more detailed technical discussion of the procedure, the reader should consult (Penoncello, 1980).

Table 5.8 shows the user input parameters required to run the program. These values are entered in a BLOCK DATA routine; therefore, the values can be easilty altered.

ORNL-DWG 81-17929

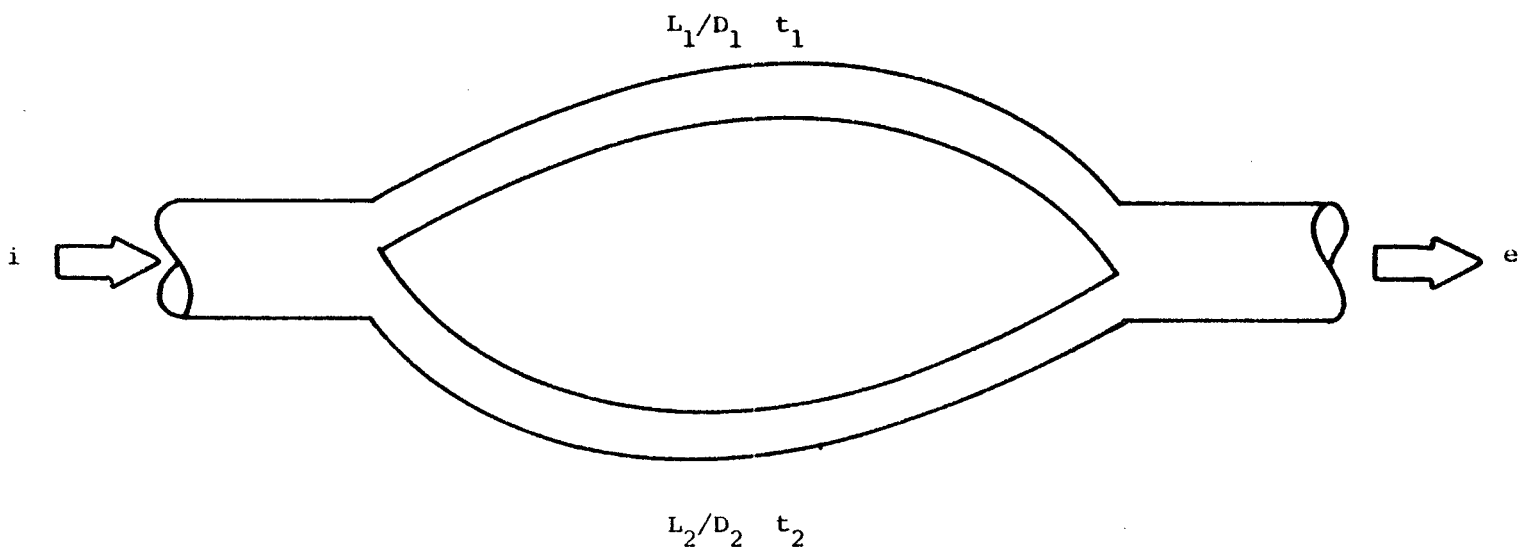

FIGURE 5.16 - PARALLEL PIPE FLOW SYSTEM

TABLE 5.8

INPUT PARAMETERS FOR SYSTEM SIMULATION PROGRAM

Parameter	Description
NR	Type of refrigerant
TH	Condenser sink temperature
TL	Active evaporator (earth) source temperature
TCOOL (1)	Environment temperature around air subcooler
TCOOL (2)	Environment temperature around earth subcooler
TEVAP	Initial guess at the saturated evaporator temperature
US (1)	Overall heat transfer coefficient of air subcooler
US (2)	Overall heat transfer coefficient of earth
AS (1)	Heat transfer area of air subcooler
AS (2)	Heat transfer area of earth subcooler
UC	Overall heat transfer coefficient for the subcooler
AC	Heat transfer area of the condenser
UE	Overall heat transfer coefficient for the evaporator
AE	Heat transfer area of the evaporator
DIMR1	L/1250D for a single restrictor cap tube
DIMR2	ϕ, for a single cap tube (from ASHRAE equipment volume - Chapter 20)
NTR	Number of parallel cap tubes in the restrictor
IEXP	Type of expansion valve
DIMX1	Sizing characteristic of expansion device
SP	Compressor speed
VD	Displacement volume of compressor
SEFF	Isentropic efficiency of the compressor

An example of the program output is seen in Table 5.9. Also, a complete listing of the program is shown in Appendix 5.a (on microfiche — see inside back cover).

TABLE 5.9

EXAMPLE OF COMPUTER MODEL OUTPUT

```
*****************************************************************************
   MULTIPLE SOURCE HEAT PUMP SIMULATION DURING STEADY STATE OPERATION
*****************************************************************************

COMPRESSOR:
 DISPLACEMENT VOLUME, CUBIC FEET =   0.0021
 SPEED, RPM =   3500.0000
 ISENTROPIC EFFICIENCY, PERCENT =   0.6000

CONDENSER:
 SURFACE AREA, SQUARE FEET =   80.000
 OVERALL HEAT TRANSFER COEFFICIENT, BTU/HR-SQ.FT-F =   50.0000

SUBCOOLER:
 SUBCOOLER 1 SURFACE AREA, SQUARE FEET =   18.00
 SUBCOOLER 1 OVERALL HEAT TRANSFER COEFFICIENT, BTU/HR-SQ.FT-F =   1.00
 SUBCOOLER 2 SURFACE AREA, SQUARE FEET =   3.00
 SUBCOOLER 2 OVERALL HEAT TRANSFER COEFFICIENT, BTU/HR-SQ.FT-F =   1.00

ACTIVE EVAPORATOR:
 SURFACE AREA, SQUARE FEET =   18.0000
 OVERALL HEAT TRANSFER COEFFICIENT, BTU/HR-SQ.FT-F =   100.0000

RESTRICTOR:
 NUMBER OF PARALLEL TUBES =   5
 FLOW FACTOR =   1.8500
 1/1250 D =   0.20000

EXPANSION DEVICE:
 TYPE OF EXPANSION DEVICE; THERMOSTATIC EXPANSION VALVE
 NOMINAL REFRIGERATION CAPACITY, TONS =   1.6146

ENVIRONMENTAL CONDITIONS:
 CONDENSER SINK TEMPERATURE, DEGREES FAHRENHEIT =   75.0000
 LINE 3620 IN OUTPUT:  PROCESSING TIME LIMIT REACHED

 ACTIVE EVAPORATOR SOURCE TEMPERATURE, DEGREES FAHRENHEIT =   30.0000
 SUBCOOLER 1 ENVIRONMENT TEMPERATURE, DEGREES FAHRENHEIT =   40.00
 SUBCOOLER 2 ENVIRONMENT TEMPERATURE, DEGREES FAHRENHEIT =   30.00

REFRIGERANT TYPE IS R-22
```

TABLE 5.9 (continued)

EXAMPLE OF COMPUTER MODEL OUTPUT

```
*****************************************************************************
                          RESULTS OF THE SIMULATION
*****************************************************************************

UNITS ARE:  TEMPERATURE IN DEGREES FAHRENHEIT
            ENTHALPY IN BTU/LBM
            QUALITY IN PERCENT
 T1 = 30.0000   H1 =   106.0057
 SATURATED EVAPORATOR TEMPERATURE =   7.50000

CONDITIONS AT THE ENTRANCE TO THE CONDENSER:
 T2 =   168.1299   H2 =   128.3031
 SATURATED CONDENSER TEMPERATURE =   78.9551

CONDITIONS AT THE EXIT FROM THE CONDENSER:
 X3 =   0.5195   H3 =   73.4181

CONDITIONS AT THE EXIT FROM THE RESTRICTOR:
 SATURATION TEMPERATURE =   53.1128
 X4 =   0.5742

CONDITIONS AT THE EXIT FROM THE SUBCOOLER:
 X5 =   0.5660   H5 =   72.5495

*****************************************************************************

HEATING CAPACITY, BTU/HR =   15820.3086

HEATING COEFFICIENT OF PERFORMANCE =   2.1267
STOP
TIME  45.5 SECS
```

6.0 WEATHER DATA ANALYSIS

6.1 Background

6.1.1 Historical

As we all know by experience, the thermal characteristics of weather are highly variable. It is not uncommon to find a temperature variation of 80 F^{o} (45 C^{o}) for any given day of the year in almost any location in the country. The average temperature for that day, however, will be representative of the season and locality; this leads one to think that City "A" is generally cooler or hotter than City "B". The thermal designer is of course, faced with the problem of quantifying the behavior of the weather. Historically, he has approached this problem utilizing a "worse case" analysis. In other words, his lack of knowledge forced him to overdesign his system to be sure that the load would be met. This approach was, of course, successful in that the load was always met; but it has created other problems which are now starting to be addressed.

The thermal designer of the past was successful in meeting the load because of three major reasons:

1. The system being installed were "demand" systems capable of meeting the worst case load and did not rely upon internal storage;

2. The systems were supported by an energy storage system which was external to the thermal delivery system and usually were very large. Examples include electric utilities, oil distribution, and gas utilities; and

3. The demand systems were usually oversized by 10 to 30 percent.

When non-renewable energy sources were inexpensive, readily available, and undergoing development, these characteristics were desirable

and consequently encouraged. This situation is now changing; some of the principal forces behind this change are:

1. The limited and foreign controlled oil and gas resources;

2. Environmental problems associated with the production of a greater demand capability (e.g., more power plants);

3. The huge capital investment in our energy production and delivery system that is only being utilized at an average load fraction of 0.6 to 0.7 and yet is being stressed by demand on some occasions; and

4. The realization that there will have to be a gradual shift to renewable resources from non-renewable ones.

6.1.2 New Thermal Design Constraints

Thus, the thermal designer is now facing a new set of constraints when designing a thermal system; these constraints include:

1. The thermal system must minimize operational costs and energy usage;

2. Thermal storage, both high and low temperature, units becoming an integral part of the system design;

3. An analysis of the system's economics under varying utility and full rate structure must be done;

4. Prediction of the total energy usage for the system is generally required;

5. Minimization of the system's demand (rate of energy usage); and

6. A capability to provide thermal conditioning upon thermal load demand without utilization of the electrical utility during peak demand periods.

Historically, none of these constraints were important. Off-peak utility rate structures had been used only sporadically in the U.S., virtually no thermal storage systems had been used, energy costs were so low that operational costs due to energy were ignored, total energy use was not important and this was rarely monitored, and the utility was always willing and capable of providing energy on demand to

thermally condition an occupied space. The outcome of this situation was that the thermal designers problem was to minimize capital expenditure, while meeting the demand thermal load. To accomplish this goal, he needed little weather information. Much of the residential heating and air-conditioning equipment is built, installed, and sized, even today, on a very crude estimated (guess) basis. This estimate usually is based upon only the demand heating load as calculated by a simplified procedure similar to ASHRAE's.

The situation changes dramatically when a thermal system utilizes storage; particularly, if this is being used to carry the thermal load during high utility demand periods or to provide thermal conditioning during severe (hot or cold) weather conditions. Since the utility load, as well as the thermal load, is strongly dependent upon weather conditions, the designer must now understand enough about the weather conditions to size the thermal storage unit. For diurnal systems, this problem is minimal; the storage system is sized on a worst case basis which is usually taken as 24 hours of peak load (either heating or cooling). In this case, the cost of the thermal storage system is small relative to other components and consequently, the worst case philosophy is acceptable. However, as the size of the storage increases, and the economics of the storage become more important, this philosophy starts to become untenable. In short, the designer of thermal systems with intermediate (three days to a week or so) or long term (months) storage must understand the weather data, as well as the other constraints in order to successfully address the problem.

Of the two design problems of thermal storage, intermediate vs. long term, the intermediate one offers by far the larger challenge.

The reason for this is simple; the variability of the thermal load's total energy requirements decreases as the term of the thermal load increases. The implication is that the designer must now know at least two major weather parameters which up to now have not been required. These are:

1. The integrated average thermal load as a function of both calendar time and an elapsed time period (e.g., four days, two weeks, etc.); and

2. The variance associated with that thermal load for the desired time period for a given level of confidence (e.g., 90 percent, 99 percent, etc.).

Neither of the above parameters are readily available in the literature. The first of the two parameters has been addressed here. The parameter allows a designer to size a thermal storage system but have little information as to what the confidence level (probability that the system will meet load) of his system is as a function of elapsed time. The second problem has not been addressed here, due to lack of funding; both problems are of top priority and need to be further addressed if thermal storage systems are to be successfully designed.

The weather analysis reported below was initiated as part of an effort to model the thermal behavior of ACES and solar systems. As the work proceeded, it became clear that the design problems associated with the weather data were of paramount importance; in fact, the analysis of the weather data may be the single most important contribution made during this project. This is in spite of the fact that it was not one of the original goals.

6.1.3 Existing Weather Data

The common sources of weather data are:

1. local weather bureau data;

2. the National Climatic Center weather tapes;

3. the Department of Defense (DOD) bin weather data; and

4. the American Society of Heating, Air Conditioning, and Refrigeration Engineers.

Often the first is difficult to obtain, and usually either does not contain sufficient information or is in a format that makes it difficult to numerically process. The second format is the highest quality data source available, although the number of stations are quite limited, and in some cases, the term of collection is short (less than ten years). The quality of the data is such that it could be used to answer the confidence level questions associated with thermal storage design. It is the only source known to us that provides data in a format and at a density that would allow the confidence level question to be answered. The third source provides bin weather data that allows a reasonable estimate of the thermal storage requirements to be made. It is this data source that has been processed here to a format that allows the designer to determine the average thermal storage requirements as a function of calendar time and elapsed time. Unfortunately, it is impossible to address the confidence level question with these data as reported. The last data source is the one that has historically been used to size demand systems.

6.1.4 Load Calculations

The thermal load on any building is a complex function of many parameters. These parameters include: the solar load, the infiltration rate, the building use, the orientation of the building, the occupant's living pattern and the quality of the buildings construction. All of these are building specific parameters and are highly

variable from building to building. Thus, it would not be reasonable to account for them in a general weather analysis, even though they must be accounted for in the final design. The weather parameters that are universal and, in residential market, paramount are the ambient temperature and relative humidity conditions.

If one is trying to determine a thermal system's load, he must know both the universal and specific conditions. The work presented here has been designed to be coupled with the results from a building specific analysis; independently of the procedure used (ASHRAE, M.B.S., or a commercial program). This can be easily done by increasing the thermal storage size calculated on the basis of the data given below (universal thermal load) in proportion to the ratio of the total thermal load (specific universal) to the universal thermal load.

No attempt has been made here to displace, generate, or replace load calculation procedures for structures. In fact, we have attempted to present the data in a fashion that will allow new undeveloped, as well as old, procedures to utilize the data. One of the biggest problems with modeling thermal loads for structures is what weather data base to use. In computer modeling, this generally requires that a "typical" year be used, with well defined temporal weather data. The word typical can, and usually does, take on a variety of definitions, making the results difficult to interpret. Unless a good statistical data base is available, it will be impossible to design thermal systems that minimize conflict with both nature and man-made systems. The work below is a first step toward trying to develop such a data base.

6.2 Presentation of Weather Data

As pointed out above, the thermal load on a structure is dependent largely upon the environment temperature and relative humidity conditions. It is only these impacts that will be considered here; other building specific loads will not be. Thus, during the heating season only the ambient temperature is important; while during the cooling season both the ambient temperature and the relative humidity play important roles. This leads to two analyses; one for the heating season and one for the cooling season.

6.2.1 Heating Season

The basic assumption used in processing the heating season weather data is that there exists a UA product for each structure which is nominally invariant, with respect to ambient temperature or time. Thus, the heat load on a structure, $\dot{q}_s$, can be expressed simply:

$$\dot{q}_s = (UA)_s \left(T_D - T_A\ (t)\right) \qquad 6.1$$

where:

$\dot{q}_s$ = heat transfer rate between the structure and the environment;

t = time;

$(UA)_s$ = overall heat transfer coefficient-area product;

T_D = the constant design temperature (65^oF, 18^oC); and

$T_A\ (t)$ = the ambient temperature which is a function of time.

If Equation 6.1 is divided by UA and integrated over a time period, we arrive at a parameter which is proportional to the energy consumed during the time period and that is independent of the structure. This parameter has the units of temperature and time. Thus, we get a specific energy parameter, E, which is equal to:

$$E = \int_{time} \frac{\dot{q}}{UA} dt = \int_{time} \left(T_D - T_A(t)\right) dt \qquad 6.2$$

A parameter that approximates E is the ASHRAE degree-day parameter (DD). This parameter is defined by ASHRAE as:

$$N = 65 - \frac{(T_H + T_L)}{2} \qquad 6.3$$

where:

N = the number of ^{o}F - Days

T_H = the high temperature in a day in ^{o}F

T_L = the low temperature in a day.

The DOD bin weather data also allows the calculation of a parameter which is proportional to E, and reasonably closer to it because averaging of the temperature is not done as it is with the ASHRAE formula. In the DOD data, the cumulative hours observed for each 5 F^{o} (2 C^{o}) interval is reported on a month by month basis. An example is given in Table 6.1. Thus, it becomes possible to calculate the numerical value of the temperature - time integral of Equation 6.2 for either the entire month or as a function of ambient temperature. This is done by simply forming the product between the temperature difference from $65^{o}F$ and the number of hours that temperature interval was observed during that month. This results in data as shown in Table 6.2. The column "Total DG Hours" gives the energy frequency distribution for the month of September (both elapsed time and calendar time). The temperature frequency distribution is given by the hours observed. The cumulative energy requirement for September is given by the last column "Total Cumul DG Hours". These data are used as the basis for calculating the entire temperature and energy frequency cumulative distributions. An example of the cumulative and distribution energy requirements is shown in Table 6.3 for both cases analyzed. These data are calculate by summing up

TABLE 6.1

EXAMPLE OF DOD BIN WEATHER DATA
BOSTON, MASSACHUSETTS
SEPTEMBER

Temp. Range F	Hrs Observed				
	02 To 09	10 To 17	18 To 01	Tot.	Mean Coin Wet Bulb
100/104	0	0	0	0	0
95/ 99	0	0	0	0	0
90/ 94	0	2	0	2	74
85/ 89	0	10	0	10	73
80/ 84	0	24	2	26	70
75/ 79	4	37	8	49	67
70/ 74	19	44	26	89	64
65/ 69	29	46	39	114	61
60/ 64	41	37	40	118	57
55/ 59	40	28	44	112	53
50/ 54	44	11	43	98	50
45/ 49	32	1	23	56	45
40/ 44	17	0	10	27	41
35/ 39	10	0	4	14	36
30/ 34	4	0	1	5	31
25/ 29	0	0	0	0	28
20/ 24	0	0	0	0	0
15/ 19	0	0	0	0	0

TABLE 6.2

CALCULATION OF THE CUMULATIVE ^{o}F-HRS FOR
BOSTON, MASSACHUSETTS
SEPTEMBER

Temp. Range	Dev. From 65	Total		
		Hours Obs.	Total DG. Hrs	Total Cumul DG. Hrs
69/65	0	114	0	0
64/60	5	118	590	590
59/55	10	112	1120	1710
54/50	15	98	1470	3180
49/45	20	56	1120	4300
44/40	25	27	675	4975
39/35	30	14	420	5395
34/30	35	5	175	5570
29/25	40	0	0	5570

TABLE 6.3

SEASON 1 CUMULATIVE FRACTION HEATING LOADS FOR
BOSTON, MASSACHUSETTS
OCTOBER 1 TO MAY 31

	Case 1: Using the Lower Limit of Each Temperature Range				Case 2: Using the Midpoint of Each Temperature Range			
Temp. Range F	Dev. From 65 F	Total DG. Hrs	Cumul. DG. Hrs	Cumul. Fraction Ht. Load	Dev. From 65 F	Total DG. Hrs	Cumul. DG. Hrs	Cumul. Fraction Ht. Load
65/ 69	0	0	0	0.00	0.	0.	0.	0.00
60/ 64	5	1270	1270	0.77	3.	762.	762.	0.50
55/ 59	10	3870	5140	3.13	8.	3096.	3858.	2.52
50/ 54	15	7215	12355	7.52	13.	6253.	10111.	6.59
45/ 49	20	10900	23255	14.15	18.	9310.	19921.	12.99
40/ 44	25	17175	40430	24.60	23.	14801.	35722.	23.29
35/ 39	30	23910	64340	39.15	28.	22316	58038.	37.84
30/ 34	35	27825	92165	56.08	33.	26235.	84273.	54.94
25/ 29	40	23000	115165	70.07	38.	21850.	106123.	69.19
20/ 24	45	17235	132400	80.56	43.	16469.	122592.	79.92
15/ 19	50	12600	145000	88.23	48.	12096.	134688.	87.81
10/ 14	55	8745	153745	93.55	53.	8427.	143115.	93.31
5/ 9	60	6300	160045	97.38	58.	6090.	149205.	97.28

TABLE 6.3 (Continued)

SEASON 1 CUMULATIVE FRACTION HEATING LOADS FOR
BOSTON, MASSACHUSETTS
OCTOBER 1 TO MAY 31

	Case 1: Using the Lower Limit of Each Temperature Range				Case 2: Using the Midpoint of Each Temperature Range			
Temp. Range F	Dev. From 65 F	Total DG. Hrs	Cumul. DG. Hrs	Cumul. Fraction Ht. Load	Dev. From 65 F	Total DG. Hrs	Cumul. DG. Hrs	Cumul. Fraction Ht. Load
0/ 4	65	2340	162385	98.80	63.	2268.	151473.	98.75
-5/ -1	70	1190	163575	99.53	68.	1156.	152629.	99.51
-10/ -6	75	450	164025	99.80	73.	438.	153067.	99.79
-15/-11	80	240	164265	99.95	78.	234.	153301.	99.95
-20/-16	85	85	164350	100.00	83.	83.	153384.	100.00

TABLE 6.4

ESTAR AND VSTAR VALUES FOR
BOSTON, MASSACHUSETTS
OCTOBER 1 TO MAY 31

	Case 1: Using the Lower Limit of Each Temp. Range			Case 2: Using the Midpoint of Each Temp. Range		
Temp. Range F	Cumul. Fraction Ht. Load	ESTAR Degree Days	VSTAR Eq. Full Load Days	Cumul. Fraction Ht. Load	ESTAR Degree Days	VSTAR Eq. Full Load Days
65/ 69	0.00	6847.9	80.6	0.00	6391.0	77.0
60/ 74	0.77	6795.0	79.9	0.50	6359.3	76.6
55/ 59	3.13	6633.7	78.0	2.52	6230.3	75.1
50/ 54	7.52	6333.1	74.5	6.59	5969.7	71.9
45/ 49	14.15	5879.0	69.2	12.99	5561.0	67.0
40/ 44	24.60	5163.3	60.7	23.29	4902.6	59.1
35/ 39	39.15	4167.1	79.0	37.84	3972.8	47.9
30/ 34	56.08	3007.7	35.4	54.94	2879.6	34.7
25/ 29	70.07	2049.4	24.1	69.19	1969.2	23.7
20/ 24	80.56	1331.3	15.7	79.92	1283.0	15.5
15/ 19	88.23	806.3	9.5	87.81	779.0	9.4
10/ 14	93.55	441.9	5.2	93.31	427.9	5.2
5/ 9	97.38	179.4	2.1	97.28	174.1	2.1

TABLE 6.4 (Continued)

ESTAR AND VSTAR VALUES FOR
BOSTON, MASSACHUSETTS
OCTOBER 1 TO MAY 31

	Case 1: Using the Lower Limit of Each Temp. Range			Case 2: Using the Midpoint of Each Temp. Range		
Temp. Range F	Cumul. Fraction Ht. Load	ESTAR Degree Days	VSTAR Eq. Full Load Days	Cumul. Fraction Ht. Load	ESTAR Degree Days	VSTAR Eq. Full Load Days
0/ 4	98.80	81.9	1.0	98.75	79.6	1.0
-5/ -1	99.53	32.3	0.4	99.51	31.5	0.4
-10/ -6	99.80	13.5	0.2	99.79	13.2	0.2
-15/-11	99.95	3.5	0.0	99.95	3.5	0.0
-10/-16	100.00	0.0	0.0	100.00	0.0	0.0

the monthly results for each bin. The two cases are reported to show the degree of dependency upon design temperature assumption. In this case the heat load changes by seven percent between the two cases. This change is caused by a temperature difference of only 2.5 F^o (1 C^o).

Two other parameters are reported which are a measure of the energy requirements. These parameters are ESTAR, E^*, and VSTAR, V^*. They are defined as:

$$E^* = \frac{(1 - CFHL) * CUMUL\ DG.\ HRS.}{24}$$

and

$$V^* = \frac{E^*}{\Delta T_{DESIGN}}$$

They represent respectively the cumulative energy distribution in ^oF - Days and in the number of days of full load operation. Table 6.4 shows the data that correspond to Table 6.3 converted to these units. VSTAR is a useful parameter because it relates the demand load to the storage energy requirements. For example, if a designer wanted to install a storage system that would meet 6.5 percent of the seasonal load, he could determine by inspection of Table 6.4 the following:

1. The total storage energy, ETOTAL, requirement would be:

$$ETOTAL = \frac{COP - 1}{COP} * ESTAR \times (UA)_s$$

where:

COP = coefficient of performance of the machine extracting energy from the storage;

$(UA)_s$ = overall heat transfer coefficient for the structure under consideration

ESTAR = 441.9 ^oF - Days

2. This amount of storage is the equivalent to operation of his demand system for 5.2 days without shutdown.

Thus, the two parameters provide the designer a quick way to calculate the energy storage requirement and a way to qualitatively measure the probability that the storage would be depleted (e.g.: how often does a demand system run, five days without shutdown?)

6.2.2 Cooling Season

The analysis of the data to determine cooling load is more complex than heating, due to the water vapor present in the air that must be accounted for during cooling operations. Thus, the cooling load analysis is broken into two parts: a load due to conduction through the walls, and a load due to air infiltration. The two analyses are separated in the tabular data so that any building can be analyzed.

The conduction load for cooling is essentially identical to that of heating. The data based upon Table 6.1, as processed for the cooling load, are shown in Table 6.5.

The calculation to air change is a bit more complex in that the changes in enthalpy of the air/water mixture must be calculated. The Keenan and Kayes equation of state and data for low pressure water vapor were used to calculate the latent portion of the enthalpy, the sensible portion was calculated using a constant specific heat for the air. The mean coincident wet bulb temperature was used to calculate saturation pressure. The details of this calculation are reported by Lindem and Somerville, 1979. In this manner both the latent and total air enthalpies can be calculated.

The specific (building independent) energy requirements due to an air change are given by:

TABLE 6.5

SEASON 2 CONDUCTION CUMULATIVE FRACTION COOLING LOADS FOR
BOSTON, MASSACHUSETTS
JULY 1 TO AUGUST 31

	Case 1: Using the Upper Limit of Each Temperature Range				Case 2: Using the Midpoint of Each Temperature Range			
Temp. Range F	Dev. From 76 F	Total DG. Hrs OBS	Cumul. DG. Hrs OBS	Cumul. Fraction Cl. Load	Dev. From 76 F	Total DG. Hrs OBS	Cumul. DG. HRS OBS	Cumul. Fraction Cl. Load
70/ 74	0	0	0	0.00	0.0	0.	0.	0.00
75/ 79	3	648	648	20.31	1.0	216.	216.	9.47
80/ 84	8	1160	1808	56.68	6.0	870.	1086.	47.63
85/ 89	13	853	2666	83.57	11.0	726.	1812.	79.47
90/ 94	18	432	3089	97.12	16.0	384.	2196.	96.32
95/ 99	23	92	3190	100.00	21.0	84.	2280.	100.00
100/104	28	0	3190	100.00	26.0	0.	2280.	100.00

$$E_{AC} = \int_t \frac{\dot{q}_{AC}}{\dot{m}C_p}\, dt = \int_t \left(h_D - h\ (t) \right) dt$$

where:

E_{AC} = energy required over the time period t;

$\dot{q}_{AC}$ = cooling load due to air changing at a mass flow rate, $\dot{m}$, with a specific heat C_p;

h_D = the design enthalpy condition 28.42 $\frac{\text{Btu}}{\#}$;

h (t) = the ambient air enthalpy.

Examples of the latent portion and the total load due to air changes are given in Tables 6.6 and 6.7. It should be noted that the basis $\left(\frac{\text{Btu-hrs}}{\text{lbm of dry air}}\right)$ for the energy calculation is different than it is for conduction (^{o}F-hrs). Thus, the two specific energy requirements cannot be added. In order to do a general analysis, either the actual building must be designed or an assumption must be made concerning the relative size of the two loads.

Finally, the month by month distribution for the cooling loads is given for both conduction and the total air change. Examples are given in Tables 6.8 and 6.9. A month by month distribution is also given for the heating loads. An example of this can be found in Table 6.10.

A computer program was used to generate all of the above data for forty cities. The forty cities analyzed together with their ASHRAE heating load are listed in Table 6.11. The program is described in the following section.

6.3 Weather Data Analysis

The OWDA input data is from the "Manual of Engineering Weather Data" by the Departments of the Air Force, the Army and the Navy.

TABLE 6.6

LATENT COOLING LOAD DUE TO AN AIR CHANGE FOR
BOSTON, MASSACHUSETTS
JULY 1 TO AUGUST 31

Temp. Range F	Total Btu Hrs. Per # Dry Air	Cumul. Btu Hrs. Per # Dry Air	Latent Cumul. Fraction Cl. Load
70/ 74	818.	818.	40.48
75/ 79	286.	1104.	54.63
80/ 84	463.	1568.	77.56
85/ 89	300.	1868.	92.39
90/ 94	132.	1999.	98.90
95/ 99	22.	2022.	100.00
100/104	0.	2022.	100.00

All negative deviations from computed design conditions have been set to zero.

TABLE 6.7

TOTAL (LATENT PLUS SENSIBLE) COOLING LOAD DUE
TO AN AIR CHANGE FOR
BOSTON, MASSACHUSETTS
JULY 1 TO AUGUST 31

Temp. Range F	Total Btu Hrs. Per # Dry Air	Cumul. Btu Hrs. Per # Dry Air	Total Cumul. Fraction Cl. Load
70/ 74	818.	818.	31.86
75/ 79	338.	1156.	45.01
80/ 84	672.	1829.	71.18
85/ 89	474.	2303.	89.64
90/ 94	224.	2526.	98.35
95/ 99	42.	2569.	100.00
100/104	0.	2569.	100.00

All negative deviations from computed design conditions have been set at zero.

TABLE 6.8

COOLING LOAD DUE TO CONDUCTION IN DEGREE HOURS
BOSTON, MASSACHUSETTS

	January		February		March		April	
Temp. Range	Total	Cumul	Total	Cumul	Total	Cumul	Total	Cumul
74/ 70	0.	0.	0.	0.	0.	0.	0.	0.
79/ 75	0.	0.	0.	0.	0.	0.	12.	12.
84/ 80	0.	0.	0.	0.	0.	0.	16.	28.
89/ 85	0.	0.	0.	0.	0.	0.	13.	41.
94/ 90	0.	0.	0.	0.	0.	0.	0.	41.
99/ 95	0.	0.	0.	0.	0.	0.	0.	41.
104/100	0.	0.	0.	0.	0.	0.	0.	41.
	May		June		July		August	
74/ 70	0.	0.	0.	0.	0.	0.	0.	0.
79/ 75	93.	93.	228.	228.	342.	342.	306.	306.
84/ 80	120.	213.	432.	660.	648.	990.	512.	818.
89/ 85	117.	330.	260.	920.	481.	1471.	377.	1195.
94/ 90	36.	366.	144.	1064.	270.	1741.	162.	1357.
99/ 95	0.	366.	23.	1087.	69.	1810.	23.	1380.
104/100	0.	366.	0.	1087.	0.	1810.	0.	1380.

TABLE 6.9

COOLING LOAD DUE TO AIR CHANGE IN B.T.U. HOURS PER LB. DRY AIR FOR BOSTON, MASSACHUSETTS

	January		February		March		April	
Temp. Range	Total	Cumul	Total	Cumul	Total	Cumul	Total	Cumul
74/ 70	0.	0.	0.	0.	0.	0.	0.	0.
79/ 75	0.	0.	0.	0.	0.	0.	1.	1.
84/ 80	0.	0.	0.	0.	0.	0.	3.	4.
89/ 85	0.	0.	0.	0.	0.	0.	3.	6.
94/ 90	0.	0.	0.	0.	0.	0.	0.	6.
99/ 95	0.	0.	0.	0.	0.	0.	0.	6.
104/100	0.	0.	0.	0.	0.	0.	0.	6.
	May		June		July		August	
74/ 70	0.	0.	110.	110.	488.	488.	330.	330.
79/ 75	7.	7.	113.	223.	27.	516.	311.	641.
84/ 80	22.	29.	206.	428.	376.	891.	297.	937.
89/ 85	41.	70.	109.	537.	266.	1157.	208.	1146.
94/ 90	13.	83.	57.	594.	134.	1291.	89.	1235.
99/ 95	0.	83.	9.	603.	30.	1321.	13.	1248.
104/100	0.	83.	0.	603.	0.	1321.	0.	1248.

TABLE 6.10

HEATING LOAD DUE TO CONDUCTION IN DEGREE HOURS FOR BOSTON, MASSACHUSETTS

	January		February		March		April	
Temp. Range	Total	Cumul	Total	Cumul	Total	Cumul	Total	Cumul
69/ 65	0.	0.	0.	0.	0.	0.	0.	0.
64/ 60	5.	5.	5.	5.	20.	20.	185.	185.
59/ 55	10.	15.	20.	25.	100.	120.	630.	815.
54/ 50	60.	75.	90.	115.	345.	465.	1320.	2135.
49/ 45	200.	275.	200.	315.	880.	1345.	2540.	4675.
44/ 40	1075.	1350.	925.	1240.	2575.	3920.	4125.	8800.
39/ 35	2880.	4230.	3240.	4480.	5580.	9500.	3480.	12280.
34/ 30	4725.	8055.	4725.	9205.	6195.	15695.	2275.	14555.
29/ 25	5120.	14075.	4880.	14085.	4280.	19975.	640.	15195.
24/ 20	4635.	18710.	4185.	18270.	2340.	22315.	180.	15375.
19/ 15	4550.	23260.	3150.	21420.	1050.	23365.	50.	15425.
14/ 10	3410.	26670.	2145.	23565.	495.	23860.	0.	15425.
9/ 5	2520.	29190.	1800.	25365.	180.	24040.	0.	15425.
4/ 0	1105.	30295.	1170.	26535.	65.	24105.	0.	15425.

TABLE 6.10 (Continued)

HEATING LOAD DUE TO CONDUCTION IN DEGREE HOURS FOR BOSTON, MASSACHUSETTS

	January		February		March		April	
Temp. Range	Total	Cumul	Total	Cumul	Total	Cumul	Total	Cumul
-1/ -5	350.	30645.	420.	26955.	0.	24105.	0.	15425.
-6/-10	225.	30870.	150.	27015.	0.	24105.	0.	15425.
-11/-15	160.	31030.	0.	27105.	0.	24105.	0.	15425.
-16/-20	85.	31115.	0.	27105.	0.	24105.	0.	15425.

TABLE 6.11

LISTING OF CITIES' WEATHER DATA STUDIED BY
A.S.H.R.A.E. DEGREE DAYS

City	Degree Days
Tampa, Florida	383
Laredo, Texas	797
New Orleans, Louisiana	1385
San Diego, California	1458
Phoenix, Arizona	1765
Charleston, North Carolina	2033
Los Angeles, California	2061
Dallas, Texas	2363
Atlanta, Georgia	2961
Santa Marie, California	2967
Memphis, Tennessee	3232
Lubbock, Texas	3578
Tulsa, Oklahoma	3860
Washington, D.C.	4224
Bishop, California	4275
Albuquerque, New Mexico	4348
Portland, Oregon	4635
Louisville, Kentucky	4882
Trenton, New Jersey	4980
Dodge City, Kansas	4985
Boston, Massachusetts	5634
Salt Lake City, Utah	6052
Chicago, Illinois	6155
Denver, Colorado	6283
Spokane, Washington	6655
Sioux City, Iowa	6951
Buffalo, New York	7062
Casper, Wyoming	7410
Great Falls, Montana	7750
Burlington, Vermont	8269
Minneapolis, Minnesota	8382
Alpena, Michigan	8506
Bismarck, North Dakota	8851
Glasgow, Montana	8996
Sault Sant Marie, Michigan	9048
Caribou, Maine	9767
Grand Forks, North Dakota	9901
Duluth, Minnesota	10000
Anchorage, Alaska	10864
Nome, Alaska	14171

This data consists of the average number of hours observed within a specific $5^{o}F$ temperature range for each month of the year. This data is further divided into three equal time periods of the day and the daily total. The three time periods are: (1) 02 to 09 hours, (2) 10 to 17 hours, and (3) 18 to 01 hours. The temperature ranges for the heating load analysis are from $65/69^{o}F$ down to the minimum temperature observed. The temperature ranges for the cooling load analysis are from $70/74^{o}F$ up to the maximum temperature observed.

The heating load due to conduction losses, cooling load due to conduction gains, and cooling load due to air change are analyzed for the entire year and for two heating/cooling seasons. Five statistics are calculated in the heating load analysis. These are: (1) temporal frequency of occurrence of temperature, (2) total and cumulative degree hours, (3) cumulative fraction heating load, (4) energy requirements (E* and V*), and (5) a comparison of calculated degree hours/24 with the ASHRAE degree days.

Five statistics are calculated in the cooling load analysis. These are: (1) temporal frequency of occurrence of temperature, (2) total and cumulative degree hours of cooling load due to conduction, (3) cumulative fraction cooling load due to conduction, (4) total and cumulative Btu hours per pound of dry air for the latent and total cooling load due to air change, and (5) cumulative fraction cooling load for the latent and total cooling load due to air change. The lengths of the heating/cooling seasons are dependent on an input design parameter. This parameter is the percentage of the yearly load the user wishes to be included within the bounds of the second heating/cooling season. The third heating/cooling season is then initialized

to start one month later and end one month earlier than the second heating/cooling season.

Both the heating load due to conduction losses and the cooling load due to conduction gains are examined for two cases. Case one uses the lower bound of each temperature range for heating and the upper bound of each range for cooling. This case yields a conservative estimate of the heating/cooling loads. Case two uses the midpoint of each temperature range for both heating and cooling and provides a less conservative estimate.

Table 6.12 provides a list of output tables generated by the OWDA. Details of the program operation are defined in Lindem and Somerville, 1979.

6.4 Design Use of the Weather Data

The weather data have been arranged to allow the designer to make a reasonable estimate as to the quantity of storage required to meet a given goal. For example:

1. Given the size of the thermal storage and the design thermal load, the fraction of the seasonal load that will be met, the equivalent number of days of full load operation, the specific building energy requirements and what the impact of incrementally changing the size of the load can all be determined. These data allow the thermal designer to perform an economic analysis on the size of the storage required for a particular application. This type of situation probably exists in an off-peak air conditioning application;

2. Given the desire to operate a multiple source heat pump at or above a given temperature, the designer can determine the specific storage volume and COP.

3. Given the desire to operate a multiple source heat pump as an off-peak air conditioner at or above a given temperature. Here, the designer can, presuming the ratio of the total air change cooling load to total cooling load is known, determine the quantity of storage required. This is an important capability because this allows the designer to design a system which has a smaller compressor size with the size of the storage. This results in a fraction of the demand that would ordinarily be experienced, can

TABLE 6.12

LIST OF OUTPUT TABLES BY OWDA

Table	Definition
1-1 through 1-6	Input Bin Weather Data and calculated enthalpy values for each month
2-1 through 2-2	Temperature frequency of occurrence for temperatures used in heating and cooling load calculations
3-1 through 3-3	Seasonal (yearly) cumulative fraction heat loads
4-1 through 4-9	Monthly cumulative fraction heat loads with 1000-1700 hour breakdown
5-1 through 5-3	Seasonal (yearly) storage energy draws at a C.O.P. = 1
6	Comparison of computer degree hours/24 and ASHRAE degree days
7-1 through 7-2	Seasonal (yearly) cumulative fraction cooling loads due to conduction gains (f-hrs.)
8	Seasonal (yearly) cumulative fraction latent cooling loads due to air change (Btu-hrs.)
9	Seasonal (yearly) cumulative fraction total cooling loads due to air change (Btu-hrs.)
10-1 through 10-7	Monthly energy draws for heating and cooling

reduce the capital investment required, and increase the payback rate. The trade off with winter heating requirements can also be examined. This application has particular value at latitudes where the cooling load dominates. This is usually found at latitudes of approximately 33°N.

4. Application to ACES design. The design steps used in designing an ACES with this data are:

   a. The design heating and cooling loads must be determined utilizing some method.

   b. The seasonal energy requirements for heating and cooling are calculated using the data of Tables 3, 7, and 9 from (Somerville, et al., 1979).

   c. A condensing unit is selected and its coefficient of perforance is determined. This unit must be capable of meeting the heating load demand;

   d. The heating storage energy requirements are determined from Table 3 with:

$$S_H = \frac{COP_H - 1}{COP_H} \cdot E_H$$

   where:

   S_H = heating storage energy requirement;

   E_H = seasonal energy requirement for the heating season;

   COP_H = the coefficient of performance <u>based upon compressor only</u> characteristics.

   e. The cooling storage energy requirements are determined directly from Tables 7 and 9 and the information provided by Step a above.

   f. The volume of the thermal storage is calculated, based upon the energy density of the storage mechanism.

   g. If the heating storage requirement is larger than the cooling one, then the excess energy that must be disposed of can be calculated.

   h. The size of the cooling load heat exchanger can be determined, using the results of Steps a, d, e, and g.

6.5 Conclusions and Recommendations

The weather analysis presented above has been shown to be useful in the designing of any system that utilizes thermal storage. A first attempt

has been made to present weather data for the cooling season in a format that allows the designer to easily estimate cooling loads due to conduction and air changes.

The data presented are based upon average weather data and, thus, can be expected to represent the expected storage requirements. These data do not address the variance of the weather, which is of utmost importance to the designer. Thus, it is recommended that a statistical analysis of the weather be undertaken which defines the confidence level of the average weather data as a function of both the elapsed time and calendar time. Thus, data to answer the questions cited below, is needed and should be determined:

1. What are the mean energy requirement for a nine day (or some other period) period in February?

2. What are the energy requirements for the same period, at the same time, at a confidence level of 90, 95, or 99 percent?

7.0 HEAT TRANSFER CHARACTERISTICS OF A FLAT PLATE ICE-MAKER

7.1 Introduction and Summary of the Work

7.1.1 Summary of Work

The use of ice-maker plate evaporators on heat pumps has shown different performance characteristics when operating in different air environments. This difference has been observed both during laboratory tests and in actual residential application.

An analytical model has been developed to predict the evaporator heat transfer rates as a function of the environmental conditions. This model consists of two principle parts. The first part models the film coefficient of the water on the plates and its dependence on the surrounding air temperature. This model makes use of Prandtl's boundary layer equations to analyze the flow, both for the water and the air. A generalized solution was obtained through the use of dimensional analysis. The second principle part of the analytical model consists of an analysis of the overall heat transfer for the ice-maker evaporator. This analysis enables the rate of ice formation on the evaporator plate to be modeled. All of the analytical results have been generalized and are presented in a dimensionless fashion.

An experimental program was undertaken to verify the results of the analytical model. The experimental apparatus made use of an insulated enclosure constructed in the laboratory to allow the control of the air temperature surrounding the evaporator plate. Experimental data was taken at four different air temperatures, ranging from 35°F (1.7^{o}C) to 85°F (29.4^{o}C).

The results of both the analytical model and the experimental program demonstrate that the temperature of the air environment surrounding the ice-maker evaporator plates has a significant influence on the evaporator's heat transfer characteristics. The influence was sufficient to effectively double the ice formation rate in testing the evaporator over the range of air temperatures stated above. The air temperature surrounding the evaporator plates, thus, has a significant impact on the operating characteristics and coefficient of performance of a plate type ice-maker heat pump.

The numerical results of the film coefficient model could not be verified by the experimental results because of difficulty in establishing the proper initial conditions. In addition, there is some uncertainty in the experimental determination of the film coefficient by the procedure undertaken. The model, however, was proven qualitatively accurate and does provide a meaningful base on which to predict the influence of the air environment on the ice-maker plate heat transfer characteristics.

7.1.2 Typical Application

In a typical ice-maker application, water is pumped up and distributed over the top edge of a flat plate and allowed to free fall down the plate, forming a thin uniform sheet of water over the plate. This creates an excellent film coefficient and allows energy to be readily extracted from the water. If the surface of the plate is below 32°F (0°C), a thin sheet of ice is formed which continues to grow as long as energy is extracted from the water. In an ice-maker application, the interior of the plate acts as the evaporating passage for low temperature and pressure freon. Since the freon is often boiling,

high internal film coefficients are often encountered. Typically, the overall heat transfer coefficient is on the order of 45 $\frac{Btu}{Hr\ Ft^2\ F^o}$ ($256\ \frac{W}{m^2\ C^o}$).

The plate tested and shown in Figure 7.1, consists of two thin, type 304 stainless steel, plates "seamed" together to form the freon flow passage. A cross-sectional view of the flow passage is highlighted in Figure 7.1. The plates are commercially available ice-maker plates, manufactured by Turbo Refrigeration in Denton, Texas. The water is pumped over the plate and frozen directly onto the plate. Periodically the ice is "harvested" by melting the layer immediately adjacent to the plate, and the ice drops into the tank.

Extensive tests of a heat pump using the ice-maker plate evaporator configuration were performed in the laboratory at the University of North Dakota (Somerville and Wendschlag, 1977). These laboratory results were used to specify the equipment in an actual residential application in North Dakota (Somerville, Mathsen, Loken, Svard, and Wendschlag, 1977). Performance data from the actual application, however, differs somewhat from the laboratory tests. One of the reasons for this difference is attributed to the differences in the air environments surrounding the ice-maker evaporators. During the laboratory tests, the surrounding air temperature was often more than 70 F^o (21.1 C^o) and never lower than 40^oF (4.4^oC). In the residential application, however, the air temperature surrounding the evaporator plates was very close to that of the ice/water mixture in the tank, or about 33^oF (1^oC). Since the film of water flowing over the plates is very thin (about 0.25 in. (.064 cm)), the surrounding air conditions can play an important role in the rate of heat transfer to the freon.

ORNL-DWG 81-17930

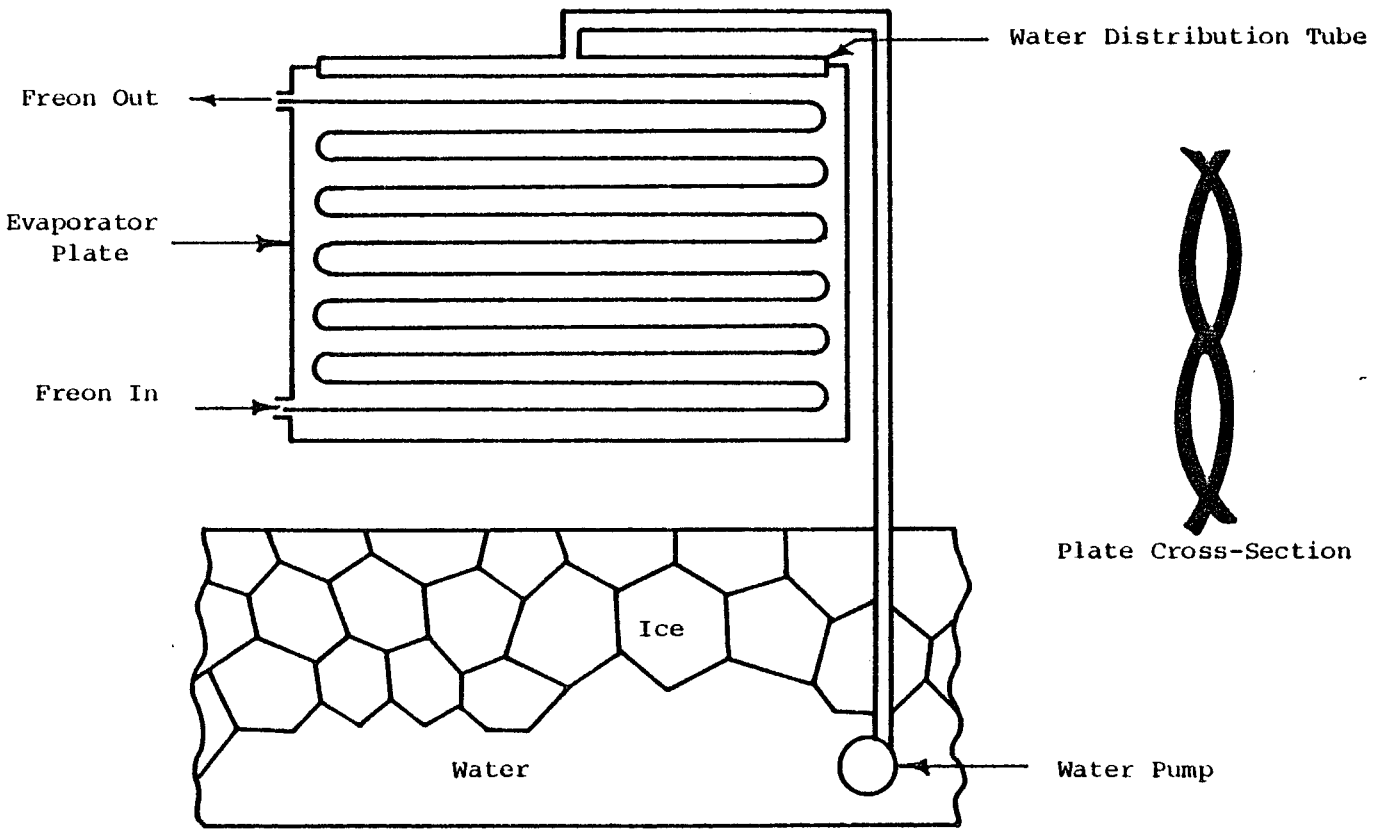

FIGURE 7.1 - FLAT PLATE ICE-MAKER EVAPORATOR CONFIGURATION

Thus, the lowering of the temperature of the air surrounding the ice-maker evaporators acts to increase the amount of heat that must be transferred from the water and, thus, increases the rate of ice formation. This, in turn, decreases the performance of the heat pump, by decreasing the freon evaporating temperature. In order to quantify the effect of the air environment on the evaporator performance, an analytical model of the heat transfer phenomenon has been developed. Figure 7.2 illustrates the situation being analyzed.

The parameter controlling the heat transfer rate is the film coefficient, h_o, of the water flowing over the plate. This film coefficient has been modeled for the configuration described above, using boundary layer theory and a finite difference method numerical solution. The model consists of a solution of the continuity, momentum, and energy boundary layer equations with the proper initial and boundary conditions. These equations and boundary equations are developed and nondimensionalized in the subsequent chapter. The dimensionless equations are then expanded in an implicit finite difference scheme and used to numerically solve for the local film coefficient down the entire length of the plate. The heat transfer from the air to the water (and consequently to the freon) is established through the proper use of the energy equation. The finite difference analysis is thus performed for both the air and the water, with the solution linked at the air/water interface.

Once h_o is established, the overall heat transfer analysis and ice formation rates can be readily computed. The differential equation which equates the heat transfer rates at the ice/water interface for the situation depicted in Figure 7.2 is written. This equation is then

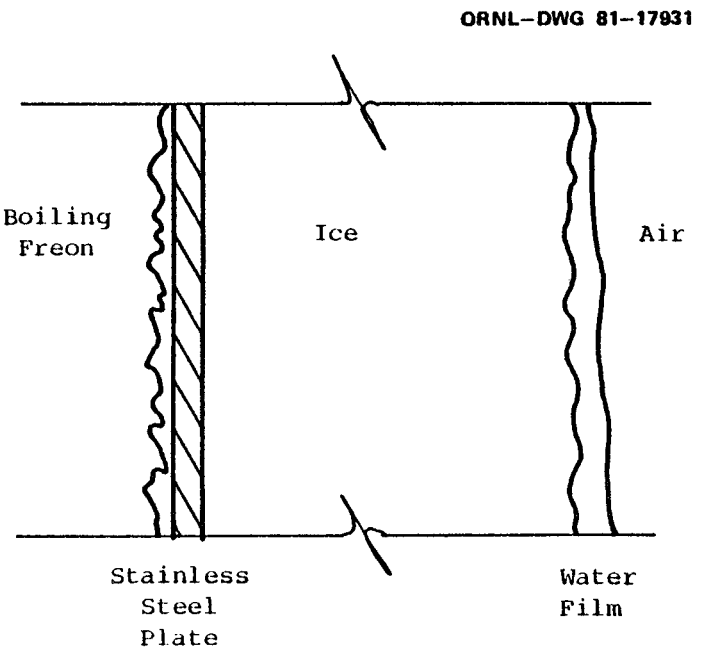

FIGURE 7.2 - ICE-MAKER PLATE HEAT TRANSFER SITUATION

nondimensionalized and solved in a manner to establish an ice formation rate versus time, in terms of the heat transfer coefficient, h_o, obtained above. The effect of the air temperature on the heat transfer coefficient can thus be related to the ice formation rate and overall heat transfer performance.

In addition to the analytical model, a laboratory experimental program was developed and undertaken to evaluate the evaporator heat transfer characteristics. An insulated enclosure was constructed to house the evaporator plates and simulate actual storage tank conditions. The evaporator performance was subsequently determined over a range of air temperatures from 35°F (1.7°C) to 85°F (29.4°C). The laboratory tests not only served as a verification of the analytical model, but also aided in establishing the proper boundary and initial conditions that are required for the analytical model.

7.2 Intent of the Summary

The following sections summarize the results of the work performed. The reader interested in the details of this work should read Wendschlag, 1979. An attempt will be made here to provide sufficient information to lead the reader through the work; but the problem presented is a difficult one and its solution is complex. Consequently, the summary presented, although comprehensive, does not contain sufficient information to reproduce the work in its entirety, where as the referenced (Wendschlag, 1979) work does.

7.3 Analytical Model

7.3.1 Analytical Model Development and Solution Procedure

The following steps are followed in the development of the analytical model:

1. The boundary layer equations for the water film are developed;

2. The boundary layer equations for the air adjacent to the water film are developed;

3. The velocities and temperature of the air and water at their common interfaced are linked;

4. The governing equations are nondimensionized;

5. The finite difference equations representing the governing partial differential boundary layer equations are written;

6. A computer algorithm is used to solve the finite difference equations. This results in the velocity and temperature profiles for both the air and the water;

7. These distributions are then used to develop the heat transfer coefficient between the water and the plate, as a function of water and air conditions;

8. The rate of water cooling and ice formation can then be calculated, as a function of freon, water, and air conditions.

7.3.2 The Governing Differential Equations

The coordinate system used for development of the boundary layer equations is shown in Figure 7.3. The result of step four (4), above, yields the following differential equations:

Continuity

$$\frac{\partial U}{\partial X} + \frac{\partial V}{\partial Y} = 0 \qquad 7.1$$

Momentum Equation for the Water

$$U\frac{\partial U}{\partial X} + V\frac{\partial U}{\partial Y} = \frac{\nu}{t_{fo}u_e}\frac{\partial^2 U}{\partial Y^2} + \frac{t_{fo}g_x}{u_e^2} \qquad 7.2$$

For the Air

$$U\frac{\partial U}{\partial X} + V\frac{\partial U}{\partial Y} = \frac{\nu}{t_{fo}u_e}\frac{\partial^2 U}{\partial Y^2} + \frac{g_x\beta t_{fo}}{u_e^2}(T_a - T_I)(1 - \Theta) \qquad 7.3$$

Energy Equation for Both the Air and the Water

$$U\frac{\partial \Theta}{\partial X} + V\frac{\partial \Theta}{\partial Y} = \frac{1}{Pr}\frac{\nu}{t_{fo}u_e}\frac{\partial^2 \Theta}{\partial_X^2} \qquad 7.4$$

ORNL-DWG 81-17932

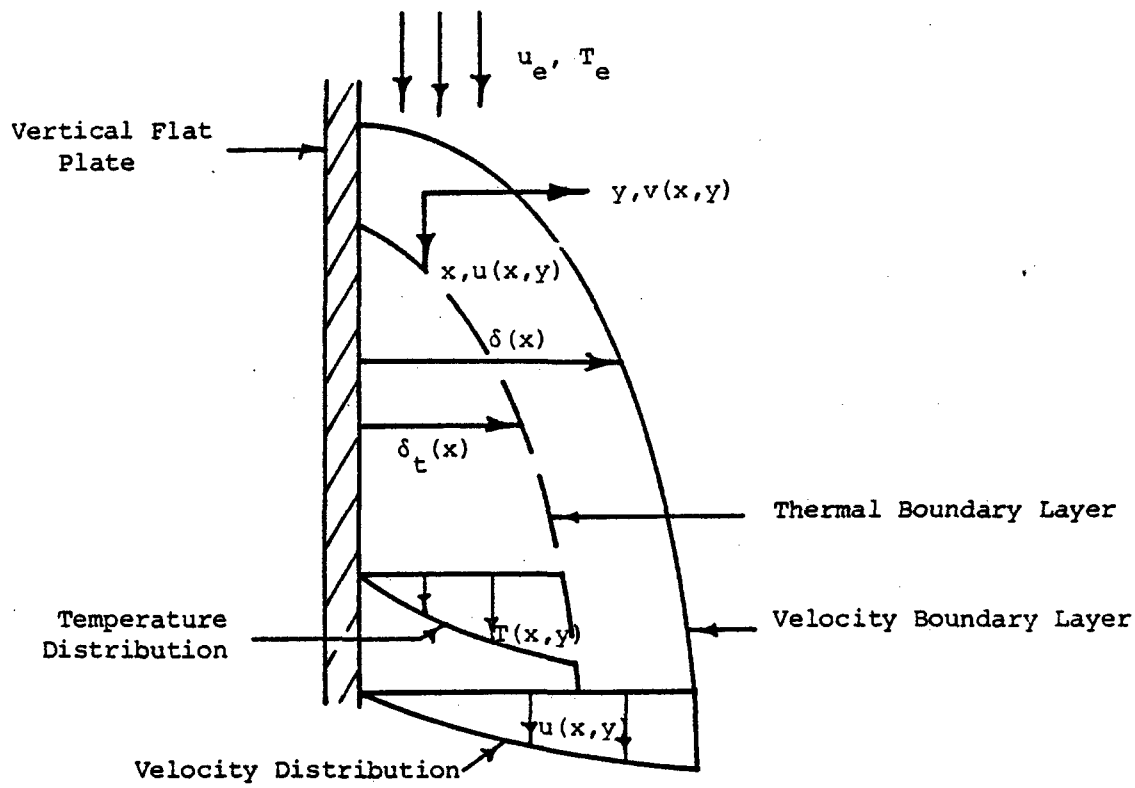

$T(x,y)$ = Temperature at Coordinates (x,y)

$\delta_t(x)$ = Thickness of Thermal Boundary Layer at x

T_e = Entering Fluid Temperature

$u(x,y)$ and $v(x,y)$ = Velocity Components in x and y directions, respectively

u_e = Entering Fluid Velocity

δ_x = Boundary Layer Thickness at Position x

FIGURE 7.3 - COORDINATES FOR THE VELOCITY AND THERMAL BOUNDARY LAYERS FOR FORCED LAMINAR FLOW ALONG A FLAT PLATE

Where:

$$X = \frac{x}{t_{fo}}, \quad Y = \frac{y}{t_{fo}},$$

$$U = \frac{u}{u_e}, \quad V = \frac{v}{u_e}$$

$$\Theta = \frac{T - T_I}{T_a - T_I},$$

and:

t_{fo} = initial film thickness of the water,

u_e = entering water velocity, which is assumed uniform, and

T_I = interface temperature between the water and the solid surface.

The boundary conditions for the above equations are:

For the Water

$$\text{At } Y = 0; \quad U = 0, \quad V = V_I, \quad \Theta = \Theta_I$$

$$\text{At } Y = \frac{\delta}{t_{fo}}; \quad U = U_w, \quad \Theta = \Theta_w, \qquad 7.5$$

For the Air

$$\text{At } Y_a = 0; \quad U = U_w, \quad V = 0, \quad \Theta = \Theta_w$$

$$\text{At } Y_a = \frac{\delta_a}{t_{fo}}; \quad U = 0, \quad \Theta = 1 \qquad 7.6$$

7.3.3 Calculation of the Film Coefficient

An implicit finite difference scheme was used to solve the governing differential equations 7.2 through 7.6. The result of solving these equations is that the velocities and temperature, U, V, and Θ, are obtained at each of the finite difference points. The Nusselt number, Nu, is then calculated from:

$$Nu_x = \left(\frac{T_a - T_I}{T_e - T_I}\right) \frac{d\Theta}{dY} \Bigg|_{Y = 0} \qquad 7.7$$

and the film coefficient, h_o, forms:

$$h_o = \frac{Nu_x \, k_{water}}{t_{fo}} \qquad 7.8$$

for each finite difference point along the plate. The average Nusselt number and film coefficient are then calculated by finding the integral average over the length of the plate.

7.3.4 Calculation of the Ice Formation Rate

Once the film coefficient, h_o, has been determined, it can be used to determine ice formation rates and the overall heat transfer as a function of the ice thickness and temperatures of the freon and water. Figure 7.4 illustrates the physical situation for the overall heat transfer analysis.

The governing differential equation for the rate of ice growth can be derived by equating the heat transfer through the ice to rate of heat removal from the water, plus the energy given up by the formation of an incremental layer of ice, dz. The resulting differential equation is:

$$\frac{T_I - T_f}{T_e - T_I} = \frac{h_o}{U} + \frac{\rho_I h_{sf}}{U(T_e - T_I)} \frac{dz}{d\tau} \qquad 7.9$$

Equation 7.9 can be integrated to yield the thickness of the ice, z, as a function of the time, τ. The result is:

$$C1 = -\frac{z^*}{C4} - \left(\frac{C3}{C4} + \frac{1}{C4^2}\right) \ln\,(1 - C4z^*) \qquad 7.10$$

where:

$$z^* \equiv \frac{z}{t},$$

$$\Theta \equiv \frac{\tau k_I \, (T_e - T_I)}{\rho_I h_{sf} t^2}$$

ORNL-DWG 81-17933

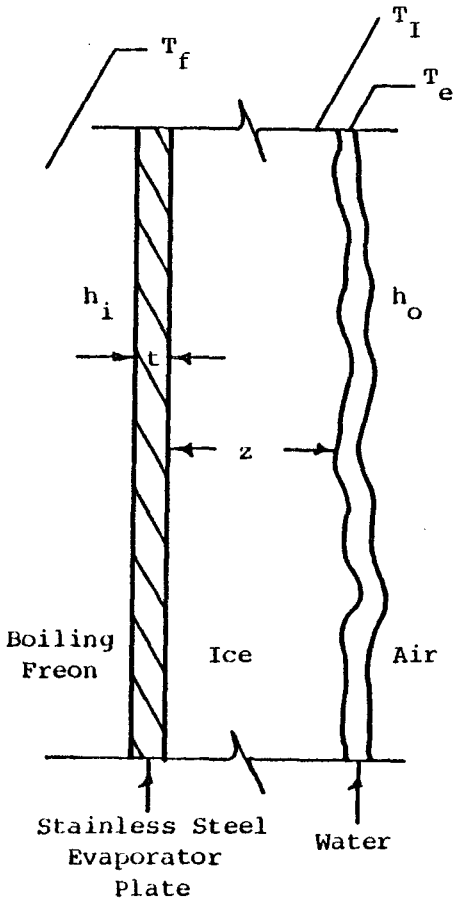

T_I = Fusion Temperature of Ice

T_f = Freon Temperature

A = Area

h_i = Inside Film Coefficient (Freon)

t = Thickness of the Plate

k_p = Thermal Conductivity of the Plate

z = Ice Thickness

k_I = Thermal Conductivity of Ice

h_o = Outside Film Coefficient (Water and Air)

T_e = Entering Water Temperature

ρ_I = Density of Ice

h_{sf} = Latent Heat of Fusion for Ice

τ = Time

FIGURE 7.4 - NOMENCLATURE FOR THE OVERALL HEAT TRANSFER ANALYSIS

$$C1 \equiv \frac{T_I - T_f}{T_e - T_I} - \frac{h_o}{h_i} - \frac{h_o t}{k_p} ,$$

$$C3 \equiv \frac{k_I}{th_i} + \frac{k_I}{k_p} , \text{ and}$$

$$C4 \equiv \frac{h_o t}{k_I C1} .$$

It should be noted that the outside film coefficient, h_o, is a strong function of the ambient air temperature. It should also be noted that $(1/h_o)$ appears in every term on the right hand side of Equation 7.10. Thus, one would expect, by inspection of Equation 7.10, that the ice formation rate is strongly dependent upon the film. Equation 7.10 is, of course, a transcendental equation and must be solved by trial and error for z*, the dimensionless ice thickness. The results of the analytical work are presented below.

7.4 Experimental Equipment

The heat pump used for test purposes was a modified 2½-ton Janitrol Wattsaver model 380380B. This unit uses a Sundstrand model H20A323AB compressor. The unit has been modified to provide test data for several experimental investigations. It was, therefore, set up on a series air and ice-maker evaporator/subcooling scheme (Chapter 3.0). For the purpose of determining the heat transfer characteristics of the ice-maker evaporator, the four-way valve will remain in the position which allows subcooling in the air evaporator and evaporation in the ice-maker plates.

To control the air temperature surrounding the ice-maker plates, the plates are enclosed in an insulated box. The air handler evaporator unit for a three-ton Westinghouse heat pump is also located in this enclosure to control the air temperature inside. This unit contains an electrical

resistance duct heater, as well, and thus allows control of the enclosure temperature both above and below the external laboratory temperature.

To evaluate the evaporator load for the heat pump, copper constantan thermocouples and pressure gauges were used to determine the state of the freon at various points in the system. A Fluke model 2240B data logger was used to monitor the temperatures indicated by the thermocouples and the power used by the compressor, by means of an AC watt transducer. The pressure gauges were Bourdon tube refrigeration gauges with dial indicators.

To measure the water flow rate over the ice-maker plate, a trough was fabricated which would direct all the water from the plate into a bucket. The water was allowed to dump into the bucket for a specified length of time. The flow rate was subsequently determined from the difference in weight of the bucket when full and when empty, and the time span.

In order to determine the velocity of the water flowing over the plate, an apparatus was devised to measure the thickness of the water film at any point on the plate. The device made use of a micrometer, attached to a special mount which enables it to slide along a horizontal rail to access any point along the width of the plate. The rail, in turn, can be moved to any vertical position desired on the plate.

The amount of ice formation of the plate was determined by the weight of ice formed as a function of time.

7.5 Experimental Procedure

It was desirable to check the analytical model over a wide range of its results. Eight different test conditions were established for the check of the film coefficient and the rate of ice formation. The test conditions made use of two different water flow rates with four different air temperatures ranging from 35°F (1.7°C) to 85°F (29.4°C). The tests to

determine the film coefficient were performed during water-chilling to avoid the inclusion of ice resistance in the heat transfer analysis.

To begin the first series of tests, the water flow rate was set at the maximum rate obtainable, using the given water pump. This flow was then used unaltered for the first four tests, varying the air temperature to change the test conditions.

Before starting the heat pump to establish the heat transfer rates, the flow characteristics of the water were first established. The trough was used to measure the flow rate of the water over the plate. Three different measurements were taken to ensure the accuracy of the method. Subsequently, the film thickness of the water on the plate was measured to establish the water velocity profile on the plate. Measurements were taken on one side of the plate only, because of the symmetrical design of the water distribution system.

After the water flow characteristics were established, the heat pump was started, to begin water-chilling. The initial water temperature was approximately that of the laboratory or $70^{\circ}F$ ($21^{\circ}C$). In order that the water conditions would not be significantly different than that during ice formation, data was not taken until the water temperature dropped below $40^{\circ}F$ ($4^{\circ}C$). This also allowed the heat pump to operate for a long enough period of time to establish steady state operation. As the water temperature approached this point, the duct heater unit inside the enclosure was turned on and thermostatically controlled, to maintain the enclosure air temperature at $85^{\circ}F$ ($29.4^{\circ}C$).

With the air in the enclosure and the water flowing over the plates at the desired temperatures and the system operating at steady state conditions, the state temperature, pressures, and compressor power were read.

In addition, the temperatures of the air entering and exiting the condenser unit were measured in order that the heat output of the unit could be determined. The heat output and compressor power were necessary to establish the refrigeration capacity or heat transfer rate to the evaporator.

Once the necessary data was acquired at the 85°F (29.4°C) air temperature, the thermostat setting was lowered to 65°F (18.3°C) and the environmental control heat pump started. Once steady state conditions were established with the air in the enclosure at 65°F (18.3°C), the data described above was again taken. This process was repeated twice more with enclosure air temperatures of 50°F (10°C) and 35°F (1.7°C).

After acquiring the data during chilling to determine the air temperature impact on the film coefficient, the water in the tank was allowed to continue cooling until ice formation began. During this time the air evaporator unit in the enclosure was left on to maintain the enclosure air conditions at 35°F (1.7°C). With the desirable air conditions established, the plate was defrosted by reversing the position of the four-way valve, and the ice formed, dropped into the tank. After defrosting of the plate was completed, the four-way valve was switched back and the unit was allowed to reach equilibrium. Upon reaching equilibrium, data was again taken, as above, at five-mintue intervals. In addition, the scales were also read at each interval to establish the amount of ice on the plate. The recording of interval data was continued over a period of one hour.

The ice formation rate data thus acquired for 35°F (1.7°C) air, the four-way was again switched to defrost the plate. During the defrosting, the thermostat temperature setting was raised to 50°F (10°C). After the enclosure reached 50°F (10°C) and the plate was de-iced, the four-way was

switched back and the process described above was repeated for the 50°F (10°C) air condition. Following this test, the procedure was again repeated at 65°F (18.3°C) and 85°F (29.4°C) enclosure air temperatures.

The second series of tests proceeded exactly as the first series. To begin these tests, the water flow was throttled, to permit the minimum flow possible which would still allow an even water distribution on the plate. The procedure to determine the flow characteristics was then repeated. With the new flow characteristics established, the tests for the determination of the film coefficient and ice formation rate were repeated at the 85°F (29.4°C), 65°F (18.3°C), 50°F (10°C), and 35°F (1.7°C) enclosure air temperatures.

7.6 Analytical and Experimental Results

The analytical results presented below are the major ones from Wendschlag, 1979. These results are dependent upon several assumptions, especially the numerical step size used and the entering water velocity. The reader interested in these and the experimental details should consult Wendschlag, 1979.

7.6.1 Analytical Results

The results of the mean Nusselt number calculation for the water/plate or water ice interface are shown in Figures 7.5 through 7.8. The results of one of the local Nusselt number calculations are presented in Figure 7.9. Figure 7.10 demonstrates the variation of the mean Nusselt number, with respect to the relative air temperature. The last figure, Figure 7.11, shows the rate of ice growth as a function of time. The definition of symbols used in all the figures can be found in Appendix 7-A.

ORNL-DWG 81-17934

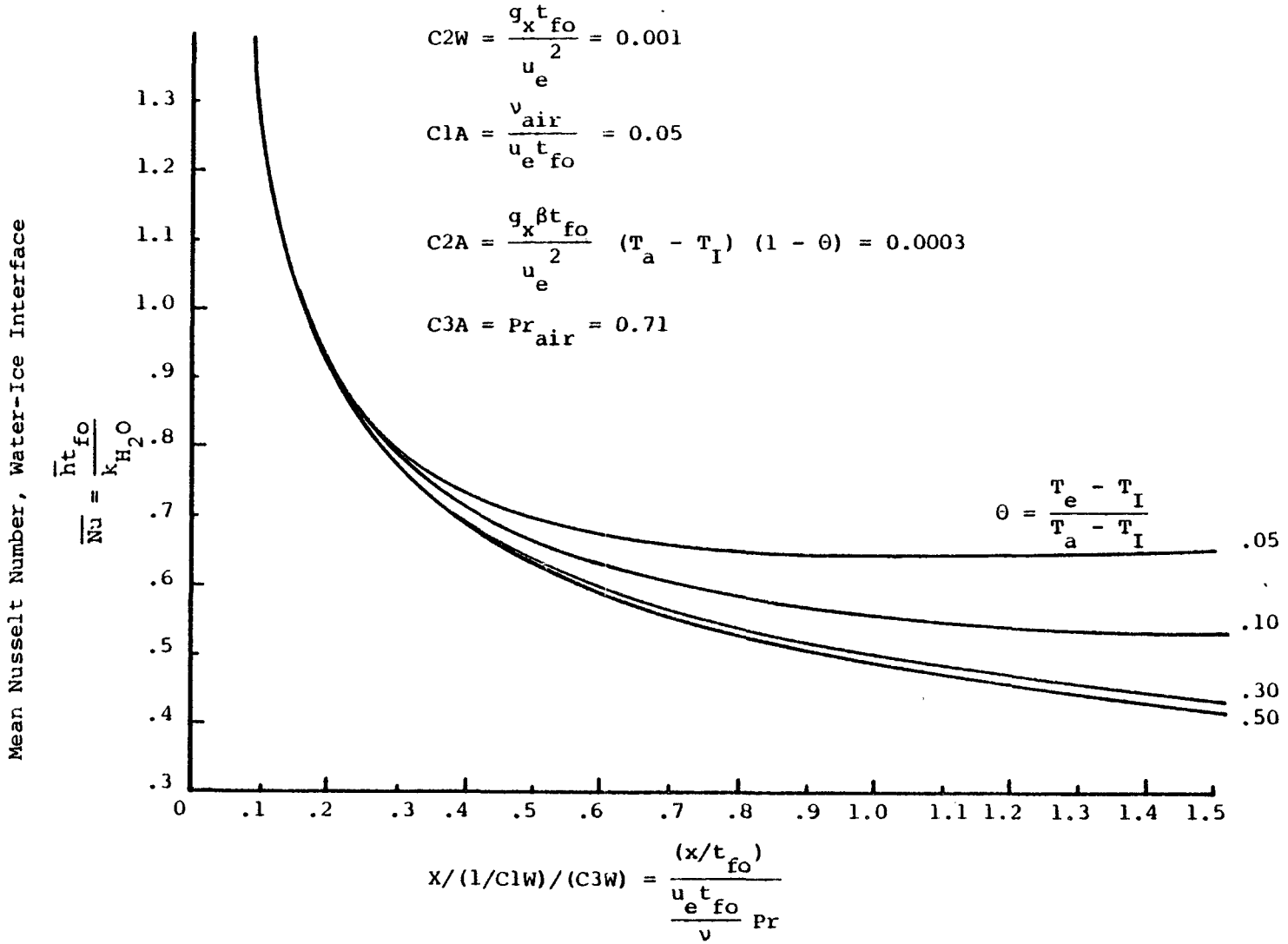

FIGURE 7.5 - ANALYTICAL CALCULATIONS OF MEAN NUSSELT NUMBER

ORNL-DWG 81-17935

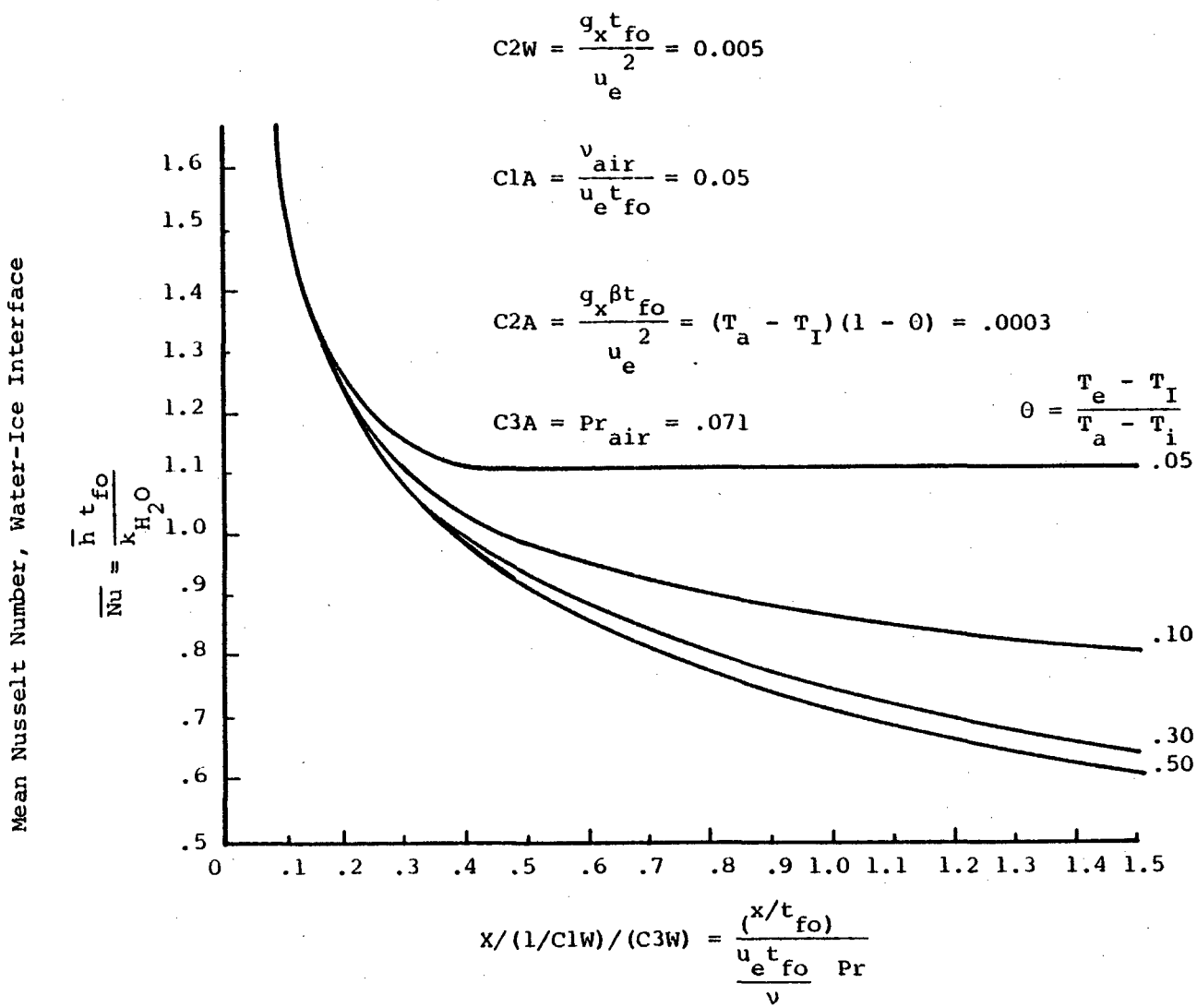

FIGURE 7.6 - ANALYTICAL CALCULATIONS OF MEAN NUSSELT NUMBER

ORNL-DWG 81-17936

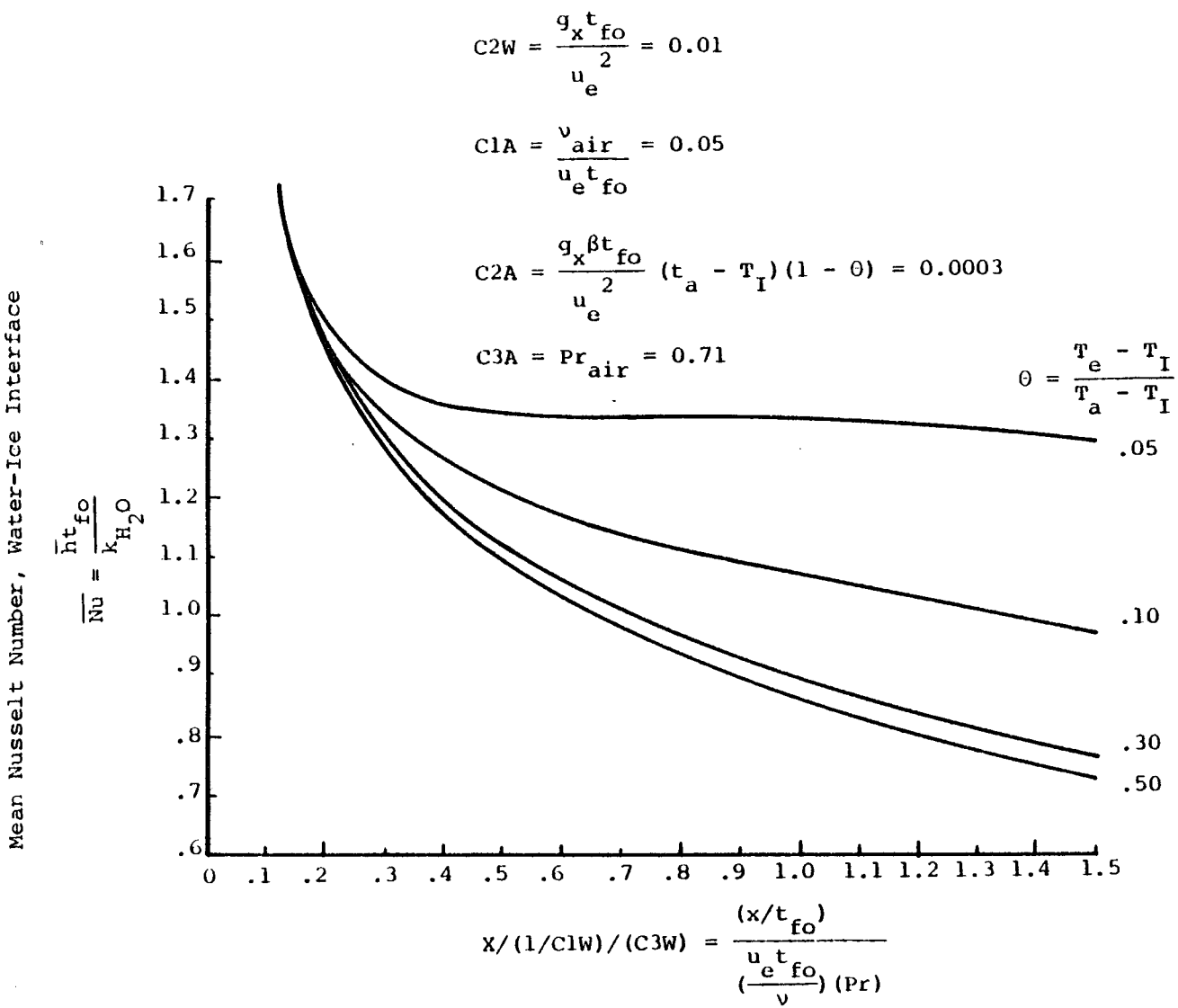

FIGURE 7.7 - ANALYTICAL CALCULATIONS OF MEAN NUSSELT NUMBER

ORNL-DWG 81-17937

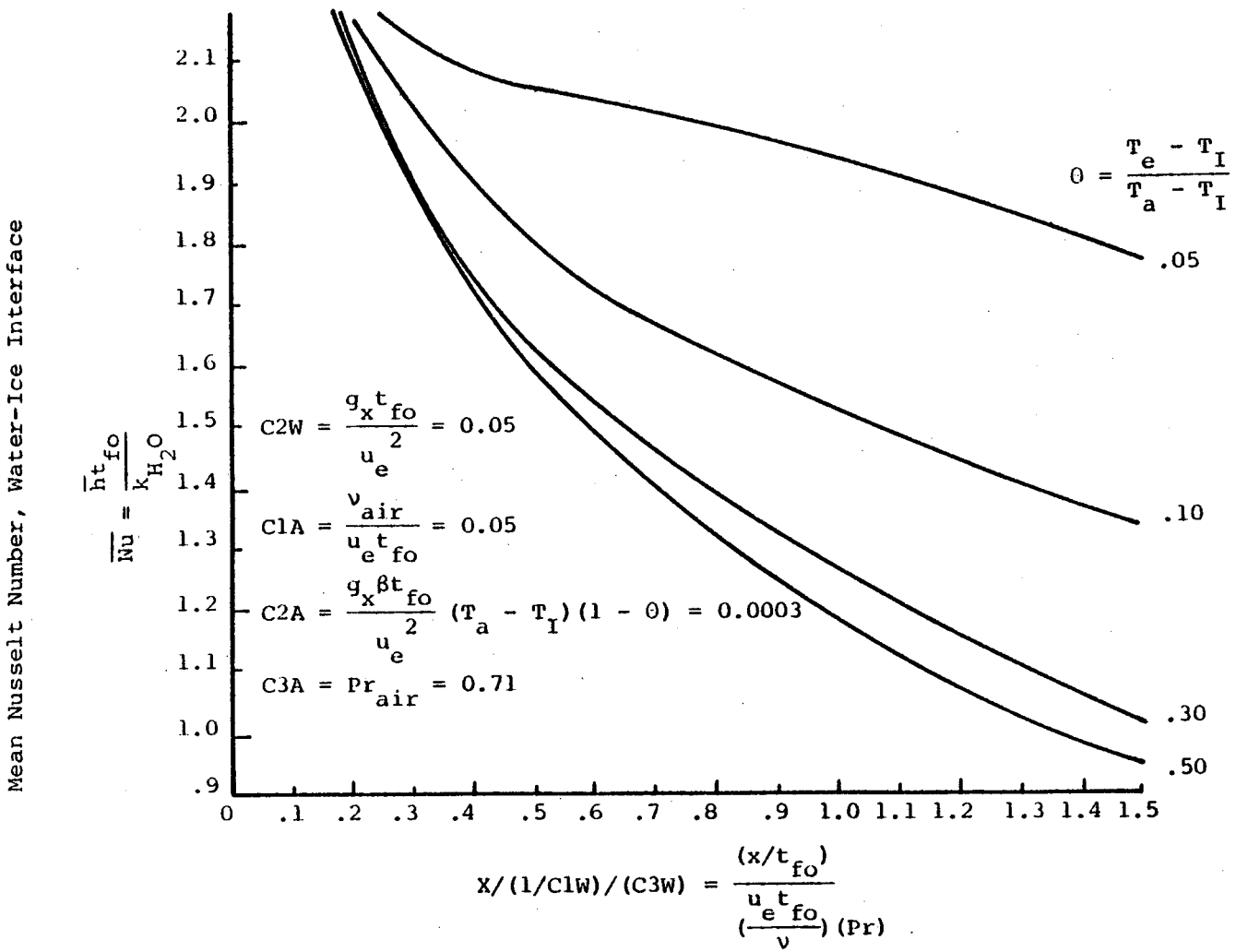

FIGURE 7.8 - ANALYTICAL CALCULATIONS OF MEAN NUSSELT NUMBER

ORNL-DWG 81-17938

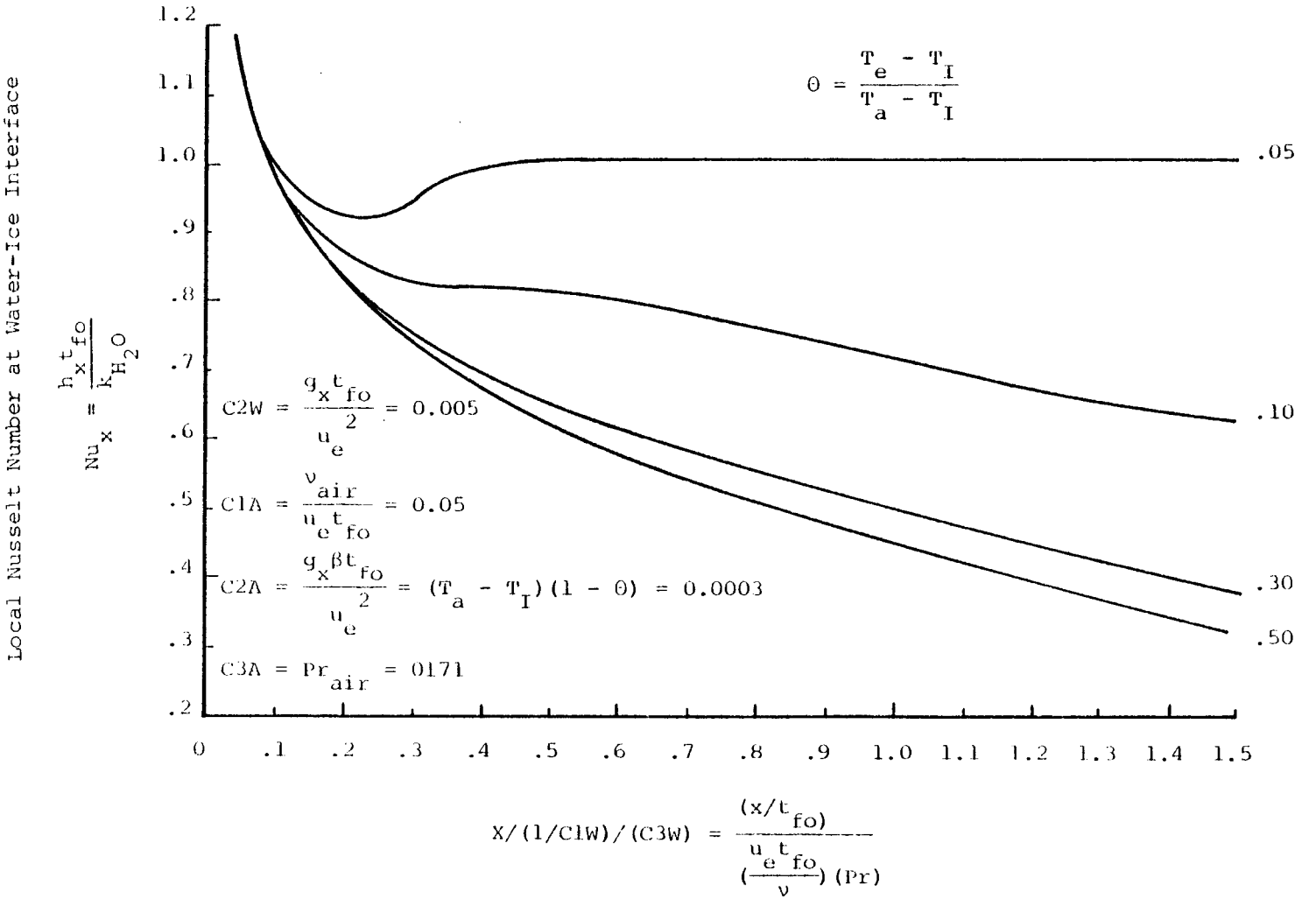

FIGURE 7.9 - ANALYTICAL CALCULATIONS OF LOCAL NUSSELT NUMBER

ORNL-DWG 81-17939

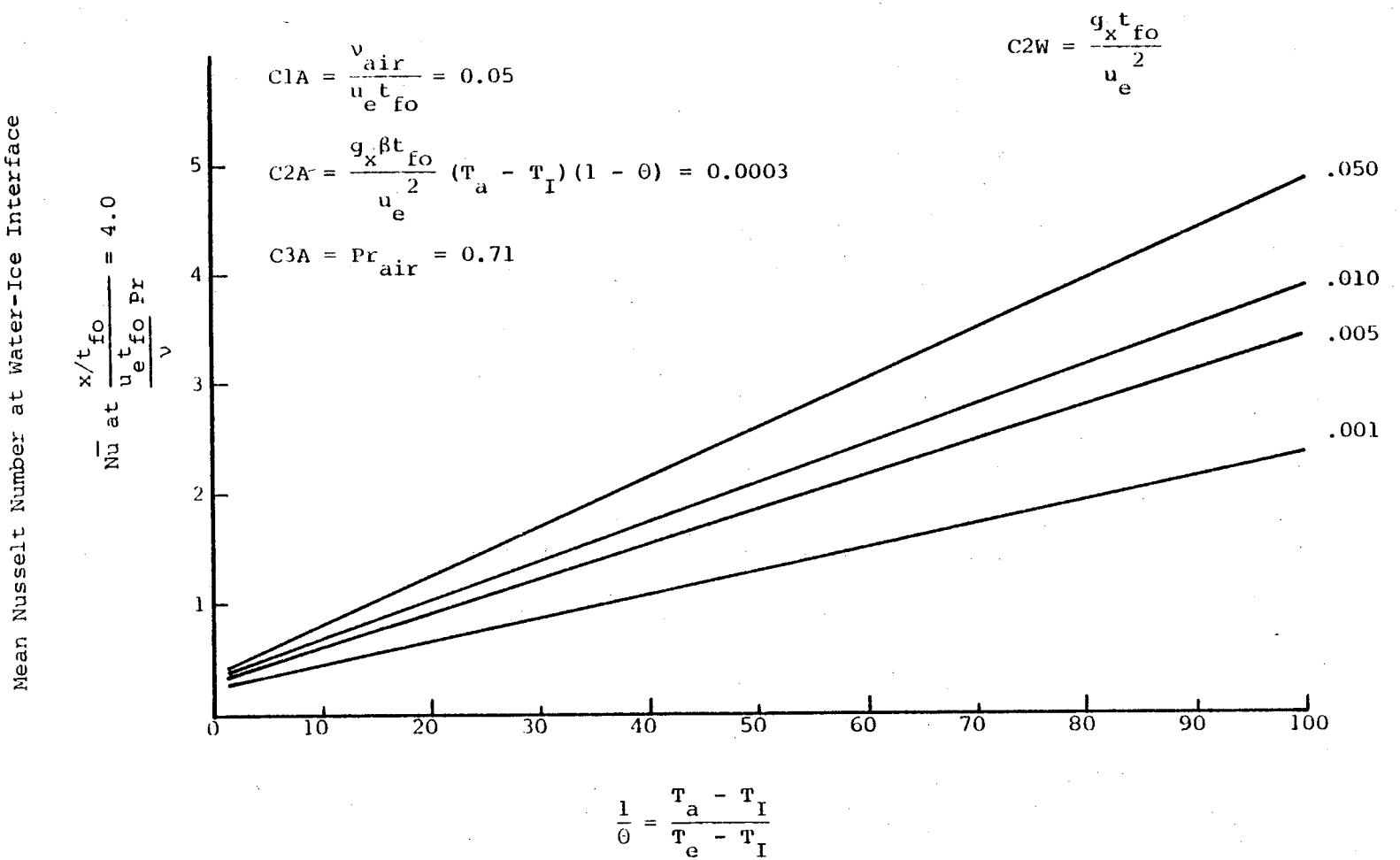

FIGURE 7.10 - VARIATION IN MEAN NUSSELT NUMBER WITH RESPECT TO THE RELATIVE AIR TEMPERATURE, θ.

ORNL-DWG 81-17940

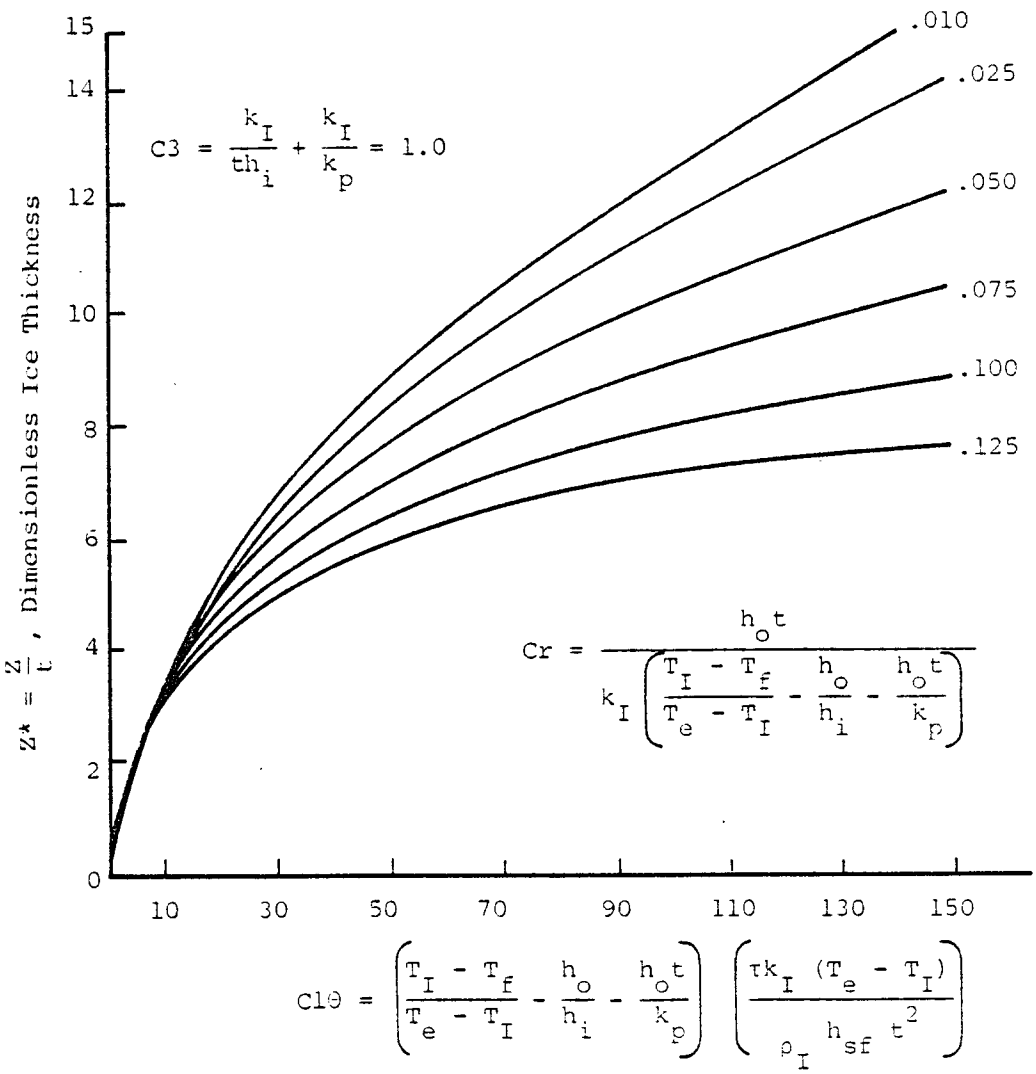

FIGURE 7.11 - ANALYTICAL DETERMINATION OF ICE FORMATION FOR AVERAGE CONDUCTION EVAPORATORS

Examination of Figure 7.5 through 7.8 reveals the following:

1. The average Nusselt number approaches a constant value with all parameters fixed, except for plate length, x. This is an expected result.

2. At all conditions chosen, the air temperature always has a pronounced impact upon the Nusselt number. This impact can be as high as a factor of approximately 2.0.

3. The major physical parameters that control the rate of heat transfer to the plate are: the entrance water velocity, the ambient air temperature, and the initial film thickness.

4. The Nusselt number can vary from 0.4 to > 2.0 for the conditions chosen.

Examination of Figure 7.9 shows that the local Nusselt number is also strongly dependent upon the air temperature, and that it approaches a constant value as one proceeds down the plate. Figure 7.10 shows the variation in the mean Nusselt number with air temperature. In evaluating this curve, one should note that in a typical application ($T_e - T_I$) has a numerical value of 2 F^o (1 C^o) to 4 F^o (2 C^o). Thus, values of "$1/\Theta$" of 10 to 30 are readily achievable, as this corresponds to an air temperature of 50 to 80°F (10 to 30°C).

In the original tests run in the laboratory, we were operating at a value of "$1/\Theta$" of approximately 15. This would correspond to a Nusselt number value of approximately 1.1 for C2W = 0.050. In moving the equipment into the field application, C2W remained the same, but $1/\Theta$ was decreased to unity. This, in turn, decreased the effective film between the water and the plate by a factor of approximately 2.7. Since the rate of heat transfer to the freon remains relatively constant, the rate of ice growth had to increase. This, of course, is what was experimentally observed and was the reason the analytical

work was undertaken. Consequently, the analytical results qualitatively verify what was experimentally observed. Figure 7.11 also shows the same result in a different graphical format.

7.6.2 Experimental Results

Two experiments were run to determine the film coefficient, h_o, one at a flow rate of 99.5 $\frac{lbm}{min}$ (445 $\frac{kg}{min}$) and 65.5 $\frac{lbm}{min}$ (29.7 $\frac{kg}{min}$). The results of the test are shown in Tables 7.1 and 7.2. The results as presented are based upon an assumption that the freon boiling film coefficient is 340 Btu/Hr Ft^2 F^o (1930 Watts/m^2 C^o) and a plate conductively of 10 Btu/Hr Ft F^o (17.3 Watts/ m C^o). The pronounced impact of the air temperature upon the film coefficient and the overall heat transfer coefficient, U, can be seen. It should be noted that these data were gathered with equipment that was not designed for this type of a test. Consequently, variable test conditions were encountered, and it is likely that the calculated film coefficients are only representative of the "real" values. A detailed discussion of these conditions can be found in Wendschlag, 1979.

A graph of the rate of ice formation as a function of time is shown in Figure 7.12. It should be noted that these data are similar to those seen in Figure 7.11. Table 7.3 compares the analytical and experimental film coefficients. The coefficients compare favorably, considering the variability of the test conditions and the difficulty of measuring the initial water velocity.

7.7 Conclusions and Recommendations

From the results presented above, it becomes apparent that the temperature of the air environment surrounding the ice-maker evaporator plates has a significant effect on the evaporator's heat transfer characteristics. It

TABLE 7.1

RESULTS OF FILM COEFFICIENT LABORATORY TESTS
WATER FLOW RATE = 99.5 lbs/min

T_{air} (^oF)	$\bar{T}_{evap}$ (a) (^oF)	T_e (a) (^oF)	Q_{cond} (b) (Btu/hr)	P_{comp} (Watts)	Q_{evap} (b) (Btu/hr)	$\bar{U}_{evap}$ (c) (Btu/hr ft^2 ^oF)	h_o (c) (Btu/hr ft^2 ^oF)
85	32.0	39.8	24,460	2,930	14,460	107	168
65	31.2	38.3	23,010	2,910	13,080	106	165
50	29.1	36.9	22,840	2,840	13,150	98	147
35	27.1	34.9	21,910	2,790	12,390	92	134

(a) $^oC = (^oF - 32) \times 5/9$

(b) For watts multiply by 0.2930

(c) For $W/m^2\ ^oC$ multiply by 5.6786

TABLE 7.2

RESULTS OF FILM COEFFICIENT LABORATORY TESTS
WATER FLOW RATE = 65.5 lbs/min

T_{air} (^oF)	$\bar{T}_{evap}$ (a) (^oF)	T_e (a) (^oF)	Q_{cond} (b) (Btu/hr)	P_{comp} (Watts)	Q_{evap} (b) (Btu/hr)	$\bar{U}_{evap}$ (c) (Btu/hr ft^2 ^oF)	$\bar{h}_o$ (c) (Btu/hr ft^2 ^oF)
85	31.1	39.5	24,910	2,798	15,360	106	165
65	30.3	37.9	24,220	2,760	14,800	113	183
50	28.0	36.5	24,560	2,719	15,280	104	161
35	22.8	33.8	22,670	2,570	13,900	73	97

(a) $^oC = (^oF - 32) \times 5/9$

(b) For watts multiply by 0.2930

(c) For $W/m^2\ ^oC$ multiply by 5.6786

ORNL-DWG 81-17941

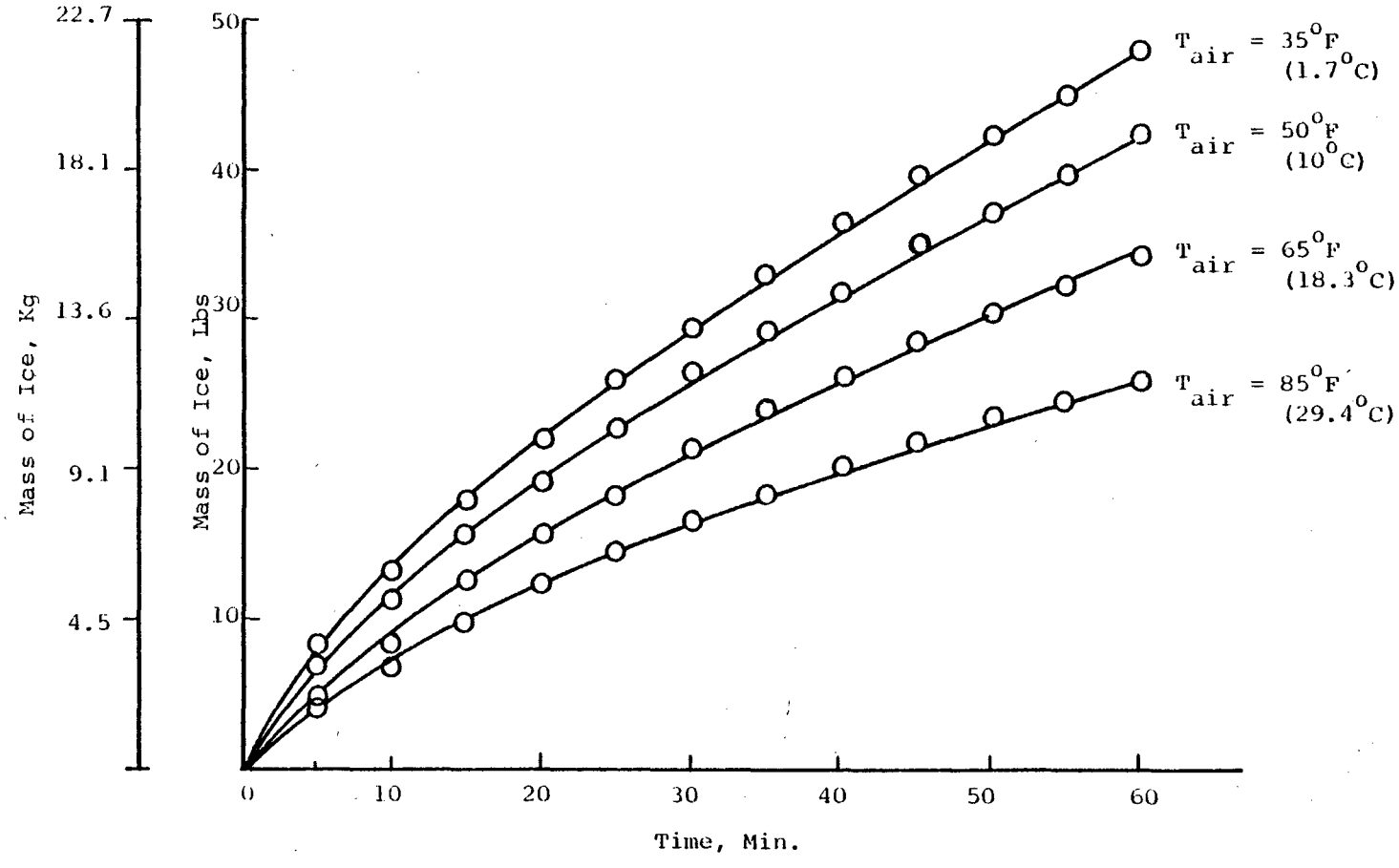

FIGURE 7.12 - EFFECT OF AIR ENVIRONMENT ON ICE FORMATION RATE AT A WATER FLOW RATE OF 65.5 LBS/MIN (29.7 KG/MIN)

TABLE 7.3

COMPARISON OF ANALYTICAL AND EXPERIMENTAL FILM COEFFICIENTS
WATER FLOW RATE = 99.5 lbs/min (45.1 kg/min)

Θ	C2W	X/C1W/C3W	$\overline{Nu}$	$\overline{h}_{predicted}$ [a] (Btu/hr ft^{2o}F)	$\overline{h}_{lab}$ [a] (Btu/hr ft^{2o}F)
0.147	0.013	0.60	1.11	236	172
0.210	0.013	0.60	1.075	228	158
0.373	0.013	0.60	1.045	222	147
0.987	0.013	0.60	1.02	217	137

[a] For W/m^{2o}C multiply by 5.6786

was demonstrated both analytically and experimentally that the air temperature can effect the evaporating temperature of the freon, which has a direct impact both on the output of the heat pump and the coefficient of performance (COP). It was also shown that a change in air temperature of 50°F (27.7°C) from 85°F (29.4°C) to 35°F (1.7°C) essentially doubles the rate of ice formation on the plate. This, in turn, doubles the frequency of the ice harvesting. The effect of the air temperature on the plate harvesting characteristics was not studied, but it is very likely the lowering of the air temperature would have a detrimental effect here as well.

It is apparent that in the continued development of the ice-maker evaporator plates that the laboratory environmental conditions under which they are tested needs to be directly considered in predicting the performance in an actual application.

The model predicting the effect of air temperature on the water to plate film coefficient was shown to be qualitatively accurate, and demonstrates the significant effects of the air environment upon the ice formation rate.

It is suggested that a test procedure be developed that could better serve as a quantitative test of the model. Characteristics of the heat pump used for the experimental analysis, such as the hunting by the expansion valve and the uncertainty of the boiling film coefficient in the evaporator, make it difficult to verify the numerical results of the model. Since it is conceivable that the results of this model may be relevant to other applications, continued verification and modification of the model is definitely warranted.

Finally, since the temperature of the air environment has been demonstrated to significantly impact the ice-maker evaporator performance,

the results of this study may be used as a basis for evaluation of already existing test data of similar ice-maker heat pumps. This study may, therefore, aid in properly predicting the heat pump performance in applications in a variety of evaporator air environments.

APPENDIX 7-A

NOMENCLATURE

A — Surface area of evaporator plate (L^2)

C1 — Dimensionless constant in ice formation model

$$\frac{T_I - T_f}{T_e \quad T_I} \quad \frac{h_o}{h_i} - \frac{h_o t}{k_p}$$

C2 — Dimensionless constant in ice formation model

$$\frac{h_o t}{k_I}$$

C3 — Dimensionless constant in ice formation model

$$\frac{k_I}{t h_i} + \frac{k_I}{k_p}$$

C4 — Dimensionless constant in ice formation model

$$\frac{h_o t}{k_I \quad \frac{T_I - T_f}{T_e - T_I} - \frac{h_o}{h_i} - \frac{h_o t}{k_p}}$$

C1A — Dimensionless constant in film coefficient model

$$\frac{\nu_{air}}{u_e t_{fo}}$$

C2A — Dimensionless constant in film coefficient model

$$\frac{g_x \beta t_{fo}}{u_e^2} (T_a - T_I) \ (1 - \Theta)$$

C3A — Dimensionless constant in film coefficient model

$$Pr_{air}$$

C1W — Dimensionless constant in film coefficient model

$$\frac{\nu_{water}}{u_e t_{fo}}$$

C2W	Dimensionless constant in film coefficient model $$\frac{g_x t_{fo}}{u_e^2}$$
C3W	Dimensionless constant in film coefficient model $$Pr_{water}$$
L	Length of evaporator plate (l)
$\overline{Nu}$	Mean Nusselt number $$\frac{\bar{h}_o t_{fo}}{k_{water}}$$
Nu_s	Local Nusselt number $$\frac{h_x t_{fo}}{k_{water}}$$
P_{comp}	Electrical power drawn by compressor (Watts)
Pr	Prandtl number of fluid
Q_{cond}	Heat output from condenser unit ($BtuT^{-1}$)
Q_{evap}	Heat transferred at evaporator plate ($BtuT^{-1}$)
T	Temperature of fluid in boundary layer (^oF)
T_a	Air temperature surrounding evaporator (^oF)
T_e	Water temperature entering plate (^oF)
T_f	Evaporating freon temperature (^oF)
T_I	Interface temperature between water and evaporator plate or ice (^oF)
T_w	Interface temperature between air and water (^oF)
$\overline{T}_{evap}$	Mean freon evaporating temperature (^oF)
U	Dimensionless X velocity $$\frac{u}{u_e}$$
U_w	U at interface between air and water (LT^{-1})

$\bar{U}_{evap}$	Mean evaporator heat transfer coefficient ($BtuT^{-1}L^{-2o}F^{-1}$)
V	Dimensionless Y velocity $\frac{v}{u_e}$
V_I	V at the ice/water interface (LT^{-1})
X	Dimensionless x distance $\frac{x}{t_{fo}}$
Y	Dimensionless y distance $\frac{y}{t_{fo}}$
Y_1	Dimensionless y distance $\frac{y_a}{t_{fo}}$
c_p	Constant pressure specific heat of fluid ($BtuM^{-1o}F^{-1}$)
g_x	Gravitational force in x direction (LT^{-2})
h_i	Evaporator internal film coefficient ($BtuT^{-1}L^{-2o}F^{-1}$)
h_o	Evaporator outside film coefficient ($BtuT^{-1}L^{-2o}F^{-1}$)
h_{sf}	Latent heat of fusion of water ($BtuM^{-1}$)
k	Thermal conductivity of fluid ($BtuT^{-1}L^{-1o}F^{-1}$)
k_I	Thermal conductivity of ice ($BtuT^{-1}L^{-1o}F^{-1}$)
k_p	Thermal conductivity of evaporator plate ($BtuT^{-1}L^{-1o}F^{-1}$)
m_{ice}	Mass of ice formed on evaporator plate (M)
t	Thickness of evaporator plate (L)
t_{fo}	Thickness of water film entering evaporator plate (L)
$\bar{t}_{film}$	Mean film thickness of water on evaporator plate (L)
$\bar{t}_{ice}$	Mean thickness of ice formed on evaporator plate (L)
u	Fluid velocity in x direction inside boundary layer (LT^{-1})

$\bar{u}$	Mean velocity of water flowing over the evaporator plate (LT^{-1})
u_e	Velocity of water in x direction entering the evaporator plate (LT^{-1})
u_w	Velocity of water in x direction at interface between air and water (LT^{-1})
v	Fluid velocity in y direction inside boundary layer (LT^{-1})
v_I	Velocity of fluid in y direction at ice/water interface (LT^{-1})
v_w	Velocity of water in y direction between air and water (LT^{-1})
x	Direction parallel to evaporator plate with origin at top of plate
y	Direction perpendicular to evaporator plate with origin at plate surface
y_a	Direction perpendicular to evaporator plate with origin at outside water surface
z	Thickness of ice on plate (L)
z^*	Dimensionless ice thickness $\frac{\bar{t}_{ice}}{t}$
α	Thermal diffusivity of fluid (L^2T^{-1})
β	Volumetric coefficient of thermal expansion for air ($^oF^{-1}$)
δ	Thickness of water boundary layer (L)
δ_a	Thickness of air boundary layer (L)
δ_t	Thickness of thermal boundary layer (L)
Θ	Dimensionless temperature parameter in film coefficient model $\frac{T - T_I}{T_a - T_I}$
Θ_I	Θ at interface between water and plate or ice
Θ_w	Θ at interface between air and water
ν	Kinematic viscosity of fluid (L^2T^{-1})

ρ	Mass density of fluid (ML^{-3})
ρ_I	Mass density of ice (ML^{-3})
τ	Time variable in ice formation model (T)

8.0 THE ICE/EARTH SOURCE EVAPORATOR

Beneath the frost line, typically 6-8 feet below the earth's surface in North Dakota, the temperature of the earth remains relatively constant throughout the year (approximately $50^{\circ}F$ ($10^{\circ}C$)). Thus, the earth provides an excellent constant low temperature energy source which can be utilized with a heat pump system. Earth coupled heat pumps have been operational for several decades, but only with limited success. Past systems can be classified as either, 1) buried coil, or 2) groundwater heat pump. The buried coil method of energy extraction has one distinct disadvantage. The earth has a relatively slow response to a load. Thus, a load of significant duration may not be satisfied due to a localized cold area around the unit. Groundwater heat pumps have had success, however, these systems require a readily available aquifer. Thus, this can only be considered for limited applications.

Research at the Engineering Experiment Station has been directed at development of the MSHP system. This includes low temperature source development (i.e., ice or earth) as well as the heat pump development. The objective of the low temperature source development is to optimize the qualities of various energy sources, one such consideration is the cost of thermal storage.

By placing a water storage system in the ground, and thermally coupling it to the earth, the size of the required storage volume can be reduced significantly over that of an ACES or MSHP system. This yields a distinct advantage over conventional storage in both space and cost requirements. A storage system of this nature can be retrofit in any residential system, unlike conventional storage which is difficult or retrofit because of space requirements.

8.1 System Description

The Earth Thermal Storage (ETS) system developed at the Engineering Experiment Station consists of four vertical cylindrical wells of depth of 20, 30, 40, and 50 feet (6.1, 9.1, 12.2, and 15.2 meters)(See Figure 8.1). The cylindrical configuration was used for several reasons. Specifically, the ratio of the area of earth contact to storage volume is maximized, and the installation costs and problems can be minimized. Each unit consists of a capped six-inch (15.2 cm) PVC pipe that contains water to a depth up to the frost line. A concentric pipe heat exchanger is located axially in each unit. A 40 percent solution of ethlyene glycol/water (brine) is utilized as the heat transfer media. The brine solution provides the intermediate energy link between the thermal storage and the evaporator. Heat is transferred from the storage water to the brine in the concentric pipe heat exchanger (Figure 8.2). The brine solution flows through the transmission piping (Figure 8.3) and eventually delivers the energy to the heat pump evaporator. Once all the sensible heat has been extracted from the storage water, ice begins to form on the surface of the concentric pipe heat exchanger.

During the heating operation, ice forms while peak load conditions occur and melts (due to the earth's energy input) over non-demand periods. This system has the opportunity to provide off-peak cooling where an off-peak structure exists. During the cooling season, the heat pump is run during off-peak periods to make ice. By de-coupling the ETS from the earth, the ice can be stored for a period of time. The brine can now be circulated through a brine-to-air heat exchanger and provide cooling for the residence. Research is being conducted on various methods of de-coupling the storage unit from the earth.

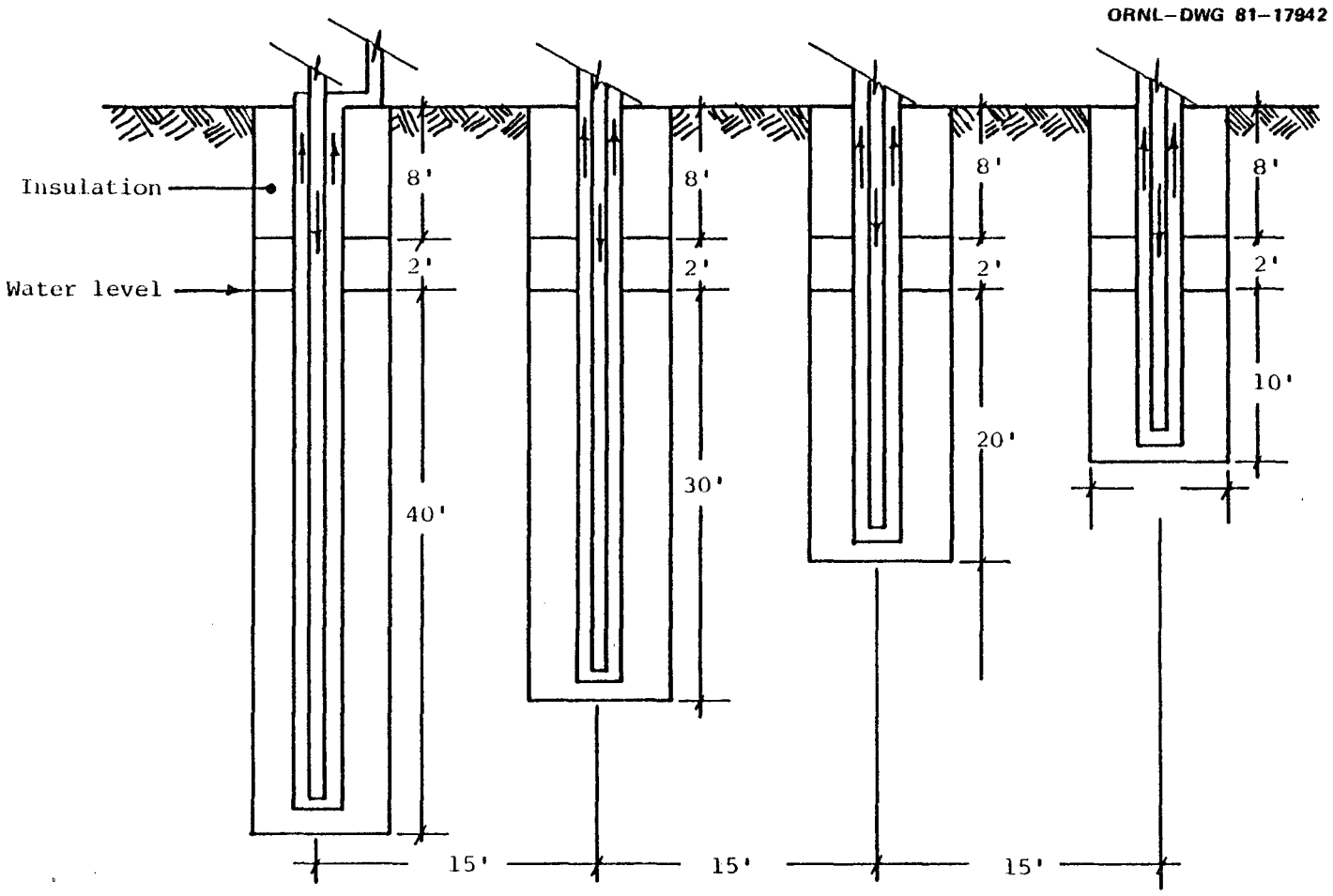

FIGURE 8.1 - CROSS-SECTION OF TEST FACILITY

ORNL-DWG 81-17943

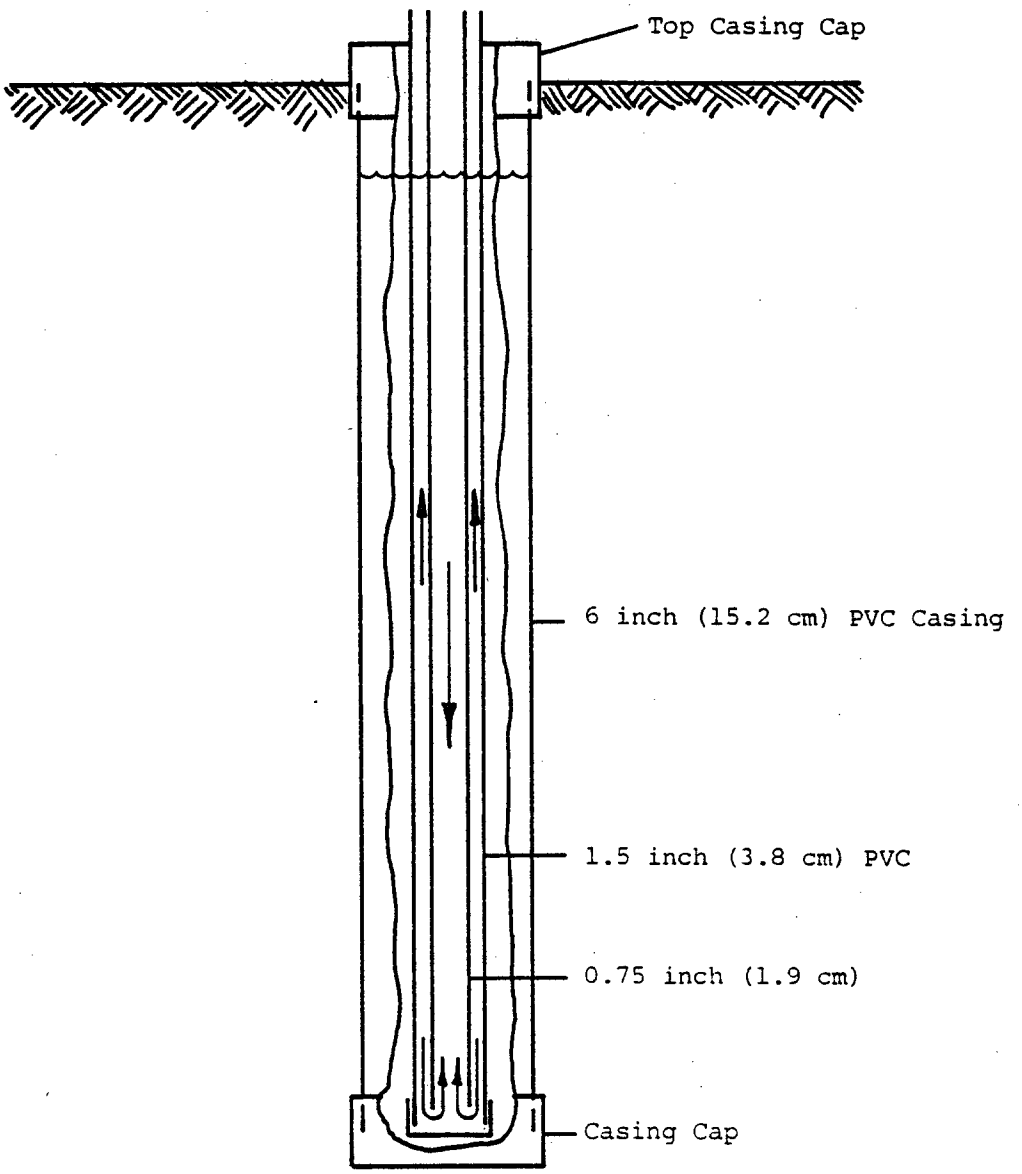

FIGURE 8.2 - TYPICAL E.T.S. UNIT

ORNL-DWG 81-17944

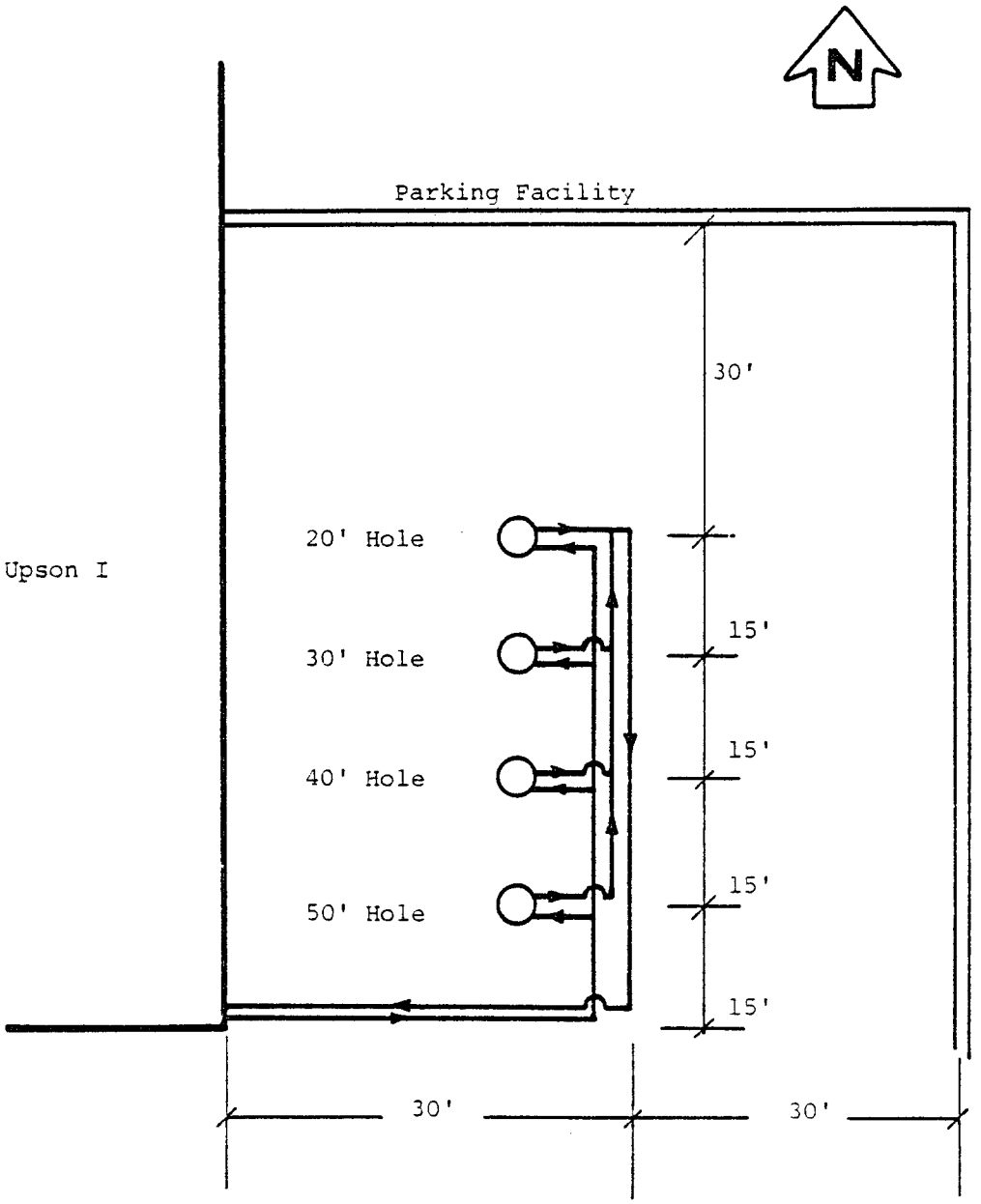

FIGURE 8.3 - REVERSE-RETURN HYDRAULIC SYSTEM

Since the ETS system consists of a number of units, the operable storage volume can be changed to meet the instantaneous load. Thus, if properly designed, a minimum quantity of thermal storage should always be available.

The heat pump evaporator (as shown in Figure 8.4) is a shell and tube evaporator in which the brine flows in the annulus between the PVC shell and the copper tubes. The copper tubes are spirally wound around a one inch (2.54 cm) core. The evaporator is a partial cross/counter flow unit. The spiralling of the inside tubes has the advantages of 1) flow patterns in the annulus are disrupted and the heat transfer increases, and 2) a more compact evaporator can be manufactured. Since this evaporator is utilized in a MSHP system, a method of subcooling must be provided. This is accomplished by using one of the seven ¼" copper tubes, which carries the subcooling liquid. (See Figure 8.4)

8.2 Analytical and Experimental Efforts with the ETS Facility

A computer model that analyzes the instantaneous thermal energy has been developed (Cox, 1980). Since the ETS facility was not operational until February 1980, a complete winter test program has not been completed. One major problem encountered during the early testing program (winter tests) was the significant gain of energy in the transmission piping. It was initially necessary to run the piping through a warm (100°F (37.8°C)) tunnel. Despite several layers of varying types of insulation, over 50 percent of the evaporator load was the result of this heat gain. Thus, the data recorded during this period is not satisfactory. Summer melt-off data (no external load) was recorded to determine the actual earth heat transfer rate. Figure 8.5 shows the results of the melt-off tests. Included on the graph is the analytical prediction of the melt-off rate.

ORNL-DWG 81-17945

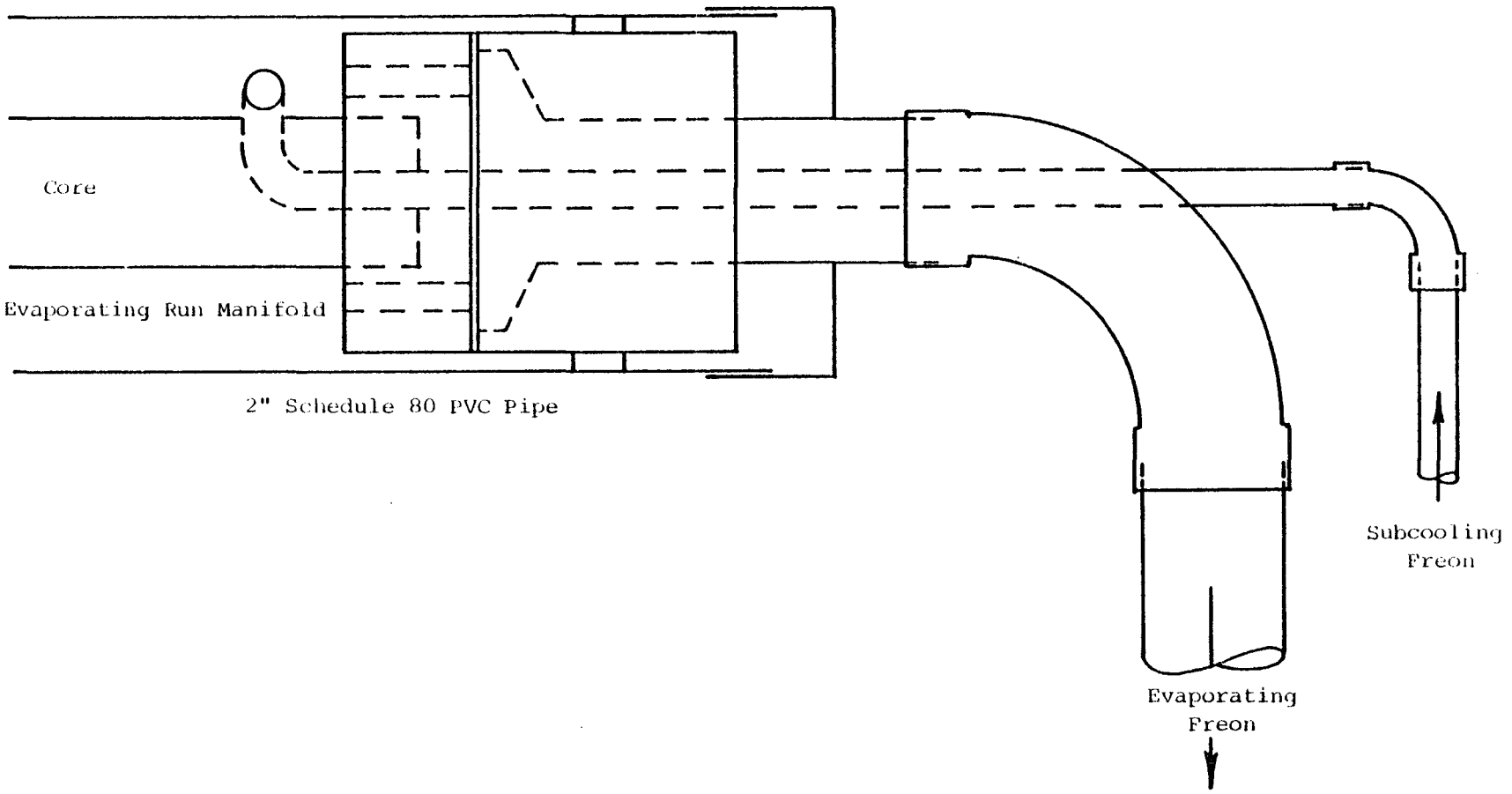

FIGURE 8.4 - DETAIL OF SUBCOOLING TUBE ENTRY, EARTH EVAPORATOR

ORNL-DWG 81-17946

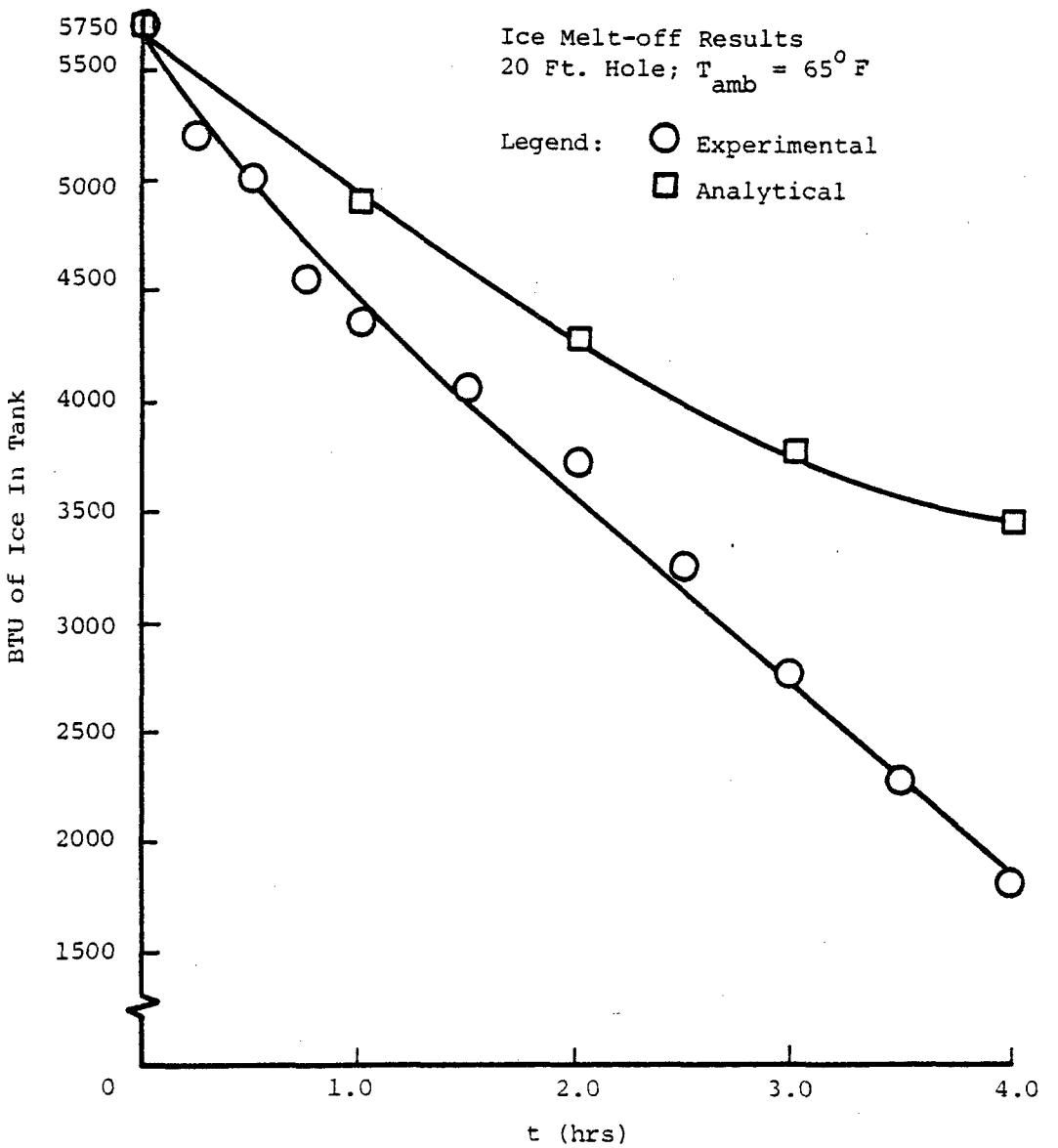

FIGURE 8.5 - ICE MELT OFF VERSUS TIME

Currently, the problem of the undesirable energy input has been resolved by moving the heat pump and associated equipment closer to the ETS site, thus, eliminating the load picked up in the transmission piping. A complete winter test program is being planned for the coming winter.

8.3 Recommendations

Preliminary analysis of the ETS facility performance has proved that the storage requirements seen in an ACES or MSHP system can be reduced, thus, reducing the capital investment in the system. Because of this, the further development of the ETS facility is justified.

Another area that research should be devoted to is the use of the ETS and associated MSHP system as an off-peak cooling system. In order to do this, various ways to de-couple the earth from the storage cylinder must be investigated.

9.0 RELATIVE ECONOMICS OF THE MULTIPLE SOURCE HEAT PUMP SYSTEM

9.1 Introduction

The purpose of this study is to provide a general comparison of the thermal and economic performance of a Multiple Source Heat Pump (MSHP) system to that of an air-to-air heat pump and an Annual Cycle Energy System (ACES)

The general case will be considered as opposed to the detailed case for several reasons:

1. The design details of any heat pump system vary significantly from location to location, as well as from application to application; hence, the specific variables controlling the design are a function of weather and application.

2. The weather data are crucial to a comparative evaluation. Since the weather data are not fully understood, it is impossible to make a detailed comparison with universal validity.

3. The rate structure (off-peak to demand ratio) and cost of energy vary widely, depending on location.

9.2 Analysis Assumptions

The weather data used in this study was based on the Department of Defense (DOD) Bin weather data. The DOD data was processed into useable tables (Somerville, Barney, and Lindem, 1979), including a cumulative heat load table and cumulative cooling load tables for conduction and air changes.

Five major cities were chosen for the study. Table 9.1 shows the five cities and their heating and cooling loads, based on the processed bin weather data analysis.

Several assumptions were made, in order to carry out the study:

TABLE 9.1

THE FIVE MAJOR CITIES CHOSEN FOR THE THERMAL AND ECONOMIC STUDY*

City	Loads (°F - hrs)			Heating/Cooling
	Heating	Cooling	Total	
Grand Forks, ND	226492	6428	232920	35.24
Boston, MA	153384	6792	160176	22.58
Memphis, TN	78754	30440	190194	2.59
Dallas, TX	58761	49940	108701	1.18
Tampa, FL	17268	43302	60570	0.40

*Taken from processed bin weather data (Somerville, Barney, and Lindem, 1979).

1. The cooling load at any location is equivalent to twice the conduction cooling load. In other words, half the cooling load is made up by infiltration.

2 The ACES at any given location costs approximately 2½ times that of an air-to-air heat pump system (capital investment).

3. Two switchover temperatures were used for the MSHP system:
   Case 1: Switchover temperature = 10°F (-12.2°C)
   This case was chosen because this temperature represents the lowest practical bound that an air to-air heat pump can operate.

   Case 2: Switchover temperature = 32°F (0°C)
   This case was chosen because this switchover temperature can eliminate the hot-gas defrost of the air evaporator.

4. The heating coefficient of performance (COP_h) of the air-to-air heat pump was based on the compressor only. The COP_h data was taken from the manufacturers published data. No hot gas defrost is considered in this data.

5. The cooling coefficient of performance (COP_c) of the air-to-air heat pump was assumed to decrease linearly from 2.0 at 70°F (21.1°C) to 1.3 at 100°F (37.8°C).

6. The cooling coefficient of the ACES is assumed to be 8.00 when the system is not used an an off-peak cooling system.

7. The heating coefficient of performance for an ACES or a MSHP during ice-making is 2.80 (compressor only).

8. The cooling coefficient of performance for an ACES or a MSHP when the compressor is used to make ice is 1.80.

9. When the ACES provides a seasonal energy carry-over, it may be used for cooling. This is accomplished by circulating the cool water through an air-to-water heat exchanger. This mode of operation provides a COP_c = 8.00 for the ACES.

   Example: Dallas, TX:
   Heating Load = 58761 °F - hrs.
   Cooling Load = 49940 °F - hrs.
   The ACES storage can supply:

$$\frac{COP_h - 1}{COP_h} \text{ (heating load)}$$

$$\frac{2.8 - 1}{2.8}(58761) = 37775 \text{ °F - hrs}$$

of cooling. However, the cooling load is 49940 °F - hrs. Therefore, the ACES tank can supply 75.6 percent of the cooling requirement, operating at a COP_c = 8.00. The remaining 24.4 percent of the cooling is provided by running the ACES as an off-peak cooling system with a COP_c = 1.80.

10. The MSHP system provides no seasonal energy carry-over from winter to summer. Therefore, the MSHP system must be run in the heating mode to make enough ice to satisfy the next day's cooling requirements.

11. All ice-making during the cooling season is done off-peak.

12. When the air-to-air heat pump is used to cool, 1/3 of the usage is off-peak, and 2/3 of the usage is demand.

13. Three off-peak to demand cost rations (O/D) are assumed. These are 1/3, 1/2, (based on current off-peak structures) and 1/1 (straight demand rate structure).

14. During the heating season, all of the heating requirements are done on a fully demand basis.

9.3 Analysis Procedure

Four systems were chosen for the analysis of each of the five cities. These systems are as follows:

Case 1 - a full Annual Cycle Energy System (ACES);

Case 2 - a MSHP system with a 32°F switchover temperature;

Case 3 - a MSHP system with a 10°F switchover temperature; and

Case 4 - an air-to-air heat pump system.

In order to clearly present the analysis method, an example will be shown for the city of Boston.

9.3.1 Determination of the Procurred Energy During the Heating Season

The first step in the analysis is to determine the heating season performance (i.e., the heating coefficinet of performance). This can be done by determining the percentage of procurred electrical energy (and thus, the heating season COP) for each system. This is done for the example city of Boston in Table 9.2.

The percentage heating load fraction (Q_f) is determined by dividing the total number of ^{o}F - hrs observed at a certain temperature by the total number of ^{o}F - hrs for the heating season. The ^{o}F - hrs

TABLE 9.2

CALCULATION OF HEATING SEASON COP FOR THE FOUR SYSTEMS ANALYZED FOR BOSTON, MASSACHUSETTS

Temperature (°F)	Q_f (%)[1]	CFHL (%)[2]	Air-to-Air[3] COP_h	Procurred energy = Q_f/COP_h[4] (%) Case 1	Case 2	Case 3	Case 4
67	0	0	3.45	0	0	0	0
62	0.50	0.50	3.40	0.18	0.15	0.15	0.15
57	2.02	2.52	3.30	0.72	0.61	0.61	0.61
52	4.08	6.59	3.20	1.46	1.27	1.27	1.27
47	6.40	12.99	3.20	2.28	2.00	2.00	2.00
42	10.30	23.29	3.10	3.68	3.32	3.32	3.32
37	14.55	37.94	2.90	5.20	5.02	5.02	5.02
32	17.10	54.94	2.80	6.11	6.11	6.11	6.11
27	14.25	69.19	2.60	5.09	5.09	5.48	5.48
22	10.74	79.92	2.50	3.83	3.83	4.29	4.29
17	7.89	87.81	2.30	2.82	2.82	3.43	3.43
12	5.49	93.31	2.10	1.96	1.96	2.62	2.62
7	3.97	97.28	1.90	1.42	1.42	1.42	2.09
2	1.48	98.75	1.70	0.53	0.53	0.53	0.87
-3	0.75	99.51	1.60	0.27	0.27	0.27	0.47
-8	0.29	99.79	1.50	0.10	0.10	0.10	0.19
-13	0.15	99.95	1.40	0.05	0.05	0.05	0.11
-18	0.05	100.00	1.30	0.02	0.02	0.02	0.04
			Total Procurred Energy (%) =	35.71	34.57	36.69	38.07
			Heating Season COP_h =	2.80	2.89	2.72	2.62

TABLE 9.2 (Continued)

CALCULATION OF HEATING SEASON COP FOR THE FOUR SYSTEMS
ANALYZED FOR BOSTON, MASSACHUSETTS

[1] $Q_f = \frac{\text{Total } ^{o}F \text{ - hrs observed at that temperature over heating season}}{\text{Total } ^{o}F \text{ - hrs during the heating season}}$

[2] CFHL = Cumulative Fraction Heating Load

[3] Based on manufacturers data for a heating only Janitrol 2½ ton heat pump (Compressor only COP)

[4] The COP_h is determined as:

a) 2.8 for an ACES (Case 1);
b) Air-to-Air heat pump COP for a MSHP until the switchover temperature, then COP_h = 2.8 (Cases 2 and 3);
c) Air-to-Air COP_h for a conventional air-to-air heat pump (Case 4).

data is taken from the processed bin weather data (Somerville, et al., 1979, Volume III).

Once this heat load fraction (Q_f) is known, the procurred energy for the four considered systems can be determined by dividing the heat load fraction by the COP_h of the system at the ambient temperature being considered for the respective heating systems (this is expressed as a percent). By summing the procurred energy values over the season (various ambient temperatures), an equivalent heating season procurred electrical energy percentage can be determined. The inverse of this procurred energy percent is the heating season coefficient of performance (COP_h)

9.3.2 Determination of the Procurred Energy During the Cooling Season

Table 9.3 shows the calculation of the total procurred energy for the cooling season for the example city of Boston. The cooling season is a more complex analysis. To simplify the calculations, the cooling load is assumed to be made up of ½ conduction load and ½ air change load. With this assumption, the cumulative fraction cooling load (CFCL) can be determined by adding ½ of the CFCL due to conduction and ½ of the CFCL due to air change. The fraction of the cooling load can then be determined by subtraction of successive values of the CFCL. Once the fraction of the cooling load is determined for a certain temperature, the procurred energy at that temperature for the four specific systems can be determined by dividing this fraction cooling load by the COP_c of the system. By summing the procurred energy for each system over the cooling season, the total procurred energy (and thus, the cooling season COP_c) can be determined for the cooling season.

TABLE 9.3

DETERMINATION OF THE PROCURED ENERGY DURING THE COOLING SEASON FOR BOSTON, MASSACHUSETTS

Temperature (°F)	CFCL (%)[1]	Q_f(%)[2]	Procurred Energy = Q_f/COP_c[3] (%) Case 1	Cases 2 & 3	Case 4
72	14.56	14.56	1.82	8.09	7.47
77	27.56	13.09	1.64	7.27	7.11
82	61.26	33.61	4.20	18.67	19.54
87	85.74	24.88	3.06	13.60	15.30
92	97.77	12.03	1.50	6.68	8.07
97	100.00	2.23	0.28	1.24	1.63
Total Procurred Energy (%)			= 12.50	55.56	59.12
Cooling Season COP_c			= 8.00	1.80	1.69

[1]CFCL = Cumulative fraction cooling load - determined by adding ½ of the CFCL due to conduction and ½ of the CFCL due to air change.

[2]Q_f = Fraction of cooling load (%)

[3]COP_c is determined as:

a) 8.00 for ACES when the tank can completely supply the cooling requirements. Otherwise COP_c = 1.80 (off-peak) ice-making).
b) 1.80 for MSHP systems.
c) Based on a linear decrease from 2.0 @ 70°F to 1.3 @ 100°F.

9.3.3 Determination of the Total Procurred Energy and Annual COP for the Heating/Cooling Systems

Table 9.4 shows the total procurred energy determined for the example city of Boston. Using the total percent procurred energy from the heating and cooling season, the amount of procurred energy in ^{o}F - hrs for each season can be calculated by multiplying these percentages by the total seasonal load. Once the procurred seasonal energies are determined, they are added together to determine the total annual procurred energy on a ^{o}F - hrs basis. The annual COP (ACOP) is then determined by dividing the total annual load (the sum of the heating load and cooling load) by the total annual procurred energy. The percent savings in procurred energy over a reversing air-to-air heat pump can then be determined. It should be noted that this percent savings is based on no off-peak incentive offered by the utilities (i.e., the electrical rate structure is based on a total demand situation).

9.3.4 The Influence of an Off-Peak to Demand Cost Ratio in the Electrical Rate Structure

The influence of an off-peak incentive offered by the utilities on the percent procurred energy savings over an air-to-air heat pump can be analyzed utilizing the assumptions listed in Section 9.2. The major assumption will reiterated here.

1. All ice-making during the cooling season is done during off-peak periods.
2. When an air-to-air heat pump is used to cool, 1/3 of the usage is off-peak and 2/3 of the usage is demand.
3. During the heating season, all of the heating is done during demand periods.

Two off-peak to demand (O/D) cost ratios were considered. These ratios are 1/2 and 1/3.

TABLE 9.4

DETERMINATION OF THE TOTAL PROCURRED ENERGY AND ANNUAL COP OF THE FOUR HEATING SYSTEMS FOR BOSTON, MASSACHUSETTS

Heating Load (^{o}F - hrs) = 153384
Cooling Load (^{o}F - hrs) = 6792

Annual Load = 160176

		Case 1	Case 2	Case 3	Case 4
Procurred Energy (^{o}F - hrs)	Heating Season	54758	53071	56292	58439
	Cooling Season	849	3774	3774	4015
	Annually	55607	56845	60066	62454
Annual COP (ACOP) = $\frac{\text{Total Annual Load}}{\text{Procurred Annual Energy}}$		2.88	2.82	2.67	2.56
Percent savings in procurred energy over an air-to-air heat pump heating/cooling system		10.96	8.98	3.82	--

Table 9.5 shows the percent savings in procurred electrical energy over an air-to-air heat pump system for the various O/D ratios for the example city of Boston. It can be seen that under an off-peak incentive, the savings for a MSHP (at 32°F switchover) system surpass that of an ACES. This is not always true, as will be shown in the next section.

9.4 Results of Analysis

9.4.1 Thermal Performance

Table 9.6 shows the thermal analysis of the four case systems for the five cities considered. It can be seen that for all cases, the ACES out-performs the other three systems, from an energy standpoint. It can also be seen that both cases of the MSHP system out-perform the air-to-air heat pump system. Therefore, from the standpoint of energy efficiency, the systems can be ranked, from best to worst as follows:

1. The ACES;
2. The MSHP with a 32°F switchover;
3. The MSHP with a 10°F switchover; and
4. The air-to-air heat pump.

Before the systems can be truly ranked, the performance of the systems from an economic viewpoint must be considered. This is the topic of the next section.

9.4.2 Economic Performance

In order to economically evaluate the heating system, we must establish some sort of comparison basis. The most useful comparison would be to the system which is commercially available today. This system is Case 4; the air-to-air heat pump system.

TABLE 9.5

THE INFLUENCE OF AN OFF-PEAK INCENTIVE ON THE PERCENT SAVINGS IN PROCURRED ENERGY FOR BOSTON, MASSACHUSETTS

O/D Cost Ratio			Case 1	Case 2	Case 3	Case 4
1/1		Heating	54758	53071	56292	58439
	Procurred Energy	Cooling	849	3774	3774	4015
		Total	55607	56845	60066	62454
	Percent Savings		10.96	8.98	3.82	--
1/2		Heating	109516	106142	112584	116879
		Cooling	849	3774	3774	6691
		Total	110365	109916	116358	123571
	Percent Savings		10.69	11.05	5.83	--
1/3		Heating	164274	159213	168876	175318
		Cooling	849	3774	3774	9368
		Total	165123	162987	172650	184686
	Percent Savings		10.59	11.75	6.52	--

TABLE 9.6

THERMAL ANALYSIS OF THE FOUR CASE SYSTEMS

City	Load (^{o}F - hrs)		Procurred (^{o}F - hrs)							
			Case 1		Case 2		Case 3		Case 4	
	Heating	Cooling	Heating	Cooling	Heating	Cooling	Heating	Cooling	Heating	Cooling
Grand Forks, ND	226492	6428	80858	804	79952	3571	84935	3571	112340	3881
			COP_h=2.80	COP_c=8.00	COP_h=2.82	COP_c=1.80	COP_h=2.67	COP_c=1.80	COP_h=2.02	COP_c=1.66
			ACOP = 2.85		ACOP = 2.79		ACOP = 2.63		ACOP = 2.00	
Boston, MA	153384	6792	54758	849	53071	3774	56292	3774	58439	4015
			COP_h=2.80	COP_c=8.00	COP_h=2.89	COP_c=1.80	COP_h=2.72	COP_c=1.80	COP_h=2.62	COP_c=1.69
			ACOP = 2.88		ACOP = 2.82		ACOP = 2.67		ACOP = 2.56	
Memphis, TN	78754	30440	28115	3805	26461	16912	27170	16912	27328	18626
			COP_h=2.80	COP_c=8.00	COP_h=2.98	COP_c=1.80	COP_h=2.90	COP_c=1.80	COP_h=2.88	COP_c=1.63
			ACOP = 3.42		ACOP = 2.52		ACOP = 2.48		ACOP = 2.38	
Dallas, TX	58761	49940	20978	16056	19509	27742	19861	27702	19861	32086
			COP_h=2.80	COP_c=3.20	COP_h=3.01	COP_c=1.80	COP_h=1.96	COP_c=1.80	COP_h=2.96	COP_c=1.56
			ACOP = 2.94		ACOP = 2.30		ACOP = 2.28		ACOP = 2.09	
Tampa, FL	17268	43302	6165	19577	5389	24059	5389	24059	5389	25834
			COP_h=2.80	COP_c=2.21	COP_h=3.21	COP_c=1.80	COP_h=3.21	COP_c=1.80	COP_h=3.21	COP_c=1.68
			ACOP = 2.35		ACOP = 2.06		ACOP = 2.06		ACOP = 1.94	

Case 1 - ACES

Case 2 - MSHP - $32^{o}F$ Switchover

Case 3 - MSHP - $10^{o}F$ Switchover

Case 4 - Air-to-Air Heat Pump

Since the air-to-air heat pump system does not require a water storage tank, the ACES was chosen to be a comparative basis for equivalent storage requirements. Table 9.7 shows the storage requirements for the two MSHP systems, based on the ACES storage requirement equal to 1.00. The fraction of ACES storage required for the MSHP systems can then be determined from the cumulative fraction heating load (CFHL) data (Somerville et al., 1979).

To determine the capial cost of a system relative to an air-to-air heat pump, the following assumptions are made:

1. The air-to-air heat pump equivalent cost = 1.00.
2. The fixed cost of a MSHP system = 1.25 (this is due to the addition of an extra evaporator).
3. The cost of storage in an ACES = 1.25, and the heat pump and peripherals have a fixed cost of 1.25 (because of the brine circulation loop and associated heat exchangers). This makes the ACES cost = 2.50.

The operating cost of the system is also relative to the air-to-air heat pump. Section 9.3.4. (and Table 9.5) show the detailed determination of the savings in procurred energy (operating cost) over an air-to-air heat pump system for the example city of Boston. Similar calculations were done for the other four cities in the study. Table 9.8 summarizes the percent savings in operating cost for various O/D ratios, as well as the relative capital cost of the system for the cities considered.

Table 9.8 reveals the following information:

1. In northern climates, the difference in operating cost savings between the ACES and the MSHP systems is generally small, whereas the relative capital cost difference is large. This favors the installation of a MSHP system over an ACES. In southern climates, the ACES may be justified over the MSHP.

TABLE 9.7

FRACTION OF ACES STORAGE VOLUME REQUIRED FOR A MSHP SYSTEM (ACES = 1.00)*

City	Switchover = 32°F	Switchover = 10°F
Grand Forks, ND	0.75	0.40
Boston, MA	0.44	0.05
Memphis, TN	0.25	0.01
Dallas, TX	0.17	0.00
Tampa, FL	0.01	0.00

* The fraction of storage was determined by using the CFHL data in the processed bin weather data (Somerville, et al., 1979).

TABLE 9.8

SUMMARY OF PERCENT OPERATING COST SAVINGS[1] FOR VARIOUS O/D RATIOS AND RELATIVE CAPITAL COST[2] OF THE SYSTEM FOR THE FIVE CITIES CONSIDERED

City	Multiple Source Heat Pump								ACES			
	Switchover = 10 F				Switchover = 32 F							
	Savings O/D[3]			Relative Capital Cost[2]	Savings O/D[3]			Relative Capital Cost[2]	Savings O/D[3]			Relative Capital Cost[2]
	1/1	1/2	1/3		1/1	1/2	1/3		1/1	1/2	1/3	
Grand Forks, ND	23.8	25.0	25.1	1.75	28.1	29.3	29.4	2.18	29.7	29.7	29.4	2.50
Boston, MA	3.8	5.8	6.5	1.30	8.9	11.1	11.8	1.80	10.9	10.7	10.6	2.50
Memphis, TN	4.1	16.9	21.5	1.27	5.6	18.5	23.2	1.56	30.5	29.9	29.7	2.50
Dallas, TX	8.4	27.6	23.8	1.25	9.0	28.4	24.7	1.47	28.7	37.8	31.1	2.50
Tampa, FL	5.7	35.3	47.8	1.25	5.7	35.3	47.8	1.27	17.6	40.7	50.2	2.50

[1] Relative to an air-to-air heat pump

[2] Based on an air-to-air heat pump = 1.00

[3] Percent savings in procurred energy for various off-peak to demand (O/D) cost ratios over that of an air-to-air heat pump

2. In northern climates, an off-peak incentive by the utilities has very little effect on the procurred energy savings. In southern climates, an off-peak incentive affects the savings considerably.

3. Under an off-peak incentive, the MSHP system out-performs an air-to-air heat pump and approaches the performance of an ACES (from the viewpoint of operating cost savings).

4. The operating costs savings for a MSHP with a 32°F switchover compared to that of a 10°F switchover is generally not justified when the relative capital costs are considered (especially in the northern climates).

9.5 Recommendations

The results of the economic analysis provides a strong case for further development of the MSHP system. In southern climates, the development of the MSHP system, along with off-peak incentives from the utilities, provide even further justification of continued development of such systems.

Further work is also recommended in the area of the weather data. Until a reliable method for analyzing the weather data exists, a detailed economic analysis cannot be made, and still hold universal validity. One suggestion for this development would be to generate tables of various "confidence" levels. Then, when the designer uses these tables, he can be assured of a certain percent confidence in the final figures.

10.0 CONCLUSIONS AND RECOMMENDATIONS

10.1 Conclusions

The following are the major conclusions of the work presented:

1. It is possible to design and build a multiple source heat pump (MSHP);

2. A MSHP with a parallel evaporator arrangement, with active sub-cooling in each evaporator was the most successful design built;

3. The hand calculational design procedure developed for a MSHP (dual series) is valid when used as a preliminary design procedure;

4. A parameter change of refrigeration effect to freon mass flow rate, as a function of evaporating or condensing temperature, as the design basis for MSHP systems is required;

5. The format utilized for the weather data analysis is sound and presents the thermal designer with the flexibility required to address the design of ACES, multiple source heat pumps, off-peak air conditioning, and solar and thermal storage systems;

6. The heat transfer characteristics of a flat plate ice-maker are strongly dependent upon the air temperature surrounding them. This phenomena must be considered in the design of a system utilizing flat plate ice-makers;

7. The storage density characteristics of an in-bin exchanger are much preferable to those of flat plate ice-maker. This is particularly true in a residential application;

8. The analytical model of a flat plate ice-maker is qualitatively sound and forms a basis for future development of flat place ice-makers;

9. The earth-ice storage system has the potential to be used in ACES, MSHP, and off peak air conditioning systems;

10. The relative economic analysis indicates that air-to-air heat pumps have a clear economic edge over both the ACES and MSHP systems for the cities analyzed (Memphis, Dallas, and Tampa);

11. The ACES system utilizes the minimum annual energy of the systems analyzed (MSHP, and air-to-air heat pumps) for cities analyzed (Grand Forks, Boston, Memphis, Dallas and Tampa);

12. The MSHP system has a lower capital investment and, in some cases, a lower operating cost than does ACES (either full or partial);

13. It is unlikely that full ACES will compete in the marketplace in the near term, unless there is a marked breakthrough in the cost of thermal storage;

14. The MSHP design with parallel evaporator and active subcooling can be used to defrost an air evaporator without loss of heat pump output.

15. It is possible to design an air-to-air MSHP that would eliminate the need for a hot-gas defrost;

16. It is possible to build a MSHP off-peak air conditioner that would eliminate the need for a hot-gas defrost during heating operations;

10.2 Recomendations

The following recommendations represent the opinions of the authors based upon the last four years of work. The recommendations are based both on the work presented here and the engineering experience of the authors:

1. The work initiated in the analysis of the weather data should be continued and expanded to include the confidence level associated with energy requirements for different elapsed times, as a function of calendar time;

2. The development of MSHP technology should be continued because of its capability to provide:

   * a known output at cold temperatures;

   * a solution to the defrosting of air coils that does not utilize high quality energy;

   * a capability to perform off-peak air conditioning; and

   * a savings of both energy and money, particularly with a demand rate structure;

3. A hand calculational design procedure should be developed for MSHP systems with active subcooling;

4. Work to simplify and improve air-to-air heat pumps should be encouraged, particularly the units reliability and energy efficiency;

5. Air-to-air heat pump start up and transients should be experimentally investigated;

6. Monitoring of some of the existing commerical off-peak air conditioning systems should be carried out.

REFERENCES

Albrecht, L.S. and M.H. Somerville, "The Dual Evaporator Heat Pump with the Parallel Alternating Arrangement," Engineering Experiment Station, Bulletin No. 78-04-EES-02, April 1978.

Cox, N.R., "Analytical Solution for the Determination of the Instantaneous Thermal Storage of an Earth Thermal Storage Facility," Engineering Experiment Station, Bulletin No. 80-04-EES-03, April 1980.

Fischer, H.C., "The Annual Cycle Energy System," Oak Ridge National Laboratory, Oak Ridge, Tennessee, 1976a.

Fischer, H.C., "Thermal Storage Applications of the Ice Maker Heat Pump," Oak Ridge National Laboratory, Oak Ridge, Tennessee, 1976b.

Kipp, C.P., "Annual Cycle Energy System (ACES) Impact Upon a Utilities Load Duration Curve," Engineering Experiment Station, Bulletin No. 78-09-EES-01, September 1978.

Loken, G.R., M.H. Somerville, and D.V. Mathsen, "A Computer Model for Performance Analysis of a Solar Heated Residential Home in North Dakota," Engineering Experiment Station, Bulletin No. 77-04-EES-05, April 1977.

Loken, G.R., "A Mathematical Model of a Residential Heating and Cooling Annual Cycle Energy System," Engineering Experiment Station, Bulletin No. 77-07-EES-01, July 1977.

Mathsen, D.V., M.H. Somerville, and G.R. Loken, "A Flat-Plate Solar Collector Using Non-Black Absorber Elements," Engineering Experiment Station, Bulletin No. 77-04-EES-02, April 1977.

Mondry, G., "The Effect of Subcooling on the Performance on a Dual-Series Evaporator Heat Pump," Engineering Experiment Station, Bulletin No. 79-06-EES-04, June 1979.

Penoncello, S.G. and M.H. Somerville, "The Analytical Prediction and Experimental Verification of the Thermal Performance of a Multiple Source Heat Pump System," Engineering Experiment Station, Bulletin No. 80-07-EES-05, May 1980.

Somerville, M.H., D.V. Mathsen, G.R. Loken, C.D. Svard and J.C. Wendschlag, "The Design and Analysis of a North Dakota Annual Cycle Residential Solar Heating System," Engineering Experiment Station, Bulletin No. 77-04-EES-01, April 1977.

Somerville, M.H. and S.G. Penoncello, "The Development of an Air-Icemaker Multiple Source Heat Pump System," Engineering Experiment Station, Bulletin No. 80-05-EES-01, June 1980.

Somerville, M.H. and J.C. Wendschlag, "The Heating Only Heat Pump, An Application in the Annual Cycle System," Engineering Experiment Station, Bulletin No. 77-04-EES-03, April 1977.

Somerville, M.H., W.G. Barney, and A.C. Lindem III, "Processed Bin Weather Data for Use in the Design of Renewable Energy Based Heating and Air Conditioning for Forty Cities," Engineering Experiment Station, Bulletin No, 79-07-EES-01, Volumes A, B, C, and D, July 1979.

Svard, C.D., M.H. Somerville, and D.V. Mathsen, "The Economics of Solar Space Heating and Cooling," Engineering Experiment Station, Bulletin No. 77-04-EES-04, April 1977.

Trellis, A., "The Backward Air Conditioners Take a Front Seat," Popular Mechanics, February 1978.

Wendschlag, J.C., "Isothermal Heat Transfer Through a Thin Fluid Undergoing a Phase Change with a Secondary Heat Transfer from a Warm Environment," Engineering Experiment Station, Bulletin No. 79-06-EES-02, June 1979.

Wood, J.A., "A Practical Design Procedure for Dual Evaporator Heat Pumps," Engineering Experiment Station, Bulletin No. 79-06-EES-03, June 1979.

INTERNAL DISTRIBUTION

1. V. D. Baxter
2. N. S. Cardell
3. R. S. Carlsmith
4. R. C. DeVault
5. R. D. Ellison
6. S. K. Fischer
7. W. Fulkerson
8. C. C. Gilmore
9. R. Eugene Goodson, Consultant
10. G. Grossman
11. D. M. Hamblin
12. V. O. Haynes
13. Todd R. LaPorte, Consultant
14. C. G. Lawson
15. W. P. Levins
16-20. P. M. Love
21. H. A. McLain
22. V. C. Mei
23. J. W. Michel
24. W. A. Miller
25-29. R. E. Minturn
30. W. R. Mixon
31. Larry I. Moss, Consultant
32. C. L. Nichols
33. F. S. Patton, Jr.
34. A. M. Perry
35. J. H. Reed
36. C. K. Rice
37. R. C. Robertson
38. M. W. Rosenthal
39. G. Samuels, Jr.
40. D. B. Trauger
41-42. Central Research Library
43. Document Reference Section
44. Laboratory Records - RC
45-47. Laboratory Records Dept.
48. ORNL Patent Section

EXTERNAL DISTRIBUTION

49. Dr. David Colvin, Triangle Research and Development Corporation, P.O. Box 12696, Research Triangle Park, NC 27709
50. Congressional Information Service, Research Building 83, Kodak Park, Rochester, NY 14050
51. J. J. Cuttica, Energy Conversion Equipment Branch, CE-113.2, Department of Energy, 1000 Independence Avenue, S.W., Washington, DC 20585
52. Edward J. Doyle, Jr., Doyle Associates, 14 East Lyon Farm Drive, Greenwich, CT 06830
53. Edison Electric Institute, Library, 8th Floor, 1111 19th Street, N.W., Washington, DC 20036
54. J. H. Gibbons, Office of Technology Assessment, U.S. Congress, 600 Pennsylvania Avenue, S.E., Washington, DC 20510
55. Tina Hobson, Building Equipment Division, CE-113.2, Department of Energy, 1000 Independence Avenue, S.W., Washington, DC 20585
56. P. L. Johnson, Oak Ridge Associated Universities, Executive Office, Administrative Building, Oak Ridge, TN 37830
57. T. Kapus, Office of Buildings Energy Research and Development, CE-11, Department of Energy, 1000 Independence Avenue, S.W., Washington, DC 20585

58. Dr. Edward A. Kush, Associate Scientist, Solar Research Group, Brookhaven National Laboratory, Upton, NY 11973
59. Arvo Lannus, Residential and Commercial Applications, Electric Power Research Institute, 3412 Hillview Avenue, P.O. Box 10412, Palo Alto, CA 94303
60. Jim Leggoe, Philadelphia Electric Company, 2301 Market Street, Philadelphia, PA 19101
61. G. S. Leighton, Department of Energy, CS-111, FORSTL, Washington, DC 20585
62. D. C. Lim, Energy Conversion Equipment Branch, CE-113.2, Department of Energy, 1000 Independence Avenue, S.W., Washington, DC 20585
63. Jack McCormick, Research Engineer, Northern States Power Company, 414 Nicollet Mall, Minneapolis, MN 55401
64. J. P. Millhone, Office of Buildings Energy Research and Development, CE-11, Department of Energy, 1000 Independence Avenue, S.W., Washington, DC 20585
65. Dan Myers, Refrigeration Systems, 611 State Street, Newberg, IN 47630
66. National Energy Information Center, Library, Room 1404, 12th and Pennsylvania Avenue, N.W., Washington, DC 20461
67. J. Rizzuto, New York State Energy Research and Development Authority, Agency Building No. 2, Empire State Plaza, Albany, NY 12223
68. J. D. Ryan, Energy Conversion Equipment Branch, CE-113.2, Department of Energy, 1000 Independence Avenue, S.W., Washington, DC 20585
69. M. L. Savitz, Deputy Assistant Secretary for Conservation, CE-10, Department of Energy, 1000 Independence Avenue, S.W., Washington, DC 20585
70. M. H. Sommerville, Dept. of Mechanical Engineering, University of Arkansas, Fayetteville, AR 72701
71. Steven Strong, Solar Design Associates, 271 Washington Street, Canton, MA 02021
72. D. J. Walukas, Foster-Miller Associates, Inc., 795 Oak Ridge Turnpike, Oak Ridge, TN 37830
73. Robert G. Werden, Werden & Associates, Inc., P.O. Box 414, Jenkintown, PA 19046
74. Office of the Assistant Manager for Energy Research and Development, Department of Energy, Oak Ridge Operations, Oak Ridge, TN 37830

75-101. Technical Information Center, U.S. Department of Energy, P.O. Box 62, Oak Ridge, TN 37830

102-125. Energy Division Library, Oak Ridge National Laboratory, P.O. Box Y, Bldg. 9102-2, Room 218, Oak Ridge, TN 37830

☆ U.S. GOVERNMENT PRINTING OFFICE: 1981-546-067/341